WHOI-89-12

Woods Hole Oceanographic Institution

Abstracts of Manuscripts Submitted in 1988 for Publication

Technical Report WHOI-89-12

WHOI-89-12

Research in Progress

Abstracts of Manuscripts Submitted in 1988 for Publication

Woods Hole Oceanographic Institution
Woods Hole, Massachusetts

Editor: Alice I. Tricca

Approved for Distribution: _____

When citing this report, it should be referenced as:
Woods Hole Oceanographic Institution
Technical Report No. WHOI-89-12

PREFACE

This volume contains the abstracts of manuscripts submitted for publication during calendar year 1988 by the staff and students of the Woods Hole Oceanographic Institution. We identify the journal for those manuscripts which are in press or have been published. The volume is intended to be informative, but not a bibliography.

The abstracts are listed by title in the Table of Contents and are grouped into one of our five departments, marine policy, or the student category. An author index is presented in the back to facilitate locating specific papers.

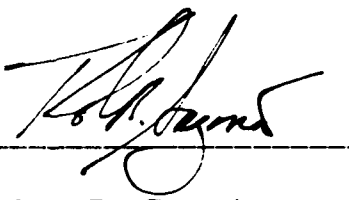

Robert B. Gagosian
Associate Director for Research

TABLE OF CONTENTS

DEPARTMENT OF BIOLOGY

ZOOPLANKTON

DEPARTMENT OF CHEMISTRY

ORGANIC AND BIOLOGICAL CHEMISTRY

RADIOCHEMISTRY

DEPARTMENT OF GEOLOGY AND GEOPHYSICS

GEOLOGY

DEPARTMENT OF OCEAN ENGINEERING

DEPARTMENT OF PHYSICAL OCEANOGRAPHY

COASTAL CIRCULATION AND DYNAMICS

INSTRUMENTATION AND EXPERIMENTAL METHODOLOGY

OCEAN CIRCULATION AND LOW FREQUENCY VARIABILITY

TECHNICAL REPORTS

MARINE POLICY CENTER

GRADUATE STUDENTS

DEPARTMENT OF BIOLOGY

Peter H. Wiebe, Chairman

BENTHOS

SPECIES DIVERSITY IN DEEP-SEA COMMUNITIES

J. Frederick Grassle

More extensive quantitative sampling of the deep-sea bottom has revealed communities much richer in species than previously thought. In situ experiments and more precise sampling using free-vehicle instruments and submersibles have provided a more accurate assessment of spatial and temporal variation on the sea floor. These studies have demonstrated the importance of small patches (mm to m) of biogenic disturbance and food input separated on spatial scales of m to km. In this respect the processes maintaining deep-sea diversity are similar to those in other species-rich environments such as rain forests.

Published in: *Trends in Ecology and Evolution*, 4, 12-15, 1989.

Supported by: NSF Grant OCE83-11201.

WHOI Contribution No. 6891.

THE INFLUENCE OF MODE OF EXPOSURE AND THE PRESENCE OF A TUBICOLOUS POLYCHAETE ON THE FATE OF BENZ(A)ANTHRACENE IN BENTHIC MICROCOSMS

Anne E. McElroy, John W. Farrington and John M. Teal

A series of experiments were run to simultaneously assess the effects of mode of introduction and the presence of large burrowing organisms on the fate of polycyclic aromatic hydrocarbons (PAH) and their metabolic breakdown products in the benthos. The distribution and metabolism of [^{14}C-12]benz(a)anthracene (BA) was followed in benthic microcosms in the presence and absence of the polychaete Nereis virens for periods of 4 to 25 days. Isotope was added to the chambers in three ways: already sorbed to the entire sediment reservoir; directly into the water column; or incorporated into food for the worms. BA added to the water column and subsequently associated with the sediment-water interface was more available for uptake and metabolism by worms, microbial mineralization to CO_2, and removal to the water column than BA previously sorbed to sediment. In experiments with the sediment reservoir uniformly labeled with BA, worms increased flux of BA from the sediment, and with time their presence led to increased rates of microbial mineralization of BA to CO_2.

Supported by: NOAA Contract 83-ABD-00012; and an Andrew W. Mellon Foundation Grant.

WHOI Contribution No. 6825.

APLACOPHORA

M. Patricia Morse and Amélie H. Scheltema

Members of the class Aplacophora (solenogasters) are wormlike, bilaterally symmetrical, nontorted mollusks found in marine environments in all oceans. They range in length from less than 1 mm to 13 cm; most are elongate (length 2 to 30 times width), but a few are nearly round while others are extremely elongate and thread-like. Some burrow within soft mud bottoms or creep on the surface; others are found wrapped around hydroids and corals; still others are interstitial in habitat and found among coarse sand grains. The meiofaunal species described here are defined as 2 mm in length (as recorded in the literature) since the diameter of a specimen this long would easily allow its passage through a 1 mm mesh sieve. There are eighteen species of Aplacophora which are interstitial and/or meiofaunal in size.

Published in: *Introduction to the Study of Meiofauna, R. P. Higgins and H. Thiel, eds. Smithsonian Press, Washington, D.C.*, pp. 447-450, 1988.

Supported by: Without support.

WHOI Contribution No. 6697.

VERTICAL DISTRIBUTIONS OF THE EPIFAUNA ON MANGANESE NODULES: IMPLICATIONS FOR FEEDING AND SETTLEMENT

Lauren Mullineaux

Over 65% of the sessile organisms living on manganese nodules from the tropical North Pacific belong to taxa whose abundances are related to vertical position on the nodule. The nodule surface texture and boundary layer flow environment, two factors that also vary vertically, were investigated to determine whether they could account for the observed faunal distributions. The surface texture of nodules from the tropical Pacific is generally rough and knobby at the nodule base and smooth near the summit. Twenty-five taxa, including 68% of the total individuals, were found in significantly different abundances on the rough vs smooth surfaces of 34 nodules. These distributions may be due to larval responses to surface texture, and can account for much of the observed vertical zonation of the fauna. Boundary layer flows over nodules were generalized from laboratory flume studies and

field observations. In flows at the field site, it is expected that mean boundary shear stress and horizontal flux of particles (food or larvae) will increase from the nodule base to the summit, while particle contact rate (deposition with no erosion) will decrease. The observations that suspension feeders persist near the nodule summit and deposit feeders concentrate near the base suggest that vertical distributions of some taxa may be determined by adult feeding requirements. Individuals of most taxa are relatively scarce at the nodule base, indicating that their larvae are not colonizing where they accumulate passively. High abundances of mat-like agglutinated foraminifers (of unknown feeding type) at the nodule summit may be due to larval responses to the relatively higher shear stresses. The relative effects of surface texture and the flow environment can be resolved for some, but not all, taxa.

Supported by: NSF Predoctoral Fellowship to author; and the Coastal Research Center.

WHOI Contribution No. 6947.

STABLE ISOTOPIC COMPOSITIONS OF HYDROTHERMAL VENT ORGANISMS

Cindy Lee Van Dover and Brian Fry

We used stable isotope analyses to study trophic relationships in two communities of deep-sea hydrothermal vent organisms in the Pacific Ocean. The community at Hanging Gardens on the East Pacific Rise (21°C) is dominated by two species of vestimentiferan tubeworms; communities at Alice Springs and Snail Pits on the Marianas Back Arc Spreading Center (western Pacific) are dominated by gastropod mollusks, barnacles, and anemones. In both locations, carbon and nitrogen isotopic values of vent invertebrates are significantly different from those non-vent invertebrates collected at 11°C on the East Pacific Rise and elsewhere in the deep sea. These distinct isotopic compositions reflect sources of organic carbon and nitrogen used by vent consumers. Many vent invertebrates lacking chemoautotrophic endosymbionts have ^{13}C-enriched values of -11 to -16 °/oo compared with the values normally observed in deep-sea fauna, -17 to -22 °/oo. This suggests that a ^{13}C-enriched food source is trophically important in both vent communities. Free-living bacteria colonizing surfaces and suspended in the water column may constitute this food resource. Nitrogen isotopic analyses show that the food web of the East Pacific Rise community has more trophic levels than the Marianas vent community.

Supported by: WHOI/MIT Education Office; WHOI Biology Department; WHOI Ocean Ventures Fund Grant; and Ecosystems Center, MBL.

WHOI Contribution No. 6886.

A NOVEL EYE IN 'EYELESS' SHRIMP FROM HYDROTHERMAL VENTS OF THE MID-ATLANTIC RIDGE

Cindy Lee Van Dover, Ete Z. Szuts, Steven C. Chamberlain and J. R. Cann

A recently described shrimp, one of several species that swarms over sulfide chimneys at Mid-Atlantic Ridge hydrothermal fields at a depth of 3600 m, lacks an externally differentiated eye. Instead, the shrimp bears a pair of hypertrophied organs within the cephalothorax that are connected via large nerve cords to the supraesophageal ganglion and contain a visual pigment with an absorption spectrum characteristic of rhodopsin. Ultrastructural evidence for degraded rhabdomeral material suggests the presence of photoreceptors. No image-forming optics are associated with the organs. We interpret the organs to be eyes adapted for the detection of low-level illumination, and we suggest that they evolved in response to some unusual source of radiation associated with the environment of hydrothermal vents.

In Press: *Nature.*

Supported by: WHOI Education Ocean Ventures Fund Grant; and NSF Graduate Fellowship.

WHOI Contribution No. 6887.

DETRITUS ON SEDIMENT SURFACE ENHANCES GROWTH OF CLYMENELLA TORQUATA, A HEAD DOWN FEEDING, TUBICOLOUS POLYCHAETE

James R. Weinberg

Food of deposit feeders tends to be concentrated in the top 2 cm of sediment. Although Clymenella torquata deposit feeds from the base of its vertical tube, 5-30 cm below the surface, it might obtain surface food in two ways: 1) "conveyor-belt" feeding involves subsurface ingestion and surface defecation. Defecation buries some surface food, and it eventually arrives at the subsurface feeding zone, and 2) use of posterior segments to "hoe" surface material directly into the tube.

A laboratory experiment was conducted to test the effect of surface food (detritus) on C. torquata's growth rate. To increase the variety of conditions under which the importance of detritus was tested, the experiment was conducted at three densities of a bivalve, Gemma gemma, which is

numerically dominant in C. torquata's natural community.

Addition of detritus to the sediment surface caused worms to grow larger than "control" worms. Clams had no effect on worm growth. Analysis of worm sizes after 34 d and 83 d suggests that enhanced growth from detritus began within 1 mo and continued throughout the experiment. The two feeding modes are discussed as they relate to C. torquata growth and the risk of predation.

In Press: *Ophelia.*

Supported by: WHOI Independent Study Award; and a Doctoral Dissertation Fellowship from the University of Connecticut.

WHOI Contribution No. 6773.

BIOGEOGRAPHY AND SYSTEMATICS

PECTINAPSEUDES CAROLINENSIS N. GEN., N. SP. (TANAIDACEA) DISCOVERED IN CONTINENTAL SLOPE WATERS OF NORTH AND SOUTH CAROLINA (U.S.A.)

Mihai Băcescu and Isabelle Williams

A new tanaid - Pectinapseudes carolinensis, new gen., n. sp. - discovered in the deep waters (800 m) off North and South Carolina (USA) is described in this paper. Ecological and catching data are also provided.

Published in: *Revue Roumaine de Biologie, Série de Biologie Animale*, 33(1), 3-6, 1988.

Supported by: Without support.

WHOI Contribution No. 6693.

AUSTRALIAN APLACOPHORAN MOLLUSKS: I. CHAETODERMOMORPHA FROM BASS STRAIT AND THE CONTINENTAL SLOPE OFF SOUTHEASTERN AUSTRALIA

Amélie H. Scheltema

Four new species of Chaetodermatidae (Chaetoderma usitatum, Falcidens chiastos, F. lipuros, and F. macrafrondis) and a new genus and species of Prochaetodermatidae (Rhabdoderma australe) are the first Chaetodermomorpha described from off Australia; all are from the shelf in Bass Strait or from the continental slope off southeastern Australia. Two species are numerous: F. chiastos occurs at densities sometimes up to 180 m^{-2} from 22 to 120 m in 20 of the 23 shelf samples that contain Chaetodermomorpha, and the prochaetodermatid R. australe is common from deeper water, 1,120 to 2,510 m. Several additional species only recently received or with a single specimen are noted but not described; three belong to Prochaetoderma, Limifossor, or Scutopus, thereby extending the recorded ranges of these genera to the western Pacific.

Of the 16 species of Chaetodermomorpha collected, 4 are shelf species occurring at depths of less than 200 m (F. chiastos, F. lipuros, one Prochaetodermatidae, one undetermined), 6 are upper slope species extending to 1,000 m (3 species of Falcidens, Chaetoderma sp., Scutopus sp., Limifossor sp.), and 6 extend below 1,000 m (C. usitatum, F. macrafrondis, R. australe, Falcidens sp., Chaetoderma sp., Prochaetoderma sp.). These depth distributions are similar to other Pacific Chaetodermomorpha genera except for Chaetoderma, a genus usually common on the shelf but missing from Bass Strait.

In Press: *Records of the Australian Museum.*

Supported by: Without support.

WHOI Contribution No. 6762.

ON AKWERKEPENTYE*: FAR-TRAVELLING CHILDREN OF BENTHIC INVERTEBRATES

Rudolf S. Scheltema

The spatial distributions of tropical benthic species may be enlarged by a capacity to disperse while, conversely, limited by ecological constraints, i.e., physical and biologic factors that control survival and reproduction. Unpredictable historic accidents at various time scales also play a role in the distribution of species and sometimes whole faunas, e.g., short-term physical catastrophies over hours or days; climatic and sea-level changes over periods of thousands of years or the opening and closing of seaways over geological epochs. Although there sometimes are alternative ways to disperse viz. adult migration, rafting, and human intervention, the principle means among most benthic invertebrates is by the transport of planktonic larvae - whose time in the plankton according to the species may vary from hours to many months. Generally, the capacity for dispersal among marine species exceeds that of terrestrial forms which often show a high localized endemism, especially on oceanic islands. It is proposed that initial colonization and subsequent gene flow between oceanic islands or other disjunct regions is largely accomplished by teleplanic or "long distance" larvae. Dispersal and the events leading

to settlement have implications for the management of benthic marine species.

Supported by: NSF Grant OCE86-14579.

WHOI Contribution No. 6902.

OCCURRENCE OF TELEPLANIC PELAGOSPHERA LARVAE OF SIPUNCULANS IN TROPICAL REGIONS OF THE PACIFIC AND INDIAN OCEANS

Rudolf S. Scheltema and Mary E. Rice

Teleplanic pelagosphera larvae of sipunculans have been found throughout the tropical epipelagic waters of the Pacific and Indian Oceans. Evidence for their widespread occurrence is based on plankton samples from 849 locations. Among 22 tropical forms distinguished and described, 9 were encountered in the eastern Pacific (east of 140°W), 13 in the central Pacific, 8 in the west Pacific, and 11 in the tropical Indian Ocean. Four of the 13 central Pacific larval forms also occur in the eastern portion of the east tropical Pacific. Approximately 69 percent of the 13 central Pacific larval forms also were shown to exist in the west Pacific and Indian Oceans. The number of central Pacific forms of pelagosphera are equal to about two-thirds of the 20 adult shoal water species reported there. Among the 22 larval forms described, four were found to range throughout the tropical Pacific and Indian Oceans (including the east Pacific); three additional pelagosphera were widely distributed throughout the Indo-Pacific as far east as the Polynesian islands. The evidence suggests that by their dispersal, larval sipunculans may play an important biogeographic and evolutionary role but until a correspondence is established between larval forms and adult species, only tentative conclusions are possible.

Supported by: NSF Grants OCE84-10262 and OCE86-14579.

WHOI Contribution No. 6888.

DIFFERENCE IN SPATIAL DISTRIBUTION OF VELIGER LARVAE BELONGING TO LITIOPA MELANOSTOMA AND ALABA INCERTA (PROSOBRANCHIA: LITOPIDAE) IN THE WARM TEMPERATE AND TROPICAL ATLANTIC OCEAN

Rudolf S. Scheltema, Isabelle P. Williams and Janice Tharpe

Litiopa melanostoma lives its adult life in pelagic Sargassum adrift on the open ocean; Alaba incerta is restricted to shallow-water Thalassia beds. Veligers of these closely related species are often confused but may be distinguished by characteristics of their larval shell (Robertson 1971, Veliger 14, pp. 5-6, pl. 2-4). Larvae of both species are found in the major oceanic currents in the western warm temperate and tropical Atlantic including the North and South Equatorial Current, the Antilles Current, the Gulf Stream and North Atlantic drift, but veligers of Litiopa also occur in the Central Atlantic "Sargasso Sea". The spatial distribution of Litiopa larvae is a consequence of both larval dispersal and rafting of the adults on Sargassum; that of Alaba is the result of larval transport only.

In Press: *Journal of Molluscan Studies.*

Supported by: NSF Grant OCE86-1457.

WHOI Contribution No. 6788.

FISHES

FURTHER ACOUSTIC TELEMETRY OBSERVATIONS OF SWORDFISH

Francis G. Carey

Five swordfish were followed in the Straits of Florida, New York Bight and Georges Bank areas. In two experiments where cranial temperature was monitored, one fish was able to maintain a cranial temperature elevation of more than 10°C, a second fish showed significant thermoregulation with cranial temperature decreasing only 5°C when water temperature dropped 10°C. Telemetry of muscle temperature indicated that swordfish may cool slowly but rewarm 10 times more rapidly on passing through the thermocline. This thermal hysteresis allows the fish to rewarm its body rapidly in the warm mixed layer and to retain this heat for many hours when foraging in cold water below the thermocline.

In general the fish were on the surface at night, but at depth during the day. In the Georges Bank area swordfish were in-shore on the bank during the day and moved offshore, on the surface at night. Use of an echosounder showed that one fish stayed with a well developed deep sound scattering layer as it moved from near the surface at night to 300 meters during the day.

Supported by: NSF Grants PCM78-03250, OCE80-18674 and OCE83-11512.

WHOI Contribution No. 6932.

MOVEMENTS OF BLUE SHARKS IN COURSE AND DEPTH

Francis G. Carey and Jill V. Scharold

Acoustic telemetry was used to follow blue sharks, Prionace glauca (Linnaeus), over the Continental Slope between Georges Bank and Cape Hatteras. The sharks make regular vertical excursions, passing between the surface and depths of several hundred meters every few hours. The vertical excursions were greatest in the daytime and were smaller in amplitude and near the thermocline at night. These oscillations were prominent in trials between August and March, but were not seen in trials with sharks between May and July. This activity is discussed in terms of a hunting tactic and behavioral thermo-regulation. Many of the sharks moved off to the east and southeast and were able to maintain a consistent course day and night over periods of several days. The ability to maintain a constant heading in the absence of celestial clues implies that the sharks may be using a magnetic compass.

Supported by: NSF Grants PCM76-81612, DCB83-08150, OCE80-18674 and OCE83-11512.

WHOI Contribution No. 6933.

SPAWNING BEHAVIOR OF CHAETODON MULTICINCTUS (CHAETODONTIDAE); PAIRS AND INTRUDERS

Phillip S. Lobel

Spawning by the banded butterflyfish, Chaetodon multicinctus (Chaetodontidae) was observed on coral reefs off Kona, Hawaii. These fish occurred in male-female pairs during normal daytime activities, a behavior which is typical for the family. Courtship is also a paired male-female activity. During spawning, however, other individuals (males?) may intrude on the spawning pair. Spawning typically takes place at least a meter or two above the bottom. The spawning position consists of the male below and behind the female with his snout against the female's ventral flank or anal fin area. Intruding individuals join in when the pair is in position and about to spawn. Intruders line-up against the male in the same position as he is against his female. Underwater photographs are included to illustrate these behaviors.

In Press: *Environmental Biology of Fishes*, 1989.

Supported by: NSF Grants OCE80-09554 and OCE81-17891; DOE Grant DE-A503-83CE89302; U.S. Army Contract DACA83-83-C0049; and Sea Grant NA86AA-D-SG090.

WHOI Contribution No. 6774.

BEHAVIOR OF THE FREE-SWIMMING BLUE SHARK PRIONACE GLAUCA: VERTICAL MOVEMENTS, SWIMMING SPEED AND TAILBEAT FREQUENCY

Jill Scharold and Francis G. Carey

Acoustic telemetry was used to record depth, swimming speed and tailbeat frequency from blue sharks in northwestern Atlantic slope waters near Hudson Canyon. Records obtained from five sharks show a consistent pattern of vertical migration between the surface and depths as great as 450 meters, with the deepest dives occurring during the daytime and shallower dives at night. Mean swimming speed was 44.5 ± 1.6 (X±S.E.) $cm.s^{-1}$ (0.179 ± 0.014 $lengths.s^{-1}$) for three sharks, with short bursts up to 180 $cm.s^{-1}$. Mean tailbeat frequency was 0.335 ± 0.021 beats.s-1. Measurement of swimming speed and rate of vertical movement during dives permits calculation of angles of ascent and descent. For 84 dives deeper than 50 m, the descent angle averaged 8.0 ± 0.7 degrees from the horizontal while the ascent angle was 6.4 ± 0.5 degrees. Tailbeat records indicate that blue sharks actively swam downward during most of the descent, with brief periods of gliding which appear to be associated with the most rapid descent rates. The observed diving behavior does not match that predicted by theory to be energetically optimum for migration, and may instead represent a strategy for encountering and capturing prey.

Supported by: NSF Grant OCE83-11512.

WHOI Contribution No. 6938.

TELEMETERED HEART RATE AS A MEASURE OF METABOLIC RATE IN THE LEMON SHARK, NEGAPRION BREVIROSTRIS

Jill Scharold and Samuel H. Gruber

Heart rate, metabolic rate, and activity were simultaneously recorded from juvenile lemon sharks for 24 hour periods to determine whether heart rate might be a suitable indicator of energy expenditure for field studies. Heart rate was monitored by acoustic telemetry using a frequency modulated ECG transmitter. Metabolic rate was measured as oxygen consumption rate in a flow through respirometer. In 7 sharks, mean resting

values for heart rate and oxygen consumption rate were 52.0 ± 0.4 (S.E.) beats.min^{-1} and 162.0 ± 2.0 (S.E.) mg O_2.kg^{-1}.hr^{-1}, respectively. Both parameters increased significantly ($p < 0.001$) during swimming, to means of 55.9 ± 0.2 beats.min^{-1} and 233.6 ± 2.3 mg O_2.kg^{-1}.hr^{-1}, at a mean swimming speed of 0.400 ± 0.003 body lengths.s^{-1}. The observed elevation in heart rate from rest to spontaneous exercise accounts for 19% of the increase in oxygen uptake, leaving the remainder to be accounted for by increases in stroke volume and/or arteriovenous oxygen difference. Although a significant linear regression of oxygen consumption rate on heart rate was obtained, the small contribution of heart rate to changes in the oxygen transport system may limit its value as a measure of metabolic rate.

Supported by: NSF Grants OCE83-11512 and OCE87-43949.

WHOI Contribution No. 6939.

METABOLIC RATE, HEART RATE, AND TAILBEAT FREQUENCY DURING SUSTAINED SWIMMING IN THE LEOPARD SHARK TRIAKIS SEMIFASCIATA

Jill Scharold, N. Chin Lai, William R. Lowell and Jeffrey B. Graham

Heart rate, metabolic rate, and tailbeat frequency were simultaneously recorded from seven leopard sharks (Triakis semi-fasciata) during steady swimming at controlled speeds to evaluate the usefulness of heart rate as a measure of field metabolic rate. Heart rate was monitored by acoustic telemetry using a frequency modulated ECG transmitter. Metabolic rate was measured as oxygen consumption in a swimming tunnel respirometer. For instrumented sharks, mean resting oxygen consumption rate and heart rate were 105.3 ± 35.6 (S.E.) mg O_2.kg^{-1}.hr^{-1} and 36.6 ± 1.8 (S.E.) beats.min^{-1}, respectively. While swimming at the maximum sustained speed (0.84 ± 0.03 lengths.s^{-1}) for 30-60 minutes, these rates were 229.3 ± 13.2 mg O_2.kg^{-1}.hr^{-1} and 46.9 ± 0.9 beats.min^{-1}. Although a significant linear regression was obtained between metabolic rate and heart rate, a low overall correlation coefficient may result from the existence of separate individual regressions and confounding changes in stroke volume and/or arteriovenous oxygen difference. Heart rate was approximately as closely correlated to oxygen consumption rate as was swimming speed. A significant linear relationship was obtained between tailbeat frequency and swimming speed to speeds of 0.75 lengths.s^{-1}.

Supported by: Grant from Coastal Research Center; and NSF Grant DCB84-16852.

WHOI Contribution No. 6940.

GEOCHEMISTRY

HYDROCARBONS IN SURFACE SEDIMENTS FROM A GUAYMAS BASIN HYDROTHERMAL VENT SITE

Dennis A. Bazylinski, John W. Farrington and Holger W. Jannasch

Petroleum-like materials found at the Guaymas Basin hydrothermal vent site (Gulf of California) are derived from pyrolysis of organic matter. Two characteristic surface sediment cores differing in temperature profiles and other parameters were collected by DSV ALVIN, sectioned and analyzed for hydrocarbons. The quantitative and qualitative composition of alkanes, steranes, diasteranes, and triterpans differed between these cores as well as within sections of the same core. These differences, apparent for scales of tens of centimeters, are related to interactive physical, chemical, and microbial processes as well as the influence of multiple sources for the petroleum.

Published in: *Organic Geochemistry*, 12, 547-558, 1988.

Supported by: NSF Grants OCE85-09859 and OCE86-00581; ONR Contract N00014-86-K-0481; and a Grant from Exxon Research and Engineering Company.

WHOI Contribution No. 6766.

GROUNDWATER-SURFACE WATER RELATIONSHIPS IN BOREAL FOREST WATERSHEDS: DISSOLVED ORGANIC CARBON AND INORGANIC NUTRIENT DYNAMICS

Timothy E. Ford and Robert J. Naiman

Dissolved organic carbon (DOC) and inorganic nutrients (NH_4-N, NO_3-N, soluble total-N, PO_4-P, soluble total P and Si) were measured in ground and surface waters in the Matamek River drainage network, Quebec, Canada. In general, concentrations of carbon and nitrogen were significantly higher in groundwater than in surface water (up to 340% for DOC and up to 700% for total N). No significant difference was detected for phosphorus while considerable variation occurred for silicon, with significantly higher groundwater

concentrations at 50% of the study sites. We hypothesize (1) that groundwater is a source of DOC and nitrogen in these systems and (2) that nutrients introduced through groundwater seepage are rapidly utilized via oxidative, biotic processes within the hyporheal zone or at the sediment/water interface.

In Press: *Canadian Journal of Fisheries and Aquatic Sciences.*

Supported by: Matamek Research Program; and NSF Grant BSR81-05677.

WHOI Contribution No. 6877.

THE ROLE OF ACANTHARIA IN THE CYCLING OF STRONTIUM AND TRACE METALS AT STATION "P" IN THE NORTH PACIFIC

Anthony F. Michaels and Kenneth H. Coale

In this paper we present new data on the standing stocks and vertical fluxes of acantharia and their primary skeletal material, strontium at Station "P". The highest Sr fluxes were at the base of the euphotic zone and only a small fraction of this particulate Sr flux was in identifiable acantharia cells. Most of the free-sinking acantharia (i.e., not associated with detritus) were the typical spiny forms, although as a class, they probably contributed less Sr than the few robust cysts in the same traps. At 300 m, the Sr flux was 20% of the Sr flux at 100 m. This decrease is due primarily to the dissolution of both the spiny acantharia and celestite in detrital material. At 300 and 500 m, most of the Sr flux can be attributed to the sinking of relatively few, large cysts. We also report new data on the trace element composition of acantharia collected in the Southern California Bight. Although the trace-metal:Sr ratios in these samples are lower than previously published (Brass 1980), the calculated metal fluxes at Station "P" due to sinking of acantharia can be a substantial fraction of estimates of total metal fluxes. The identification of unique carrier phases, like acantharia, is an important step in understanding the rates and mechanisms of trace metal fluxes in the upper ocean.

Supported by: NSF Grants OCE86-00459 and OCE86-00452; and ONR Contract NOOOO14-87-0683.

WHOI Contribution No. 6925.

MARINE MAMMALS

A SONAR TRANSPONDER TAG FOR UNDERWATER TRACKING OF SPERM WHALES (PHYSETER CATODON)

William Watkins

A transponder tag with depth telemetry and display on omni (simultaneous 360) sonar was tested in the southeast Caribbean off Dominica Island from 22 April to 8 May 1987 to assess its potential for underwater tracking of sperm whales (Physeter catodon). The transponder was interrogated on demand at 40 kHz and responded with 36-kHz signals compatible with the sonar. With little energy in pulse envelopes, these frequencies were apparently ignored by whales. One transponder tag and one radio tag were attached to different sperm whales with the system developed for the WHOI radio whale tags. The 1-km range of the transponder proved too short for successful sperm whale tracking, but modifications were indicated to increase the range. Sperm whales could be approached for tagging (transponder and radio tags) without chasing. As with other species previously tagged with this implanted attachment system, whales did not react to tag attachment, but they obviously reacted to tags that missed and splashed into the water. Four signals were received from the transponder tag on the whale. The farthest was 1.4 km, and all were apparently within a few m of the surface.

In Press: *Marine Mammal Science.*

Supported by: National Geographic Society NGS 3452-86; NSF Grant BNS85-08047; The Environmental Preservation Support Trust; and the Laurel Foundation.

WHOI Contribution No. 6735.

REFERENCE DATABASE MARINE MAMMAL LITERATURE

William A. Watkins, James E. Bird, Karen E. Moore and Peter Tyack

A comprehensive Reference Database has been designed for the marine mammal literature. The system used INMAGIC programming (Cambridge, MA) to file, store, search, retrieve, and format the data records. The database was organized to be complementary to features developed by William E. Schevill for his library of older cetacean literature, and it uses direct association of species with some 300 indexed subjects, observation dates, locations, etc. Every component and detail of the references and annotations are available for rapid search by a wide variety of simple and complex strategies. In addition, separately indexed fields

provide immediate retrieval of author, editor, year, journal, type of publication, language, genus/species (searchable by order/suborder and family as well), major subject, subject, picture, observation date, geographic location (including area name and latitude/longitude), as well as the location and library call numbers of the document referred to. Codes have been adapted for ease in identifying and searching species, subjects, journals, languages, and geographic areas. These codes may be used separately or in connection with the associated terms and texts. It is anticipated that the Reference Database will be a continuing resource for marine mammal research.

Published in: *Woods Hole Oceanographic Institution Technical Report*, WHOI-88-2, 1988.

Supported by: Marine Mammal Commission MM4465702-4; and NMFS Grant 40EANF702277.

MARINE POLLUTION

INDUCED CYTOCHROME P-450 IN FUNDULUS HETEROCLITUS ASSOCIATED WITH ENVIRONMENTAL CONTAMINATION BY POLYCHLORINATED BIPHENYLS AND POLYNUCLEAR AROMATIC HYDROCARBONS

Adria A. Elskus and John J. Stegeman

Fundulus heteroclitus were collected from two sites in Rhode Island during the non-spawning season and analyzed for hepatic monooxygenase activities and for whole body concentrations of polychlorinated biphenyls (PCB) and polynuclear aromatic hydrocarbons (PAH). Microsomal protein, total spectral cytochrome P-450 and cytochrome b_5 content did not differ between Seekonk River and Succotash Salt Marsh fish. Ethoxyresorufin O-deethylase (EROD) activity was significantly higher (3-fold) in Fundulus from the Seekonk River than in fish from Succotash Salt Marsh. Similarly, levels of the immunodetectable homolog of P-450E in Fundulus, a representative of the major PAH-inducible P-450 form (P-450IA1) in teleosts, were higher in fish from the Seekonk River. In contrast, rates of aldrin epoxidase (AE) activity were the same in fish from the two sites. Concentrations of PCB were 1000-fold, and PAH 60-fold, greater in Seekonk River sediment than in Succotash Salt Marsh sediment. The bioavailability of these contaminants is not known, but the relative degree of contamination in the sediments is reflected in the fish tissues. Fish from both sites had very low concentrations of PAH in their tissues representing as little as 0.1% of the concentration in the sediment, with tissue concentrations in Seekonk River fish exceeding those of Succotash fish by 4-fold. Polychlorinated biphenyl concentrations in Seekonk fish (1860 ± 176 ng/g dry weight) were 3-fold higher than in Succotash Marsh fish (636 ± 217 ng/g). These concentrations were nearly the same (Seekonk fish) or 300-fold greater (Succotash Marsh fish) than PCB concentrations in the surrounding sediment. The result is consistent with a rapid metabolism of PAH while PCBs appear to be slowly eliminated by these fish. Tissue PCB concentrations in Seekonk River fish were similiar to those known to elicit strong P-450 induction in Fundulus. Thus, levels of hepatic P-450E and EROD, but not AE activity, reflect relative tissue concentrations of PCB and PAH in Fundulus from two sites. Liver hypertrophy was also observed in Seekonk River fish, indicating that altered liver function may have occurred in these animals.

In Press: *Marine Environmental Research.*

Supported by: EPA Cooperative Agreement CR-813155-01-0; and USPHS Grant ES-04220.

WHOI Contribution No. 6874.

EFFECTS OF ORTHO-AND NON-ORTHO SUBSTITUTED POLYCHLORINATED BIPHENYL CONGENERS ON THE HEPATIC MONOOXYGENASE SYSTEM IN SCUP (STENOTOMUS CHRYSOPS)

Jay W. Gooch, Adria A. Elskus, Pamela J. Kloepper-Sams, Mark E. Hahn and John J. Stegeman

Polychlorinated biphenyl congeners that are abundant in environmental samples, and known to induce hepatic monooxygenase isozymes in the P-450IA gene subfamily in mammals, were examined for their ability to induce hepatic monooxygenase activity in scup, a marine teleost. Scup were dosed i.p. with 3,3',4,4'-tetrachlorobiphenyl (congener 77), 2,3,3',4,4'-pentachlorobiphenyl (congener 105), 2,3',4,4',5-pentachlorobiphenyl (congener 118), 2,2',3,4, 4',5'-hexachlorobiphenyl (congener 138), 2,2',3,3',4,4'-hexachlorobiphenyl (congener 128) or β-naphthoflavone and examined for increases in ethoxyresorufin-O-deethylase (EROD) activity, immunodetectable cytochrome P-450E (the EROD catalyst in scup) and in vitro translatable mRNA for cytochrome P-450E. Monooxygenase parameters were significantly induced only by 3,3', 4,4'-tetrachlorobiphenyl (TCB). However, while translatable mRNA for P-450E was induced at all doses (1, 5 and 10 mg/kg), EROD activity and P-450E were decreased at the 5 and 10 mg/kg

doses, relative to the response at 1 mg/kg. A strong relationship between residual TCB concentration in the liver and the decreased EROD activity was evident at the higher doses of TCB. Aminopyrine N-demethylase, a monooxygenase activity not catalyzed by P-450E, was unaffected by TCB treatment, indicating a specificity in the TCB effect. Analysis in vitro revealed that TCB was a potent competitive inhibitor of EROD activity, with half-maximal inhibition at 0.3 μM, near the K_m for ethoxyresorufin, suggesting one mechanism for the in vivo effect of TCB. These results demonstrate that PCB congeners with ortho chlorine substitution and which are effective inducers of AHH and EROD activity in mammals, are ineffective, at the doses tested, as inducers in the teleost scup.

In Press: *Toxicology and Applied Pharmacology.*

Supported by: U.S. PHS Grant ES-04220; and EPA Grants CR-813155-01-0 and CX-813567-01-1.

WHOI Contribution No. 6918.

MICROBIOLOGY

ANAEROBIC MAGNETITE PRODUCTION BY A MARINE, MAGNETOTACTIC BACTERIUM

Dennis A. Bazylinski, Richard B. Frankel and Holger W. Jannasch

Report on the first isolation and axenic culture of a marine, magnetotactic bacterium, designated MV-1, that can synthesize intracellular, single-domain magnetite crystals under strictly anaerobic conditions. It is concluded that magnetitotactic bacteria do not necessarily require molecular oxygen for magnetite synthesis and suggest that they, as well as dissimilatory iron-reducing bacteria, can contribute to the natural remanent magnetism of long-term anaerobic sediments.

Published in: *Nature*, 334, 518-519, 1988.

Supported by: NSF Grants OCE86-08241 and OCE87-00581.

WHOI Contribution No. 6741.

PREFACE TO THE CYANOBACTERIA

R. W. Castenholz and J. B. Waterbury

General properties of the cyanobacteria are described including: their phylogenetic positioning taxonomic systems (both botanical and bacterial), characteristics and criteria needed to describe new species, extent of cyanobacterial taxa currently in culture, culture collections containing cyanobacteria, the general characteristics of cyanobacteria (morphology, cytology, developmental patterns, modes of reproduction, cell differentiation, physiology and biochemistry) and their ecology.

In Press: *Bergey's Manual of Systematic Bacteriology*, J. G. Holt and J. T. Staley, eds.

Supported by: NSF Grants BSR86-07386 and OCE84-16960.

WHOI Contribution No. 6795.

A THERMOPHILIC BACILLUS SP. WHICH SHOWS THE DENITRIFICATION PHENOTYPE OF PSEUDOMONAS AERUGINOSA

Noyan Gokce, Thomas C. Hollocher, Dennis A. Bazylinski and Holger W. Jannasch

A thermophilic Bacillus sp. of marine origin was observed to grow anaerobically with nitrite, nitrous oxide (N_2O) in the presence of nitrite, and N_2O alone for a few hours after exhaustion of nitrite. This represents the second example of a denitrification phenotype originally observed to occur with Pseudomonas aeruginosa.

Supported by: NSF Grant OCE87-00581.

WHOI Contribution No. 6823.

LIFE AT DEEP-SEA HYDROTHERMAL VENTS

Holger W. Jannasch

An overview with emphasis on the geochemical-biochemical transfer of energy and the chemolithotrophic sustenance of various parts of the vent communities.

In Press: *Proceedings of the Royal Norwegian Society of Science, Trondheim.*

Supported by: NSF Grant OCE87-00581; and ONR Contract N00014-88-0386.

WHOI Contribution No. 6893.

BIOLOGY OF GEOTHERMAL ENVIRONMENTS

Holger W. Jannasch, Douglas E. Caldwell and Vittorio Buonocore

An overview over geochemical, physiological and molecular aspects of procaryotes and

eukaryotes in marine terrestrial hot spring environments.

Published in: *Current Perspectives in Environmental Biogeochemistry.* G. Giovannozzi-Sermanni and P. Nannipieri, eds., C.N.R. - I.R.R.A., Rome, 1988.

Supported by: NSF Grant OCE87-00581.

WHOI Contribution No. 6976.

COMPARISON OF THERMOPHILIC METHANOGENS FROM SUBMARINE HYDROTHERMAL VENTS

William Jack Jones, Carol E. Stugard and Holger W. Jannasch

An extremely thermophilic methanogen was isolated from hydrothermal vent sediment (80-120°C) collected from the Guaymas Basin, Gulf of California, at a depth of approximately 2000 m. The isolate was a characteristic member of the genus Methanococcus based on its coccoid morphology, ability to produce methane from CO_2 and H_2, and DNA base composition (31.4 mol % G+C); it appears to be similar to previously described vent methanogens. The methanogen was an osmotically fragile motile coccus which grew and produced CH_4 from formate and a mixture of H_2 plus CO_2. The temperature range for growth was 48-94°C (optimum near 85°C); the pH optimum was 6.0. The isolate grew autotrophically but was stimulated by selenium and growth nutrients supplied by yeast extract and trypticase. Extracted polar lipids consisted primarily of diphytanyl glycerol diether (62%), macrocyclic glycerol diether (15.3%), and dibiphytanyl glycerol tetraether (11.8%). Neutral lipids were dominated by a series of C_{30} isoprenoids; in addition, a novel series of C_{35} isoprenoids were detected. The isolate appears to be a close relative of the previously described Methanococcus jannaschii, isolated from the East Pacific Rise hydrothermal vent system.

From the frequency of its isolation, it appears that this extremely thermophilic organism is the predominant representative of the methanogenic archaebacteria occurring at deep-sea hydrothermal vents.

Supported by: NSF Grant OCE87-00581.

WHOI Contribution No. 6824.

GROUP II - THE PLEUROCAPSALES

John B. Waterbury

The systematics of the order Pleurocapsales is presented based on the properties of pure cultures. This system of classification is compared with traditional botanical taxonomic treatments. The order is subdivided into six genera whose descriptions are based on the Geitlerium system but modified to incorporate new properties revealed by the study of their developmental cycles under controlled culture conditions.

In Press: *Bergey's Manual of Systematic Bacteriology*, J. G. Holt and J. T. Staley, eds..

Supported by: NSF Grant BSR86-07386.

WHOI Contribution No. 6792.

THE PLANKTONIC CYANOBACTERIA

John B. Waterbury and Edward J. Carpenter

The biology and ecology of the two principal marine planktonic cyanobacteria: Synechococcus sp. and Trichodesmium spp. are reviewed. The properties of the organisms, their distributions and their contribution to the oceanic carbon and nitrogen cycles are discussed.

Supported by: NSF Grant OCE84-16960.

WHOI Contribution No. 6814.

GROUP I - THE CHROOCOCCALES

John B. Waterbury and Rosmarie Rippka

The systematics of the order Chroococcales is presented based on the properties of pure cultures. This system is compared with traditional botanical taxonomic treatments. The order is subdivided into three clearly defined genera and four "Groups" that are artificial assemblages that in the future will be subdivided into genera when phenotypic and genetic characterization has been completed.

In Press: *Bergey's Manual of Systematic Bacteriology*, J. G. Holt and J. T. Staley, eds.

Supported by: NSF Grants BSR86-07386 and OCE84-19690.

WHOI Contribution No. 6794.

RIBULOSE BISPHOSPHATE CARBOXYLASE OF THE PROCARYOTIC SYMBIONT OF A HYDROTHERMAL VENT TUBE WORM: KINETICS, ACTIVITY AND GENE HYBRIDIZATION

C. A. Williams, Douglas C. Nelson, B. A. Farah, Holger W. Jannasch and J. M. Shively

The giant tube worm, Riftia pachyptila, which is abundant at deep-sea hydrothermal vents,

contains an extremely high density of bacterial symbionts in a specialized 'trophosome' tissue. Although the symbiont has not been cultured, enzymatic studies by others indicate that the symbiont is capable of hydrogen-sulfide-or sulfur-based lithoautotrophy and fixes CO_2 via the Calvin-Benson cycle. Here we report additional findings for a specimen from the Guaymas Basin vent site (Gulf of California, 2000 m). Under assay conditions where activity was proportional to cell-free extract concentration, ribulose bisphosphate carboxylase/oxygenase (RuBisCO) activity was 6.3 nmol CO_2/mg protein per min (30°C). This is within the range observed for non-CO_2 limited cultures of sulfur bacteria. The activity vs. temperature profile suggests that the symbiont is a mesophile and not a thermophile. A substrate saturation curve shows an apparent K_m (with respect to ribulose 1,5-bisphosphate) of 65 μM which is considerably lower than the single previous report for a sulfur bacterial symbiont. Strong hybridization was detected between a gene probe derived from the RuBisCO large subunit gene of Anacystis nidulans and Riftia trophosome DNA. A Rhodospirillum rubrum-derived probe also showed hybridization with the same restriction fragments of symbiont DNA.

Published in: *FEMS Microbiological Letters 50*, 107-112, 1988.

Supported by: NSF Grant OCE87-00581.

WHOI Contribution No. 6670.

PHYSIOLOGY AND BIOCHEMISTRY

ACTIVE VERTICAL TRANSPORT OF PARTICULATE FATTY ACIDS IN AN OLIGOTROPHIC GULF STREAM WARM-CORE RING

Maureen H. Conte, James K. B. Bishop and Peter H. Wiebe

Rapidly sinking particles are believed to transport most labile organic compounds through the oceanic water column. Here we report that active transport by animals, not passive settling, dominated the vertical flux of labile fatty acids and appeared to account for 25% of the total carbon flux out of the euphotic zone. The active vertical transport pathway: bioassimilation of dietary compounds by animals, net downward transport of biomass and loss by predation into the particle pool, may be important for other bioaccumulated compounds. Measurements of the sinking particle flux of such compounds alone may severely underestimate vertical transport rates.

Supported by: ONR Contracts N000014-80-C-0098 and N00014-87-K-0204; and NSF Grants OCE-8017468 and OCE-8017248.

WHOI Contribution No. 6863.

FURTHER CONSIDERATION OF PHENOBARBITAL EFFECTS ON CYTOCHROME P-450 ACTIVITY IN THE KILLIFISH, FUNDULUS HETEROCLITUS

Adria A. Elskus and John J. Stegeman

1. Ethoxyresorufin O-deethylase (EROD) activity, aldrin epoxidase (AE) activity, cytochrome P-450 content, and levels of cytochrome P-450E (the major BNF-inducible P-450 form and primary EROD catalyst in scup) or its homologues were measured in hepatic microsomes isolated from Fundulus heteroclitus, scup (Stenotomus chrysops) and brook trout (Salvelinus fontinalis) treated with β-naphthoflavone (BNF) or phenobarbital (PB).

2. In all three teleost species, BNF treatment caused expected increases in P-450 content, EROD activity and P-450E level; but either no change or a slight decrease in AE turnover rate (nmol/min/nmol P-450).

3. Polyclonal antibodies to P-450E did not inhibit AE activity in microsomes from BNF-treated scup, confirming that this major BNF-inducible P-450 form does not catalyze AE activity in fish.

4. In contrast, PB treatment did not affect hepatic AE activity, P-450 content or levels of "P-450E" in F. heteroclitus, but did variably affect EROD activity which was suppressed in one experiment and elevated in another.

5. The results indicate that (i) contrary to previous reports, neither PB nor MC-type inducers increase AE activity in F. heteroclitus, (ii) MC-type inducers do not affect AE activity in the other teleost species examined, and (iii) AE activity is not a reliable indicator of P-450 induction by environmental chemicals.

6. We emphasize the need to establish the mechanism of PB action, and the nature of any fish P-450 forms analogous to PB-inducible forms in mammals, in order to conclusively evaluate PB-responses in fish.

In Press: *Comparative Biochemistry and Physiology.*

Supported by: Public Health Service Grant ES-04220; and EPA Grant CR-813155-01-2.

WHOI Contribution No. 6733.

XENOBIOTIC AND STEROID METABOLISM IN ADULT AND FOETAL PIKED (MINKE WHALES), BALAENOPTERA ACUTOROSTRATA

Anders Goksøyr, Tommy Andersson, Lars Forlin, Jørgen Stenersen, Elisabeth A. Snowberger, Bruce R. Woodin and John J. Stegeman

Cytochrome P-450 monooxygenase, glutathione S-transferase and UDP-glucuronyl transferase activities with both xenobiotic and steroid substrates, and immunochemical cross-reactivity with antibodies of fish cytochromes P-450, were examined in piked (minke) whale. Foetal liver samples showed generally lower activities than adults, with a few noteworthy exceptions in the conjugating enzymes. Adult kidney samples had substantial amounts of P-450 (0.1-0.1 nmol/mg microsomal protein), but low monooxygenase activities even compared with foetal livers (which had c. 0.06 nmol P-450/mg). In kidney, androstendione-5a-reductase and certain conjugating activities dominated. Most activities were high in adult liver (which had 0.25-0.5 nmol P-450/mg). Liver samples cross-reacted strongly with antibodies towards scup P-450E (MAb 1-12-3) or cod P-450c (IgC), two BNF-inducible P-450 forms from fish. Only female adult specimens were obtained for this study. No significant differences were observed between immature and mature females. The results give new information on the xenobiotic and steroid biotransformation in this little studied species.

Published in: *Marine Environmental Research*, 24, 9-13, 1988.

Supported by: NIH Grant 1ROZ ES-04220.

WHOI Contribution No. 6740.

THE TEMPORAL RELATIONSHIPS BETWEEN CYTOCHROME P-450E PROTEIN CONTENT, CATALYTIC ACTIVITY AND MRNA IN THE TELEOST FUNDULUS HETEROCLITUS FOLLOWING TREATMENT WITH β-NAPHTHOFLAVONE

Pamela J. Kloepper-Sams and John J. Stegeman

P-450 induction occurs in some marine organisms following chemical exposure. The mode of 3-methylcholanthrene (MC)-type induction was evaluated by examining hepatic isozyme P-450E content, catalytic activity, and mRNA levels in the marine teleost Fundulus heteroclitus after exposure to a single dose of β-naphthoflavone (BNF). P-450E is the major teleost P-450 induced by MC-type compounds and is the catalyst for aryl hydrocarbon hydroxylase (AHH) and ethoxyresorufin O-deethylase (EROD) activities. In a 20 day experiment, EROD activity was elevated in BNF-treated animals from Day 4 through Day 20. Increases in immunodetectable P-450E showed the same trend as EROD activity, with consistently low control values and at least a 19-fold increase in the BNF-treated fish. Precipitation of liver RNA in vitro translation products with anti-P-450E antibody gave no detectable signal from control fish, while the BNF-treated animals showed incorporation of [^{3}H]-leucine in a single 56,000 M_r band. In a shorter term experiment, EROD activity and P-450E levels were again coordinately increased in response to BNF treatment, and immunoprecipitation of translation products from these fish showed a clear trend of increased P-450E mRNA levels for all time points 6 hours or more post-treatment. Hybridization of RNA from BNF-treated Fundulus with a trout P-450IA1 cDNA also showed increases in a single band with time. The increases in P-450E mRNA preceded increases in P-450E protein and enzyme activity by about 25 h. However, P-450E mRNA declined rapidly, reaching control levels by 5 days, while protein levels remained elevated for at least 13 days. The results support a hypothesis that transcriptional enhancement is involved in induction of MC-inducible P-450s in fish, but indicate that P-450E induction is also under forms of regulatory control.

Published in: *Archives of Biochemistry and Biophysics*, 268, 525-535, 1989.

Supported by: MIT/WHOI Joint Program; and NIH Grant 1 RO1 ES-04220.

WHOI Contribution No. 6744.

MUTATIONS IN C-KI-RAS ONCOGENES: PREVALENCE IN LIVER DISEASE AND NEOPLASIA IN WINTER FLOUNDER FROM BOSTON HARBOR

Gerald McMahon, L. Julie Huber, Michael J. Moore, John J. Stegeman and Gerald N. Wogan

A natural population of winter flounder exhibiting liver lesions was examined for the presence of transforming genes (oncogenes) by transfection of liver DNA into NIH3T3 mouse fibroblasts, followed by selection for tumorigenicity in athymic (nude) mice. Seven of 13 DNA samples from diseased livers induced tumors in nude mice; a flounder c-Ki-ras oncogene was detected in all mouse tumors. Direct DNA sequencing and allele-specific oligonucleotide hybridization of

polymerase chain reaction amplified-DNA showed mutations in the 12th codon of flounder c-Ki-ras sequences in the DNA from all nude mouse tumors, and from liver samples of all 13 fish exhibiting lesions. The mutations appeared as G-C to A-T or G-C to T-A base changes resulting in AGT, GTT, and TGT mutant codons. Liver DNA from 5 histologically normal flounder livers did not induce tumors in nude mice, and contained only wild-type DNA sequences in the 12th codon. The high incidence of liver lesions, including neoplasia, occurring in winter flounder from Boston Harbor could be associated with 12th codon mutations in proto-oncogenes, and these could in turn result from environmental chemical contamination.

Supported by: USPHS Grant CA44306.

WHOI Contribution No. 6882.

CYTOCHROME P-450E INDUCTION AND LOCALIZATION IN GILL PILLAR (ENDOTHELIAL) CELLS OF SCUP AND RAINBOW TROUT

Michael R. Miller, David E. Hinton and John J. Stegeman

The i.p. administration of β-naphthoflavone (BNF) to scup Stenotomus chrysops increased the specific content of total cytochrome P-450 (P-450) in gill microsomes nearly ten-fold. This increase in P-450 content was accompanied by an increase in microsomal ethoxyresorufin O-deethylase activity from undetectable levels to 0.16 nmol/min/mg, and a shift in P-450 Fe^{2+}-CO absorption maximum from 450 to 447 nm. Western blot analysis of microsomes from control and BNF-treated scup gills, with monoclonal antibody (MAb) 1-12-3 directed against scup P-450E (the BNF-inducible EROD catalyst), confirmed that P-450E was induced from essentially undetectable levels in control animals to levels comprising at least 60% of the spectrally measured P-450 in BNF-treated animals. Immunohistochemical analysis of scup gills with MAb 1-12-3 and fluorescently-labeled second antibody demonstrated that the P-450E was induced primarily in the endothelium (pillar cells) of the secondary lamellae. Immunohistochemical analysis of gills from rainbow trout (Salmo gairdneri) showed that BNF treatment also induced a P-450E counterpart in trout gills and that, as in scup, this P-450 was localized principally in the endothelium of gill lamellae. P-450E catalyzes formation of promutagenic benzo-ring dihydrodiols of benzo[a]pyrene, which suggests possible toxicological consequences for the induction of this isozyme in gill.

In Press: *Aquatic Toxicology.*

Supported by: USPHS Grant CA-45131 to MRM and DEH; The Bowden Federal Fish Hatchery; and USPHS Grants ES-04220 and CA-44306 to JJS.

WHOI Contribution No. 6782.

CYTOCHROME P-450 INDUCTION AND LOCALIZATION IN ENDOTHELIUM OF VERTEBRATE HEART

John J. Stegeman, Michael R. Miller and David E. Hinton

A strong (8-10-fold) induction of microsomal cytochrome P-450 by β-naphthoflavone was observed in teleost heart, with specific content reaching levels (0.5 nmol/mg) similar to those in liver. Catalytic activities and immunoblot analysis showed that the hydrocarbon- and chlorobiphenyl-inducible P-450E (P-450IA1) is the dominant and possibly sole P-450 form in heart microsomes of experimentally induced animals. P-450E is also present in heart microsomes of untreated animals from contaminated environments. Induced P-450E is localized primarily in the endothelial cells in the heart, where it accounts for as much as 25% of the microsomal protein. Strongly induced P-450 in endothelium could play a critical role in drug and chemical-biological interactions affecting the heart and the vasculature of other organs.

Supported by: USPHS Grants ES-04220 and CA-44306.

WHOI Contribution No. 6883.

PHYTOPLANKTON

TOXIC ALGAL BLOOMS AND RED TIDES: A GLOBAL PERSPECTIVE

Donald M. Anderson

The literature on toxic algal blooms and red tides documents a global increase in the frequency, magnitude, and geographic extent of these events over the last two decades. Some of this increase is undoubtedly a result of the increased awareness and analytical capabilities of the scientific community, but a strong correlation between the number of red tides and the degree of coastal pollution or utilization of coastal waters for aquaculture argue that there are other contributing factors. It also appears likely that toxic algal species have spread within regions over spatial scales of hundreds of kilometers, moving with major water currents and storms. Long distance transport of species across oceans may

have occurred as well, but the evidence is not conclusive and the hypothesis controversial.

Published in: *Red Tides: Biology, Environmental Science and Toxicology.* T. Okaiichi, D. M. Anderson and T. Nemoto, eds., 1988.

Supported by: NSF Grant OCE86-14210; and NOAA, Office of Sea Grant, Grant NA86AA-D-SG090, R/B-76.

WHOI Contribution No. 6669.

PARALYTIC SHELLFISH POISONING IN NORTHWEST SPAIN: THE TOXICITY OF GYMNODINIUM CATENATUM

Donald M. Anderson, John J. Sullivan and Beatriz Reguera

The highly productive mussel fishery in the Rias Bajas region of northwest Spain has experienced several outbreaks of paralytic shellfish poisoning (PSP) beginning in 1976. In this study, similarities in the HPLC analyses of extracts from toxic shellfish, plankton tows, and cultured dinoflagellates from the Rias Vigo and Pontevedra clearly indicate that Gymnodinium catenatum Graham is the organism responsible for the recent PSP episodes. The toxin profile of the dinoflagellate contains an unusually high proportion of the low potency sulfocarbamoyl toxins (ca. 90-95 mole %), although a major portion of the overall toxicity is due to the more potent saxitoxin that is present at 5-10% of the total. Toxin profiles of shellfish showed approximately the same composition as that of the dinoflagellate, although the shellfish contained several carbamate toxins (GTX I, GTX II, GTX IV, and NEO) that were not detected in G. catenatum culture extracts. The shellfish also contained decarbamoyl toxins (dc-GTX II and dc-GTX-III) at approximately 2% of the total profile. The small relative abundance of these decarbamoyl toxins suggests that they may be the result of chemical rather than enzymatic conversion within the shellfish.

In Press: *Toxicon.*

Supported by: U.S./Spain Joint Committee for Scientific and Technological Cooperation; NSF Grant OCE86-14210; and NOAA, Sea Grant No. N86-AA-D-SG090, WHOI No. R/B-76.

WHOI Contribution No. 6864.

VERTICAL DISTRIBUTION OF AMMONIUM IN STRATIFIED OLIGOTROPHIC WATERS

Mark Brzezinski

A method for measuring nanomolar concentrations of ammonium in seawater was used for the first time under field conditions in the Sargasso Sea and Gulf Stream. Ammonium concentrations ranged from below the limit of detection (3.5 nM) to 164 nM NH_4^+. Subsurface ammonium maximum (16-59 nM NH_4^+) occurred within the seasonal thermocline and near the deep chlorophyll a maximum in association with the primary nitrite maximum. The latter feature was observed in both the Sargasso Sea and Gulf Stream suggesting that it may be common in stratified oligotrophic waters. Vertically integrated nitrite concentrations in the upper 140 m generally exceeded those for ammonium suggesting more efficient use of reduced nitrogen by the microplankton.

Published in: *Limnology and Oceanography*, 33(5), 1176-1182, 1988.

Supported by: WHOI Postdoctoral Fellowship Award.

WHOI Contribution No. 6829.

CHAIN-FORMING DINOFLAGELLATES: AN ADAPTATION TO RED TIDES

Santiago Fraga, Scott M. Gallager and Donald M. Anderson

Swimming speeds of two chain-forming dinoflagellates, the toxic Gymnodinium catenatum and the non-toxic Alexandrium affine, were measured as a function of chain lengths. Long chains swam faster than short chains. The increase in speed from a single cell to a chain of four cells for both species was about a factor of 1.5-1.6. Populations of both dinoflagellate species were coincident with red tides in areas of coastal upwelling relaxation and downwelling in the Ria de Vigo, northwest Spain. The higher swimming speeds of long chains may allow more cells to remain in the photic zone during downwellings or convergences. This may be a mechanism for local concentration of cells leading to a red tide.

Published in: *Red Tides, Biological Environmental Science and Toxicology,* T. Okaichi, D. M. Anderson and T. Nemoto, eds. Elsevier, New York, pp. 281-284, 1989.

Supported by: Sea Grant NA86-AA-D-SG090, R/B-76; USA-Spain Joint Committee for the Scientific and Technological Cooperation, Grant No. CCA-8411089; and NSF Grant OCE87-11386.

WHOI Contribution No. 6810.

FRONTS, UPWELLING AND COASTAL CIRCULATION: SPATIAL HETEROGENEITY OF CERATIUM IN THE GULF OF MAINE

Peter J. S. Franks, Donald M. Anderson and Bruce A. Keafer

The accumulation of dinoflagellates at tidal fronts has been a popular explanation for the distribution of blooms in coastal waters throughout the world. We sought to test this hypothesis with frequent sampling from March to September, 1987, along a 30 km transect from Portsmouth, New Hampshire into the southwestern Gulf of Maine, a region subject to recurrent outbreaks of PSP. No evidence of a tidal front was found in the CTD profiles; however, a dense bloom of Ceratium longipes was found offshore in June, closely linked to a wind-driven coastal upwelling. Distributions of Alexandrium tamarense (= Protogonyaulax tamarensis) suggest that it may respond to the same physical forcings as C. longipes even though it remained a small fraction of the total phytoplankton biomass.

Published in: *"Red Tides"*, T. Okaichi, D. M. Anderson and T. Nemoto, eds., Elsevier, New York, pp. 153-156, 1989.

Supported by: ONR Contract N00014-87-K-0007; and NOAA, Office of Sea Grant, Grant NA86AA-D-SG090, R/B-76.

WHOI Contribution No. 6772.

ULTRASTRUCTURAL ASPECTS OF SEXUAL REPRODUCTION IN THE RED TIDE DINOFLAGELLATE GONYAULAX TAMARENSIS.

Lawrence Fritz, Donald M. Anderson and Richard E. Triemer

The marine dinoflagellate Gonyaulax tamarensis Lebour is best known for its propensity to form blooms as red tides in coastal waters worldwide. This paper examines the sexual cycle of this organism using light and electron microscopy. Sexual reproduction begins with contact between thecate gametes which subsequently shed their thecae to fuse along their pellicular layers. Nuclear fusion occurs well after cytoplasmic fusion and is characterized by several distinctive features: a highly vesiculate nucleoplasm without microtubules; nucleoli and V-shaped chromosomes abut the nuclear envelope distal to the region of nuclear contact and each chromosome possesses a longitudinal line, the central chromosomal axis. Fusion results in a planozygote with numerous cytoplasmic storage products and a slightly thickened layer beneath the pellicle. Subsequent loss of thecal plates and additional accumulation of wall material results in a non-motile hypnozygote. A newly-formed hypnozygote possesses numerous minute papillae along its outer surface, formed by the upfolding of the accumulating wall layer. Maturation of the hypnozygote wall results in a smooth three-layered wall. Hypnozygote germination produces a large quadriflagellate planomeiocyte with a single nucleus and thecal plates identical to vegetative cells. Two subsequent divisions, presumably meiotic, result in four cells morphologically identical to vegetative cells.

Supported by: Bureau of Biological Research, Rutgers University; the Charles and Johanna Busch Memorial Fellowship, Rutgers; NOAA National Sea Grant Program, NOAA Grant NA86-AA-D-SG090; and NSF Grants OCE84-00292 and OCE86-14210.

WHOI Contribution No. 6879.

THE CYST AND THECA OF GONYAULAX VERIOR SOURNIA AND THEIR IMPLICATION FOR THE SYSTEMATICS OF THE GENUS GONYAULAX

Kazumi Matsuoka, Yasuwo Fukuyo and Donald M. Anderson

On the basis of unialgal cultures established from living cysts recovered from surface sediments, thecate and encysted forms of the dinoflagellate Gonyaulax verior Sournia are described from Japan and the United States. The cyst is ovoidal, lacks ornamentation, and is sometimes surrounded by mucilaginous material. The thecal plate formula of this species is identical to that of the Spinifera group of the genus Gonyaulax, but the G. verior cyst is distinctly different in shape, lacks ornamentation, and has a different archeopyle. These observations emphasize the need for a careful re-examination of the systematics of the genus Gonyaulax, with due consideration of both the cyst and motile stage morphology.

In Press: *Japanese Journal of Phycology.*

Supported by: NSF Grant OCE84-00292.

WHOI Contribution No. 6695.

DISCRIMINATION OF EUKARYOTIC PHYTOPLANKTON CELL TYPES FROM LIGHT SCATTER AND AUTOFLUORESCENCE PROPERTIES MEASURED BY FLOW CYTOMETRY

Robert J. Olson, Eric R. Zettler and K. O. Anderson

Flow cytometric methods for recognizing several groups of eukaryotic marine phytoplankton were tested using 26 laboratory cultures. Measurements of Coulter volume, light scatter (magnitude and polarizaton properties of forward scattered light, and right angle scattered light), and autofluorescence (emission and excitation properties) can be used as diagnostic tools to distinguish crytophytes, coccolithophores, pennate diatoms, and chlorophytes from other cell types. Forward light scatter and Coulter volume were closely related except for the pennate diatoms) over the range from about 0.01 to 30 pL (equivalent spherical diameter about 3 to 40 um), according to a logarithmic function.

Supported by: NSF Grants OCE84-16964 and OCE86-14332; and ONR Contracts NOOO14-83-K-0661, NOOO14-84-C-0278 and NOOO14-87-K-0007.

WHOI Contribution No. 6924.

TESTING AND APPLICATION OF BIOMONITORING METHODOLOGIES FOR ASSESSING ENVIRONMENTAL EFFECTS OF NOXIOUS ALGAL BLOOMS

Gregory A. Tracey, Richard L. Steele, Jenifer Gatzke, Donald K. Phelps, Robert Nuzzi, Robert M. Waters and Donald M. Anderson

The goal of the U.S. Environmental Protection Agency's Biomonitoring research program is to produce test methods for assessing environmental effects of anthropogenic activities in marine waters. Two biomonitoring methods using the blue mussel, Mytilus edulis, are under evaluation for their use in areas threatened by noxious algal blooms. In the nutrition bioassay method, feeding (clearance) rates of mussels were measured in response to diets containing natural particulates from Peconic Bay and Great South Bay waters from June-September, 1988. In the transplant method, growth and physiological performance of mussels were measured in the laboratory under standardized conditions after a 30-day field exposure in the Peconics. Results of the nutrition bioassay method show a marked reduction in mussel clearance rates over the summer at all Peconic Bay stations. In Great South Bay, clearance rates were initially minimal at all bay stations, but recovered with time. In transplant experiments, growth and physiological performance of mussels deployed at inshore stations were reduced relative to the control station (Gardiners Bay). The comparison of mussel clearance rates observed in response to brown tide conditions occurring in the Peconics, Great South Bay and in the laboratory suggest significant differences in brown tide effects which are independent of Aureococcus anophagefferens cell concentration. The implications of these results in regards to the utility of these biomonitoring methods are discussed.

Supported by: Dept. of Commerce - Grant NA86-AA-D-SG090 WHOI Sea Grant R/B 91; and Schumann Foundation.

WHOI Contribution No. 6937.

CHEMOTAXIS TOWARD NITROGENOUS COMPOUNDS BY SWIMMING STRAINS OF MARINE SYNECHOCOCCUS

Joanne M. Willey and John B. Waterbury

The majority of open ocean isolates of the marine unicellular cyanobacterium Synechococcus are capable of swimming motility, whereas coastal isolates are nonmotile. Surprisingly, the motile strains do not display either phototactic or photophobic responses to light, but instead demonstrate positive chemoresponses to several nitrogenous compounds. The chemotactic responses of Synechococcus (WH8113) were investigated using blind-well chemotaxis chambers fitted with 3.0 μm Nucleopore filters. One well of the chamber contained cells suspended in aged Sargasso seawater (SSW) and the other well of the chamber contained the potential chemoattractant in SSW. The number of cells that crossed the filter into the attractant-SSW was measured by direct cell counts and was compared with values obtained in chambers lacking a gradient. Twenty-two compounds were tested including sugars, amino acids and simple nitrogenous substrates at concentrations ranging from 10^{-5} to 10^{-10} M. Strain WH8113 responded positively only to ammonia, nitrate, β-alanine, glycine and urea. Typically, there was a 1.5- to 2-fold increase in cell concentrations above control levels in chambers containing these compounds, which is comparable to results from similar experiments using enteric and photoheterotrophic bacteria. However, the threshold levels of 10^{-9} to 10^{-10} M found for Synechococcus chemoresponses were several orders of magnitude lower than those reported for other bacteria and in a range that could be ecologically

significant in the oligotrophic oceans. The presence of chemotaxis in motile Synechococcus supports the notion that regions of nutrient enrichment, such as the proposed microzones and patches, may play an important role in picoplankton nutrient dynamics.

Supported by: NSF Grants OCE84-16960 and DCB86-08698.

WHOI Contribution No. 6934.

PLANKTON ECOLOGY

EFFECTS OF THE BROWN TIDE ALGA ON GROWTH, FEEDING PHYSIOLOGY AND LOCOMOTORY BEHAVIOR OF SCALLOP LARVAE (ARGOPECTEN IRRADIANS)

Scott M. Gallager, V. Monica Bricelj and Diane K. Stoecker

Growth and survival of scallop larvae in laboratory culture are deleteriously affected by the presence of Aureococcus anophagefferens gen. et sp. nov. Sieburth et al. when applied at near bloom concentrations. Relative to controls, shell growth rates were reduced three-fold and mortality increased by a factor of 3.5 when scallop larvae were fed A. anophagefferens with or without an alternative food source supplied at equivalent carbon levels. Etiology appeared to involve larval starvation as indicated by empty guts and low lipid levels in the digestive glands. Food-limited larval growth was not a function of poor assimilation of cell carbon from A. anophagefferens or inhibition of larval swimming activity, but due to inefficient capture of this unusual alga. High-speed video analysis of larval feeding behavior showed that when A. anophagefferens was present in the medium together with cells of an easily captured and nutritious alga, Isochrysis aff. galbana clone TISO, the latter are rendered unpalatable to scallop larvae and very few cells are ingested. Results suggest that some specific surface or chemical characteristic of brown tide cells interferes with capture by the preoral cirri and modulates selection of particles for ingestion.

Supported by: NSF Grant OCE87-11386; and NOAA Sea Grant NA86A-D-SG090.

WHOI Contribution No. 6944.

NITROGEN UPTAKE AND NH_4^+ REGENERATION BY PELAGIC MICROPLANKTON AND MARINE SNOW FROM THE NORTH ATLANTIC

Patricia M. Glibert, Mark R. Dennett and David A. Caron

Comparative rates of nitrogen uptake and NH_4^+ regeneration by plankton of < 153 and < 5 μm in size were determined in the Sargasso Sea and Gulf Stream, and by plankton associated with marine snow in the Gulf Stream during May 1982. Rates of total nitrogen uptake of Sargasso Sea phytoplankton exceeded those of the Gulf Stream phytoplankton by factors ranging from 1.8 to 5.6. Rates of microplankton NH_4^+ regeneration equaled or exceeded rates of NH_4^+ uptake in the Sargasso Sea, but in the Gulf Stream were negligible in all but one case. Significant rates of NH_4^+ regeneration were measured for Gulf Stream marine snow, and, in all but one case, exceeded those of NH_4^+ uptake. Rates of NO_3^- and urea uptake by the snow were less than half those of NH_4^+. Protozoan densities were enumerated on aliquots of the same snow particles and compared with previously reported bacterial estimates; enrichment factors of the cultivable ciliates and flagellates were 6500-9000 relative to ambient seawater. These organisms were also grazing and reproducing rapidly. Bacterial densities were also moderately enriched, but their productivity was lower than surrounding seawater bacteria. Thus, the large bacterivorous population associated with marine snow may have accounted for a substantial fraction of the observed NH_4^+ regeneration.

Published in: *Journal of Marine Research*, 46, 837-852, 1988.

Supported by: Leopold Schepp Foundation Award; NSF Grants OCE85-15629 and OCE80-24445; and WHOI Education Program.

WHOI Contribution No. 6830.

DYNAMICS OF HERBIVOROUS GRAZING BY THE HETEROTROPHIC DINOFLAGELLATE OXYRRHIS MARINA

Joel C. Goldman and Mark R. Dennett

In a series of batch experiments in the dark, the heterotrophic dinoflagellate Oxyhrris marina grazed three phytoplankton prey (Phaeodactylum tricornutum, Isochrysis galbana, and Dunaliella tertiolecta) with equal efficiency. Growth rates of the dinoflagellate ranged between 0.8/d and 1.3/d. Maximum observed ingestion rates on a cell basis varied according to the size of the prey from about

50 cells/flagellate/day when D. tertiolecta was the prey up to 250-350 cells/flagellate/d when the other species were eaten. However, when compared on a nitrogen basis, ingestion rates were independent of prey type. Both ingestion and growth ceased when prey cell concentrations fell below a threshold concentration of about 10^5 cells/ml. Maximum specific clearance rates were 2.7×10^4/d - 7.9×10^4/d, which is considerably lower than that found for heterotrophic dinoflagellates in oceanic waters, and may explain why O. marina generally thrives only in productive waters. The timing of NH_4^+ regeneration was linked to the C:N ratio of the prey at the start of grazing. Regeneration efficiencies for NH_4^+ never exceeded 13% during the exponential phase and 45% well into the stationary phase. These results are comparable to those obtained with heterotrophic flagellates and demonstrate that the bioenergetic patterns of grazing and nutrient cycling by protozoa are very similar. Moreover, they support the notion that to achieve 90^+% nutrient regeneration in the open ocean, as is currently believed, the microbial food loop must consist of multiple feeding steps. Alternatively, nutrient regeneration efficiences may be considerably lower than 90%.

In Press: *Journal of Plankton Research.*

Supported by: NSF Grant OCE85-11283; and U.S. Israel Binational Agricultural Research and Development Fund (BARD) Grant I-626-83.

WHOI Contribution No. 6808.

EQUIVALENCE AND ITS USE

Edward M. Hulburt

When we plot A against B in a graph we have an equivalence: If more A then more B saying that if not more B then not more (less) A. A relationship is an equivalence. But when there are three things, A, B, and C, there are quite a number of equivalences. In this article 16 expressions are presented; when these are taken in pairs, each pair is an equivalence. For example, Verity and Stoecker (1982) found that abundance of the alga Olisthodiscus luteus in flasks with tintinnids prevented the tintinnids growth, while the tintinnids grew well with lesser amounts of the alga. The same occurred in Narragansett Bay (U.S.A.); with abundance of the alga there was low amount of tintinnids while tintinnids thrived with less alga. An equivalence description is this: 'If O. luteus is abundant experimentally or is abundant observationally in nature, then it is lethal to tintinnids' is equivalent to 'If O. luteus is not lethal to tintinnids then it is neither experimentally nor observationally abundant'. This illustrates: 'If A or B then C' equivalent to 'If not C then not A and not B'. A wholly different path of endeavor is to choose an equivalence and then to fit all the data to it. This is done in the last of five cases presented.

In Press: *Ecological Modelling*, 44.

Supported by: Woods Hole Oceanographic Institution.

WHOI Contribution No. 6919.

IN SITU OBSERVATIONS OF DEEPWATER MEDUSAE IN THE GENUS DEEPSTARIA WITH A DESCRIPTION OF D. RECTICULUM, SP. NOV.

Ronald J. Larson, Laurence P. Madin and G. Richard Harbison

Two medusae in the poorly known genus Deepstaria were observed during submersible dives in the Pacific and Atlantic Oceans. The first specimen, identified here as D. enigmatica Russel, 1967, was observed, photographed and videotaped at a depth of about 600 m in the Catalina Basin off California. The second specimen was observed and collected at a depth of 915 m near Bermuda, and is described here as a new species, D. reticulum. Both medusae have a voluminous, thin-walled umbrella, a gastrovascular system of anastomosing canals, elongate oral arms and no tentacles. Behavioral observations made from the submersibles suggest that the medusae trap prey by pursing their voluminous bells shut around organisms which swim into them.

Published in: *Marine Biological Association of the United Kingdom*, 68, 689-699, 1988.

Supported by: NOAA Office of Undersea Research Program; and NSF Grant OCE77-22511.

WHOI Contribution No. 6746.

BEEBE PROJECT: ZOOPLANKTON STUDIES IN THE 1987 FIELD SEASON

Laurence P. Madin

Zooplankton research was conducted on 11 dives with the JOHNSON SEA-LINK during the Beebe Project off Bermuda in 1987. The work included documentation of abundance and vertical distribution, collection of new or unusual species, and observations of behavior. A lighted platform was deployed at the site to attract midwater animals, but weather prevented completion of these experiments. Observations on vertical and diel distribution showed evidence of vertical migration in narcomedusae, euphausiids, sergestids and squid. Some near surface gelatinous species were found throughout the water column, whereas other mesospelagic forms were found only below 300 m. A distinctive fauna of red pigmented organisms from several groups occurred below 700 m. Several new species were seen or collected, including a scyphomedusa in the genus Deepstaria.

Published in: *National Undersea Research Program Research Report*, 88-4, 1988.

Supported by: NOAA National Undersea Research Program; National Geographic Society; and NSF Grant OCE86-08961.

WHOI Contribution No. 6745.

FEEDING BEHAVIOR OF TENTACULATE PREDATORS: IN SITU OBSERVATIONS AND A CONCEPTUAL MODEL

Laurence P. Madin

The recent focus on behavior of individual zooplankters has led to several models describing predatory encounters; in this paper a general model is extended to gelatinous zooplankton that catch prey with tentacles. Because of their large size and fragility, these organisms are best observed in situ by divers. Observations on the feeding behavior of several medusae, siphonophores, and ctenophores are reported, along with information on diet composition and measurements of tentacle size, spacing, and deployment pattern made from photographs or videotapes. From these data two additional parameters affecting the probability of prey capture can be estimated. The "encounter zone" is the space around the predator in which the tentacles may be found, and the "tentacle density" is the fraction of that space actually filled with tentacles. These spatial parameters, and others relating to predator size, prey swimming speed and pattern, prey size and type, and nematocyst characteristics are incorporated into a conceptual model of prey selection and capture by tentaculate feeders.

In Press: *Bulletin of Marine Science*, 43, 1988.

Supported by: NSF Grants OCE83-15297 and OCE86-08961.

WHOI Contribution No. 6747.

AN EXPERIMENTALLY DETERMINED CARBON:VOLUME RATIO FOR MARINE "OLIGOTRICHOUS" CILIATES FROM ESTUARINE AND COASTAL WATERS

Mary Putt and Diane K. Stoecker

The biomass of marine "oligotrichous" ciliates has often been estimated by measuring the biovolume of preserved samples and converting to units of carbon based on theoretical carbon:volume (C:vol) ratios of 70 to 110 fg·μm^3. Using laboratory cultures of several strains of Laboea strobila, Strombidium spp. and Strobilidium spiralis we experimentally derived a C:vol conversion factor of 190 fg·μm^3 for cells preserved with 2% vol:vol Lugol's iodine. Biovolume estimates of Lugol's preserved cells average 76% of biovolume estimates of formalin preserved cells. Hence a C:vol ratio of 150 fg·μm^3 applies to formalin preserved cells. Our study indicates that the biomass of oligotrichous ciliates in marine systems has been significantly underestimated by the use of inappropriate C:vol ratios.

Supported by: WHOI Postdoctoral Scholarship (MP); and NSF Grants OCE88-10235 (MP) and OCE88-00684 (DKS).

WHOI Contribution No. 6957.

MOLLUSCS IN THE PLANKTON

Rudolf S. Scheltema

Molluscs in the plankton can be divided into two major categories, the holoplankton and meroplankton. Included among the permanent or holoplankton are the opisthobranch pteropod orders Thecostomata and Gymnostomata and also the prosobranch order Heteropoda. The temporary or meroplankton is the free-drifting larvae of benthic species. During their planktonic life, most veliger larvae feed upon unicellular algae; some bivalves probably can also utilize dissolved organic matter. The length of planktonic life can vary greatly within the same species. Cues for settlement and metamorphosis are distinct for a species though usually there may be a hierarchy of cues. How larvae will actually make contact with

the bottom under the hydrodynamic conditions at the bottom boundary layer is not fully understood. Larvae of most Australian marine molluscs have not been described even though they constitute a significant fraction of the total plankton at certain times of the year. Among prosobranchs there are at least 20 families known to include species with teleplanic larvae. Long-distance dispersal by such larvae is of considerable biogeographic interest since it offers one explanation of how Indo-Pacific species may have become widely distributed and recruited onto Pacific islands. Knowledge of larvae is important to aquaculture.

In Press: *The Fauna of Australia*, Vol. 5. Mollusca.

Supported by: NSF Grant OCE86-14579; and Woods Hole Oceanographic Institution.

WHOI Contribution No. 6901.

ABUNDANCE OF AUTOTROPHIC, MIXOTROPHIC AND HETEROTROPHIC PLANKTONIC CILIATES IN SHELF AND SLOPE WATERS

Diane K. Stoecker, Akira Taniguchi and Ann E. Michaels

During early summer, the density of microplanktonic ciliates in the euphotic zone on Georges Bank (Northwest Atlantic) ranged from 600 to 13,000 cells l^{-1}; in the slope waters to the southeast of the bank, densities ranged from 1900 to 2800 cells l^{-1}. Myrionecta rubra, a photosynthetic autotroph with a reduced algal endosymbiont, comprised an average of 30% of the microplanktonic ciliate fauna at stations in < 100 m depth, but 3% or less of the ciliate fauna at the deeper stations. Oligotrichous ciliates with chloroplasts are estimated to have contributed 34% of the ciliate fauna and were abundant at both shallow, unstratified stations on the bank and at deeper, stratified stations on the slope of the continental shelf and in the Gulf of Maine. Overall, about 50% of the ciliates in the euphotic zone contained chlorophyll.

At the shallow water stations, two species, M. rubra and Laboea strobila (a mixotrophic oligotrichous ciliate) accounted for over 50% of the biomass of ciliates with chlorophyll. At an irradiance of 100 $\mu E\ m^{-2}s^{-1}$, M. rubra and L. strobila had photosynthetic rates of 85 and 465 pg C fixed $cell^{-1}h^{-1}$, respectively. During the summer, when phytoplankton biomass is low, autotrophic and mixotrophic ciliates may make an important contribution to photosynthesis in the larger size fractions and be an important source of food for larger organisms that rely on high quality, $\geq$15-20 μm food particles.

In Press: *Marine Ecology Progress Series.*

Supported by: NSF Grant OCE86-00765.

WHOI Contribution No. 6789.

POPULATION ECOLOGY

LIFE HISTORY STRATEGIES

Hal Caswell

The study of life history strategies originated in the late 1940's and early 1950's from the combination of animal demography and evolutionary theory. The application (by Lotka, Pearl, Bodenheimer, Lack, Leslie, and Deevey) of demographic methods (especially the life table and stable age theory) to animals provided a description of the life cycle and a way to derive its population dynamic consequences. That description was couched in terms of age-specific rates of mortality and reproduction, and ecologists were well aware that those rates showed interesting patterns both within and between species. The development of population genetics provided rigorous basis for Darwinian arguments about the adaptive value of phenotypic traits.

Supported by: NSF Grants OCE85-16177, BSR86-09395 and BSR87-04936.

WHOI Contribution No. 6775.

THE ANALYSIS OF LIFE TABLE RESPONSE EXPERIMENTS I: DECOMPOSITION OF EFFECTS ON POPULATION GROWTH RATE

Hal Caswell

Life table response experiments use the life table as a response variable in studies of the population level response to environmental or biological factors. Demographic indices, particularly the asymptotic population growth rate γ (or $r = \ln\gamma$), are commonly used as summary statistics to integrate the multifarious effects of the environmental factors on the life table. This raises the question of how to decompose the overall effect of a treatment on γ into contributions due to its effects on the individual survival and fertility rates. These contributions can be calculated from matrix projection models. Examples are shown, including a two-way factorial experiment in which both main effects and interactions are decomposed into contributions. In general, changes in the vital rates are only poorly correlated with the contributions of those changes to effects on γ.

Supported by: NOAA Grant NA83AA-D-00058; NSF Grant OCE85-16177; and a Cooperative Agreement from the EPA.

WHOI Contribution No. 6837.

ESTIMATION OF STAGE-SPECIFIC DEMOGRAPHIC PARAMETERS FOR ZOOPLANKTON POPULATIONS: METHODS BASED ON STAGE-CLASSIFIED MATRIX PROJECTION MODELS

Hal Caswell and Saran Twombly

Our understanding of zooplankton dynamics is constrained by the difficulty of estimating stage-specific vital rates from field data. In this paper, we approach demographic estimation as an inverse problem, using stage-classified matrix projection models. We allow the vital rates to vary between stages and over time, and do not assume stable age distributions or that discrete cohorts can be identified. We obtain least-squares estimates of survival and growth probabilities, which can be obtained from as few as three consecutive censuses. However, the estimates are ill-conditioned in the presence of sampling noise. Two regularization methods, truncated singular value decomposition and Tikhonov regularization (ridge regression) are examined as possible solutions.

Supported by: NSF Grant BSR86-09395.

WHOI Contribution No. 6718.

PLANKTONIC AND NON-PLANKTONIC DEVELOPMENT AMONG PROSOBRANCH GASTROPODS AND ITS RELATIONSHIP TO THE GEOGRAPHIC RANGE OF SPECIES

Rudolf S. Scheltema

Evidence from a quasi non-biased sample of intertidal and sublittoral prosobranchs from the east coast of the United States shows that species with a planktonic larva have on the average a greater range than those lacking a free-drifting veliger stage. However, among those that have a planktonic stage, the length of larval development is unrelated to the extent of geographic range so long as there are no major barriers to dispersal. Consequently, along the continental coastlines of North, Central and South America there is on the average no significant difference in the geographic range between species with a planktonic development of 2 to 6 weeks duration and those having teleplanic or "long distance" larvae with a development of 2 to 6 months or even more. If one considers however a barrier such as the Atlantic basin, species with the shorter planktonic life seldom exhibit amphi-Atlantic distributions whereas among species having teleplanic veligers, three-fourths are known to have a range extending across the Atlantic Ocean. The generalizations which emerge cannot be regarded as exact. Means of dispersal other than the drift of planktonic larvae may extend species ranges beyond expectation or, alternatively, ecological constraints can determine where species cannot survive and restrict geographic range despite the capacity for dispersal.

In Press: *Proceedings of the 23rd European Marine Biology Symposium.*

Supported by: NSF Grant OCE86-14579.

WHOI Contribution No. 5820.

ZOOPLANKTON

ANALYZING ZOOPLANKTON SIZE DISTRIBUTIONS USING HIGH-FREQUENCY SOUND

Charles H. Greene, Peter H. Wiebe and Janusz Burczynski

A high-frequency, dual-beam acoustical technique for directly estimating the size distributions within zooplankton assemblages has been developed. In combination with data from echo integration, acoustical size distributions can be used to apportion zooplankton numerical density and biomass into concentration into different size classes. Two major conclusions can be drawn from calibration experiments and preliminary field studies using the technique: the backscattering intensities from individual zooplankters increase proportionally with the cubes of their lengths; and the combination of dual-beam and echo-integration techniques has the potential to produce rapid, high-resolution, size-specific data on zooplankton distributions in the water column.

Published in: *Limnology and Oceanography*, 34(1), 1989.

Supported by: ONR Contract N00014-87; and NOAA National Undersea Research Program.

WHOI Contribution No. 6761.

ACOUSTICAL DETECTION OF HIGH-DENSITY DEMERSAL KRILL LAYERS IN THE SUBMARINE CANYONS OFF GEORGES BANK

Charles H. Greene, Peter H. Wiebe, Janusz Burczynski and Marsh J. Youngbluth

High-density demersal layers of krill have been detected in the submarine canyons off Georges Bank by means of a high-frequency, dual-beam bioacoustical technique. Krill densities in these demersal layers were observed to be two to three orders of magnitude greater than the highest densities observed in water-column scattering layers. Such abundances may help explain the unusually high squid and demersal fish production estimates attributed to the Georges Bank ecosystem.

Supported by: ONR Contract N00014-87-K-0007; and NOAA National Undersea Research Program.

WHOI Contribution No. 6760.

FUNCTIONAL REGRESSION OF EQUATIONS FOR ZOOPLANKTON DISPLACEMENT VOLUME, WET WEIGHT, DRY WEIGHT AND CARBON: A CORRECTION

Peter H. Wiebe

A corrected set of functional regression equations relating zooplankton displacement volume, wet weight, dry weight and carbon are presented to update those presented by Wiebe et al. (1975). In addition a relationship between zooplankton carbon and nitrogen which is presented indicates that zooplankton are nitrogen rich relative to their phytoplankton counterparts.

Supported by: NSF Grant OCE87-09962.

WHOI Contribution No. 6839.

COARSE-SCALE HORIZONTAL PATCHINESS AND VERTICAL MIGRATION IN NEWLY FORMED GULF STREAM WARM-CORE RING 82-H

Peter H. Wiebe, Nancy J. Copley and Steven H. Boyd

A 1-m^2 MOCNESS with 20 nets was used to make a series of tows in Gulf Stream meander/ring 82-H (Sept/Oct 1982) including two 0-100 m towyo's. One towyo, made at dusk in the core of 82-H (of Sargasso Sea/ Gulf Stream origin) permitted study of the effect of diel migration on the spatial variability of copepod and euphausiid species abundance, and species composition in a region of low physical variability. The other towyo taken across a front on the outer edge of 82-H (a mixture of Gulf Stream, shelf, and Slope Water) allowed comparison of spatial variability of the same biological properties in a region of strong physical variability. A sharp transition in species composition occurred in the ring core after sunset as diel migrating euphausiid species moved into the surface waters. A similar, but less extreme change took place in copepod species composition because a smaller proportion of these migrated. All copepod migrants also entered surface waters after sunset with species living deeper in the water column during the day arriving in the surface waters later than those living shallower. Estimated swimming speeds (typically 50-200 m/hr) of migrating euphausiids and copepods were similar in spite of large differences in body size between the two groups. Variations in species composition were substantially larger at the edge of the ring where species proportions changed radically in concert with changes in water mass properties. There were also large differences in species composition between the samples from the ring core and the front which equaled those which occurred across the front. Streamers of surface water which originated within the frontal region and spiraled into the ring core could provide colonizers of many species not present at the time of ring formation.

Supported by: NSF Grants OCE80-12748, OCE85-08350 and OCE87-09962.

WHOI Contribution No. 6815.

DEPARTMENT OF CHEMISTRY

Frederick L. Sayles, Chairman

ORGANIC AND BIOLOGICAL CHEMISTRY

PARTICULATE NEW NITROGEN FLUXES IN THE SARGASSO SEA

Mark A. Altabet

Seasonal variations in the flux of new nitrogen as sinking particles of up to 7-fold are observed at a site near Bermuda. Maxima occur in the late winter with minima in the late fall. While this particle flux is dependent on levels of suspended PN in the euphotic zone, NO_3^- flux modulated by seasonal variations in the magnitude of vertical transport appears to be the ultimate forcing function. However, high particle fluxes are not dependent on the large wintertime increases in euphotic zone NO_3^- which are observed when the mixed layer depth exceeds 100 m. Surprisingly, the gradient in NO_3^- concentration at 100 m is inversely correlated with particle flux causing the annual amplitude in new nitrogen flux to be well below the amplitude in vertical transport.

Annualized flux of sinking PN is 0.2 M m^{-2} yr^{-1}, 1/3 the highest estimate reported for new nitrogen flux in this region. The downward mixing of suspended PN makes a significant contribution to the downward flux, particularly in the winter, and its inclusion raises the annual new nitrogen flux to 0.33 M m^{-2} yr^{-1}. This estimate is most likely conservative since sporadic events may not have been adequately sampled and the downward flux of non-particulate forms of nitrogen has not been taken into account. Fluxes of particulate new nitrogen are consistent with high rates of new production in the oligotrophic, open ocean.

Supported by: NSF Grants OCE87-17508 and OCE85-16296.

WHOI Contribution No. 6786.

WITHER ORGANIC CARBON?

Werner G. Deuser

Two-thirds of the particulate organic carbon (POC) carried by rivers (150 x 10^{12} grams per year), most of it associated with clay minerals, is resistant to degradation in the terrestrial and fluvial environment, according to a recent report in Nature. That amount is comparable to most current estimates of the rate of burial of organic matter in the entire ocean, including deltaic and shelf areas. Does this suggest that all organic matter buried in the ocean is of terrestrial origin? If not, where does all the terrestrial carbon go? Does it reach the ocean and become oxidized there? If it is not oxidized, do marine sediments preserve mostly terrestrial carbon?

It seems to be easier to point out additional discrepancies in our understanding of the land-ocean carbon balance than to answer the questions raised by the report. Besides their POC load, rivers carry an approximately equal load of dissolved organic carbon (DOC) - about $200x10^{12}$ grams per year. If all this were to reach the ocean, and if it were as resistant to degradation as is POC, it would take less than 3,000 years to "fill up" the oceans' reservoir of DOC by rivers alone. But DOC in the deep Pacific is reported to have an average radiocarbon age of 6,000 years and is believed to be mostly (90 per cent) of marine origin. Although many qualifications could be added, it seems that there is much more organic matter coming down the rivers than can be accounted for in the ocean. Where does it go?

The complex physical, chemical and biological processes at the interface between fresh and salt water in estuaries and deltas can only dispose of part of the load. Neither near-shore burial rates nor oxidation and attendant release of nutrients are high enough to accommodate the excess carbon. Deep-sea fans are one place to look for it. Another, more provocative, supposition is that the ocean is comparable to a heterotrophic organism. That is to say that it depends on an import of terrestrial organic matter to maintain its level of metabolism, because there is an excess of respiration over primary production of organic matter.

Published in: *Nature*, 332, 396-397, 1988.

RADIOCARBON LEVELS AND CONCENTRATIONS OF DISSOLVED ORGANIC MATTER IN PACIFIC OCEAN WATERS

Ellen R. M. Druffel, Peter M. Williams, and Yoshimi Suzuki

The apparent mean ^{14}C age of UV-oxidizable dissolved organic carbon (DOC) in the deep waters of the central North Pacific gyre is 6000 yrs B.P., several thousand years older than that of the far more abundant dissolved inorganic carbon (DIC). This older age indicates that a portion of the DOC is recycled numerous times within the ocean. Radiocarbon dating of organic compound classes is necessary to determine the sources and turnover times of various fractions within the organic matter pool in the ocean, though the problems involved are enormous. We report AMS (accelerator mass spectrometry) $\Delta^{14}C$ results of humic, fulvic and hydrophilic acid fractions isolated from water collected at 180 m in the North Pacific (19°N, 158°W) using XAD macro- reticular resins. Results show that the $\Delta^{14}C$ values of these

fractions are less than or equal to the $\Delta^{14}C$ of the UV-oxidizable DOC (DOC_{uv}) from the same depth 900 km further north. Total (free plus combined) amino acid and carbohydrate concentrations (THAA, TCHO) are also reported for the same water samples used to make the $DO^{14}C$ measurements. We present two lines of evidence that indicate only a portion of the DOC in the sea water analyzed previously may have been oxidized by the UV-method: 1) higher DOC was obtained for the first 7 samples oxidized by UV[1], presumably due to greater energy output of the Hg-arc lamp, and 2) high temperature catalytic (HTC) methods used to reoxidize the central North Pacific gyre water samples reveal additional DOC of the order of the original DOC_{uv}. Evidence suggests that the portion of DOC that is chemically unoxidizable by UV-radiation contains higher amounts of radiocarbon than DOC_{uv}, contrary to expectations. It appears that the DOC fraction dated originally is more refractory with respect to biological utilization and is more chemically reactive with respect to photooxidation than the fraction resistant to UV-oxidation.

Supported by: NSF Grant OCE84-16632.

WHOI Contribution No. 6850.

ICES/IOC INTERCOMPARISON EXERCISES ON THE DETERMINATION OF PETROLEUM HYDROCARBONS IN BIOLOGICAL TISSUES (MUSSEL HOMOGENATE) - ICES (2/HC/BT)

John W. Farrington, Alan C. Davis, Nelson M. Frew, and Anthony Knap

A homogenate was prepared from approximately 4,000 Mytilus edulis sampled near the municipal sewer outfall of Boston, Massachusetts, U.S.A. Subsamples were placed in jars. Then a set of subsamples were freeze-dried. Both wet homogenate and freeze-dried homogenate samples were checked for non-homogeneity by analyses of randomly selected subsamples by the W.H.O.I. coordinating laboratory. Three randomly selected freeze-dried subsamples were distributed to each of fifty participating laboratories from twenty-four countries.

Twenty-two laboratories reported U.V.-fluorescence data giving $x = 24 \times 10^{-6}$ g chrysene equivalents/g dry weight $\pm 24 \times 10^{-6}$ g/g dry weight for a $\pm$ 100% r.s.d. Twenty laboratories reported U.V.-fluorescence data in Arabian Light Crude Oil equivalents; $x = 235 \times 10^{-6}$ g/g dry weight $\pm$ 234 for a $\pm$ 98% r.s.d. Between twenty-two and thirty laboratories reported data for n-alkanes, pristane and phytane determined by GC analyses giving between $\pm$ 69% and $\pm$ 297% r.s.d. depending on the compound. Elimination of outliers reduced the range of r.s.d.'s to $\pm$ 67 to $\pm$ 104% r.s.d. A similar experience was noted for data for individual polynuclear aromatic hydrocarbons when combining data from HPLC, GC, and GC/MS analyses. There is a need for much improvement for within and between laboratory precision.

Published in: *Marine Pollution Bulletin* 18, 372-280, 1988.

Supported by: Ocean Assessment Division, NMFS, NOAA; UNEP Regional Seas Programme; and A. W. Mellon Foundation Grant to Coastal Research Center.

WHOI Contribution No. 6822.

BIOGEOCHEMISTRY OF LIPIDS IN SURFACE SEDIMENTS OF THE PERU UPWELLING AREA AT 15°S

John W. Farrington, Alan C. Davis, Jacek Sulanowski, Mark A. McCaffrey, Matt McCarthy, C. Hovey Clifford, Peggy Dickinson, and John K. Volkman

Organic carbon, lycopane, $C_{20:1}$ branched alkane, C_{37} alkenones, and 20:5 and 22:6 polyunsaturated fatty acid concentrations in two box cores from the Peru continental margin area at 15°S in 90 meters and 268 meters water depth have depth profiles that are synchronous and appear to indicate an historical record of fluctuating higher productivity-lower productivity (ENSO) periods. The UK_{37} ratio of the $C_{37:2}$ and $C_{37:3}$ alkenones in the 268 meter core in the center of the upwelling zone varies with depth in a manner consistent with the UK_{37} functioning as a historical recorder of euphotic zone temperature.

Concentrations and CPI for n-alkanes are reported for both cores. A C_{27} anthrasteroid from cholest-5-en-3β-ol has been identified and quantified in the 268 meter core.

In Press: *Advances in Organic Geochemistry* 1987: Organic Geochemistry.

Supported by: NSF Grants OCE85-09859, OCE79-18665 and OCE77-26184; and ONR Contract N00014-79-C-1171.

WHOI Contribution No. 6696.

BITUMEN MOLECULAR MATURITY PARAMETERS IN THE IKPIKPUK WELL ALASKAN NORTH SLOPE

John W. Farrington, Alan C. Davis, Martha E. Tarafa, Mark A. McCaffrey, Jean K. Whelan and John M. Hunt

Several bitumen molecular maturity parameters: methylnaphthalene ratios - MNR, ENR, DNR; methylphenanthrene indices - MPI_1, MPI_2, DPI; n-C_{17}/pristane; pristane/phytane; C_{15+} alkane distributions and GC-MS analyses of triterpanes, steranes, diasteranes, triaromatic steroids, and monoaromatic steroids for samples of the Ikpikpuk well, Alaskan North Slope, are reported. The molecular maturity parameters are compared and contrasted with previous data for lower molecular weight C_1 to C_7 hydrocarbons, production index, vitrinite reflectance, and thermal alteration index.

Bitumen maturation indices, C_{15+} alkane distributions, and distributions of steranes, diasteranes, triterpanes, triaromatic and monoaromatic steroids agree with kerogen maturation indices in the Kingak section of Ikpikpuk well. Bitumen maturation indices and distributions of steranes, diasteranes, triterpanes, triaromatic and monoaromatic steroids diverge from vitrinite maturation profiles for the Shublik section of Ikpikpuk indicating either a major influence of changes in kerogen type or the presence of residues of expulsion/migration in the Shublik. The data are consistent with the Shublik being a source and/or conduit of migration of oil.

In Press: *Advances in Organic Geochemistry* 1987: Organic Geochemistry.

Supported by: DoE Contract EG-77-02-4392 and DoE Grant DE-FGO2-86ER-13466.

WHOI Contribution No. 6835.

GEOCHEMICAL IMPLICATIONS OF THE LIPID COMPOSITION OF THIOPLOCA SPP. FROM THE PERU UPWELLING REGION - 15°S

Mark A. McCaffrey, John W. Farrington, and Daniel J. Repeta

Thioploca, a genus of colorless, sulphur-oxidizing, filamentous bacteria, constitutes as much as 80% of the biomass in dysaerobic surface sediments ([O_2 <0.1 ml/l bottom water) in the coastal upwelling regimes of Peru and Chile. The lipid composition of Thioploca collected from sediments from the oxygen minimum zone in the Peru upwelling region near 15°S is presented here, and we provide the first assessment of the influence of Thioploca on organic compound distributions in upwelling regime sediments. Since marine species of Thioploca have been found only in dysaerobic surface sediments of upwelling regimes, biomarkers for this organism may be useful in identifying similar depositional conditions in the sedimentary record. Thioploca (dry) was found to be ≈3.8-4.1 wt.% lipid. three fatty acids: cis 16:1Δ9, 16:0 and cis 18:1Δ11 accounted for 69-72% of this lipid. Hydroxy fatty acids, hopanoids and hydrocarbons were conspicuously absent from the Thioploca. The Thioploca was found to contain cyclolaudenol, a C_{31} sterol with an unusual structure; diagenetic alteration products of this sterol may serve as markers for Thioploca input to sedimentary organic matter, and hence as markers for paleo-upwelling depositional environments in the sedimentary record.

In Press: *Organic Geochemistry.*

Supported by: Ocean Ventures Fund and NSF Grant OCE85-09859.

WHOI Contribution No. 6757.

CAROTENOID DIAGENESIS IN RECENT MARINE SEDIMENTS-II. DEGRADATION OF FUCOXANTHIN TO LOLIOLIDE

Daniel J. Repeta

The quantitative distributions of major phytoplankton carotenoids: fucoxanthin, diadinoxanthin, diatoxanthin, and β-carotene in two cores of anoxic marine sediment recovered from the Peru continental shelf are reported. Our results demonstrate that the rapid degradation of carotenoids in sediments is not a result of their high degree of unsaturation as has been previously suggested. Instead, carotenoids exhibit a wide range of degradation rates that are proportional to the ability of specific pigments to form unstable bicyclic furanoxides. Carotenoid furanoxides undergo subsequent fragmentation to loliolide, isololiolide, dihydroactinidiolide and other, as yet undetermined, low molecular weight products. This degradation pathway accounts for the relative rates of removal for specific carotenoids (fucoxanthin = fucoxanthinol > diadinoxanthin > diatoxanthin = carotene), the distribution of carotenoids reported by Watts and Maxwell (1977) and Cardoso et al. (1978) in ancient sediments, the occurrence of novel carotenoid transformation products in surface sediments reported by Ridout et al. (1984), and the distribution of loliolides in recent sediments recovered from the Namibian shelf as reported by Klok et al. (1984a,b). We predict that loliolide and isololiolide will inherit a specific

stereochemistry from their carotenoid precursors, but that dihydroactinidiolide will be racemic.

For every mmole of fucoxanthin degraded in Peru sediments, 0.7-1.1 μmole of loliolide is produced. Summation of fucoxanthin and loliolide at each subsurface horizon yields an estimate of the total deposition of fucoxanthin at t = 0. Throughout the 0-20 cm depth of our samples, this parameter is remarkably constant to ± 16%, suggesting a depositional regime approaching steady state. Individual horizons exhibit excursions which may reflect changes in surface productivity. Extrapolation of our measurements to deeper sediments may therefore be of some value in deciphering questions on environmental conditions of deposition and paleoproductivity.

Supported by: NSF Grant OCE83-10004, OCE85-09859, PRF 17791-G2.

WHOI Contribution No. 6856.

LONG CHAIN UNSATURATED KETONES AS A POTENTIAL TOOL TO EVALUATE THE ATMOSPHERIC TRANSPORT OF MARINE DERIVED PARTICLES

Marie-Alexandrine Sicre, Robert B. Gagosian, and Edward T. Peltzer

Long chain alkenones (LCA) in the range of C_{37}-C_{39} were found in significant amounts in aerosols collected in New Zealand. The occurrence of these compounds in the atmosphere probably stem from their ejection due to bubbling processes during wave breaking. The surface water temperatures during LCA production calculated from the U^K_{37} ratios suggested a local origin and short atmospheric residence times of the LCA. They were not detected in aerosol samples collected on American Samoa due to the absence of the source organisms in surface waters. The distribution of LCA over the particle size spectrum demonstrated that they were only associated with large particles suggesting a direct ejection of the algae cell or its fragments into the atmosphere.

In Press: *Journal of Geophysical Research-Atmosphere.*

Supported by: NSF Grant OCE84-06666.

WHOI Contribution No. 6724.

THERMAL DESORPTION AND PYROLYSIS OF C_1-C_3 HYDROCARBONS IN SOURCE ROCKS - INDICATOR OF MATURITY AND GAS GENERATION POTENTIAL

Jean K. Whelan, Martha E. Tarafa, and John M. Hunt

Hydrocarbon gas (C_1-C_3) generation characteristics were determined by pyrolysis for three Alaskan North Slope wells (Ikpikpuk, Seabee, and Inigok in the Naval Petroleum Reserve) which go to high maturities (maximum vitrinite reflectances 2.5, 2.5%, and 5% respectively). Both P_l (sorbed generated gas) and P_2 (pyrolysis generated or pyrolyzable gas) were measured. The maximum P_2 C_2-C_3 occurs at R_o = 0.7-1.2% with all pyrolyzable P_2 C_2 and C_3 (wet gas) disappearing at R_o = 2.0-2.4% for these marine sediments containing predominantly type III organic matter. Maximum methane generation potential occurs in about the same range with most generation capacity disappearing at about R_o = 2.4-3%. In the Inigok well, a second deeper maximum in both P_l and P_2 methane (C_l) generation capacity, possibly from anthracite coals, was observed at R_o = 4.8% with all C_l generation capacity disappearing at R_o of 4.9- 5%. Small amounts of residual C_2 (but not C_3) generation capacity were also observed which maximized at R_o = 4.3% and then disappeared by R_o = 4.8%. The Seabee well which is extensively affected by migrated hydrocarbons shows trends very similar to those found for the Ikpikpuk well, but with the maximum generated C_l (expressed as a percentage of total P_l and P_2 C_l) in the bottom of the well being considerably weaker than for the other two wells.

In fine-grained intervals of all three wells, individual P_2 C_l-C_3 concentrations were at least 10 to 100 times those of P_l so that an in situ C_l- C_3 source would be able to produce all of the sorbed gas found in any particular formation without invoking an outside (i.e., deeper or lateral) gas source.

High proportions of sorbed (P_l) in comparison to total (P_l+P_2) gas tend to concentrate at: i) intervals containing coarse grained sediments such as sand layers or discontinuities between formations, and ii) in the deepest sections of the Inigok and Ikpikpuk wells, particularly for Cl.

The sorbed methane from one Seabee sample (14,550 ft, R_o = 2.3%) has a $\delta^{13}C$ value of -35.1, consistent with a source from a kerogen from the same depth (maturity) and not consistent with a major contamination source (e.g. microbiological, downhole slumping, or drilling contaminant). The very low concentrations of sorbed alkenes and

C_4-C_5 hydrocarbons in the same sample also minimize the possibility of significant drilling artifact contamination of this sorbed gas.

P_2 ratios of $C_l/(C_l+C_2+C_3)$ show a good correlation with R_o for the Ikpikpuk well and a generally positive, but poorer correlation, with R_o in the other two wells.

Supported by: DOE Grant DE-FG02-86ER-13466.

WHOI Contribution No. 6751.

RADIOCHEMISTRY

REMOVAL OF THORIUM-234 BY SCAVENGING IN THE BOTTOM NEPHELOID LAYER OF THE OCEAN

Michael P. Bacon and
Michiel M. Rutgers van der Loeff

Concentrations of ^{234}Th were measured in deep-sea bottom waters to assess the extent of chemical scavenging near the ocean floor. At five stations in the eastern tropical Pacific, where no appreciable bottom nepheloid layer (BNL) was observed, total ^{234}Th was in secular equilibrium with its parent ^{238}U, confirming earlier published results. In contrast, samples from a well-developed BNL in the western North Atlantic showed a significant depletion of ^{234}Th due to its removal by scavenging. The largest depletions were observed in the two samples closest to the bottom (25 and 64 m above bottom) and amounted to 19% of the equilibrium value. The results can be used to test models that have been proposed to explain the existence of a BNL. It is concluded that only a model which includes local or nearby resuspension of sediment can account for the observations. From a steady-state model that assumes local resuspension, the average residence time of resuspended particles in the BNL is estimated to be 25 days.

In Press: *Earth and Planetary Science Letters.*

Supported by: NSF Grants OCE78-25724, OCE78-26318, and OCE84-17910.

WHOI Contribution No. 6785.

DETERMINATION OF FISSION-PRODUCTS AND ACTINIDES IN THE BLACK SEA FOLLOWING THE CHERNOBYL ACCIDENT

Ken O. Buesseler, Susan A. Casso,
Mary C. Hartman, and Hugh D. Livingston

Radiochemical procedures are discussed for the isolation and determination of a suite of radionuclides in samples from the Black Sea following their input from the Chernobyl reactor accident. The samples analyzed include discrete water samples and both suspended and dissolved phases collected by in-situ chemisorption techniques. The radiochemical scheme permits the separation and analysis of ^{134}Cs, ^{137}Cs, ^{90}Sr, ^{144}Ce, ^{147}Pm, ^{106}Ru, ^{239}Pu, ^{240}Pu, and in some instances ^{242}Cm, ^{238}Pu, and ^{241}Am. The detection techniques employed include various instrumental gamma spectrometric methods, low-level beta counting, alpha spectrometry, and mass spectrometry.

The methods developments are described and data are presented on some representative samples from the Black Sea. The sensitivity of the analysis for the various nuclides and sample types is summarized and questions of radiochemical interferences addressed.

In Press: *Second International Conference on Low Level Measurements of Actinides and Long-Lived Radionuclides in Biological and Environmental Samples, Akita City, Japan*, 16-20 May, 1988.

Supported by: Coastal Research Center, ONR Contract N00014-85-C-0715, and NSF Grant OCE87-00715.

WHOI Contribution No. 6798.

DECADE TIMESCALE VARIABILITY OF VENTILATION IN THE NORTH ATLANTIC: HIGH PRECISION MEASUREMENTS OF BOMB RADIOCARBON IN BANDED CORALS

Ellen R. M. Druffel

The first high precision radiocarbon measurements for the upper ocean are presented for banded corals from two sites in the North Atlantic Ocean. The striking dissimilarities between the post-1950 records at Bermuda in the Sargasso Sea and the Florida Straits in the Gulf Stream illustrate the different mixing processes in the upper ocean at each site. Convective overturn associated with eighteen degree water formation during late winter in the northern Sargasso Sea facilitates storage of considerable quantities of bomb radiocarbon at depth, which accounts for the damping of the $\Delta^{14}C$ signal at Bermuda during the 1960's.

A multi-box isopycnal mixing model is used to estimate the ventilation rate of the upper 700 meters of the water column in the Sargasso Sea from 1950-1983. An inverse model is used, that is, the water mass renewal rate was calculated for the post-bomb period in order to satisfy the bomb radiocarbon time-history in the corals. Sea water radiocarbon measurements made during the

Geosecs (1972- 73) and TTO (1980-81) surveys are used to constrain the sub-surface radiocarbon values calculated by the model. Results show that the rate of water mass renewal in the Sargasso Sea was high during 1963-64 and decreased during the late 1960's and remained low during most of the 1970's. The ^{14}C-derived record of water mass renewal precedes by about 4 years that derived from isopycnal salinity in the Sargasso Sea (Jenkins, 1982), illustrating that the coral ^{14}C record is controlled to a large extent by changes in ocean circulation, rather than by atmospheric exchange of CO_2.

In Press: *Journal of Geophysical Research.*

Supported by: NSF Grants OCE83-15260 and OCE86-16532, and a Grant from The Mellon Foundation.

WHOI Contribution No. 6732.

PREDICTING THE OCEANIC FLUX OF RADIONUCLIDES ON SINKING BIOGENIC DEBRIS

Nicholas S. Fisher, J. Kirk Cochran, S. Krishnaswami and Hugh D. Livingston

The vertical flux of long-lived radionuclides and metals in general has been linked to the flux of particulate matter in marine systems. Various forms of particulate matter have been shown to be capable of transporting radionuclides in the sea, with greatest interest in recent years focusing on debris of biological origin. The degree to which radionuclide flux exiting the euphotic zone can be attributed to sinking biodetritus deriving ultimately from phytoplankton can be calculated using experimentally determined concentration factors in phytoplankton, dissolved radionuclide concentrations in surface waters, and new production estimates for specific ocean regions. Predictions of radionuclide fluxes are generally comparable with sediment trap measurements of radionuclide fluxes in these waters, suggesting that the downward flux from open ocean surface waters of particlereactive radionuclides is governed principally by sinking biogenic debris.

Published in: *Nature*, 335, 622-625, 1988.

Supported by: Sandia National Laboratory Subseabed Disposal Program #25-5713 and NSF Grant OCE86-14545.

WHOI Contribution No. 6861.

CHARACTERISTICS OF CHERNOBYL FALLOUT IN THE SOUTHERN BLACK SEA

Hugh D. Livingston, Ken O. Buesseler, Erol Izdar, and T. Konuk

The input to the Black Sea of fallout radioisotopes from the 26 April 1986 Chernobyl nuclear accident may be used to study both physical and biogeochemical processes in this unusual oceanic setting. We describe measurements of the concentrations, distributions, and paticle associations of ^{134}Cs, ^{137}Cs, ^{144}Ce, ^{106}Ru, and transuranic elements in surface waters of the southern Black Sea sampled in June and September 1986. Our measurements indicate that the Chernobyl tracer signal in surface waters of the southern Black Sea is both substantial and widespread - ^{137}Cs concentrations in the range 40-250 Bq/m^3 characterized waters from the Bosporus to the Caucasus. In addition, several vertical profiles of Cs isotopes down to the upper boundary of the anoxic bottom waters are used to address the question of the extent of physical mixing of the Chernobyl tracer signal after delivery to the sea surface. The vertical profile data permit an evaluation of the total Chernobyl Cs isotope deposition to these Black Sea water masses.

A comparison of the relative nuclide composition of surface waters sampled at different locations over time permits preliminary conclusions be drawn on the extent and relative rates of removal of reactive radionuclides from Black Sea surface waters. other data relevant to these questions come from measurements of the partition of the Chernobyl radiotracers between the filterable suspended particulate and dissolved phases of surface waters.

In Press: *International Symposium on Radioactivity and Oceanography, Radionuclides: A Tool for Oceanography*, June 2-5, 1987, Cherbourg, France.

Supported by: Coastal Research Center, ONR Contract N00014-85-C-0715, and NSF Grant OCE87-00715.

WHOI Contribution No. 6800.

ANOMALOUS LEVELS OF ^{90}SR AND $^{239,240}PU$ IN FLORIDA CORALS: EVIDENCE OF COASTAL PROCESSES

Caroline B. Purdy, Ellen R. M. Druffel and Hugh D. Livingston

Strontium-90, a radionuclide whose primary source is fallout from nuclear weapons testing, serves as a tritium-like tracer of ocean circulation.

The historical record of ^{90}Sr activities in the annual bands of island corals have been shown by other investigators to reflect the ^{90}Sr concentration in surface waters at those sites.

Strontium-90 activities measured in annual and seasonal bands in Montastrea annularis from the Florida Keys are 30-120% higher than that in corresponding peak activity years (1960-1965) of a Bermuda coral (Diploria). The Bermuda ^{90}Sr activity record reflects the fallout source only, whereas the additional ^{90}Sr activity in the Florida Keys is expected to reflect a coastal runoff source as well as the fallout. The coastal circulation patterns off the northern and western edge of the Florida Current further act to concentrate and prolong the exposure of the corals to runoff ^{90}Sr. Six measured $^{239,240}Pu$ activities in the Florida coral are 30% lower than $^{239,240}Pu$ activities in island coral records previously reported. Since Pu is expected to be scavenged by particles in coastal waters, this decrease in $^{239,240}Pu$ substantiates the importance of coastal influences in the Florida ^{90}Sr record.

Strontium-90 activities measured in subannual coral bands from 1973 to 1974 reflect seasonal changes in the ^{90}Sr concentrations in the surface layer of the coastal waters. This may reflect Loop Current intrusion events.

In Press: *Geochimica et Cosmochimica Acta.*

Supported by: NSF Grant OCE86-14545.

WHOI Contribution No. 6907.

VARIATIONS IN HOLOCENE SEDIMENTATION IN THE NORTH AMERICAN BASIN DETERMINED FROM TH-230 MEASUREMENTS

Daniel O. Suman and Michael P. Bacon

Excess ^{230}Th was measured in 20 sediment samples from the upper 251 cm of KNR31 GPC5, a giant piston core taken at a depth of 4583 m from a drift deposit on the northeastern Bermuda Rise, in an attempt to determine the cause of fluctuations in calcium carbonate percentage within the Holocene section. The excess ^{230}Th activity, corrected for radioactive decay since the time of deposition, is strongly correlated with $CaCO_3$ percentage, suggesting that both are controlled by the same factor(s). We conclude that the fluctuations in $CaCO_3$ percentage are due primarily to variations in the supply of the terrigenous (non-carbonate) components. From a simple model that assumes a constant supply of excess ^{230}Th, we estimate that during the past 11,000 yr the $CaCO_3$ flux in this region has remained within the narrow range 0.58 - 0.79 g cm $^{-2}$ kyr^{-1}. Non-carbonate flux, on the other hand, has varied during the same period by as much as a factor of 2.3 (1.25 - 2.84 g cm^{-2} kyr^{-1}). Non-carbonate flux maxima occur at ~1580 and ~3360 yr BP and coincide with enrichments of high latitude clay minerals. These features may reflect variations in the rate at which terrigenous sediment has been resuspended from the continental slope and transported to the interior of the basin. From the measured accumulation of excess ^{230}Th in radiocarbon-dated intervals, it can be shown that the degree of sediment focussing at the core site has increased by more than a factor of three since the beginning of the Holocene.

In Press: *Deep-Sea Research.*

Supported by: NSF Grant OCE84-17910.

WHOI Contribution No. 6873.

SEAWATER AND GEOCHEMISTRY

A TIME-SERIES STUDY OF THE VERTICAL STRUCTURE OF NITROGEN AND PARTICLE DYNAMICS IN THE SARGASSO SEA

Mark A. Altabet

Results are presented for the first 3 years of a time-series study of nitrogen and particle dynamics at a site near Bermuda using natural nitrogen isotopic ratios as an in situ tracer. Vertical structure in $\delta^{15}N$ values and other quantities vary both seasonally and interannually. At times during stratification, a $\delta^{15}N$ minimum and a concentration maxima in suspended PN are observed in association with the top of the nitracline at the base of the euphotic zone, and are indicative of NO_3^- utilization. However, the net transport of PN as sinking particles enriched in ^{15}N from the upper to lower half of the euphotic zone tend to weaken or erase these features. A return flux of nitrogen from the lower to upper half of the euphotic zone is required to prevent depletion of suspended PN in the upper 50 m on a 1 to 3 week time scale. The form that this flux takes remains uncertain. Previous applications of concepts of new versus regenerated production to subsections of the euphotic zone are, as a result, questioned. Persistently higher particle flux at 50 versus 100 m is opposite the findings of the VERTEX study for the N.E. Pacific; the upper half of the euphotic zone in the Sargasso Sea appears to be substantially less efficient at recycling nutrients than the euphotic zone as a whole, perhaps due to ecological differences between the two sites. Destruction of sinking particles within the euphotic zone is critical for determining both the overall

efficiency of nutrient recycling and the vertical variations observed. The particle flux entering the ocean's interior appears to originate from both the upper and lower halves of the euphotic zone.

Supported by: NSF Grants OCE84-16296 and OCE87-17508.

WHOI Contribution No. 6881.

TESTING MODELS OF PAST OCEAN CHEMISTRY USING FORAMINIFERAL $^{15}N/^{14}N$

Mark A. Altabet and William B. Curry

Previous models have attempted to explain glacial to interglacial changes in atmospheric pCO_2 by invoking changes in the ocean's nutrient concentration or regional changes in nutrient utilization. Nitrogen is limiting to primary production and has a residence time in the ocean compatible with glacial to interglacial variations. But, up to now, there has been no geological indicator for glacial to interglacial changes in the ocean's nitrogen cycle. We propose that $^{15}N/^{14}N$ ratios for the organic matrix of preserved foraminifera are likely to yield an interpretable $\delta^{15}N$ record. We have developed models to study the relationship between plausible changes in the ocean's nitrogen cycle and resulting changes in the $^{15}N/^{14}N$ ratio of dissolved NO_3^-. Our model results clearly demonstrate that $^{15}N/^{14}N$ ratios exhibit excursions during periods in which the oceans are accumulating or losing nitrogen regardless of the means by which these changes occur. Foraminiferal $^{15}N/^{14}N$ results for a Pacific and an Atlantic core provide evidence against wide-spread glacial anoxia, a consequence of many models of ocean chemistry. We suggest that increasing shelf-sediment denitrification upon deglaciation led to reduced nitrogen concentrations in the modern ocean. Ambiguities between the two foraminiferal $^{15}N/^{14}N$ records indicate that local effects associated with changes in hydrography or ecology need to be studied further.

Supported by: Mellon Award and NSF Grants OCE83-09124, OCE85-11014 and OCE88-00693.

WHOI Contribution No. 6854.

CHEMISTRY OF HOT SPRINGS ON THE MID-ATLANTIC RIDGE

A. C. Campbell, M. R. Palmer, G. P. Klinkhammer, T. S. Bowers J. M. Edmond, J. R. Lawrence, J. F. Casey, G. Thompson, S. Humphris, P. Rona, and J. A. Karson

The first hydrothermal fluid samples collected along the slow-spreading Mid Atlantic Ridge (MAR) are remarkably similar in composition and temperature to fluids collected along the shallower, faster-spreading East Pacific Rise (EPR). The MAR fluids, like those from the EPR, appear to be in equilibrium with a greenschist-facies mineral assemblage. In contrast to the EPR, the more fractured nature of the MAR apparently allows fluids at one of the MAR sites to interact with weathered basalt.

Published in: *Nature* 335, 514-519.

Supported by: NSF Grant OCE84-11979.

THE EFFECT OF BOUNDARY CONDITIONS ON TRACER ESTIMATES OF THERMOCLINE VENTILATION RATES

Scott C. Doney and William J. Jenkins

Using a simple box mixing model, we show that ventilation rate estimates are inherently tracer specific, controlled by the surface boundary condition for the particular tracer. Ventilation rates for rapidly exchanging tracers (e.g., ^3He) are close to the fluid ventilation rate while tracers with limited surface exchange (e.g., tritium) ventilate more slowly. The ratio of ventilation rates for rapidly equilibrating tracers to limited surface exchange tracers is equal to the ratio of winter to summer mixed layer depths. The distribution of rapidly equilibrating tracers more accurately tracks climatological fluctuations in water mass formation rates compared to limited surface exchange tracers which show a damping proportional to the ratio of summer to winter mixed layer depths. To compare model results with observations, we calculate ^3He and tritium ventilation rates for data from the eastern subtropical North Atlantic. In calculating the tritium ventilation, we develop a North Atlantic tritium source function for the model from reported surface data. On shallow density surfaces ($\sigma\theta$ <27.0), the tritium ventilation rates are 2-3 times lower than those of ^3He. Deeper in the thermocline, the two ventilation rates approach each other. This trend with increasing density is related to the decreasing effectiveness of ^3He gas exchange at the more northerly isopycnal outcrops. Finally, box models using limited surface exchange tracers (e.g., ^{14}C and tritium) can underpredict oxygen utilization rates (OUR) by up to 3 times due to the difference between tritium and oxygen boundary conditions. In contrast, 3He ventilation ages overpredict OUR by about 20%.

Published in: *Journal of Marine Research* 46, 947-965, 1988.

Supported by: NSF Grants OCE78-19815 and OCE78-21378; a Graduate Fellowship from the

National Science Foundation, and the WHOI/MIT Joint Program.

WHOI Contribution No. 6765.

SEASONALLY ABUNDANT PLANKTONIC FORAMINIFERA OF THE SARGASSO SEA: SUCCESSION, DEEP-WATER FLUXES, ISOTOPIC COMPOSITIONS, AND PALEOCEANOGRAPHIC IMPLICATIONS

Werner G. Deuser and Edith H. Ross

A suite of 31 two-month sediment-trap samples from the deep Sargasso Sea, collected over six years, provided data on seasonal variations in flux and oxygen and carbon isotopic composition of twelve species of seasonally abundant planktonic foraminifera. The order of succession in the course of the calendar year was Pulleniatina obliquiloculata, Globorotalia truncatulinoides, Globigerina bulloides, Globorotalia inflata, Globorotalia hirsuta, Globigerinita glutinata, Neogloboquadrina dutertrei, Globorotalia crassaformis, Globigerinoides sacculifer, Globigerinoides ruber (pink var.), Globigerina rubescens, and Globigerinoides conglobatus. The timing and succession of the flux peaks is very similar to population data derived from plankton tows two decades earlier. The pink variety of G. ruber occurs only during times of surface-water stratification and has several characterisitics besides pigmentation, especially size and isotopic composition, which distinguish it clearly from the perennially abundant white variety. All twelve species occurred in significant numbers for two to six months each year and were very rare or completely absent during the remaining months. Peak fluxes of different species ranged from single tests to 300 tests per square meter and day. Most species underwent distinct annual cycles in average weight of their tests. Average annual flux of all planktonic foraminifera, including perennially abundant species, is close to 100,000 individuals or 1 g m^{-2}. The total flux of foraminiferal calcite is about one-third that of coccolith calcite, but slighly greater than that of pteropod/heteropod aragonite. Comparisons of the oxygen isotopic composition of the eight more abundant species with equilibrium compositions for calcite, calculated from Station "S" temperature and salinity data for the upper 1200 m, place tight constraints on their depth habitats and deviations from isotopic equilibrium. For paleoceanographic purposes, different species can be used as indicators of hydrographic conditions (mainly temperature) as follows: P. obliquiloculata, G. inflata, and N. dutertrei for winter mixed-layer (0-100 m); G. bulloides for 50-100 m throughout the year, but very rare during summer; G. conglobatus for 75-100 m during fall; G. ruber (pink) for surface water in summer. Whole tests of G. truncatulinoides and G. hirsuta appear to record average conditions at 200 and 600 m, respectively, but in reality those averages are the result early-life test building near the surface and later calcite-crust deposition near 800 m for G. truncatulinoides and near 1000 m for G. hirsuta. Analyses of specimens taken from the surface sediment at the study site yielded reasonable "paleotemperatures" for the seasons and depths characterized by the different species and confirmed the practicality of deriving past seasonality and mixed- layer depths from sedimentary assemblages. The seasonal variations of the carbon isotopic compositions of G. ruber (pink) and G. truncatulinoides appear to reflect the extent of photosynthetic carbon fixation near the surface and of its respiration above 800 m. Extension of this type of study to other parts of the ocean could significantly enhance our ability to read paleoclimatic and paleoceanographic fine print in the sedimentary record.

Supported by: NSF Grants OCE76-21280, OCE78-19813, OCE80-24130, OCE82-19588, OCE84-17910 and OCE85-01955.

WHOI Contribution No. 6904.

ESTIMATES OF WINTERTIME MIXED LAYER NUTRIENT CONCENTRATIONS IN THE NORTH ATLANTIC

David M. Glover and Peter G. Brewer

Nonlinear, time dependent model sensitivity to initial conditions poses a challenging problem when attempting to initialize such a model. In order to initialize a chemical-physical model of the upper several hundred meters of the North Atlantic, we have calculated the initial concentrations of several chemical species from three estimation methods by a combination of the Climatological Atlas of the World Ocean (Levitus, 1982) and the TTO north, and tropical, Atlantic study databases. A 1°x1°grid of the average initial concentrations over the mixed layer depth was generated for the method of preference and added to the initialization data base of the model. Contour maps of this calculated initial concentration set are presented and comparisons with the other methods and actual data are made.

Published in: *Deep-Sea Research* 35, 1525-1546, 1988.

Supported by: ONR Contract No. N00014-85-C-0001 and University of New Hampshire subcontract No. 85-12.

WHOI Contribution No. 6726.

HELIUM, LEAD, STRONTIUM AND NEODYMIUM ISOTOPE CONSTRAINTS ON MAGMA GENESIS AND MANTLE HETEROGENEITY BENEATH YOUNG PACIFIC SEAMOUNTS

David W. Graham, Alan Zindler, Mark D. Kurz, William J. Jenkins, Rodey Batiza, and Hubert Staudigel

Pb, Sr and Nd isotope variations are correlated in diverse lavas erupted at small seamounts near the East Pacific Rise. Tholeiites are isotopically indistinguishable from MORB ($^{206}Pb/^{204}Pb$ = 18.1-18.5; $^{87}Sr/^{86}Sr$ = 0.7023-0.7028; $^{143}Nd/^{144}Nd$ = 0.51326-0.51308); associated alkali basalts always show more radiogenic Pb and Sr signatures ($^{206}Pb/^{204}Pb$ = 18.8-19.2; $^{87}Sr/^{86}Sr$ = 0.7029-0.7031) and less radiogenic Nd ($^{143}Nd/^{144}Nd$ = 0.51289-0.51301. The isotopic variability covers ~80% of the variability for Pacific MORB, due to the presence of small-scale heterogeneity in the underlying mantle. Isotope compositions also correlate with trace element ratios such as La/Sm.

Tholeiites at these seamounts have $^{3}He/^{4}He$ between 7.8-8.7 RA (RA = atmospheric ratio), also indistinguishable from MORB. He trapped in vesicles of alkali basalts, released by crushing in vacuo, has low $^{3}He/^{4}He$ (1.2-2.6 R_A) in conjunction with low helium concentrations ([He] $<5 \times 10^{-8}$ ccSTP/g). In many cases post-eruptive radiogenic ingrowth has produced He isotope disequilibrium between vesicles and glass in the alkali basalts; subatmospheric $^{3}He/^{4}He$ ratios characterize the He dissolved in the glass which is released by melting the crushed powders. The narrow range of $^{3}He/^{4}He$ in the vesicles of the alkali basalts suggests that low $^{3}He/^{4}He$ is a source characteristic, but given their low [He] and high (U+Th), pre-eruptive radiogenic ingrowth cannot be excluded as a cause for low inherited $^{3}He/^{4}He$ ratios.

Pb, Sr, and Nd isotope compositions in lavas erupted at Shimada Seamount, an isolated volcano on 20 m.g. old seafloor at 17°N, are distinctly different from other seamounts in the East Pacific ($^{206}Pb/^{204}Pb$ = 18.8-19.0, $^{87}Sr/^{86}Sr \cong 0.7048$ and $^{143}Nd/^{144}Nd \cong 0.51264$). Relatively high $^{206}Pb/^{204}Pb$ (15.6-15.7) indicates ancient (>2 Ga) isolation of the source from the depleted upper mantle, similar to Dupal components which are more prevalent in the southern hemisphere mantle. $^{3}He/^{4}He$ at Shimada Seamount is between 3.9-4.8 R_A. Because the helium concentrations range up to 1.5×10^{-6}, the low $^{3}He/^{4}He$ cannot be due to radiogenic accumulation of ^{4}He in the magma for reasonable volcanic evolution times. The low $^{3}He/^{4}He$ may be due to the presence of "enriched" domains within the lithosphere with high (U+Th)/He ratios, possibly formed during its accretion near the ridge. Alternatively, the low $^{3}He/^{4}He$ may be an inherent characteristic of an enriched component in the mantle beneath the East Pacific.

Collectively, the He-Pb-Sr-Nd isotope systematics at East Pacific seamounts suggest that the range of isotope compositions present in the mantle is more readily sampled by seamount and island volcanism than by axial volcanism. Beneath thicker lithosphere away from the ridge axis, smaller degrees of melting in the source regions are less efficient in averaging the chemical characteristics of small-scale heterogeneities.

Supported by: NSF Grants OCE85-15270 and OCE85-16082.

WHOI Contribution No. 6719.

MORPHOLOGY, GEOCHEMISTRY, AND EVOLUTION OF SEROCKI VOLCANO

Susan E. Humphris, Wilfred B. Bryan, Geoffrey Thompson and Laurie K. Autio

Basalts collected during drilling and diving programs on Serocki Volcano mostly fall within a limited compositional range, and are moderately evolved, normal MORBs with distinctive high MgO contents (averaging 7.60 wt%) and high Al_2O_3 concentrations (averaging 16.14 wt% in whole rocks samples). However, samples recovered from within the central crater have lower TiO_2 and FeO*/MgO, and higher MgO and Al_2O_3 concentrations, and are most similar to glasses recovered at Site 649 about 45 km to the north. Comparison of the observed geochemical variations with experimental work and other samples from the region suggests that the Serocki Volcano and Site 649 data are compatible with crystal- liquid fractionation involving both olivine and early-stage clinopyroxene, as well as plagioclase, and that the sources may be similar even though Sites 648 and 649 are located in different, but adjacent, spreading cells.

Consideration of the stratigraphy and morphology of Serocki Volcano suggests that this function is more properly described as a megatumulus or lava delta, associated with a steeper, conical peak to the southwest. The evolution of Serocki Volcano involved early construction of a marginal rampart of pillows, followed by doming of this feature and the formation of a perched lava pond. Draining of this pond resulted in collapse and the formation of the central crater.

In Press: *Initial Reports Ocean Drilling Program Legs* 106/109.

Supported by: USSAC Grants through Texas A&M Foundation and NSF Grants OCE85-11979 and OCE85-10847.

WHOI Contribution No. 6821.

EXPOSURE-AGE DATING WITH COSMOGENIC ^{3}HE AND ITS APPLICATION TO GEOMAGNETISM

Mark D. Kurz, Debra Colodner, Thomas W. Trull, and Daniel E. Sampson

The presence of in situ produced cosmogenic ^{3}He in terrestrial surface rocks is now well documented; if the production rate of ^{3}He can be accurately predicted, then the accumulation of cosmogenic ^{3}He will become a valuable geochronological tool. In a previous paper, we attempted to constrain the production rate by measuring the cosmogenic ^{3}He in a single Hawaiian radiocarbon dated lava flow. This paper extends the approach to a number of ^{14}C dated Hawaiian lava flows ranging in age from 640 to 13000 years. The production rate varies from 40 to 200 atoms g^{-1} yr^{-1} over this time period, with a pronounced minimum between 2000 and 5000 years (before present), which we attribute to modulation of cosmic ray flux due to fluctuations in the strength of the earth's dipole field. The results demonstrate that cosmogenic helium will be a valuable tool not only for exposure age dating but for constraining paleomagnetic field intensities.

Supported by: NSF Grant No. EAR76-10611.

WHOI Contribution No. 6698.

RADIONUCLIDE GRADIENTS IN TWO MN OXIDE DEPOSITS FROM THE MID-ATLANTIC RIDGE: POSSIBLE INFLUENCE OF A HYDROTHERMAL PLUME

Claude Lalou, Evelyne Brichet, and Geoffrey Thompson

During a 1973 Atlantic II oceanographic cruise in the North Atlantic, two MnFe oxide deposits were recovered in the same dredge haul, 135 km west of the Mid Atlantic Ridge axis at 23°N. One of them is Mn-rich and has mineralogical and chemical characteristics generally attributed to hydrothermal deposits; the other is more comparable to typical hydrogenous ferromanganese deposits. A radiochemical study based on the observed decrease of $^{230}Th_{excess}$ with depth in the sample suggests a hydrogenous origin for both samples, with growth rates around 20 mm/10^6 years. However, one of the samples consists mainly of well- crystallized todorokite, with a very low U content (1 ppm) and no detectable Th; these features point to a hydrothermal origin for one of the samples. In both samples decreasing gradients with depth for ^{232}Th and ^{238}U, as well as the near-constant ^{230}Th/^{232}Th ratios, render questionable the use of the excess ^{230}Th method to calculate growth rates. To explain the observed gradients with depth, a qualitative model based on the scavenging properties of oxyhydroxides for trace elements is proposed. In this model the gradients reflect primary chemical rather than radioactive decay gradients, and result from change in the composition of a hydrothermal plume.

Published in: *Canadian Mineralogist 26*, 713-720, 1988.

Supported by: NSF Grant No. OCE85-10847.

WHOI Contribution No. 6227.

CARBON CYCLING IN COASTAL SEDIMENTS: 1. A QUANTITATIVE ESTIMATE OF THE REMINERALIZATION OF ORGANIC CARBON IN THE SEDIMENTS OF BUZZARDS BAY, MA

Ann P. McNichol, Cindy Lee, and Ellen R. M. Druffel

Seasonal remineralization rates of organic carbon are calculated in the top 20-30 cm of biologically irrigated, organic-rich sediments of Buzzards Bay, MA. Six cores were collected over a period of two years, and the pore water concentrations of the following species were measured: dissolved inorganic carbon (ΣCO_2), PO_4^{3-}, ΣH_2S, Alk, and Ca^{2+}. Overall, these constituents showed large gradients with depth, which are larger in summer than in winter.

Remineralization rates in the sediments were estimated by applying a nonlocal exchange, vertical molecular diffusion, reaction model to the ΣCO_2 depth profiles. The major processes affecting the pore water concentration of ΣCO_2 described in the model are diffusion, irrigation, and the oxidation of organic carbon. The calculated remineralization rates varied seasonally with the high of 7.5 x 10^{-9} mol/L-sec observed in August 84 and the low (0.6 x 10^{-9}) in December 1983. The remineralization rates were dependent on the amount of irrigation in the sediments. It was possible to calculate remineralization rates between 0 and 20 cm because the amount of irrigation was well-characterized at this site. We calculated that 69 gC/m^2 are oxidized annually and 5-33 gC/m^2-yr are buried. It appears that there is a highly reactive portion of organic matter which is oxidized at the sediment water interface.

Examination of the Alk and dissolved Ca^{2+} profiles indicates that there was significant production of acid which dissolved $CaCO_3$ in the spring and early summer.

Published in: *Geochimica et Cosmochimica Acta*, 52, 1531-1543, 1988.

Supported by: NSF Grants OCE83-15412, OCE84-2179, and OCE84-16632; Coastal Research Center Grant; and WHOI/MIT Joint Program.

WHOI Contribution No. 6763.

$\delta^{13}C$, TCO_2, AND THE METABOLISM OF ORGANIC CARBON IN THE DEEP SEA SEDIMENTS

Frederick L. Sayles and William B. Curry

The stoichiometry and rates of benthic sediment metabolism at five stations have been determined on the basis of the carbon released to the pore waters as TCO_2. The stations cover a range of redox conditions permitting an evaluation of stoichiometry in oxic environments and under conditions where both denitrification and manganese reduction occur. At four of the five stations the flux of TCO_2 from the sediment is significantly enriched in ^{13}C relative to predictions from traditional Redfield ratio based stoichiometry. The Ca^{2+}:TCO_2 stoichiometry under oxic conditions also appears to depart systematically from predicted values, being consistently lower than model calculations.

The heavy isotopic composition of the flux can be explained in two ways. The TCO_2 derived from organic matter may be fractionated relative to the organic matter intercepted in sediment traps set in the general areas studied. Alternatively, the heavy isotopic composition of the flux may result from the neutralization of as much as 1/3 of the metabolic acid produced in diagenesis by CO_3^{2-} diffusing into the sediment from the overlying water.

Rates of sub-oxic diagenesis, determined from flux estimates across redox boundaries, are usually small compared to oxic rates. However, at the most reduced stations studied sub-oxic rates are quite substantial, accounting for up to 30-45% of the total TCO_2 flux.

Published in: *Geochimica et Cosmochimica Acta 52*, 2963-2978, 1988.

Supported by: NSF Grants OCE84-12142 and OCE87-11962.

WHOI Contribution No. 6870.

ARTIFACTS ASSOCIATED WITH THE CHEMICAL LEACHING OF SEDIMENTS FOR RARE EARTH ELEMENTS

Edward R. Sholkovitz

Using radioactive europium as a tracer for rare earth elements (REE), simple experiments were carried out to determine if a readsorption artifact occurs during the chemical leaching of marine sediments. Commonly used chemical leaching solutions (14 in total) were used with and without (controls) the presence of Buzzards Bay sediment. All controls show 100% recovery of soluble ^{152}Eu, indicating no adsorption or precipitation during handling. In contrast, almost all chemical leaching solutions show poor recoveries even at low (2-4) pH. Even for HCl and HNO_3, recoveries ranged from 85% to 25% at 0.2 M or less. Hydroxylamine hydrochloride in acetic acid, for example, shows only 33% and 57% recoveries for 0.02 M and 0.04 M concentrations.

The results show that large-scale readsorption of REE onto sediments occurs even at low pH associated with mineral acids, organic chelators, and reductive solutions. Given their large hydrolysis constants, a case is made that one would expect that REE, like Pb and Th, to exhibit significant readsorption onto sediments following their dissolution from specific phases. The results reinforce concerns in the literature that chemical leaching techniques have major artifacts associated with non-selectivity and readsorption of trace metals. Interpretations of REE diagenesis and authigenesis, based on chemical leaching data, should be viewed with caution.

Supported by: NSF Grant OCE85-15695.

WHOI Contribution No. 6911.

THE PORE WATER CHEMISTRY OF RARE EARTH ELEMENTS IN BUZZARDS BAY SEDIMENTS

Edward R. Sholkovitz, Donald J. Piepgras, and Stein B. Jacobsen

A 72 cm pore water profile of rare earth elements (REE) is presented from Buzzards Bay sediments and extends our understanding of the diagenetic chemistry of REE beyond that of an earlier study at this location. In the upper half of the core, the diagenetic input of REE into pore waters is accompanied by the preferential release of light REE (LREE) and middle REE (MREE) relative to heavy REE (HREE). Near 40 cm, pore water concentrations reach values 10-20 times (30 times for Ce) those of bottom water. In the lower half of the core, removal of all REE occurs with

LREE and MREE being preferentially removed relative to HREE (Er, Yb, Lu). Concentrations of REE in the 66-72 cm horizon are 7-8 times (Ce, 16 times) bottom water values. Ce behaves anomalously with the greatest positive anomalies restricted to the upper 9 cm where Ce redox cycling is most active. The REE are involved in complex diagenetic chemistries of unknown kinds. As recently reported for the Cariaco Trench water column, the cycling and fractionation of REE is strongly influenced by redox conditions. The active diagenesis of REE in reducing coastal sediments indicates that caution must be applied when using Ce anomalies of sedimentary biogenic phases as paleoredox indicators of ancient oceans.

Supported by: NSF Grant OCE85-15695.

WHOI Contribution No. 6931.

RATES OF VERTICAL MIXING, GAS EXCHANGE, AND NEW PRODUCTION: ESTIMATES FROM SEASONAL GAS CYCLES IN THE UPPER OCEAN NEAR BERMUDA

William S. Spitzer and William J. Jenkins

Argon measurements, obtained from more than one year of monthly detailed vertical profiles near Bermuda (32°N 64°W), show a maximum in argon super- saturation of about 4% in the seasonal thermocline in late summer. Since the argon supersaturation is 3-4 times smaller than that of oxygen, most of the oxygen supersaturation is not of physical origin and hence must result from biological production.

In the winter mixed layer, air injection produces argon supersaturation in spite of high gas exchange rates. During spring and summer, radiative heating, air injection, and an upward argon flux create an even larger supersaturation in the mixed layer. In the seasonal thermocline, radiative heating maintains argon concentrations above solubility equilibrium in spite of vertical mixing.

The observed seasonal cycles of temperature, argon, helium, and oxygen are coupled with an upper ocean model. We linearized the model's response to variations in vertical diffusivity, air injection, gas exchange rate, and new production, and then used an inverse technique to determine the values of these parameters that best fit the data. A vertical turbulent diffusivity of $0.9\pm0.1 \times 10^{-4}$ m^2 s^{-1} is consistent with both the thermal history and subsurface argon distribution. The rate of air injection, determined to ±25%, is similar to previous estimates. The seasonally-averaged gas exchange rate is 17±12% lower than predicted by Liss and Merlivat (1986). We estimate a lower limit to depth- integrated new production of 4.4 ± 1.8 moles O_2 m^{-2} yr^{-1} during 1985, and obtain an estimate of 5.5 ± 1.5 moles O_2 m^{-2} yr^{-1} if new production near the surface is fixed at zero.

Published in: *Journal of Marine Research 47*, 169-196, 1989.

Supported by: NSF Grant OCE85-01171.

WHOI Contribution No. 6799.

AXIAL VOLCANISM ON THE EAST PACIFIC RISE, 10-12°N

Geoffrey Thompson, Wilfred B. Bryan, and Susan E. Humphris

The East Pacific Rise axis, 10-12°N, consists of three discrete topographic or tectonic units each of which has erupted compositionally distinct magmas. The two major units have an axial bathymetric high, are bounded by transform or overlapping spreading centers, and are shown to be discrete volcanoes. One of the units shows systematic variation in magma composition along the rift consistent with injection of lava down-rift and concomitant low pressure fractional crystallization with distance from the topographic high. Compositional variation within and between magmatic units is largely controlled by fractional crystallization at low and intermediate pressures. The eastern and western limbs of a large over-lapping spreading centre about 11°45'N have compositionally distinct lavas apparently from separate magma batches. Axial eruptions in the vicinity of a large transform fault (Clipperton Fracture Zone) show a large variation in composition and at least one independent magma injection. Highly fractionated lavas with compositions up to 59% silica are included in these eruptions. One of the axial tectonic units has, in addition to normal tholeiitic eruptions, some lavas highly enriched in incompatible elements such as K, Ti, Sr, Ba, Zr and La. These lavas are also isotopically enriched with respect to $^{87}Sr/^{86}Sr$, suggesting that the mantle beneath some portions of the axis is compositionally heterogenous. The presence of compositionally distinct magma batches, often in close proximity, suggests that magma chambers underlying the EPR axis are small and probably intermittent.

Published in: *"Magmatism in the Ocean Basins", eds. A. D. Saunders and M. J. Narry, Geol. Soc. Sp. Publ. 42*, pp. 181-200.

Supported by: NSF Grant No. OCE83-09977.

WHOI Contribution No. 6729.

HELIUM AND STRONTIUM ISOTOPIC CONSTRAINTS ON THE ORIGIN OF ISLAND ARC MAGMAS IN THE WOODLARK BASIN-SOLOMON ISLANDS REGION

Thomas W. Trull, Michael R. Perfit, and Mark D. Kurz

In an effort to better understand the sources of volatiles and compositional variations in island arc magmas helium and strontium isotopes were measured in lavas from the northeastern edge of the Woodlark Basin, the site of subduction of the Woodlark spreading center (WSC) beneath the volcanically active New Georgia island group of the Solomon Islands arc in the western Pacific. Helium isotope ratios ($^3He/^4He$) range from less than 1 to more than 9 times the atmospheric ratio (R_a) in glasses, whole rocks, and mineral separates of dredged volcanic rocks. Low concentrations and isotopic disequilibrium between helium released by crushing and melting in vacuo suggest that addition of helium by radiogenic decay and diffusion from seawater produces part of this variability. In other samples, where the magmatic $^3He/^4He$ ratio can be recovered, an important result is that Kavachi Volcano, presently active in the Solomon Islands forearc, exhibits $^3He/^4He$ ratios of $6.9\pm .2$ R_a, significantly lower than is observed in WSC tholeiitic basalts (8-9 R_a, similar to mid-ocean-ridge-basalts). This difference may be explained as a contribution of radiogenic helium from subducted oceanic crust, or less probably as the result of degassing and 4He ingrowth during long (more than 10,000 yr.) magma transport times.

Strontium isotope ratios ($^{87}Sr/^{86}Sr$) range from lows near 0.7026 in normal Mid-ocean-ridge-basalts (MORB) and NaTi basalts from the Woodlark Basin to a high greater than 0.7040 in a calcalkaline dacite in the forearc region; transistional rock types have intermediate values. Strontium isotopes and concentrations in fresh samples exhibit systematic increases from the WSC toward the active arc, suggesting a smooth spatial variation in source composition. Examined together the helium and strontium isotope data suggest that the Kavachi magmas are derived from an upper mantle source that was contaminated by subduction of Pacific lithosphere during the Miocene. Involvement of a fluid phase distinct from silicate melt in their formation may occur in the source region, but does not appear to be directly related to magmagenesis.

Supported by: NSF Grants OCE85-16082 and OCE87-16970.

WHOI Contribution No. 6720.

DEPARTMENT OF GEOLOGY AND GEOPHYSICS

David A. Ross, Chairman

PERFORMANCE OF BEACH NOURISHMENT AT JUPITER ISLAND, FLORIDA

D. G. Aubrey and N. M. Dekimpe

The Town of Jupiter Island, Florida, has a five mile length of shoreline that is undergoing significant erosion. The dominant factors contributing to erosion along Jupiter Island are the narrowness of the continental shelf offshore, lack of sheltering of ocean waves by the Bahama Banks, and interruption of longshore sand transport by the jetties protecting the entrance to the artificially-opened St. Lucie Inlet to the north. Since the mid-1950's, beach stabilization measures have been carried out in an attempt to preserve the shoreline. Four major beach nourishment efforts contributing more than 8 million cubic yards of sediment (at a cost of $11,500,000), several earlier smaller nourishment efforts contributing an additional 1 million cubic yards, and the construction of nearly 5 miles of seawalls and revetments combined with more than 3 miles of coast protected by groins, all have been used to mitigate the widespread erosion at this location. Beach nourishment since 1972 has relied on sand dredged from a barrow area located 3500 feet offshore of the beach. Economic considerations preclude the use of the higher quality material off St. Lucie Inlet, whose extent and quality have not been proven yet by extensive coring and profiling. Cost per cubic yard for coarser St. Lucie sands is approximately 4 to 6 times that of the offshore borrow area (where in the latest 1987 nourishment effort sand was obtained at a cost of $1.62 per cubic yard placed). While the poorer quality borrow material results in higher turbidity, greater losses in the fill, and reduced duration of the nourishment effort, the economics of using coarser sands are purely theoretical at this point and have not convinced the Town of Jupiter Island that the coarser sand is worth the higher initial cost and the risks of losing the sands equally rapidly. Scientific and engineering understanding of the performance of beach fill must be improved before complete confidence can be placed in the calculations of beach stability. Without this improved understanding, considerable risks are taken by project proponents who elect to use much higher cost, but better quality, beach sands for nourishment projects.

In Press: *Performance of Beach Nourishment at Jupiter Island, Florida.*

Supported by: WHOI Coastal Research Center; Aubrey Consulting Incorporated.

WHOI Contribution No. 6759.

RECENT GLOBAL SEA LEVELS AND LAND LEVELS

David G. Aubrey and K.O. Emery

Tide gauge records from around the world ambiguously document the rise and fall of relative sea levels during the past century. Analysis of these records, nonuniformly distributed in time and space, reveals that land levels as well as ocean levels are changing, making difficult the estimation of sea-level change alone. Because most tide gauges are concentrated in the northern hemisphere instead of the southern hemisphere (where most ocean area is located), tide-gauge data reflect major continental motions due to glacio-isostasy and neotectonism, suppressing and masking the signal from eustatic sea-level change. Estimation of the magnitude of sea-level change is important for many reasons, including interpretation of possible effects of global climate change resulting from carbon dioxide and other trace-gas loading of the atmosphere. Proper interpretation of past sea-level changes is required to calibrate and assess global climate models and observations of past climate change. The oceanic lag to atmospheric temperature change can be determined from study of tide-gauge records and other records of relative sea levels only if land level changes are separated from sea-level changes.

In Press: *Proceedings Climate Change Workshop, Norwich, U.K.*

Supported by: NSF Grant OCE85-01174, the Coastal Research Center, & Ocean Industry Program.

WHOI Contribution No. 6876.

UPPER TRIASSIC-LOWER JURASSIC SALT BASIN SOUTHEAST OF THE GRAND BANKS

James A. Austin, Brian E. Tucholke and Elazar Uchupi

A grid of multichannel seismic reflection (MCS) profiles has been used to delineate and map a large evaporite basin (Salar basin) beneath the continental slope and rise southeast of the Grand Banks of Newfoundland. The Salar basin is a major, hitherto unrecognized rift basin that is approximately 400 km long, 35-70 km wide, and covers an area of approximately 20,000 km^2. It parallels the Carson basin which lies beneath the Grand Banks immediately to the west and merges with this basin north of 45°20'N. The southern end of the basin is marked by the intersection of the

Southeast Newfoundland Ridge with the South Bank High on the Grand Banks, and the northern end is bounded by the southwestern margin of Flemish Cap. Based upon correlation with contiguous deposits sampled by drilling in the Carson basin, the evaporites filling the Salar basin are inferred to be of Late Triassic-Early Jurassic age, and they probably are predominantly halite.

An early Mesozoic age for the Salar basin implies a multi-stage rifting history for the Newfoundland Basin as has been documented for the adjacent Grand Banks. Initial rifting occurred in Late Triassic-Early Jurassic time, and was associated with rifting of North American from Africa and extension in western Europe. The presence of a large evaporite basin suggests development of a significant, but shallow and restricted, seaway between the Grand Banks and the Iberian peninsula, most likely connected northward with the salt provinces of northwestern Europe. During the Early and Middle Jurassic, evaporites in the Salar basin probably were capped with clastic and carbonate deposits as the basin subsided epeirogenically. A second rift phase associated with the separation of Iberia and the Grand Banks affected the Grand Banks and Salar basin in Late Jurassic to Early Cretaceous time. Uplift related to this rifting led to the development of the widespread "U" (Avalon) unconformity across the Grand Banks, the Salar basin, and the Newfoundland Basin out to the J Anomaly. Associated tectonism may have induced the first halokinesis in the Salar basin. The second rift phase culminated in the initiation of sea-floor spreading in mid-Cretaceous (Aptian) time at a location now marked by the J Anomaly.

In Press: *Earth and Planetary Science Letters.*

Supported by: NSF Grant OCE83-09085.

WHOI Contribution No. 6734.

TIDE GAUGES OF INDIA

K.O. Emery and D.G. Aubrey

India contains most of the tide-gauge stations (12) of the Indian Ocean from which mean annual relative sea levels can be computed for estimating long-term trends. However, two records are too short, three have poor statistical confidence, and four appear to be much influenced by episodic high sea levels caused by cyclonic storm surges or monsoonal floods, or alternately by poor tide-gauge recordings. The five remaining station records that appear usable (three on the west coast and two on the east coast) reveal trends between +1.33 and -2.27 mm/year with an average of minus 0.67 mm/year, indicating relative sinking of land. The evidence is unclear whether these records document real sinking of land or real eustatic rise of sea level. Regardless of the present cause, increased submergence may be expected in coming decades owing to higher temperatures (greenhouse effect of worldwide burning of fossil fuels) that can expand the volume of ocean water as well as augment the return of glacial meltwater. The making and study of repeated precise leveling surveys on land combined with information from satellites may quantify the relative roles of sinking coastal land belts relative to inland areas (subsidence of coasts) versus increasing volume of ocean water in causing intrusion of the ocean.

In Press: *Journal of Coastal Research.*

Supported by: NSF Grant OCE85-01174 and the Ocean Industry Program.

WHOI Contribution No. 6809.

AN OVERVIEW – MARINE MINERAL RESERVES AND RESOURCES – 1988

K.O. Emery and J.M. Broadus

Marine mining has been conducted on a local and generally small scale for thousands of years. Large-scale recovery from beaches and piers began only about forty years ago, and soon afterward powered ships and tools and new exploration methods revealed the presence of economic concentrations of oil and gas, sand and gravel, and some heavy minerals beyond the beach. These materials are in relatively shallow waters of the continental shelf and snow are known well enough to be considered reserve ores. Rapid success for them led to immediate expectation of marine mining of many other minerals that have higher value per unit weight, but they occur in deeper waters beyond the shelf where conditions are more difficult and costs are higher. They include phosphorite, ferromanganese nodules and crusts, and (less than a decade ago) polymetallic sulfides. All are still potential resources that cannot yet be considered reserve ores.

Increased knowledge of the deep-ocean floor and its natural processes is likely to be applied first to expanding the reserves of similar deposits now on land and perhaps later to ocean-floor mining. Moreover, ocean-floor mining must compete economically with improved methods of recovery from existing low-grade resources on land and from waste piles left from earlier and less efficient methods of mineral recovery.

In Press: *1988 International Far East Conference on Marine Mineral Resources. Also in Marine Mining.*

Supported by: Pew Charitable Trust and NOAA Sea Grant NA86-AA-D-SG090.

WHOI Contribution No. 6738.

BALLAST FROM H.M.S. ENDEAVOUR LEFT AT GREAT BARRIER REEF, AUSTRALIA, IN 1770

K.O. Emery and W.B. Bryan

A piece of ballast, offloaded by Captain James Cook when his ship grounded on a reef in the long lagoon off the eastern coast of Australia more than two hundred years ago, was examined for its mineralogy and chemical composition. Cook's log indicates that the original ballast was supplemented at Cook Strait in New Zealand and at Raiatea in the Society Islands before the grounding. The chemistry and petrography of this rock shows that this particular piece of ballast came from Raiatea, illustrating the usefulness of geology as a supplement for historical and archaeological records.

In Press: *Queensland Geological Survey Bulletin.*

Supported by: Ocean Industry Program.

WHOI Contribution No. 6936.

CHANGED LATE QUATERNARY MARINE ENVIRONMENTS ON ATLANTIC CONTINENTAL SHELF AND UPPER SLOPE

K.O. Emery, A.S. Merrill and E.R.M. Druffel

About 2000 large sediment samples were collected during the early 1960s throughout the continental shelf off the Atlantic coast of the United States to establish and map sediment types including sediments relict from times of glacially low (and subsequently higher) sea levels. In about 510 of these samples we found fossil shells of mollusks remaining from environmental conditions different from those at present. Publications and collections by others contain about 70 additional samples having relict mollusks. Some of these shells indicate lower sea levels, others–colder water, and still others–warmer water than now is present. Radiocarbon measurements from earlier studies by us and others established the dates of colder water (Late Pleistocene), and we made additional measurements to learn the dates of warmer water (about 1000 to 2000 years ago). The results show reasonably enough that continental shelves are the sites of relict faunas as well as of sediments that indicate changed and complex environmental histories.

Published in: *Quaternary Research*, 70, 251-269, 1988.

Supported by: Ocean Industry Program.

WHOI Contribution No. 6818.

NON-LINEAR TIDAL DISTORTION IN SHALLOW WELL-MIXED ESTUARIES: A SYNTHESIS

Carl T. Friedrichs and David G. Aubrey

The importance of asymmetric tidal cycles in the transport and accumulation of sediment in shallow well-mixed estuaries is well established. Along the U.S. Atlantic Coast, tidal amplitude, bottom friction, and system geometry determine tidal distortion as documented at 54 tide gauges in 26 tidally dominated estuaries of varying geometry having negligible freshwater inflow. Analyses of sea-surface heights are compared to the results of one-dimensional numerical modeling to clarify the physics of tidal response in well-mixed estuaries. Concise measurements of estuarine geometry and ocean tidal range are used to predict consistently the nature of tidal seasurface distortion. Numerical modeling then is utilized to extend theoretical and observational relationships between geometry and sea-height to predict trends in velocity distortion and near bed sediment transport. Non-linear tidal distortion is a composite of two principal effects: (1) frictional interaction between the tide and channel bottoms (reflected in a/h = tidal amplitude/channel depth) causes relatively shorter floods; (2) intertidal storage (measured by V_s/V_c = volume of intertidal storage/volume of channels at mean sea level) causes relatively shorter ebbs. Variations in V_s/V_c and a/h trigger consistent and predictable changes in tidal distortion as measured through the first harmonic of the principal tidal constituent.

Published in: *Estuarine, Coastal and Shelf Science*, 27, 521-545.

Supported by: ONR/American Society for Engineering Education, NOAA Sea Grants NA79-AA-D-0102 and NA80-AA- D-00077, CERC Waterways Experiment Station, Naval Civil Engineering Laboratory and WHOI Coastal Research Center.

TIDAL VELOCITY ASYMMETRIES AND BEDLOAD TRANSPORT IN SHALLOW EMBAYMENTS

Virginia A. Fry and David G. Aubrey

Tidal circulation can cause a net nearbed transport sediment when the tidal velocity is asymmetric about a zero mean (flood or ebb dominant) and the transport rate is related nonlinearly to velocity. The relationship between elevation and velocity is elucidated here to enable one to determine from tide gauge data and sediment transport relations whether tidal

asymmetry may cause net sediment transport. Tidal elevation and tidal velocity are related through the equations of motion of the fluid. If the estuary is shallow, the change in cross-sectional area of the channel with the tide is significant with respect to total area: the equations become nonlinear and an exact solution does not exist. A relationship between elevation and velocity in a nonlinear system is derived through the continuity equation and shown to be significantly different than the linear relation. Finite difference numerical solutions of the one-dimensional, shallow water nonlinear equations are compared to the continuity relation and are in good agreement.

The relationship between elevation asymmetry and ratio of flood-to-ebb bedload transport is calculated from the nonlinear relation between elevation and velocity is similar to the flood-to-ebb ratio calculated from the linear relation because of offsetting effects.

In Press: *1988 Estuarine, Coastal and Shelf Science.*

Supported by: WHOI Education Office; WHOI Coastal Research Center; NOAA Sea Grant NA86-AA-D-SG090; U.S. Army Coastal Engineering Research Center (Inlet Channel work no. 31716).

WHOI Contribution No. 6759.

CYCLICAL BEHAVIOR OF THE TIDAL INLET AT NAUSET BEACH, CHATHAM, MASSACHUSETTS

Graham S. Giese

Study of geological indicators and historical data relating to shoreline forms and change on southeastern Cape Cod revealed a cyclical pattern of change in the barrier beach system off Chatham, Massachusetts, with a period of approximately 150 years. Based on the observed patterns and deductions concerning the processes controlling those patterns. predictions of breaching of the barrier beach and new inlet formation were provided to local coastal resource managers, reducing the negative impacts accompanying the formation of the new inlet when it eventually occurred.

In Press: *Lecture Notes on Coastal and Estuarine Studies, Springer-Verlag.*

Supported by: NOAA Sea Grant NA86-AA-D-SG090.

WHOI Contribution No. 6797.

GLACIAL-HOLOCENE STRATIGRAPHY, CHRONOLOGY, AND SOME PALEOCEANOGRAPHIC OBSERVATIONS ON SOME NORTH ATLANTIC SEDIMENT DRIFTS

L.D. Keigwin and G.A. Jones

Several sediment drifts in the deep North Atlantic have been studied using oxygen isotopes, percent CaCO, clay mineralogy, tephra content and Accelerator Mass Spectrometer (AMS) radiocarbon dating. Because enhanced deposition of fine-grained terrigenous sediment increases rates of sedimentation by as much as 100 times the regional mean, sediment drifts contain high-resolution records of climate and oceanographic change. The major results of this study are that: 1) Patterns of sedimentation rate are regionally variable. In the western North Atlantic (Bermuda Rise, Blake-Bahama Outer Ridges), rates of sedimentation have been relatively low during the Holocene, but were as high as 200 cm/1000 yrs during the latest glacial episode, reflecting a greater supply of sediment due to glaciation and sea level lowering. Deep circulation patterns were probably similar to today. In the northern North Atlantic (Gardar Drift), which is dominated today by Norwegian Sea Overflow Water (NSOW), sedimentation rates were lowest during the glacial, despite the availability of sediment, because NSOW production was stopped. Rates peaked during the early Holocene as NSOW resumed. Glacial and Holocene rates of sedimentation were roughly comparable in the northeast Atlantic (Feni Drift) because sedimentation at that location is influenced less by NSOW than by Northeast Atlantic Deep Water (NEADW), which has a large southernsource component. 2) Stable isotopic events of deglacial age are preserved with unprecedented clarity in the sediments of North Atlantic drifts. Where the Younger Dryas cooling and Vedde Ash occurred together, at 56°N on Feni Drift, direct AMS dating suggests that the radiocarbon age difference between the surface ocean and atmosphere reservoirs in the northeast Atlantic was the same 10,500 yrs ago as it is today (about 400 yrs). A $\delta^{18}0$ maximum of Younger Dryas age indicates cooler or more saline surface waters above the Bermuda Rise at 33°N and as far south as 28°N on the Bahama Outer Ridge. Two $\delta^{18}0$ minima at 12,000 and 13,500 radiocarbon years BP on the Bahama Outer Ridge and the Bermuda Rise probably resulted from lowered surface water salinity. These low salinity events most likely originated as meltwater discharge down the Mississippi and into the Gulf of Mexico, followed by advection into the open North Atlantic via the

Gulf Stream.

In Press: *Deep-Sea Research.*

Supported by: NSF Grants ATM84-14335 and ATM87-06617.

WHOI Contribution No. 6945.

SHOREFACE DYNAMICS: EVIDENCE FROM THE BATHYMETRY AND SURFICIAL SEDIMENTS

James T. Liu and Gary A. Zarillo

A conceptual model for the maintenance of an equilibrium shoreface is tested on the shoreface of Long Island, New York, by using empirical eigenfunction analysis on sediment grain size data. A bluff, composed of morainal material in the headland section, and backbarrier lagoons in the barrier island section are two external sediment sources for the study area. Within the shoreface system, a remnant terminal moraine lobe-complex, sediments associated with old tidal inlet outer channels and the relict outwash plain deposits are permanent (irreversible) internal sediment sources. The present shoreface sediments are derived primarily from the 'relict' outwash plain sediments as a result of in situ re-working by the present shoreface hydrodynamic regime. Other temporary (reversible) internal sediment sources are storm deposits, and modern shoreface depositional features such as nearshore bars, sand ridges and active ebb tidal deltas.

As sea-level rises, the shoreface probably will continue to migrate landward. The recessional shoreface also will leave behind a sheet of relict transgressive sand, composed of mainly medium sands as the result of the winnowing of fine-grained sediments by hydrodynamic processes of the traversing shoreface.

In Press: *Marine Geology.*

Supported by: New York Community Trust Fund, the U.S. Army Corps of Engineers, NY District, and the Marine Sciences Research Center of SUNY at Stony Brook.

WHOI Contribution No. 6943.

SONOSTRATIGRAPHIC RECORDS FROM EQ. ATLANTIC DEEP-SEA CARBONATES: PALEOCEANOGRAPHIC AND CLIMATE RELATIONSHIPS

J. Mienert, W.B. Curry and H.S. Sarnthein

Paleoceanographic and stratigraphic methods, based on high-resolution compressional wave (p-wave) velocity measurements, have been applied to the studies of late Quaternary deep-sea carbonates in the western and eastern equatorial Atlantic. The measurements provide sonostratigraphic records in which changes in p-wave velocity parallel the changes from a glacial to an interglacial climate: Maxima in p-wave velocity (greater than 1540 m/s) occur during interglacial oxygen isotope stages 1, 5 and 7. Minima (1490 m/s) occur during glacial oxygen isotope stages 2, 4 and 6. Changes in p-wave velocity parallel past changes in carbonate accumulation and sediment coarse fraction, and allow a detailed core to core correlation. From these results two main patterns emerge: (1) In cores from shallower than 4300 m and from well above the present lysocline, large temporal changes in p-wave velocity parallel the production of planktonic foraminifera and the climatic history recorded in the sediments, and (2) below 4300 m, the position of the foraminiferal lysocline in the western equatorial Atlantic, large downcore p-wave velocity fluctuations gradually disappear due to dissolution of carbonate sediments. Dissolution also causes a distinct decrease in p-wave velocity and acoustic reflectivity in surface sediments across the present foraminiferal lysocline. Thus, past changes in the position of the foraminimiferal lysocline or calcite compensation depth that caused distinct changes in reflectivity of sediments should lead to distinct reflectors within sediment columns. Their distribution can be utilized to map paleowater masses with different degrees of carbonate saturation.

Published in: *Marine Geology*, 83, 9-20.

Supported by: NSF Grants OCE83-09124, OCE85-11014 and the German Science Foundation Sa 207/26-2.

WHOI Contribution No. 6743.

PHYSICAL PROPERTIES OF SEDIMENTARY ENVIRONMENTS IN OCEANIC HIGH (SITE 658A) AND OCEANIC LOW (SITE 659A) PRODUCTIVITY ZONES

Jüergen Mienert and Peter Schultheiss

Understanding the changes and characteristics of sediment physical properties beneath coastal upwelling and non-upwelling areas was one of the major objectives in physical property studies on Leg 108 drilling. Increased biogenic silica concentrations in sediments beneath the upwelling area (Hole 658A) cause a relatively low average grain density ($<2.4 g/cm^3$),low bulk density ($<1.6 g/cm^3$), and low shear strength (<60kPa). Sediments from the non-upwelling area (Hole

659A) have higher average carbonate concentrations (40-90%) and reflect a steady increase in wet bulk density (decrease in porosity) with subbottom depth (0.12 g/cm^3/100 m). Organic carbon concentrations, which are high at the upwelling site (<3.5%) and very low at the non-upwelling site (<0.4%), have no significant influence (R-<0.4) on the physical properties of sediment. The most substantial difference between the upwelling (Hole 658A) and the non-upwelling area (Hole 659A) is the presence of high biogenic silica concentration (Hole 658A) that marks a Plio-Pleistocene interval in which biogenic gas concentrations drastically increase at subbottom depths greater than 25 m. The distinct changes in the sediment physical properties observed beneath areas of intense upwelling should provide large enough impedance contrasts for mapping the distribution of upwelling cells in sediments by high resolution acoustic methods.

In Press: *ODP*, Vol. B, Leg 108.

Supported by: Ocean Drilling Program.

WHOI Contribution No. 6796.

CORRELATION OF 3.5 KHZ ACOUSTIC PENETRATION AND DEPOSITION/EROSION IN THE ARGENTINE BASIN: A NOTE

John D. Milliman

3.5 kHz profiles show that sediments in the Argentine Basin have acoustic penetrations ranging from nil to greater than 300 msec. The acoustically opaque sand- and silt-rich sediments on the proximal abyssal plain seaward of the Rio de la Plata appear to be winnowed by the Antarctic Bottom Water as it flows north. The northern and eastern parts of this gyre, however, appear to be depositional, explaining the acoustically transparent sediments on the southern slopes of the Rio Grande Rise and the Ewing-Argyros-Zapiola Drifts.

In Press: *Deep-Sea Research.*

Supported by: ONR Contract N00014-86-K-0578.

WHOI Contribution No. 6783.

ENVIRONMENTAL AND ECONOMIC IMPACT OF RISING SEA LEVEL AND SUBSIDING DELTAS: THE NILE AND BENGAL EXAMPLES

J.D. Milliman, J.M. Broadus and F. Gable

The effects of natural and accelerated subsidence, combined with a probable decreased influx of fluvial sediment, may accentuate greatly the rise of sea level in low-lying deltas over the next 100 years. By the year 2100 local sea level at the Nile and Bangladesh deltas (respectively) could be as much as 3.3 to 4.5 m higher than at present. At the higher calculated ranges, Egypt and Bangladesh could lose 26 and 34 percent of their currently habitable land. The additional loss of shoreline by erosion, loss of mangrove forests and decreased agriculture and fisheries would exacerbate environmental and economic impacts.

In Press: *Nature.*

Supported by: EPA Cooperative Agreement CR-812921-01-0, Pew Charitable Trust, and Andrew Mellon Foundation.

WHOI Contribution No. 6806.

LATE QUATERNARY SEDIMENTATION ON THE OUTER AND MIDDLE NEW JERSEY CONTINENTAL SHELF: RESULT OF HUDSON RIVER DISCHARGE?

John D. Milliman, Zhuang Jiezao, Li Anchun and John I. Ewing

High resolution seismic profiles from the outer and middle New Jersey continental shelf show two prominent sediment wedges deposited by Hudson River during the last glacial retreat. An extensive wedge along the outermost shelf and upper slope reaches thicknesses as great as 50 meters. The northern portion of this wedge apparently was deposited during an early melting of the late-Wisconsin Laurentide ice sheet, about 16 to 18 thousand years ago (ka), and reworked during sea level regression, still-stand and subsequent transgression. The mid-shelf sediment wedge, which forms the Fortune shore, probably was deposited during a second major melt event, 11 to 12 ka.

In Press: *Journal of Geology.*

Supported by: ONR Contracts N00014-86-C-0141 and N00014-86-C-0198.

WHOI Contribution No. 6753.

LATE QUATERNARY SEDIMENTATION IN A RIVER-DOMINATED EPICONTINENTAL SHELF: WESTERN YELLOW SEA

J.D. Milliman, Y.S. Qin, J.Z. Zhuang and A.C. Li

High resolution seismic profiles from the western Yellow Sea show a series of erosional-depositional cycles, each related sea level

regression, low stand and subsequent transgression. An erosional surface, presumably formed during the last major regression of sea level, has numerous channels that mark the drainage pattern of the Yellow River during lowered sea level.

Three sedimentary sequences overlie this erosional surface: 1) The oldest sediments include channel fill (in the east) and two prominent deltas (in the west), locally thicker than 30 m. At least one local unconformity and subsequent sediment fill within the deltaic sequence may have occurred during a local or eustatic fluctuation in sea level. In the central part of the study area deltaic sediments (or reworked deltaic sediments) are exposed at the sea floor. 2) The overlying sedimentary sequence consists of a thin (generally less than 5 m) acoustically dark horizon containing peats and fine-grained sediments deposited during the last transgression, 11 to 12 thousand years ago. 3) The youngest sedimentary sequence consists of Holocene sediments, ranging from less than 2 m thick to more than 30 m thick off the Jiangsu coast and on the Shandong sediment wedge.

Although present-day topographic relief in the western Yellow Sea largely reflects late Quaternary deposition, much of this sediment (particularly the deltas and sediment wedges) will be eroded and transported seaward during the next regression of sea level.

In Press: *Bulletin of the American Association of Petroleum Geologists.*

Supported by: ONR Contract N00014-81-C-0009 and NSF Grant INT85-01366.

WHOI Contribution No. 6805.

SMALL FRACTURE ZONES: SYMMETRIC IN CROSS-SECTION?

Peter R. Shaw

Oceanic crust is discontinuous in age across oceanic fracture zones (FZ's), long linear scars formed at ridge crest offsets. Models of lithospheric cooling predict a change in water depth and geoid height across FZ's. Topographyand geoid profiles across large-offset (>10 m.y.) FZ's resemble step functions modified by lithospheric flexure and mantle convection having length scales of hundreds of km. In this study I analyze geoid profiles across 17 small-offset FZ's, investigating the correlation of profile asymmetry with the sense of age offset. Pairs of profiles representing the FZ on conjugate sides of the ridge are compared for fit, aligned either geographically (north-south) or by age contrast. No clear evidence is found for alignment by age providing a superior fit, implying that small-offset FZ's are symmetric in cross section.

Supported by: NSF Grant OCE86-14512 and ONR Contract N00014-87-K-0007.

WHOI Contribution No. 6742.

SEDIMENT DISTRIBUTION IN THE NORTH ATLANTIC OCEAN, 50°N TO 72°N

Brian E. Tucholke

The sediment isopachs compiled in the accompanying maps give a detailed regional synthesis of sediment distribution in the northern North Atlantic and Norwegian-Greenland Sea. All contours are expressed in kilometers rather than reflection time in order to present a realistic picture of actual geologic relations. Conversion of reflection-time data to thickness was accomplished by application of sediment sound-velocity data in various provinces as described later. This text provides a brief summary of previous work and outlines the principal factors affecting sediment distribution in the northern North Atlantic. A more detailed interpretation, together with presentation and discussion of accompanying maps of basement structure, is being developed separately.

Previous mapping of sediment distribution in this area began with a map of sediment isopachs that covered the entire Atlantic (Ewing et al., 1973). Although this map was highly generalized and it presented isopachs in reflection time rather than in true thickness, it offered the first comprehensive overview of sediment distribution in the North Atlantic south of about 62°N. Updated isopachs for the same region were published by Emery and Uchupi (1984), who mapped sediment thickness in kilometers using an assumed sound speed in sediments of 2.0 km/sec. The most recent and most detailed mapping of sediment distribution was published by Tucholke and Fry (1985) for the western part of the northern North Atlantic as far north as 69°N. Their isopachs are in kilometers, based on sediment velocities determined from sonobuoy wide-angle reflection profiles.

Sediment isopachs in the Norwegian-Greenland Sea north of 62°N have been mapped by Eldholm and Windisch (1974) and Gronlie and Talwani (1978); both maps were presented in seconds reflection time. These compilations recently have been updated with additional seismic reflection data by Eldholm (written comm., 1983) and Eldholm et al. (1987).

Numerous, usually more detailed, isopach maps have been constructed for smaller areas or for specific physiographic provinces (e.g. continental shelf) in the northern North Atlantic

and Norwegian-Greenland Sea. A summary of these studies is given in Table 1.

In Press: *Deutsches Hydrographisches Institute Atlas of the North Atlantic Ocean.*

Supported by: ONR Contracts N00014-79-C-0071 and N00014-82-C-0019.

WHOI Contribution No. 6712.

CRUSTAL STRUCTURE AND RIFT/DRIFT EVOLUTION OF THE NEWFOUNDLAND BASIN

Brian E. Tucholke, James A. Austin, Jr. and Elazar Uchupi

A multichannel seismic reflection survey of the Newfoundland Basin southeast of the Grand Banks was conducted to examine the rift-drift history of the basin and to determine the nature and location of the continent-ocean boundary. The data suggest that the continet-ocean boundary is marked by the "M" magnetic anomaly (M1-M0 which separates crust having a relatively smooth magnetic field to the west from higher-amplitude anomalies to the east. Basement at the boundary is characterized by a set of large volcanic ridges that were constructed simultaneously with the adjacent Southeast Newfoundland Ridge and the J-Anomaly Ridge. The ridges appear to have formed from magma derived from a mantle plume then located beneath the Southeast Newfoundland Ridge.

The Newfoundland basin west of the interpreted continent-ocean boundary exhibits two distinct structural provinces in basement. A large (60x400km) rift basin, the Salar basin, occurs beneath the continental slope and upper rise and is filled with probably Upper Triassic to Lower Jurassic evaporites. Seaward of Salar basin, a zone of complexly faulted basement blocks with intervening, probably syn-rift sedimentary and volcanic fill extends to the J anomaly. Both the blocks and fill are capped by a high-amplitude, relatively flat seismic unconformity. The unconformity pinches out at the J anomaly and appears to correlate with the "U", or Avalon, breakup unconformity on the adjacent Grand Banks.

Late Triassic rifting formed the Salar basin and caused an unknown amount of extension in adjacent continental crust to the east. A second phase of Late Jurassic through Early Cretaceous rifting reactivated parts of the western margin of the Salar basin and probably caused substantial extension and thinning of continental crust to the east. The rifting culminated in broad uplift or doming of this extended crust, erosion of the breakup unconformity, and Barremian-Aptian emplacement of volcanic ridges marking the continent-ocean boundary at the J-Anomaly ridges, oldest oceanic crust) appear to have experienced unusually rapid subsidence, much faster than age/depth relations of normal oceanic crust, following continental breakup.

In Press: *AAPG Memoir.*

Supported by: NSF Grant OCE83-09085.

WHOI Contribution No. 6859.

KANE FRACTURE ZONE

Brian E. Tucholke and Hans Schouten

The Kane Fracture Zone probably is better covered by geophysical survey data, acquired both deliberately and unintentionally, than any other fracture zone in the North Atlantic Ocean. We have used this data to map the basement morphology of the fracture zone and the adjacent crust for nearly 5700 km, from near Cape Hatteras to the middle of the M-series magnetic anomalies west of Cap Blanc. We use the basement structural data at the Kane transform valley, and in the adjacent inactive fracture valleys, to interpret how the transform has evolved in response to changes in plate motion, and we then examine the record of plate motion changes recorded in the structure of the older fracture valley. Prior to about 135 Ma the Kane was a small-offset transform and its fracture valley is structurally expressed as a shallow (<0.5 km) trough. In younger crust, the offset increased to as much as 200 km (present offset 150 km) and the fracture valley is typically 1.2 km deep. The fracture valley in this crust clearly records significant changes in direction of plate motion (5°-30°) near 100 Ma, 90 Ma, 59 Ma, 22 Ma, and 17 Ma. Each change corresponds to a major reorganization of plate boundaries in areas around the Atlantic, and the fracture-zone structure appears to be a sensitive recorder of these events. The Kane transform has exhibited characteristic responses to changes in plate motion. Counterclockwise shifts in plate motion put the left-lateral transform zone into extension, and the response has been for ridge tips at the ridge-transform intersections to propagate across the transform valley and against the truncating lithosphere. Heating of this lithosphere produces uplift and formation of a transverse ridge that bounds the adjacent inactive fracture valley. The propagating ridge tips also rotate toward the transform fault in response to the local stress field, forming hooked ridges that extend across the fracture valley. Clockwise (compressional) shifts in relative plate motion produce none of these features and the resulting fracture valleys typically have a wide-v shape. The fracture-valley structure produced during extensional and compressional

shifts can be decidedly asymmetrical in conjugate limbs of the fracture zone. This asymmetry appears to be directly explicable by the motion of the plate boundary with respect to the asthenosphere. The Kane transform underwent severe adaptions to the changes in plate motion at about 100 Ma and 90 Ma, forming new transform faults in older crust outside the existing transform domain. Subsequently, the transform offset has been smaller and the rates of change in plate motion have generally been more gradual, so transform adjustment has been contained within the contemporaneous transform domain.

In Press: *Marine Geophysical Researches.*

Supported by: ONR Contracts N00014-85-C-0001 and N00014-87-K-0007.

WHOI Contribution No. 6711.

SEDIMENT THICKNESS MAP OF THE NORTH ATLANTIC

Brian E. Tucholke and Elazar Uchupi

The sediment thickness map of the North Atlantic is compiled from maps by Tucholke et al. (1982), Tucholke and Fry (1985), Tucholke (1988), and Emery and Uchupi (1984). Contours are in kilometers, based on sediment sound velocities that were determined for various North Atlantic provinces by wide-angle reflection and refraction profiling. The application of such velocities gives sediment thickness values that are estimated to be within about 5-10% of true thicknesses. Along continental margins where sediments are very thick (10-15 km), velocity determinations usually are sparse and the uncertainties in true sediment thickness may be greater. The data base from which the four original isopach maps cited above were constructed is comprised of about one million line kilometers of seismic reflection profiles, not including profiles represented in previous compilations that were incorporated into the maps. Sediment thicknesses also are controlled by Deep Sea Drilling Project (DSDP), Ocean Drilling Project (ODP), and commercial borehole results.

The isopach contours represent total thickness of syn-rift and post-rift sediments. In most oceanic areas seaward of the ocean-continent boundary, the base of the sediment column is oceanic crust that was accreted at mid-ocean ridges. Notable exceptions occur near or along the Thulean volcanic line (e.g. Hall, 1981) extending from eastern Baffin Island to the northern British Isles. Along this trend Cretaceous to Eocene basalts which may cover significant accumulations of syn- and post-rift sediment probably have been mapped as basement, at least locally. Basement in a few deep-ocean areas is Precambrian and Paleozoic continental crust, covered in part by Cretaceous to Eocene basalts. Known or suspected examples are the microcontinental fragments of Rockall Plateau, Jan Mayen Ridge, and perhaps the Davis Strait High. Pre-rift "basement" along the continental margins landward of the ocean-continent boundary is mostly Precambrian to Paleozoic, although it locally consists of Triassic and even Jurassic rocks. Rift-related volcanics and intrusives, taken to be basement, undoubtedly have masked older, syn-rift sediments in many areas along the continental margins. Given the uncertainties about the exact distribution of syn-rift and post-rift igneous activity, and its common masking of older sedimentary deposits, the mapped sediment thicknesses should be considered minimum values along the continental margins and along the Thulean volcanic line as noted above.

The distribution of sediments in the North Atlantic is controlled primarily by five factors: 1) age of the underlying crust (in basalt-floored ocean basins), 2) tectonic history of the crust, 3) structural trends in basement, 4) nature and location of sediment sources, and 5) the nature of the sedimentary processes delivering sediments to depocenters. The relative importance of each of these factors has varied in space and time across the North Atlantic, and the details of their interrelations during the geologic evolution of the Atlantic basins are discussed fully in the aforementioned references.

In Press: *IOC International Geological/Geophysical Atlases of the Atlantic and Pacific Oceans.*

Supported by: ONR Contracts N00014-79-C-0071, N00014-82-C-0019 and NSF Grant OCE79-09382.

WHOI Contribution No. 6710.

THE TECTONIC STYLE OF THE ATLANTIC MESOZOIC RIFT SYSTEM

Elazar Uchupi

The Atlantic Mesozoic rift system consists of four branches separated from one another by fracture zones. Morphologically it resembles the ridge transform-ridge topography of mid-ocean ridges. The branches include the northern North Atlantic between the Newfoundland/Gibraltar and Bahamas/Guinea fracture zones, the Southern North Atlantic between the Bahama/Guinea and Equatorial fracture zones, the Equatorial Atlantic between the Equatorial Fracture Zone and the Torres/Walvis Ridge, and the South Atlantic between the Torres/Walvis Ridge, and the Falkland/Agulhas Fracture Zone. The fundamental structure along the shear zones is the graben, and within the rift branches the half graben. Rifting

began in Late Triassic at the northern end of the Northern North Atlantic Branch and in Early Jurassic at the South Atlantic Branch. The rifts propagated toward one another cutting through the equatorial region sometime in latest Middle Jurassic. Seafloor spreading at the northern end of the Northern North Atlantic Branch began in Middle Jurassic reaching the Bahama/Guinea Fracture Zone toward the end of Middle Jurassic. Seafloor spreading in the South Atlantic Branch began in earliest Early Cretaceous, in the Southern North Atlantic Branch in early Aptian and in the Equatorial Atlantic Branch in the Albian. A continuous North/South Atlantic oceanic basin was formed with the separation of the African and South American continents in the Turonian.

In Press: *Journal of African Earth Sciences.*

Supported by: ONR Contract N00014-87-K-0007.

WHOI Contribution No. 6725.

THE GEOLOGIC ENIGMA OF THE RED SEA RIFT

Elazar Uchupi and David A. Ross

Three models have been proposed for the origin of the Red Sea rift. One proposes that the whole width of the Red sea is underlain by oceanic crust which was emplaced in two stages, from 25 to 15 m.y. ago and from 4.5 m.y. ago to the present. In this model the middle and late Miocene evaporites pervasive in the region were deposited atop oceanic crust. In the intermediate model, the main trough is underlain by oceanic crust landward of which is an intruded rifted continental crust. Under this regime, the evaporites were deposited on both continental and oceanic crusts. The third model, the attenuated continental crustal, model assumes that the Red Sea has a rifted continental crust with oceanic crust being restricted to a narrow belt between 15°30'N and 20°N and in a series of isolated deeps from 20°N to 23°30'N. Rifting began about 20 m.y. ago and seafloor spreading in the narrow oceanic crustal belt 5 m.y. ago and in the isolated deeps less than 2 m.y. ago. In this model the evaporites were deposited on continental crust. Geological and geophysical data available to date does not allow us to determine which of these three models is applicable to the Red Sea.

In Press: *Degens Volume.*

Supported by: NOAA Sea Grant NA86-AA-D-SG090.

WHOI Contribution No. 6767.

GEOPHYSICS

TIDAL CURRENT EFFECTS ON TEMPERATURE IN DIFFUSE HYDROTHERMAL FLOW: GUAYMAS BASIN

S.A. Little, K.D. Stolzenbach and F.J. Grassle

A twelve day record of temperature collected from the diffuse flow area of a Guaymas Basin hydrothermal site exhibits variations, from a minimum of 3.05°C to a maximum of 4.87°C, whose periodicity is correlated with tides measured at the nearby town of Guaymas. A simple model, based on the hypothesis that temperature variations result as changes in tidal bottom currents induce changes in the height of the thermal boundary layer, is in good quantitative agreement with observed temperatures for most of the record. The success of this model illustrates that the effects of tidal currents can be strong enough to dominate the time variability of a temperature signal at a fixed point in hydrothermal flow. Therefore, tidal currents must be taken into account when using temperature measurements to estimate time varying heat fluxes from hydrothermal diffuse flow regions.

In Press: *Geophysical Research Letters.*

Supported by: NSF Grant OCE83-11201.

WHOI Contribution No. 6807.

SHAPE ANALYSIS OF PACIFIC SEAMOUNTS

Deborah K. Smith

Shape statistics have been compiled from 85 profiles of well-surveyed Pacific seamounts in the height range 140-3800 m. A flat-topped cone was fit to each seamount's cross-sectional profile maintaining the slopes of the sides as closely as possible. On each profile a basal width d_b, a summit width d_t, and a maximum height h, were measured. The height-to-basal-radius ratio ξ_h is estimated by the ratio $2h/d_b$ and flatness f by the ratio d_t/d_b. Slope angle $\Phi=\arctan(\varepsilon)$ is estimated from $\varepsilon=2h/(d_b-d_t)$. Summit height and basal radius are found to be highly correlated (r=0.93). The 85-point sample mean of the height-to-basal-radius ratio is $\xi_h=0.21\pm0.08$ implying that a seamount's summit height is typically one fifth its basal radius. Despite the high correlation, individual points show some scatter, and there may be groupings into different morphological types. For example, all but one of the seamounts with summit heights above 1000 m

have values of ξ_h that are larger than the sample mean. The 85-point sample mean of flatness is f=0.31±0.18. Data points show a large scatter with values of f varying between 0 (a pointy cone) and 0.69 (a flat-topped cone). A histogram representation of flatness, however, indicates that certain values of f may be more common than others: the histogram shows a bimodal distribution with maxima occurring at values of f in the ranges 0.10-0.20 and 0.35-0.50. Moreover, there is some evidence that the mean flatness decreases with summit height so that the preferred shape of a large-size seamount may be a pointy cone. Slope angle has an 85-point sample mean of Φ=18°±6°; individual values of Φ vary between 5°and 36°. In addition to having a lower than average mean flatness seamounts with heights above 2600 m also have a lower than average mean slope angle (15°). To determine which variables account for most of the observed variation in the seamount shapes, a multivariate principal component analysis was performed on the data using five shape variables (summit height, basal radius, summit radius, flatness, and slope). The analysis indicates that most of the variation is described by two variables: flatness and summit height.

In Press: *Earth & Planetary Science Letters*, 90, 457-466.

Supported by: NSF Grant OCE88-00497.

WHOI Contribution No. 6868.

A REVIEW OF FINITE DIFFERENCE METHODS FOR SEISMO-ACOUSTICS PROBLEMS AT THE SEAFLOOR

Ralph A. Stephen

Understanding seismic wave propagation in realistic seafloor environments is essential for many problems in marine seismology. Finite difference methods are becoming increasingly popular in solving propagation problems as the limitations of other techniques which apply only at high frequency or for flat lying media become fully appreciated. The seafloor problem, a high contrast in Poisson's ratio at a sharp, rough interface, is particularly challenging, and many published finite difference formulations for the elastic wave equation and to outline their applicability to sea floor problems.

Published in: *Reviews of Geophysics*, 26, 445-458.

Supported by: ONR Contracts N00014-85-C-0001 and N00014-87-K-0007.

WHOI Contribution No. 6727.

LATERAL HETEROGENEITY IN THE UPPER OCEANIC CRUST AT DSDP SITE 504

Ralph A. Stephen

The lateral variability of the upper oceanic crust can be studied by mapping the amplitude (or power) content of arrivals from a dense array of identical sources to a single receiver. In this paper, we present the results from a borehole seismic experiment at Deep Sea Drilling Project (DSDP) Site 504 in the eastern equatorial Pacific. Seismic amplitude anomalies of 20 db and more are present with a horizontal correlation length of 1-3 km. Finite difference synthetic seismogram techniques are used to predict seismic wave propagation through realistic bathymetry, basement relief and lateral variations within basement. A three dimensional model of the velocity structure around the borehole can be constructed. The resultant model has horizontal gradients greater than 2.0 sec. in the upper crust. These gradients are comparable to the vertical gradients normally associated with oceanic crust. Assuming that velocity anomalies in the upper crust reflect changes in porosity, the resultant structure provides constraints on the hydrothermal circulation at the site. An addition, the finite difference modelling indicates that polarity reversals can be generated by lateral velocity variations near the source and receiver.

Published in: *Journal of Geophysical Research*, 93, 6571-6584.

Supported by: NSF Grants OCE84-09155 and OCE84-16633.

WHOI Contribution No. 6721.

PALEOCEANOGRAPHY

CHANGES IN THE DISTRIBUTION OF $\delta^{13}C$

W.B. Curry, J.C. Duplessy, L.D. Labeyrie and N.J. Shackleton

Carbon isotopic measurements on the benthic foraminiferal genus Cibicidoides document that mean deep ocean $\delta^{13}C$ values were $0.46°/_{oo}$ lower during the last glacial maximum than during the Late Holocene. The geographic distribution of $\delta^{13}C$ was altered by changes in the production rate of nutrient-depleted deep water in the North Atlantic. During the Late Holocene, North Atlantic Deep Water, with high $\delta^{13}C$ values and low nutrient values can be found throughout the

Atlantic Ocean, and its effects can be traced into the Southern Ocean where it mixes with recirculated Pacific deep water. During the glaciation, decreased production of North Atlantic Deep Water allowed Southern Ocean deep water to penetrate farther into the North Atlantic and across low-latitude fracture zones into the eastern Atlantic. Mean Southern Ocean $\delta^{13}C$ values during the glaciation are lower than both North Atlantic and Pacific $\delta^{13}C$ values, suggesting that production of nutrient-depleted water occurred in both oceans during the glaciation. Enriched ^{13}C values in shallow cores within the Atlantic Ocean indicate the existence of a nutrient-depleted water mass above 2000 meters in this ocean.

Supported by: NSF Grants OCE85-11014 and OCE83-9124.

WHOI Contribution No. 6813.

OXYGEN AND CARBON ISOTOPIC VARIATION IN PLIOCENE BENTHIC FORAMINIFERA OF THE EQUATORIAL ATLANTIC

W.B. Curry and K.G. Miller

Large changes in benthic foraminifera $\delta^{18}O$ and $\delta^{13}C$ occurred during the Pliocene (between 3.0 and 2.0 Ma) at Hole 665A. Oxygen isotopic compoistions increased to maximum values at 2.4 Ma, correlating with an ^{18}O enrichment observed at Hole 552A and other locations (Shackleton et al., 1984). As at Hole 606 (Keigwin, 1986), however, maximum $\delta^{18}O$ values at 2.4 Ma were not as great as at 552A, and enrichments in $\delta^{18}O$ also occurred before 2.4 Ma. We believe that the section representing from 2.5 to 2.7 or 2.8 Ma is missing at Hole 552A because of incomplete core recovery. Consequently the older $\delta^{18}O$ increases are not found at 552A. Benthic foraminiferal $\delta^{13}C$ values are much lower at Hole 665A than at Hole 552A, approaching the low values observed in the Pliocene Pacific Ocean. This geographic distribution of $\delta^{13}C$ suggests that, like late Quaternary glaciations, the equatorial Atlantic Ocean was dominated during the Pliocene by deep water that originated in the Southern Ocean and had chemical characteristics very similar to the Pacific Ocean. Reduced $[O_2]$ values were probably associated with the low $\delta^{13}C$ values, and contributed to increased preservation of organic carbon during enriched ^{18}O intervals of the Pliocene equatorial Atlantic.

Published in: *ODP*, Vol. B, Leg 108.

Supported by: NSF Grant OCE85-11014 and Ocean Drilling Program.

WHOI Contribution No. 6930.

EVIDENCE FROM FRAM STRAIT (78°N) FOR EARLY DEGLACIATION

Glenn A. Jones and Lloyd D. Keigwin

Recent syntheses of the history of the last Northern Hemisphere glaciation and deglaciation illustrate our limited understanding of the mechanisms and timing of deglaciation prior to approximately 12,000 yrs B.P.. After 12,000 yrs B.P., however, there is sufficient evidence from radiocarbon dated moraines, raised beaches, varved lake sediments, and pollen records to provide a reasonable temporal and geographic picture of the decay of the ice sheets. We report on the first oxygen isotope record from the Norwegian-Greenland Sea that is radiocarbon dated directly by accelerator mass spectrometry (AMS). A significant light oxygen isotopic event is recorded at approximately 15,000 yrs B.P. suggesting that the marine-based Barents Shelf Ice Sheet disintegrated rapidly at this time. Recent studies have estimated the decay of this ice sheet could have contributed as much as 15 meters to eustatic sealevel rise. The decay of the Barents Shelf Ice Sheet is the earliest major deglacial event yet dated, and may have triggered subsequent deglacial events via eustatic sea level effects.

Published in: *Nature*, 336, 55-59.

Supported by: NSF Grant DPP87-22235 and ONR Contract N00014-85-C-0714.

WHOI Contribution No. 6826.

LATE QUATERNARY PALEOCHEMISTRY OF HIGH-LATITUDE SURFACE WATERS

L.D. Keigwin and E.A. Boyle

Recent studies have stressed the role of high latitude nutrient levels and productivity in controlling the carbon isotopic composition of the deep sea and the CO content of the atmosphere. We undertook a study of the chemical composition of the polar planktonic foraminifer Neogloboquadrina pachyderma (s., sinistral coiling) from 30 late Holocene samples and 49 down core records from the high-latitude North and South Atlantic Oceans to evaluate the record of sea surface chemical change from glacial to interglacial time. Stable isotopic analysis of coretop samples from the Atlantic, Pacific, and Southern Oceans shows no significant correlation between the $\delta^{13}C$ of N. pachyderma and either $\delta^{13}C$ or PO_4 in seawater. Conversely, Cd/Ca ratios in planktonic foraminifera are consistent with the PO content of surface waters. The level of

maximum glaciation (18,000 yr B.P.), identified by CLIMAP and $\delta^{18}O$, was chosen for mapping. Isopleths of $\delta^{18}O$ on N. pachyderma (s.) in the North Atlantic reveal a pattern largely influenced by sea surface temperature (SST) and generally support the SST reconstruction of CLIMAP. Differences between the two suggest significantly lower salinity in North Atlantic surface waters at high latitudes than in lower latitudes.

Down core $\delta^{13}C$ records of N. pachyderma confirm that low $\delta^{13}C$ occurs values in the northeast Atlantic during the latest glacial maximum (Labeyrie and Duplessy, Palaeo. 3, 1985). However, a map of $\delta^{13}C$ for the 18,000 yr B.P. level for a much larger region in the North Atlantic shows that minimum N. pachyderma $\delta^{13}C$ occurred in temperate waters. N. pachyderma $\delta^{13}C$ decreases toward the southwest, reaching a minimum of $-1°/_{oo}$ at 37°N. Despite the variability seen in $\delta^{13}C$ records of N. pachyderma, none of our cores show significant temporal variability in Cd/Ca. From the combined Cd/Ca and $\delta^{13}C$ data we conclude that there was no upwelling gyre in the eastern North Atlantic during the latest glacial maximum, and that neither tracer suggests that the southern or northern oceans were marked by significantly different levels of performed nutrients than they are today.

In Press: *Palaeogeography, Palaeoclimatology, Palaeoecology.*

Supported by: NSF Grants OCE84-10789 and OCE87-19012.

WHOI Contribution No. 6803.

DEGLACIAL CLIMATIC OSCILLATIONS IN THE GULF OF CALIFORNIA

L.D. Keigwin and G.A. Jones

A high-resolution, accelerator radio-carbon dated climate record of the interval 8,000-18,000 yrs B.P. from Pacific Ocean DSDP Site 480 (Guaymas Basin, Gulf of California), shows a significant climatic oscillation centered on 10,500 yrs B.P. This event is identical in age to the Younger Dryas cooling, which is well known in northern Europe and the North Atlantic Ocean. In the Gulf of California this oscillation is manifested as lowered salinity at 10,200 and 12,200 yrs B.P. due to excess precipitation over evaporation. These results suggest that either the climate forcing mechanism for the Younger Dryas oscillation is global in scope or there are additional unrelated forcing mechanisms of Younger Dryas age in regions other than the North Atlantic.

At a quarter past midnight on New Year's Day 1979, the first Hydraulic Piston Core (HPC) was brought aboard D/V GLOMAR CHALLENGER. Successful recovery at Deep Sea Drilling Project (DSDP) Site 480 (Guaymas Basin, Gulf of California) of a long, continuous sequence of late Quaternary sediment with undistrubed laminae (1), opened a new era in scientific ocean drilling. The DSDP was extended for HPC coring at locations where soft sediment was previously distrubed by rotary drilling, and that project led to its successor, the Ocean Drilling Program. Despite the technical success of the HPC in the Guaymas Basin, few studies of DSDP Site 480 continued beyond the initial scientific reports (2) because this core was not accurately dated. We have made eight Accelerator Mass Spectrometer (AMS) radiocarbon analyses within the upper 18 m of Site 480. In addition to reporting a high resolution chronology for this core, we discuss the climatic and oceanographic significance of abrupt oxygen isotopic oscillations during the most recent deglaciation.

Supported by: NSF Grant ATM87-00617.

WHOI Contribution No. 6802.

OCEANOGRAPHY

MARINE SCIENTIFIC RESEARCH: U.S. PERSPECTIVE ON JURISDICTION AND INTERNATIONAL COOPERATION

David A. Ross and Judith Fenwick

Many U.S. marine scientists and administrators in the late 1970s and early 1980s were skeptical about continued research access to foreign waters. Their uncertainties were heightened with the signing of the UN Convention on the Law of the Sea in 1982 and with the U.S. decision not to participate in this signing. What the treaty's impact would be on marine scientific research (MSR) access was unknown and the answer is still not obvious. By the end of 1987, 105 coastal nations (from a base of 139) have claimed jurisdiction over 200-nm zones and 78 have some form of jurisdiction over research in their coastal waters. This paper assesses the impact of this increased coastal state jurisdiction on the U.S. MSR effort, discusses factors that may determine geographic choices by U.S. marine scientists for their sea-going research, and offers some speculation from the U.S. perspective on the future for access and international cooperation in marine scientific research.

In Press: *New Developments in Marine Science and Technology: Economic, Legal, and Political Aspects of Change, Proceedings of the 22nd Annual Conference, Law of the Sea Institute,* 1988.

Supported by: NOAA Sea Grant NA86-AA-D-SG090.

WHOI Contribution No. 6840.

SILICOFLAGELLATE PRODUCTIVITY AS SEASONAL MIXED LAYER PROXY: TEMPORAL AND SPATIAL VARIABILITY IN THE NORTHEASTERN PACIFIC 1982-1986

Kozo Takahashi

To study the temporal variability of oceanic productivity, time series particle fluxes were monitored at pelagic Station Papa (50°N, 145°W) in the eastern subarctic Pacific from September 1982 through August 1986. Automated Particle Flux (PARFLUX) time series sediment traps were deployed at 3800 m and 1000 m in the 4200-m deep pelagic ocean. The traps collected samples for 2-week periods for almost continuous 4-year-long particle flux record. In order to study spatial flux variability, an additional trap at Station C (49.5°N, 138°W) was occupied during 1985-1986 where particle fluxes were measured at 3500m in the 3900-m deep water. Time series flux samples from Station C were synchronized with those at Station Papa for comparison with each other. In order to evaluate their value as productivity or temperature indicators, species of silicoflagellates and Actiniscus, a dinoflagellate genus with siliceous endoskeletons, were examined from the time series trap samples. Their fluxes were enumerated for a total of 119 samples from Station Papa and 24 samples from Station C. Among seven silicoflagellate taxa, Distephanus speculum and Dictyocha mandraiapa were dominant taxa which constantly represented >70% of total silicoflagellate assemblages. All of the taxa showed significantly suppressed fluxes during 1984 which were correlated with the σ_t changes centered around 100 m depth. It is hypothesized that the suppressed fluxes were attributable to a decrease in convective nutrient (or trace elements) supply. The flux of Distephanus speculum, a productivity indicator, was negatively correlated with the diversity index of silicoflagellates which is considered to be another productivity measure. Seasonal patterns of D. speculum and D. mandrai percentages also follow patterns of D. speculum flux and silicoflagellate diversity, either parallel or inversely. Thus, D. speculum flux trends, diversity indices and percent contribution to silicoflagellate assemblages reflect variability in upper water silicoflagellate production rate which is a consequence of hydrographic conditions. It is concluded that Stations Papa and C, 600 km apart, are situated in the same oceanic province with similar ecosystems. This is based on their exhibiting the same species composition, and very similar seasonal patterns of fluxes, and their percentage of species in the assemblages from the two stations. Most silicoflagellate species fluxes at Station C were approximately one half of those measured at Station Papa which can be explained by differences in upper water σ_t values relative to those below 200 m. Thus, silicoflagellate data clearly suggested lower fertility of the upper waters at Station C than that at Station Papa. Flux maxima at Station C generally lagged behind Station Papa by two weeks, resulting from lower σ_t values in the seasonal mixed layer. The importance of silicoflagellate fluxes as an indicator of seasonal mixed layer σ is demonstrated in the regional comparisons of fluxes and hydrography. Generic ratios of Dictyocha/Distephanus were more dependent on production rates than temperature, on the contrary to a previous hypothesis in the literature. Apparent correlations between the ratios and tempertures which were obtained in previous basin-wide studies may be indirect results of the fertility of upper water masses which are in part governed by temperature and hence stability of the waters on a global scale.

In Press: *Global Biogeochemical Cycles.*

Supported by: NSF Grants OCE85-02472 and OCE86-08255.

WHOI Contribution No. 6842.

MINERAL FLUX AND BIOGEOCHEMICAL CYCLES OF MARINE PLANKTONIC PROTOZOA

Kozo Takahashi

This paper is a synthesis of the lectures and resulting discussions from the "Mineral Flux" session held during the NATO-ASI Workshop on "Protozoa and their Role in Marine Processes" held at Plymouth, England, 24 July-5 August 1988. The session was devoted to fluxes of biogenically precipitated minerals and their biogeochemical cycles. In the session, four lectures including an invited keynote lecture were presented by pertinent workers in the field. Each lecture is summarized and future research trends for some specific research fields are discussed.

In Press: *NATO-ASI Conference Series, IV: Marine Sciences.*

Supported by: NSF Grant OCE86-08255.

WHOI Contribution No. 6878.

OCEANIC PROVINCE: ASSESSMENT FROM THE TIME-SERIES DIATOM PRODUCTIVITY IN THE NORTHEASTERN PACIFIC

Kozo Takahashi, John D. Billings and Julia K. Morgan

A pelagic domain normally can be subdivided into oceanic provinces with reference to physical or biological properties and processes. Within a single province the ecosystem is similar and hence similar biological processes would take place at different locations within a province. The biological process and productivity vary with time and thus time-series observations are essential for seasonal provincial studies. We focused on the eastern subarctic Pacific where the seasonal amplitude of biological productivity is high relative to the lower latitudes so that comparisons between different sites can be clearly made. Time-series sediment trap samples for one year (1985-1986) recovered from two sites approximately 600 km apart in the pelagic Gulf of Alaska were examined for regional differences and similarities in siliceous plankton productivity measured as vertical flux. Hydrographic data were also examined in order to relate them to the siliceous plankton productivity.

Overall similarity was overwhelming despite minor differences, suggesting the similarity of ecosystems at the two sites. We conclude that the two sites are situated within a single oceanic province based on the following findings: (1) Species compositions of diatom and other siliceous plankton assemblages were the same; (2) Seasonal flux patterns were similar; and (3) Percentage contributions of species fluxes within each of the major taxonomic groups were similar. On the other hand, levels of siliceous phytoplankton productivity differed by a factor of two between the two sites. The difference is due to hydrography: $\Delta\sigma_t$ in the upper 200 m was almost always greater at Station C than at Station Papa, and also was responsible for a less degree of surface water mixing with waters below and hence a less convective nutrient supply.

Supported by: NSF Grants OCE85-02472 and OCE86-08255.

WHOI Contribution No. 6885.

SILICEOUS PHYTOPLANKTON FLUX: INTERANNUAL VARIABILITY AND RESPONSE TO HYDROGRAPHIC CHANGES IN THE NORTHEASTERN PACIFIC

Kozo Takahashi, Susumu Honjo and Susumu Tabata

Time-series fluxes of diatoms and silicoflagellates were measured nearly continuously at pelagic Station Papa in the northeastern subarctic Pacific during September 1982 through August 1986. Significantly large interannual flux variability was observed. In 1984 the fluxes were notably low relative to other years: either flux peaks were absent or slightly above the base line values depending on taxa. Such flux suppression is attributed to changes in upper water hydrography. Within a limited physical oceanography data set a significantly shallower thermocline was observed during April 1984 than other years except for 1983. This shallow and probable maximum winter mixing of 1984 is interpreted to have resulted in limited convective nutrient supply. Production of siliceous phytoplankton, which can be measured as vertical flux, is related with the hydrography and thus the flux is a useful oceanographic proxy for mixed layer conditions.

In Press: *In Interdisciplinary Aspects of Climate Variability in the Pacific and Western Americas*, ed. David Peterson, AGU Monograph Volume.

Supported by: NSF Grants OCE85-02427 and OCE86-08255.

WHOI Contribution No. 6838.

PALEONTOLOGY

THE RELATIONSHIP BETWEEN PORE WATER CARBON ISOTOPIC COMPOSITION AND BOTTOM WATER OXYGEN CONCENTRATION

Daniel C. McCorkle and Steven R. Emerson

We present pore water $\delta^{13}C$ profiles from the Western North Atlantic and the Eastern Pacific oceans, and interpret them using a stoichiometric model of the relationship between carbon isotopic composition and oxygen concentration. Pore water $\delta^{13}C$ at the depth in the sediments where oxygen approaches zero is largely determined by the oxygen concentration of the overlying bottom water, although sulfate reduction adds a significant amount of isotopically light carbon at some locations. The $\delta^{13}C$ difference between bottom water and pore water at 0_2=0 ("$\Delta\delta^{13}C$") increases

from 1‰ in sediments of three low bottom water oxygen basins in the Southern California Borderlands to 4‰ in sediments underlying well oxygenated water in the Western North Atlantic.

We suggest that the relationship between bottom water oxygen and $\Delta\delta^{13}C$ could form the basis for a new way to use the benthic foraminifera $\delta^{13}C$ record to estimate bottom water oxygen concentration. Paleo-oxygen values derived from a pair of benthic foraminifera species which record the bottom water/pore water (0_2=0) $\delta^{13}C$ difference will be independent of the preformed $\delta^{13}C$ of the deep water mass.

Published in: *Geochimica et Cosmochimica Acta*, 52, 1169-1178.

Supported by: NSF Grants OCE86-10043 and OCE86-14514.

WHOI Contribution No. 6748.

RADIOLARIAN BIOSTRATIGRAPHY IN THE CENTRAL INDIAN OCEAN, OCEAN DRILLING PROJECT LEG 115

David A. Johnson

Identifiable Radiolaria of stratigraphic importance were recovered at 8 of the sites drilled on Leg 115. The assemblages range in age from Recent to Middle Eocene (Dictyoprora mongolfieri Zone, about 48 Ma). Faunal preservation is particularly good in 2 stratigraphic intervals: the Recent through Upper Miocene (0 to 9 Ma), and the lowermost Oligocene to Middle Eocene (35 Ma to 48 Ma). Fluctuating rates of silica accumulation at these drill sites during the Cenozoic reflect changing tectonic and paleo-oceanographic conditions. In particular, the gradual closure of the Indonesian and Tethyan seaways and the northward migration of the Indian subcontinent severely restricted zonal circulation and silica accumulation in tropical latitudes during the Late Oligocene through Middle Miocene. By the Late Miocene the Indian subcontinent had moved sufficiently north of the equator to allow trans-Indian zonal circulation patterns to become reestablished, and biosiliceous sedimentation resumed.

The composition of the radiolarian assemblages in the tropical Indian Ocean is closely comparable to that of the "stratotype" sequences in the equatorial Pacific (e.g. Riedel and Sanfilippo, 1971; 1978; Nigrini, 1985). However, there are some notable exceptions in Indian Ocean assemblages: 1) The scarcity of the genera Pterocanium and Spongaster in the Neogene; 2) The absence of the stratigraphically-important Podocyrtis lineage, P. diamesa→ P. phyxis→ P. ampla, in the Middle Eocene; and 3) The scarcity of taxa of the genus Dorcadospyris, with the exception of D. ateuchus.

In Press: *ODP*, Vol. B, Leg 115.

Supported by: Ocean Drilling Program and NSF Grant OCE87-15956.

WHOI Contribution No. 6935.

PETROLOGY

ABYSSAL PERIDOTITES, VERY-SLOW SPREADING RIDGES AND OCEAN RIDGE MAGMATISM

Henry J. B. Dick

The SW Indian and American-Antarctic Ridges are two of the world's slowest spreading ocean ridges (<1 cm/yr), making them the low end-members for rate of ocean ridge magma supply. Two thirds of the rocks dredged at the numerous large offset transforms along the ridges are residual mantle peridotites. Gabbroic rocks, however, representing layer 3 and possible paleo-magma chambers are rare. This suggests a highly segmented crustal structure, with anomalously thin crust near fracture zones that may consist of only a thin veneer of pillow basalts erupted over mantle peridotite.

The dredged peridotites underwent high degrees of melting, spanning the believed range producing abyssal basalt. Their depleted composition show that the melt was almost entirely removed. At the same time, the spatially-associated basalts have a large range of compositions, similar to those from the rift valleys, requiring extensive shallow level fractional crystallization. Since there is little evidence for magma chambers at these fracture zones, it is concluded that melts formed in the underlying mantle flowed laterally through the mantle beneath the crust towards magmatic center at the mid-point of an adjacent ridge segment. Magma was then subsequently intruded down the rift valley fissure system from the magmatic center to erupt onto the fracture zone floor. Alternatively, the melt was drained from a mantle diapir beneath the mid-point of a ridge segment, prior to lateral flow of the residual peridotite beneath the ridge axis to the fracture zone. These processes suggest behavvior of the partially molten layer beneath the ridge axis to the fracture zone. These processes suggest behavior of the partially molten layer beneath ocean ridges analogous to Rayleigh-Taylor fluid instability, where a light less viscous fluid layer floating upwards in a denser medium goes unstable and drains at regularly spaced points into protrusions which rise rapidly to the surface. Evidence for such dynamically driven, non-uniform melt flow in the mantle is seen in locally abundant

plagioclase peridotites, where the plagioclase crystallized from impregnated trapped melt. These rocks can contain up to 30% trapped melt, contrasting sharply with the typical abyssal peridotite which contains virtually none.

Basalts erupted along these ridges provide a classic case of trace and major element decoupling during magma genesis. Despite trace element and isotopic diversity, basalts from individual ridge segments were derived from primary magmas with similar major element compositions. These observations can be explained if melt flows locally through the depleted mantle at the end of melting towards the mid-point of a ridge segment. This would cause melts originating at different points in an initially heterogeneous mantle to migrate through and equilibrate with the same section of mantle immediately prior to segregation - which, for the most part, would homogenize the melt's major element compositions. This would, however, by virtue of the lever rule, have little effect on critical incompatible trace element or isotopic ratios of the migrating melts due to the very low incompatible trace element content of residual peridotite.

Ocean ridges, then, appear to be marked by strings of regularly spaced volcanic centers overlying instability points in the partially molten upwelling asthenosphere much as has been postulated for arc volcanism and early continental rifting (e.g. Marsh, 1979, Mohr and Wood 1976). Unlike arcs, the asthenosphere upwells to the base of the crust and the magmatic centers undergo continuous extension. Thus, large volcanos are not constructed, and instead, ribbons of basaltic crust form parallel to the spreading direction. This is most evident in the SW Indian and American-Antarctic Ridges due to their highly attenuated magma supply. Where the magma supply is more robust, and the magma chambers are correspondingly larger, the chambers could merge and eliminate the surficial morphological and chemical expression of punctuated magmatism at ocean ridges.

Supported by: NSF Grants OCE84-16634, DPP83-16490, DPP87-20002 and WHOI Geodynamics Program.

WHOI Contribution No. 6776.

PETROLOGY AND GEOCHEMISTRY OF MORB FROM 25°E TO 46°E ALONG THE SOUTHWEST INDIAN RIDGE: EVIDENCE FOR CONTRASTING STYLES OF MANTLE ENRICHMENT

Antone P. le Roex, Henry J. B. Dick and Robert L. Fisher

The PROTEA 5 expedition to the central Southwest Indian Ridge recovered basaltic lavas from fracture zones and ridge segments between 25°E and 48°E. In terms of petrography and major element variations the samples are unremarkable and range from aphyric to highly plagioclase phyric and from moderately primitive (Mg#=70) to moderately evolved (Mg#=40) in composition. Multiple saturated (i.e. olivine, plagioclase and clinopyroxene) basalts are common within this region. There is no systematic difference is compositional characteristics between basalts dredged from fracture zone walls and those dredged from ridge segments, and fractional crystallization has played an important role in controlling the overall range to lava composition in both tectonic environments.

Incompatible element abundance ratios in the basalts are more notable and distinguish between geochemically depleted (N-type) MORB with high Zr/Nb (16->68) and Y/Nb (4.7->23) ratios and low $(La/Sm)_n$ ratios ( ), and geochemically enriched (E-type) MORB with low Zr/Nb (3.4-15.8) and Y/Nb (0.5-8.8) and high $(La/Sm)_n$ ratios ( ). The former MORB type occur throughout the study area, but are less abundant along the section of ridge closest to Marion Island. Geochemically enriched MORB occur at scattered localities along the ridge but are particularly abundant along the section of ridge closest to the Marion hotspot.

Two distinct varieties of E-type morb are recognized. The one type has incompatible element and isotopic ratios similar to, although slightly less enriched than, those characteristic of the Marion hotspot (Zr/Nb=5.8-8.6; Y/Nb=0.5-0.8; Ba/Nb=5.1-9.0). The second type can be distinguished by having high Ba/Nb ratios (9-22), unlike any lavas directly associated with the Marion hotspot, but similar to those characteristic of DUPAL ocean island basalts. A single sample from this group for which there is isotopic data indicates derivation from an isotopically anomalous source region.

A model is proposed whereby the sub-oceanic mantle below this portion of the Southwest Indian Ocean has experienced at least two distinct enrichment events. The one is associated with the upwelling of the Marion mantle plume (geochemically characterized by having low Ba/Nb

ratios and normal OIB isotopic ratios). The other is associated with upwelling from a DUPAL source (characterized by having high Ba/Nb ratio and unusual isotopic ratios) which has been proposed to exist beneath this portion of the Southwest Indian Ocean (Hart, 1984). On the basis of Ba/Nb and Nb/U ratios, recycled oceanic lithosphere is favored as a source for the Marion hotspot, while recycled oceanic lithosphere plus ancient pelagic sediment appears to be the most likely source for the DUPAL anomaly and the DUPAL E-type MORB in this region.

Supported by: NSF Grant DPP87-20002.

WHOI Contribution No. 6777.

MAJOR ELEMENT EVOLUTION OF BASALTIC MAGMAS: A COMPARISON OF THE INFORMATION IN CMAS AND ALFE PROJECTIONS

John B. Reid, Jr., Eric Steig and Wilfred B. Bryan

Basalt petrologists disagree as to whether the commonly used projection, forsterite-diopside-silica, in the system CMAS (CaO-MgO-Al_2O_3-SiO_2, can adequately resolve differences in basaltic glass compositions for purposes of petrogenetic modelling. Here, we suggest that an analogous plot, the aluminum-factor diagram (ALFE) of Nesbitt and Cramer (1981), has greater diagnostic value than Fo-Di-Sil. A plot of molar $(Al_2O_3$-CaO-Na_2O-$K_2O)/(FeO+MgO)$ vs $FeO/(FeO+MgO)$, it produces more coherent patterns both for experimental basalt glasses, and for natural lavas. It is, like Fo-Di-Sil, a projection through plagioclase, but has the advantage that it monitors changes in $Fe/(Fe+Mg)$ in melts and associated crystalline phases, and is particularly useful in assessing the timing of clinopyroxene crystallization in a suite of lavas. The diagram owes its greater resolving power to the fact that the computation of its coordinates is less sensitive to analytical uncertainty than for Fo-Di-Sil. In the latter diagram, normative quartz is calculated as a residual and thus manifests the uncertainties in all the major elements.

Supported by: NSF Grant OCE85-10847.

WHOI Contribution No. 6865.

SEDIMENTOLOGY

CARBONATE LITHOFACIES AS PALEOLATITUDE INDICATORS: PROBLEMS AND LIMITATIONS

G. Carannante, M. Esteban, J.D. Milliman and L. Simone

Detailed study of Miocene carbonates in the Mediterranean region and their analogy on modern carbonate shelves (in the Mediterranean Sea, Brazil and other areas) reveals at least three major types of carbonate platform lithofacies in addition to the clasic tropical coral reef (chlorozoan) lithofacies: (a) Chloralgal lithofacies, similar to the chlorozoan, but without hermatypic corals: (b) Rhodalgal lithofacies, characterized by abundant encrusting coralline algae; and (c) Molechfor lithofacies, consisting of benthic foraminifers, molluscs, echinoids, bryozoans and barnacles. These carbonate lithofacies present complex distribution patterns seemingly related primarily to latitude and depth that control water temperature, although other factors (e.g., water circulation, river discharge, suspended sediment) controlling water salinity and temperature, nutrient content, light penetration, etc., also play important roles. Chloralgal and rhodalgal lithofacies can be considered two transitional terms between the two end-members: the chlorozoan lithofacies, which characterizes shallow tropical shelves; and the molechfor lithofacies, which characterizes colder and/or deeper areas. Detailed texural and sequential analysis are required for satisfactory interpretation of these lithofacies in ancient rocks.

In Press: *Sedimentary Geology.*

Supported by: ONR Contract N00014-86-K-0578.

WHOI Contribution No. 6804.

OCEAN PARTICLES AND FLUXES OF MATERIAL TO THE INTERIOR OF THE DEEP OCEAN; THE AZOIC THEORY 120 YEARS LATER

Susumu Honjo

About 120 years ago the influential Azoic theory, that no life existed on the deep ocean floor, was finally defeated by Charles Wyville Thomson. He described many types of animals collected from the North Atlantic abyssal floor using dredges during the HMS LIGHTNING and HMS PORCUPINE cruises in 1868 and 1870. Without doubt, the establishment of a lively deep sea realm had a serious impact on the philosophy of science at that time, and this was a powerful encouragement to wider and deeper recognition of Charles Darwin's "Origin of Species," published

about a decade before Thomson's cruises (Mills, 1983). For the past century since Thomson's discovery and the legendary HMS CHALLENGER voyage, scientists have collected innumerable specimens from every corner of the oceanic abyss. Deep-sea biology is now well established, resulting from an increase in the critical mass of benthic biologists, better quality and quantity shiptime, and improved equipment (Rowe, 1983).

Ironically, during this seemingly glorious century of deep sea research, the important question of what supported life in the abyssal environment was answered by sheer speculation, particularly with reference to the quantities and mechanisms of energy and nutrient supply. Until very recently this "knowledge" remained essentially unchanged from the late 19th century views of Alexander Agassiz who postulated that slowly descending plankton detritus nourished the benthos when, or if, it arrived at the abyssal sea floor. The great insight of Agassiz was that he also mentioned that the benthic population was positively related to the abundance of plankton in the ocean's surface (cited from Uda, 1955).

Supported by: NSF Grant OCE87-14363.

WHOI Contribution No. 6946.

PARTICLE FLUXES AND MODERN SEDIMENTATION IN THE POLAR OCEANS

Susumu Honjo

The finding of living animals on the abyssal ocean floor by one of the first oceanographic scientific expeditions (the H.M.S. Lightning and Porcupine by C. W. Thompson in 1868 and 1870; in: Mills, 1983), provoked vigorous discussions on the quality and quantity of energy resources and nutrients which must be supplied to a habitat miles below the productive ocean surface. The mechanism which allowed the surface layer community to share nutrients with that in the deep ocean was also debated for many years (e.g., Menzies, 1962; Vingradov, 1962). Meanwhile, the mass accumulation rate of skeletal, preserved, and refractory particles on the ocean floor is the key to understanding the geological evolution of the oceans and the earth itself (e.g., Lizitsin, 1972). These major questions in oceanography have been revised more recently in light of the urgent need to understand the biogeochemical cycle of carbon on this planet in relation to the anthropogenic increase of atmospheric CO_2 contents (Brewer et al., 1986).

Supported by: ONR Contract N00014-87-K-0007 and NSF Grant OCE83-21472.

WHOI Contribution No. 6929.

THE CENTRAL ARCTIC OCEAN SEDIMENT RECORD: CURRENT PROGRESS IN MOVING FROM A LITHO- TO A CHRONOSTRATIGRAPHY

Glenn A. Jones

In recent years there has arisen a major controversy surrounding the ages of the sediments recovered from the central Arctic Ocean. Earlier interpretations (Steuerwald et al. 1968; Clark 1970, 1971; Hunkins et al. 1971; Clark et al. 1980) inferred that the rates were very low, and of the order of 0.2 to 0.005 cm/1,000 years. These ages were based primarily upon published interpretations of the paleomagnetic polarity records of central Arctic Ocean sediments. These interpretations have been challenged by Scjrup et al. (1984). These authors measured amino acid D/L ratios of planktronic and benthonic foraminifera in core T3-67-11. They interpreted their results to mean that central Arctic Ocean sedimentation rates were 10 to 20 times higher than had been previously reported. These authors pointed out that since the actual paleomagnetics data had only been published from one Arctic Ocean core, the published polarity interpretations could not be fully evaluated. In this study all of the existing paleomagneitcs data from 110 Central Arctic Ocean cores were evaluated and the inclinations calculated (~10,000 analyses). This dataset suggests an average sedimentation rate of 0.15 cm/1000 yrs for the central Arctic. The oldest continuously accumulating sediment (i.e. not found below a hiatus) recovered from the T-3 platform is approximately 2.5 million years old, and is not Miocene in age as previously interpreted by Clark et al., 1980).

Supported by: NSF Grant OCE86-8119.

WHOI Contribution No. 6801.

RADIOCARBON DATING OF DEEP SEA SEDIMENTS: A COMPARISON OF ACCELERATOR MASS SPECTROMETER AND BETA-DECAY METHODS

G.A. Jones, A.J.T. Jull, T.W. Linick and D.J. Donahue

The radiocarbon method of age dating (Libby, 1955) has been an important tool in the marine sciences since the early 1950's (e.g. Arrhenius et al., 1951; Ericson et al., 1956; Broecker et al., 1960; Emery and Bray, 1962) and the basic principles and analytic procedures of the method have changed little. In the late 1970's the Accelerator Mass Spectrometer (AMS) method of radiocarbon

dating was developed (Bennett et al., 1977; 1978), with the major advantages being that samples several thousand times smaller than needed for beta-decay counting can be dated, and analysis time is reduced to approximately one hour from the one to six days needed for beta-decay methods.

Despite the wide acceptance and clear utility of the AMS method of radiocarbon dating in the marine geological sciences (e.g. Broecker et al., 1984; Duplessey et al., 1986; Bard et al., 1987; Andree et al., 1986) there has been no direct comparison of this method with the well-established beta-decay method of radio-carbon dating deep-sea sediments.

In this paper we compare directly the advantages, disadvantages, and limitations of both the conventional and accelerator methods. As they are applied to marine sediments. We conclude that for chronostratigraphic purposes, there is no unambiguous method determining precisely the "true" radiocarbon age for any horizon within a deepsea sediment core. Both methods give similar results however, and the small ample size required for the AMS method makes it superior to the beta-decay method in determining detailed overall sedimentation rates, and in more efficiently utilizing deep-sea sedimentary materials.

In Press: *Radiocarbon.*

Supported by: NOAA Sea Grant NA84-AA-D-0033.

WHOI Contribution No. 6749.

TECHNICAL REPORTS

THERMAL AND MECHANICAL DEVELOPMENT OF THE EAST AFRICAN RIFT SYSTEM

Cynthia J. Ebinger

The deep basins, uplifted flanks, and volcanoes of the Western and Kenya rift systems have developed along the western and eastern margins of the 1300 km-wide East African plateau. Structural patterns deduced from field, Landsat, and geophysical studies in the Western rift reveal a series of asymmetric basins bounded by approximately 100 km-long segments of the border fault system. These basins are linked by oblique-slip and strike-slip faults cross-cutting the rift valley. Faults bounding the Kenya and Western rift valleys delineate two north-south-trending, 40-75 km wide zones of crustal extension, and little or no crustal thinning has occurred beneath the uplifted flanks or the central plateau. In the Western rift, volcanism in Late Miocene time began prior to or concurrent with basinal subsidence, followed by rift flank uplift. Individual extensional basins developed diachronously, and basinal propagation may give rise to the along-axis segmentation of the rift valley. The coherence between gravity and topography data indicates that the mechanical lithosphere beneath the two rift valleys has been weakened relative to the central plateau and adjacent cratonic regions. Gravity and topography data at wavelengths corresponding to the overcompensated East African plateau can be explained by density variations within the upper mantle that are dynamically maintained.

Supported by: NSF Grant EAR84-18120 and NOAA Sea Grant NA84-AA-D-0033.

WHOI Technical Report 88-27.

HEAT FLOW AND TECTONICS OF THE LIGURIAN SEA BASIN AND MARGINS

John P. Jemsek

Heat flow, tectonic subsidence and crustal thickness distributions in the Ligurian Basin are best explained by asymmetric lithospheric thinning mechanisms. Over 150 heat flow measurements are made on several transects between Nice, France and Calvi, Corsica on continental slop and rise settings. Thermal gradient determinations are improved using an optimization technique. Piston core data and surface sediment 3.5 kHz reflectivity patterns help constrain thermal conductivity obtained from over 100 in situ stations. Plio-Quaternary stratigraphy is revised using new seismic reflection profiles: a boundary fault system associated with postrift margin uplift, a Pleistocene-age Var Fan construction, and recent diapirism of Messinian salt are indicated. After assessing local thermal disturbances (mass-wasting, microtopography, and salt refraction), positive heat flow corrections are made for multilithologic sedimentation histories and glacial paleotemperatures. Using boundary-layer cooling models, equilibrium heat flow estimates support geologic evidence for Oligocene and early Miocene rifting. Heat flow maxima correlate well with two "oceanic" sub-basins, suggesting that the southeastern trough near Corsica is ~5 Myr younger, consistent with the southeastern progression of volcanism and back arc rifting in the Western Mediterranean. Tectonic subsidence-crustal thickness trends indicate lithospheric stretching, with heat flow supporting asymmetric sub-crustal lithospheric thinning during the conjugate margin formation.

Supported by: NSF Grants OCE80-25181 and OCE84-09170.

WHOI Technical Report 88-25.

CENOZOIC DEEP-WATER AGGLUTINATED FORAMINIFERA IN THE NORTH ATLANTIC

Michael A. Kaminski

Cenozoic (predominantly Paleogene) "flysch-type" agglutinated foraminiferal assemblages and their modern analogs in the North Atlantic and adjacent areas have been studied to provide an overview of their spatial and temporal distribution and utility for paleoenvironmental analysis. Over 200 species of agglutinated foraminifera have been recognized in Paleogene sediments from North Atlantic and Tethyan basins. This unified taxonomic data base enables the first general synthesis of biostratigraphic, paleobiogeographic and paleobathymetric patterns in flysch-type agglutinated assemblages from upper Cretaceous to Neogene sediments in the North Atlantic. The majority of taxa are cosmopolitan, but latitudinal, temporal and depth-related trends in diversity and species composition are observed among flysch-type assemblages.

Supported by: NSF Grant OCE82-17586 and Ocean Drilling Program.

WHOI Technical Report 88-3.

FLUID FLOW AND SOUND GENERATION AT HYDROTHERMAL VENT FIELDS

Sarah A. Little

Several experiments are presented in this thesis which examine methods to measure and monitor fluid flow from hydrothermal vent fields.

Simultaneous velocity, temperature, and conductivity data were collected in the convective flow emanating from a hydrothermal vent field located at 10°56'N, 103°41'W on the East Pacific rise. The horizontal profiles obtained indicate that the flow field approaches an ideal plume in the temperature and velocity distribution. Such parameters as total heat flow and maximum plume height can be estimated using either the velocity or the temperature information. The results of these independent calculations are in close agreement, yielding a total heat flow from this vent site of 3.7 $\pm$ 0.8 MW and a maximum height of 150 $\pm$ 10 m. The nonlinear effects of large temperature variations on heat capacity and volume changes slightly alter the calculations applied to obtain these values.

In Guaymas Basin, a twelve day time series of temperature data was collected from a point three centimeters above a diffuse hydrothermal flow area. Using concurrent tidal gauge data from the town of Guaymas it is shown that the effects of tidal currents can be strong enough to dominate the time variability of a temperature signal at a fixed point in hydrothermal flow and are a plausible explanation for the variations seen in the Guaymas Basin temperature data.

Theoretical examination of hot, turbulent, buoyant jets exiting from hydrothermal chimneys revealed acoustic source mechanisms capable of producing sound at levels higher than ambient ocean noise. Pressure levels and frequency generated by hydrothermal jets are dependent on chimney dimensions, fluid velocity and temperature and therefore can be used to monitor changes in these parameters over time.

A laboratory study of low Mach number jet noise and amplification by flow inhomogeneities confirmed theoretical predictions for homogeneous jet noise power and frequency. The increase in power due to convected flow inhomogeneities, however, was lower in the near field than expected.

Indirect evidence of hydrothermal sound fields (Reidesel et al., 1982; Bibee and Jacobson, 1986) showing anomalous high power and low frequency noise associated with vents is due to processes other than jet noise.

On Axial Seamount, Juan de Fuca Ridge, high quality acoustic noise measurements were obtained by two hydrophones located 3 m and 40 m from an active hydrothermal vent, in an effort to determine the feasibility of monitoring hydrothermal vent activity through flow noise generation. Most of the noise field could be attributed to ambient ocean noise sources of microseisms, distant shipping and weather, punctuated by local ships and biological sources. Water/rock interface waves of local origin were detected which showed high pressure amplitudes near the seafloor and, decaying with vertical distance, produced low pressures at 40 m above the bottom.

Detection of vent signals was hampered by unexpected spatial non-stationarity due to shadowing effects of the caldera wall. No continuous vent signals were deemed significant based on a criterion of 90% probability of detection and 5% probability of false alarm. However, a small signal near 40 Hz, with a power level of 1×10^{-4} Pa^2/Hz was noticed on two records taken near the Inferno black smoker. The frequency of this signal is consistent with predictions and the power level suggests the occurrence of jet noise amplification due to convected density inhomogeneities.

Supported by: ONR Contract N00014-87-K-0007, NSF Grant OCE83-10175 and NOAA Sea Grant NA86-AA-D-SG090.

WHOI Technical Report 88-21.

DEPARTMENT OF OCEAN ENGINEERING

Albert J. Williams III, Chairman

THE TITANIC SITE RESTING IN PIECES

Elazar Uchupi, Robert D. Ballard, and William N. Lange

The story of the RMS Titanic is well known (Lord, 1978; Anonymous, 1983; Eaton and Haas, 1986; Lord, 1986; Wade, 1986; Davie, 1987). She was built by Harland and Wolff of Belfast with the keel laid on March 31, 1909 and the launching taking place on May 31, 1911. The ship was 271.5 m long, 28.5 m wide, 18.6 m high from water line to her boat deck, or 53.8 m from her keel to the top of her four stacks. Her weight was 46,328 gross tons having a displacement of 66,000 tons. She was triple screw with two four-cylinder reciprocating engines driving the wing screws, and a low pressure turbine driving the center one forward of the rudder. She had 50,000 registered horsepower, could develop at least 55,000 horsepower and could make a maximum speed of 24 to 25 knots (44 to 46 km/hour). She consumed 650 tons of coal per day to feed her 150 furnaces, and had 29 boilers with five singles located in Boiler Room 1 aft, five double boilers in rooms 2 to 5, and four double boilers in Boiler Room 6 at the forward end of the vessel. She was divided into 16 water-tight compartments by 15 water tight bulkheads the first two of which went as high as D deck, and the middle eight up to E deck.

Published in: *Oceanus*, 31(4), Winter 1988/89, 53-60.

Supported by: NSF Grant OCE-8316601; Navy Chair Contract No. N00014-85-G-0242.

WHOI Contribution No. 6730.

SEDIMENT CONCENTRATION PROFILING IN HEBBLE USING A ONE MEGAHERTZ ACOUSTIC BACKSCATTER SYSTEM

James F. Lynch, Thomas F. Gross, Blair Brumley, and Richard A. Filyo

As part of the High Energy Benthic Layer Experiment (HEBBLE), a one megahertz acoustic backscatter system (ABSS) was deployed in 4800m of water on the Nova Scotian continental rise. The purpose of the instrument was to non-intrusively measure a concentration vertical profile time series over the course of one year, from September 1985 to September 1986. In this paper, we discuss the details of the ABSS instrument, the results of the time series data analysis, and the ramifications of the results on sediment transport modeling. The variability of ABSS and light transmissometry calibration with changes of particle size distribution caused by environmental variability is discussed. A comparison of the ABSS estimates with those obtained from light transmissometers indicates that the particle size distribution changes surprisingly little throughout the experiment.

In Press: *Deep Sea Research.*

Supported by: ONR Contracts N00014-82-C-0019 and N00014-85-C-0001.

WHOI Contribution No. 6756.

BOTTOM STRESS IN WIND-DRIVEN DEPTH-AVERAGED COASTAL FLOWS

Harry L. Jenter and Ole Secher Madsen

The relationship between depth-averaged velocity and bottom stress for wind-driven coastal waters is examined using a 1-D (vertically-resolving) current model. Results indicate that conventional drag laws employed in depth-averaged coastal circulation models may produce large directional errors in bottom stress estimates. A drag tensor is suggested as an alternative to conventional drag coefficient formulations. The drag tensor allows for variation in direction between depth-averaged velocity and bottom stress. Two physically relevant cases are studied in order to quantify drag tensor variation as a function of water depth, wind stress and bottom roughness. The drag tensor allows for phenomena excluded by drag coefficient formulations. Results indicate that the drag tensor is a simple, yet physically pleasing, alternative to drag coefficients.

In Press: *Journal of Physical Oceanography.*

Supported by: NSF Grant No. OCE-8403249.

WHOI Contribution No. 6844.

GEOLOGIC RECONNAISSANCE ALONG THE AXIS OF THE REYKJANES RIDGE AT 61°30'-62°N

Robin T. Holcomb, Elazar Uchupi, and Robert D. Ballard

Diving by the U.S. Navy research submarine NR-1 has confirmed that the zone of recent volcanism along the Reykjanes Ridge is less than 15 km wide, with volcanic landforms dominating over tectonic features. Fault scarps higher than a few tens of meters were not found within 10 km of the axis, though non-eruptive fissures and faults of small displacement do occur. Broad swells, 200-300 m high, 3-6 km wide, and 20-30 km long in a right-stepping en echelon pattern along the Ridge axis, appear to be polygenetic volcanoes. Each swell is

corrugated by narrow monogenetic ridges that differ widely from each other in age. The age ranges for the ridges on adjacent swells overlap greatly, such that overall age differences between swells are not apparent. Trends of the ridges are more complex than expected with some ridges paralleling the axes of the broader swells beneath them, whereas other ridges and structures follow different trends. Each monogenetic volcanic ridge is composed of mixed sheet and pillowed flows. Some of them are remarkably narrow and steep-sided, resembling "pillow walls," others are steep-sided and flat-topped, resembling subaerial tablemountains or tuyas, and still others are asymmetric in cross-section. Circular shields and craters also occur in the neovolcanic zone. No active hydrothermal vents were found in localities examined.

In Press: *Journal of Volcanology.*

Supported by: ONR Contract No. N00014-86-C-0038.

WHOI Contribution No. 6843.

SURFACE TELEMETRY ENGINEERING MOORING (STEM)

Henri O. Berteaux, Daniel E. Frye, Peter R. Clay, Edward C. Mellinger

A Surface Telemetry Engineering Mooring (STEM) has been developed to collect and transmit oceanographic and meteorological data via satellite links. Data telemetered included currents (from 50 and 250 meters) water and air temperature, wind, relative humidity, barometric pressure, and various engineering parameters.

The unique aspect of the STEM design was the use of electromechanical cable for both the strength member of the mooring and the electrical connection between the subsurface instruments and the surface buoy.

The surface mooring was deployed 150 miles south of Cape Cod in 2700 meters of water. It was deployed in November 1987 and retrieved in May 1988, operating successfully through the harsh winter in the N. Atlantic.

Published in: *Marine Technology Society Oceans '88 Conference Proceedings*, Vol. 2, 670-680, Baltimore, MD (October 31 - November 2, 1988).

Supported by: ONR Contract Nos. N00014-86-K-0751, N00014-84-C-0134, and NR 083-400.

WHOI Contribution No. 6862.

TIME DELAY ESTIMATION IN STATIONARY AND NON-STATIONARY ENVIRONMENTS

Mordechai Segal and Ehud Weinstein

We developed computationally efficient iterative algorithms for finding the Maximum Likelihood estimates of the delay and spectral parameters of a noise-like Gaussian signal radiated from a common point source and observed by two or more spatially separated receivers. We first consider the stationary case in which the source is stationary (not moving) and the observed signals are modeled as wide sense stationary processes. We then extend the scope by considering a non-stationary (moving) source radiating a possible non-stationary stochastic signal. In that context, we address the practical problem of estimation given discrete-time observations. We also present efficient methods for calculating the log-likelihood gradient (score), the Hessian, and the Fisher's information matrix under stationary and non-stationary conditions.

In Press: *IEEE Transactions on Acoustics, Speech, and Signal Processing.*

Supported by: ONR Contract No. N00014-85-K-0272.

WHOI Contribution No. 6866.

LARVAL SWIMMING AND SUBSTRATE SELECTION IN THE BRITTLE STAR OPHIODERMA BREVISPINUM

Christine M. Webb

The general vertical distribution (in still water), passive sinking speeds and near-bottom swimming behaviours and speeds of the lecithotrophic larvae of Ophioderma brevispinum (Say) were studied over development from early to vitellaria larval stages. Substrate selectivity of the settling vitellaria larvae was examined using a range of sediment and eelgrass substrates. Early larvae mainly occupied the midwater region of a 15-cm water column and swam in vertically expansive spiral paths while the vitellariae were found close to the bottom, swimming in vertically limited circular or hovering paths. As larvae developed, their fall velocities increased. Linear swimming speeds of the vitellariae, with banded cilation, were similar to those of the uniformly ciliated early larvae, and also to other ophiuroid and echinoderm larvae, but were low compared to other ciliated, marine invertebrate larvae. The circular swimming motion, with minimal net horizontal displacement, and the slow linear speeds

of the settling larvae may limit horizontally directed search in this species. Settling larvae were not selective among the substrates tested and metamorphosed with little delay in the absence of such substrates. These preliminary findings on the larval behaviours of Ophioderma brevispinum may have implications for larval dispersal and substrate selection.

In Press: *Proceedings of the 23rd European Marine Biology Symposium.*

Supported by: Minerals Management Service, U.S. Dept. of the Interior, Contract No. 14-12-0001-30262, and the Coastal Research Center (WHOI).

WHOI Contribution No. 6890.

ACTIVE HABITAT SELECTION BY LARVAE OF THE POLYCHAETES, CAPITELLA SPP. I AND II, IN A LABORATORY FLUME

Judith P. Grassle and Cheryl Ann Butman

Horizontal swim speeds and behavior under dark and directed white light conditions, gravitational fall velocities, and habitat selection in still water and a laboratory flume flow are compared for competent larvae of the sibling species, Capitella spp. I and II (Annelida: Polychaeta). Despite marked genetic differences between the species, both selectively settle in organically-rich mud rather than in abiotic glass beads in two-hour still-water and flume experiments. The percentage of larvae settling in the flow experiments is three to four time greater, however, for Capitella sp. I compared to Capitella sp. II. This may be due to small differences between the species in near-bottom behavior, and may help to explain differences in the small-scale distributions of the adults.

In Press: *Proceedings of the 23rd European Marine Biology Symposium.*

Supported by: NSF Contract No. OCE-85000875, Minerals Management Service, U.S. Dept. of the Interior, Contract. No. 14-12-0001-30262, and the Coastal Research Center (WHOI).

WHOI Contribution No. 6903.

SEDIMENTARY PROCESSES IN THE TONGUE OF THE OCEAN, BAHAMAS: AN ARGO/SEAMARC SURVEY

William C. Schwab, Elazar Uchupi, Robert D. Ballard, and Thomas K. Dettweiler

SeaMARC 1B sidescan sonographs and Argo video and photographic data reveal the recent sedimentary environment of the floor of the Tongue of the Ocean is controlled by an interplay of turbidity current flow from the south, sediment spill-over from the carbonate platform to the east (windward side), and rock falls from the west carbonate escarpment (lee side). This environmental model is more complex than previously proposed models of platform-basin transition, which stress the concept of a carbonate platform as a line source of sediment input into the basin. The spill-over from the platform to the east forms a sandy sedimentary deposit that acts as a topographic obstruction to the turbidity current flow from the south. This obstruction is expressed by the westward migration of a northwest-southeast oriented turbidity-current-cut channel.

In Press: *Geology.*

Supported by: NSF Contract No. OCE-8702836.

WHOI Contribution No. 6896.

CONSISTENT CRITERIA FOR MODEL ORDER ESTIMATION

David Burshtein and Ehud Weinstein

We present a consistent criterion for model order selection based on the Wald's statistic. The criterion only requires the estimation of the model parameters under the highest model order. The criterion is compared with Akaike's information criterion (AIC), and with the Minimum Description Length (MDL) criterion. The application of the proposed criterion to order estimation of Auto-Regressive-Moving-Average (ARMA) models is considered.

In Press: *IEEE Transactions on Acoustics, Speech, and Signal Processing.*

Supported by: ONR Contract No. N00014-85-K-0272.

WHOI Contribution No. 6912.

OPTICAL DISK USE AND EVALUATION IN HARSH FIELD ENVIRONMENTS

Kenneth E. Prada

The need for large volume storage for oceanographic and environmental measurement applications is critical to the success of modern instrument systems. The use of similar media in differing recording applications (ships, buoys, or land stations) strongly enhances ease of analysis. Magnetic media have been used in many forms for years, accompanied by the inherent problems this media presents. Recent magnetic disk technology

presents unique potential but, for many reasons, is not suitable for field use in applications where extremes of temperature and motion prevail.

Optical disk technology, a recent development, is ideally suited to the needs of field data collection. The problems encountered with magnetic media are not associated with optical media. However, this new storage method has been untested in the harsh environments encountered in typical field operations.

Published in: *EOS Transactions, American Geophysical Union*, 69(49), December 6, 1988.

Supported by: ONR Contract No. N00014-86-C-0126.

WHOI Contribution No. 6908.

TIDE INDUCED VARIATION OF THE DYNAMICS OF A SALT WEDGE ESTUARY

W. Rockwell Geyer and David M. Farmer

The time variations of the salt wedge intrusion in the Fraser estuary, British Columbia, were monitored during a variety of tidal and run-off conditions using instruments and sampling methods that provided high resolution of the velocity and water properties in space and time. The salt wedge was found to vary considerably in position and vertical structure through the tidal cycle due to interaction of the tidal flow with the baroclinic dynamics of the salt wedge. During the flood, the salt wedge progressed up the estuary as a gravity current, while during the ebb the salinity structure was eroded by shear instability. The difference in the character of the flow between flood and ebb is attributed to the transition between a subcritical and supercritical internal Froude number. During the flood, the internal state is subcritical, and the estuarine shear flow is maintained with a small amount of vertical mixing, while in the supercritical ebb flow, vertical shears become so large that the pycnocline becomes unstable, and the salt wedge structure breaks down.

In Press: *Journal of Physical Oceanography.*

Supported by: NSF Contract No. OCE-8308586.

WHOI Contribution No. 6914.

SAND TRANSPORT BY UNBROKEN WATER WAVES UNDER SHEET FLOW CONDITIONS

John Trowbridge and Donald Young

A simple model is presented for one-dimensional sediment transport and topographical changes seaward of the break point on a natural sand beach. The model incorporates a realistic representation of the shoaling random wave field, a systematic treatment of the bottom boundary layer, and a new expression for the rate of sediment transport in oscillatory sheet flow conditions. The model contains a single adjustable constant, which is determined from high-quality laboratory measurements of sediment transport at relevant large scales. Without empirical tuning, the model produces quantitative results in good agreement with recently reported field observations of evolution of an offshore bar.

In Press: *Journal of Geophysical Research.*

Supported by: NSF Grant Number CEE-8404258 and OCE-8710768; Sea Grant No. NA86AA-D-FG090, and NA85AA-D-SG033.

WHOI Contribution No. 6754.

FIELD CALIBRATION OF MIXED-LAYER DRIFTERS

Dr. Wayne Geyer

A set of field experiments was conducted to determine the water- following characteristics of mixed layer drifters with holey sock drogues. Through the use of a drifting current meter array, direct estimates of slip velocity (or the difference between the velocity of the drifter and that of the water surrounding the drogue) were obtained with precision of better than ± 1 cm s^{-1}. The range of slip velocities was 1 to 4 cm s^{-1}, with the orientation of the slip principally in the downward direction. The results are consistent with a simple model for slip induced by a wind-drift current, assuming a static balance of drag forces.

In Press: *Journal of Atmospheric and Oceanic Technology*, February 1989.

Supported by: NSF Grant No. ATM 82-17015.

WHOI Contribution No. 6771.

STORM-GENERATED SURFACE WAVES AND SEDIMENT RESUSPENSION IN THE EAST CHINA AND YELLOW SEAS

Hans C. Graber, Robert C. Beardsley, and William D. Grant

Surface winds derived from atmospheric pressure fields are input to a finite-depth wind-wave model to predict the sea state during a cold air frontal passage over the Yellow and East China Seas which occurred during November 15-18, 1983. The predicted maximum wave stress field near the bottom is used to examine the

concept of turbulent wave intensities causing sediment resuspension. The temporal variability of the wave field at three sites are used to illustrate the dependence of the bottom response of depth within the Yellow Sea. Maps of the temporal and spatial distribution of index for initiation of sediment movement are computed for different non- cohesive sediment materials during this storm period and compared to sedimentological results for this region.

This study demonstrates that wave action is a mechanism which can significantly influence the sediment transport pattern induced by the regional circulation existing in this marginal sea. The results also identify regions where winter storm-generated surface waves are too weak to affect bottom sediments. Although the spatial variability of sediment resuspension depends on sea state and sediment material, the predicted wave-induced bottom shear stresses during a characteristic winter storm show that fine-grained material can be resuspended as far out as the 100 m isobath in the East China Sea.

These numerical simulation results suggest that the present-day distribution of sediments in the Yellow and East China Seas is in part a direct consequences of storm-generated surface waves during the winter season. The numerical model results further suggest that erosion of sand along Chinese and Korean coasts is largely determined by surface wave action. Furthermore, the present-day mud patch south of Cheju Island appears to be a consequence of the circulation pattern in the Yellow and East China Seas, which could trap fine-grained sediment resuspended by surface waves off the Chinese coast from escaping into the Pacific Ocean.

In Press: *Journal of Physical Oceanography.*

Supported by: ONR Contract Nos. N00014-82-C-0019, N00014-85-C-0001. NSF Contract Nos. OCE-8501366, OCE-8403249.

WHOI Contribution No. 6852.

OPTIMAL SOURCE LOCALIZATION AND TRACKING USING ARRAYS WITH UNCERTAINTIES IN SENSOR LOCATIONS

Mordechai Segal and Ehud Weinstein

We develop a computationally efficient algorithm for source localization and tracking, using active/passive arrays with uncertainties in sensor locations. We consider a general scenario in which the uncertainties may be correlated in time and space. The proposed algorithm is optimal in the sense that it converges iteratively to a stationary point of the likelihood function where each iteration increases the likelihood of the estimated location parameters. In the case of multiple sources, the algorithm makes an essential use of the information available from all sources to reduce the array uncertainties (the so-called array calibration) and thus to improve the localization accuracy of each signal source. We also present new expressions for the log-likelihood gradient (score), the Hessian and the Fisher's information matrix, that may be used for efficient implementation of gradient-based algorithms, and for assessing the mean square error of the resulting Maximum Likelihood (ML) parameter estimates.

Submitted to: *IEEE Transactions on Acoustic, Speech, and Signal Processing.*

Supported by: ONR Contract No. N00014-85-K-0272.

WHOI Contribution No. 6867.

EVIDENCE OF HYDROTHERMAL ACTIVITY ON MARSILI SEAMOUNT, TYRRHENIAN BASIN

Elazar Uchupi and Robert Ballard

Mid-place seamounts with their potential (now or in the past) for intense open hydrothermal circulation make ideal sites for hydrothermal precipitation. OHMOTO (1978) reports that many volcanogenic massive sulfides are associated with submarine calderas, e.g. some of the Kuroko deposits and part of the Troodos ores. Dredging on some of these highs on the flanks of the East Pacific Rise, for example, have yielded spongy masses of iron oxide (BONATTI and JOENSUU, 1966), polymetallic sulfides rich in cobalt from a cone 6 km east of the East Pacific Rise (HEKINIAN et al, 1981), copper-rich polymetallic sulfides within a caldera and on the summit bench of an 800 m high seamount 11 km north-west of the Rise, and red oxides on small peaks at the caldera margins from a seamount from an older crust 18 km from the East Pacific Rise (LONSDALE et al, 1982). MALAHOFF et al (1982) and MALAHOFF (1988) also have described surficial oxide an nontronite deposits enriched in gold from Loihi Seamount, a hot spot volcano south of Hawaii at a water depth of 980 m. In this interim report we describe the finding of what appears to be an extensive hydrothermal mineral deposit on the crest of Marsili Seamount in the Tyrrhenian Basin, western Mediterranean Sea. The deposit on the seamount was discovered during a study of the geology of the Tyrrhenian Basin with the Argo video system (HARRIS and BALLARD, 1986) aboard the R/V Starella during June, 1988. Mounted on the vehicle were three Silicon Intensified Target (SIT) cameras, a digital

Charge Couple Device (CCD) camera and a 35 mm camera with a 16 mm lens. The CCD and 35 mm cameras triggered from the vessel were used to take high resolution black and white (CCD camera) and color (35 mm camera) photographs of significant geologic features crossed by Argo. The site was revisited in mid August aboard the R/V Knorr during a cruise to test the dynamic position system on the Knorr, a fiber optic cable used to transmit color video images, and a traction winch.

Submitted to: *Deep Sea Research.*

Supported by: NSF Grant No. OCE-8511431; ONR No. N00014-87-J-1111, Navy Chair No. N00014-85-J-1242.

WHOI Contribution No. 6884.

OCEAN ACOUSTIC TOMOGRAPHY: ESTIMATING THE ACOUSTIC TRAVEL TIME WITH PHASE

John L. Spiesberger, Paul J. Bushong, Kurt Metzger, Jr., and Theodore G. Birdsall

Continuous acoustic transmission (133 Hz, 60 ms resolution) between a bottom-mounted source near Oahu, Hawaii, and a bottom-mounted receiver at 4000 km range near the coast of northern California are recorded during a 5-day interval in 1983. One of the purposes of these transmissions is to learn how to make more precise measurements of the travel time so that basin-scale fluctuations in the Pacific can be detected. Daily incoherent averages of some of the multipaths exhibit stability during this period. The standard deviation of the travel time of the resolved peaks in the daily incoherent averages is about 30 ms. An acoustic method, based on cross correlation, is derived to estimate the change in the average acoustic phase (travel time) to a precision of about 0.018 cycles (135 μS) every 2 min. Travel time estimates based on the cross correlator reduce the aberrations due to internal waves by about 19 dB in comparison with CW transmissions in this experiment. The new travel-time estimator is applied to the measurements to examine some of the fluctuations of the Pacific. Power spectra of the phase, at periods less than about 34 h, exhibit several significant peaks at nontidal periods whose equivalent rms travel times are between 1 and 10 ms. The travel times along different ray paths oscillate in phase with each other at periods near the prominent nontidal periods of 20 and 15.6 h. This observation leads to the conclusion that the ocean process is either barotropic or else it consists of the first or the second baroclinic mode with a horizontal scale which is larger than 50 km. The observation of the nontidal oscillations would not be possible if the travel times were estimated from the amplitudes of the received multipaths.

Published in: *IEEE Journal of Oceanic Engineering*, 14(1), 108-119, (1989).

Supported by: ONR Contract No. N00014-86-C-0358.

WHOI Contribution No. 6898.

INVERSE METHODS IN OCEAN BOTTOM ACOUSTICS

George V. Frisk

A review is presented of inverse methods used to determine the acoustic properties of the bottom in both deep and shallow water. The discussion concentrates primarily on inversions for properties in the top few hundred meters of sediment using input data in the frequency range 25-500 Hz. The one dimensional, horizontally stratified case is emphasized, although implications for problems of higher dimensionality are discussed. Descriptions of theoretical methods and experimental techniques as well as examples of inversions of synthetic and experimental data are presented.

Submitted to: *Geophysical Tomography*, edited by Y. Desaubies, A. Tarantola, and J. Zinn-Justin.

Supported by: ONR Contract No. N00014-86-C-0338.

WHOI Contribution No. 6892.

A MODAL/WKB INVERSION METHOD FOR DETERMINING SOUND SPEED PROFILES IN THE OCEAN AND OCEAN BOTTOM

Kevin D. Casey and George V. Frisk

Two approaches to determining sound speed profiles in the ocean and ocean bottom using measured acoustic modal eigenvalues are examined. Both methods use measured eigenvalues and mode dependent assumed values of the WKB phase integral as input data and use the WKB phase integral as a starting point for relating the index of refraction to depth. Inversion method 1 is restricted to monotonic or symmetric sound speed profiles and requires a measurement of the sound speed at one depth to convert the index of refraction profile to a sound speed profile. Inversion method 2 assumes that the sound speed at the ocean surface and the minimum sound speed in the profile are known and is applicable to monotonic profiles and to general single duct sound speed profiles. For asymmetric profiles, inverse method 2 gives the depth difference between two points of equal sound speed in the portion of the profile having two turning points, and in the

remainder of the profile it gives sound speed versus depth directly. A numerical implementation of the method is demonstrated using idealized ocean sound speed profiles, and numerical experiments are used to test the performance of the inversions using noisy data. The two methods are also used to determine the sediment sound speed profiles in two shallow water waveguide models, and inversion method 1 is used to find the sediment sound speed profile using data from an experiment performed in the Gulf of Mexico.

Submitted to: *Journal of the Acoustical Society of America.*

Supported by: ONR Contract No. N00014-86-C-0338.

WHOI Contribution No. 6849.

PHASE AND TRAVEL-TIME VARIABILITY OF ADIABATIC ACOUSTIC NORMAL MODES DUE TO SCATTERING FROM A ROUGH SEA SURFACE, WITH APPLICATIONS TO PROPAGATION IN SHALLOW WATER AND HIGH-LATITUDE REGIONS

James F. Lynch, James H. Miller, and Ching Sang Chiu

Simple theoretical expressions are generated for the phase and travel time variations (specifically wander and bias) of normal modes due to scattering by a rough ocean surface. These expressions are explicitly demonstrated for two canonical waveguide examples, the hard bottom (shallow water) waveguide and the n^2 - linear (high latitude) waveguide. Numerical examples of the scattering statistics generated for both waveguides are given, and the implications of the examples for shallow water acoustics, high latitude acoustics, and ocean acoustic tomography are discussed. An application of the theory developed to the cross coherence of modes measured in an Arctic waveguide during FRAM IV is also shown.

Published in: *Journal of the Acoustical Society of America*, 85(1), 83-89 (1989).

Supported by: ONR Contract Nos. N00014-86-C-0127, N00014-85-C-0001, and N00014-82-C-0152.

WHOI Contribution No. 6651.

MEASUREMENTS OF A BAROTROPIC PLANETARY VORTICITY MODE IN AN EDDY-RESOLVING QUASI-GEOSTROPHIC MODEL USING ACOUSTIC TOMOGRAPHY

Wendy B. Lawrence and John L. Spiesberger

An acoustic source and receiver are placed at 800 m depth and are separated by 4000 km in a 2-layer, steady-wind driven, flat bottom eddy-resolving quasi-geostrophic circulation model. Time series of sea surface elevation and upper and lower layer meridional currents are generated for comparison against a series of acoustic travel time. The spectra of the time series exhibit a broad mesoscale peak near a period of 40 days. The spectrum of the acoustic travel time contains a significant peak, which is not present in the spectra of the point measurements, due to a resonant barotropic oscillation with a period of 29.0 days. In this numerical model, basin-scale tomographic measurements are a useful method of sensing the large-scale resonant barotrophic oscillations because the tomographic system attenuates the "noise" from the mesoscale.

In Press: *Journal of Physical Oceanography*, (1989).

Supported by: ONR Contract No. N00014-86-C-0358.

WHOI Contribution No. 6942.

CONTROL OF REMOTELY OPERATED VEHICLES FOR PRECISE SURVEY

Dana R. Yoerger and James B. Newman

Remotely operated vehicles can be made more useful for a wide range of survey tasks through the use of precision navigation and automatic control. Tasks ranging from scientific survey to ship hull inspection can be done more productively and produce a more useful result if the motions of the ROV are tightly controlled. A key benefit of automatic control is the ability to repeat a track at a later time to study dynamic processes.

This paper presents experimental results of the control system for the JASON ROV that has been designed for precision survey and other automated applications. The JASON control system emphasizes a form of supervisory control where the human pilot and the automatic system share the control task. Results presented include hovering, automatic track following, and several interactive modes.

Submitted to: *Intervention 1989 Proceedings.*

Supported by: ONR Contract Nos. N00014-86-C-0038, N00014-88-K-2022, and ONR grant N00014-87-J-1111.

WHOI Contribution No. 6977.

CONTROL CAPABILITIES OF JASON AND ITS MANIPULATOR

Dana R. Yoerger and David M. DiPietro

Underwater work systems can be made more effective if vehicles and manipulators are automatically controlled and can work together in a coordinated fashion. Coordinated control can greatly increase the workspace of the manipulator without the need for additional or larger manipulator links. Such control will also minimize the need for attachment points, which is especially important in unprepared or poorly structured environments.

This paper reviews two major elements of the JASON system that will support such control. The first element is a hover control system for JASON, and results from a recent experiment in shallow water are presented. The second element concerns the design of a manipulator that is especially suited to tasks requiring force control that will fit very naturally into a combined vehicle-manipulator control system. The overall philosophy and design of the arm are summarized.

Submitted to: *Conference on International Ocean Technology Congress EEZ Resources: Technology Assessment.*

Supported by: ONR Contract nos. N00014-86-C-0038, N00014-88-K-2022, and N00014-87-J-1111.

WHOI Contribution No. 6959.

RECRUITMENT OF BENTHIC INVERTEBRATES IN BOUNDARY-LAYER FLOWS: A DEEP-WATER EXPERIMENT ON CROSS SEAMOUNT

Lauren S. Mullineaux and Cheryl Ann Butman

The response of metazoan larvae and other propagules (e.g., foraminifers) of deep-water, encrusting invertebrates to different flow conditions was investigated by deploying circulat flat plates with differing thicknesses and surfaces on the summit of Cross Seamount, Central North Pacific (410-m water depth). Measurements of currents 1.8 m above the study site during the 48-day experiment were combined with dissolution patterns on alabaster disks and previous laboratory flume studies to describe the flow patterns expected to occur over the experimental plates. In the flume studies, plates with thin edges (1.5 mm) developed a gradually thickening boundary layer downstream from the edge oriented into the current, while plates with thick edges (10.0 mm) developed a separation eddy extending 2-3 cm downstream from the leading edge; patterns of dissolution on alabaster discs in the field confirmed these patterns. Recruitment of organisms (mostly benthic foraminifers) onto the thin plates was significantly lower at the edges than near the centers of the plates. On the thick plates, recruits were most abundant 2-3 cm in from the edges of the plates, where the attachment point of the separation eddy was expected to occur most frequently. These patterns may result from variations in larval supply to responses to variations in the flow regime over the plates. In addition, several taxa recruited exclusively onto thick plates covered with finely powdered ferromaganese crust, suggesting that some taxa actively select for substratum composition or texture. Thus, although much of the variation in recruitment of deep-water invertebrates onto experimental plates can be explained by flow patterns, some taxa may be actively responding to other cues during settlement.

Submitted to: *Limnology and Oceanography.*

Supported by: ONR Contract No. N00014-87-K-0007, a grant of submersible time from NOAA, and the Coastal Research Center.

WHOI Contribution No. 6953.

PASSIVE LOCALIZATION OF CALLING ANIMALS AND SENSING OF THEIR ACOUSTIC ENVIRONMENT USING ACOUSTIC TOMOGRAPHY

John L. Spiesberger and Kurt M. Fristrup

The sounds emitted by terrestrial and marine animals can be used to localize their positions when monitored by several acoustic receivers. The localization can proceed quickly and automatically with the use of computers when cross-correlation of the acoustic records is used to optimally estimate the travel-time difference between signals at different receivers. The time-bandwidth product (call duration X acoustic bandwidth) of the call is an important parameter. When the time-bandwidth product of the acoustic call equals or exceeds 10, localization is possible even when the signal-to-noise ratios of the call are below the noise level as long as cross- correlation is used to estimate the travel time difference. Use of cross-correlation significantly increases the range at which a calling animal may be detected over that possible by visual inspection of acoustic records.

The calls of many animals have time- bandwidth products which exceed 10. The error maps for the localization can be improved by factors between 2 and 100 when the fluctuation in winds (currents) and the sound speed, and the errors in the receiver positions are accounted for with tomographic techniques. In addition, useful tomographic maps of the atmospheric wind and the sound speed fields can be obtained from the sounds emitted by the animals. Tomographic maps of the currents and the sound speed in water are much less precise because the fractional change in the acoustic propagation speed due to currents and sound speed fluctuations are much smaller in water than in the air. Studies in ecology, behavior, and conservation could be significantly enhanced using acoustic tomography.

In Press: *The American Naturalist*, (1989).

Supported by: ONR Contract Nos. N00014-86-C-0358, N00014-88-K-0273 and the National Institute of Health N525290-01.

WHOI Contribution No. 6968.

EXPERIMENTS ON THE IMPORTANCE OF HYDRODYNAMICAL PROCESSES IN DISTRIBUTING SETTLING INVERTEBRATE LARVAE IN NEAR-BOTTOM WATERS AND IMPLICATIONS FOR SETTLEMENT

Cheryl Ann Butman

The hypothesis that planktonic larvae of benthic invertebrates sink through the water like passive particles in turbulent flows near the seabed was tested in the field by exploiting the biased sampling characteristics of sediment traps. The particle collection efficiency of a given sediment-trap design depends on its geometry, the particles, and the flow. Traps were calibrated in a laboratory flume using, as passively sinking larval mimics, glass spheres having fall velocities of coarse silt sediments, similar to those measured on nonswimming polychaete larvae. The flume study was conducted using full-scale traps (to maintain geometric similarity) and for flow conditions designed for approximate dynamical similarity to mean tidal flow conditions in the field. A priori predictions regarding the rank order in which various trap designs would collect passively sinking larvae in the field were thus specified by the rank order in which the traps collected the passively sinking larvae mimics (spheres) in the flume. The field experiments were conducted at two sites, 10- and 14-m depth, in Buzzards Bay, MA (USA), and traps were moored ~1-m above the seabed.

In experiments during four field seasons, the deployments lasting from several hours to eleven days, trap collections of Mediomastus ambiseta (a polychaete worm) postlarvae, total bivalve and postlarvae, spionid/sabellariid polycheate larvae (individuals too small to identify definitively to family), spionid polychaete larvae, enteropneust larvae, and gastropod larvae generally corresponded to the patterns predicted for passive particle collections between or among sediment-trap designs. While the results were statistically more significant during some collection intervals than during others, the rank order of larval collections within each group of traps (deployed simultaneously) nearly always corresponded to the rank order of passive particle collections by the traps in the flume. Collections of the polychaete Pectinaria gouldii, were much more similar between or among trap designs (i.e., not biased, as predicted for passive particle collections) than for the groups listed above. It is speculated that the passive sinking characteristics of this organism may differ substantially from those of the organisms mentioned above because Pectinaria larvae are known to build a tube while still in the water column. If the worm-tube assembly sinks more like coarser sands, than like silts, then collections normalized to mouth area are expected to be similar among trap designs. Collections of metamorphosing seastar larvae also were in the predicted passive rank order, which may be due, at least in part, to larvae adhering to solid trap surfaces during metamorphosis.

The passive sinking hypothesis could not be falsified in most of the field experiments, indicating that hydrodynamical processes may determine the distribution of larvae in very near-bottom waters. Passive sinking by larvae is not, however, an explicit result of this experimental study. Other processes that may have produced the observed collections, such as differences among trap designs in the chemical, sedimentary or biological environments, must now be tested against the passive sinking alternative hypothesis. If larvae do sink like passive particles to within 0.5-m of the seabed, as the results of this study suggest, then it is possible that larvae initially reach the seafloor at sites where particulates, with fall velocities similar to larvae, initially settle. Passive deposition may thus determine the relatively large-scale distribution of larvae, with active or passive redistribution of larvae, post-settlement selection, or post- settlement mortality determining more localized distributions.

Submitted to: *Journal of Experimental Marine Biology and Ecology.*

Supported by: The Coastal Research Center, the Education Program and a PEW Memorial Trust Fellowship at WHOI, the Diving Equipment Manufacturers Association, an Association for Women in Science Predoctoral Award, a National Ocean Survey/Sea Grant Fellowship

(NOAA NA80-AA-D00077), a NSF Dissertation Improvement Grant (OCE-8119865), and a NSF grant (OCE-85000875) to C.A. Butman and J.P. Grassle.

WHOI Contribution No. 6950.

SPATIAL AND SPECTRAL PARAMETER ESTIMATION OF MULTIPLE SOURCE SIGNALS

Mordechai Segal and Ehud Weinstein

We propose a computationally efficient scheme for estimating the spatial (location) and spectral parameters of multiple source signals using passive array data. The source signals using passive array data. The source signals are modeled as possibly correlated narrow-band/wideband Gaussian random processes. We also allow sensor-to-sensor noise correlation. The proposed algorithm is optimal in the sense that it converges monotonically to the Maximum Likelihood (ML) estimates (or, at least, to a stationary point of the likelihood function) of the unknown spatial and spectral parameters.

Submitted to: *IEEE International Conference on Acoustics, Speech, and Signal Processing,* May 1989, Scotland.

Supported by: ONR Contract No. N00014-85-K-0272.

WHOI Contribution No. 6955.

BASIN-SCALE TOMOGRAPHY: SYNOPTIC MEASUREMENTS OF A 4000 KM LENGTH SECTION IN THE PACIFIC

John L. Spiesberger, Paul J. Bushong, Kurt Metzger, Theodore G. Birdsall

Continuous acoustic transmissions (133 Hz, 60 ms resolution), between a bottom-mounted source near Oahu and a bottom-mounted receiver at about 4000 km range near the coast of Northern California, are recorded during a five day interval in 1983 and a 21 day interval in 1987. Measurements of the acoustic travel-time change, based on the acoustic phase, are made every two minutes to a precision of about 135 μS. Power spectra of the acoustic phases, at periods less that about 34 hours, exhibit many significant peaks at non-tidal periods whose equivalent rms travel times are between 1 and 10 ms. The periods and amplitudes of these peaks change significantly over intervals of five days. The 1983 data set is used to demonstrate that the travel times along different ray paths oscillate in phase with each other at periods near the prominent non-tidal periods of 20 and 15.6 hours. This observation leads to the conclusion that the ocean process is either barotropic or it consists of the first or the second baroclinic mode with a horizontal scale of at least 50 km.

Several hypotheses are considered for the non-tidal oscillations. The internal wave field is too baroclinic and too weak to generate the non-tidal acoustic oscillations. Simple linear models, forced by peak values of the atmospheric pressure and the wind, are unable to generate an ocean response of sufficient size to account for the acoustic spectra. It is possible that the small non-tidal peaks (1 ms rms) are caused by resonant gravity wave modes. The large non-tidal peaks have rms travel times as large as that due to the semi-diurnal tide (about 10 ms). However, historical observations from tide and bottom pressure gauges may rule out the possibility that shallow-water gravity wave modes cause the large travel time oscillations unless the modes are excited intermittently or unless the structure of the modal shapes computed by Platzman are incorrect. If the modes are responsible for some of the non-tidal peaks, then some excitation mechanism must be found for them other than pressure and wind forcing of the ocean through linear models. In conclusion, we cannot reconcile the acoustic observations with historical measurements and contemporary theories.

The internal wave field and the acoustic noise impose an ultimate limit on the ability of a tomographic array (which utilizes acoustic frequencies above 100 Hz) to detect basin-scale currents. For an array consisting of an acoustic source and ten acoustic receivers, the threshold at which a basin- scale current can be detected with a confidence of ninety-five percent is given by $u \cong 33.6T$ micro-meters per second where the amplitude of the current is u and the period of the oscillation, T, is expressed in days. Other fluctuations in the ocean may place more severe limits on the ability to detect basin-scale currents.

Submitted to: *Journal of Physical Oceanography.*

Supported by: ONR Contract No. N00014-86-C-0358.

WHOI Contribution No. 7005.

REMOTE SENSING OF WESTERN BOUNDARY CURRENTS USING ACOUSTIC TOMOGRAPHY

John L. Spiesberger

The advantages and limitations of using long-range acoustic tomography, between fixed sources and receivers, to infer the position changes

of the front of a western boundary current are investigated. When the acoustic phases of the ray paths are used, the position change of a front can probably be estimated with an accuracy of a few kilometers over periods of a few days under many conditions. Hourly estimates of the propagation speed of the front along the acoustic path have a precision of about 8 cm/s. The limitations of the position and speed estimates of the front arise from the random fluctuations of the internal wave field. Since the meanders can propagate more than 20 km a day and the speeds can be several meters per second, useful estimates of the unstable region of a western boundary current can be achieved. The principal limitation of the technique is imposed by the horizontal refraction of the ray paths by rotations of the front by 60 degrees or more. When the rotations of the front are less than 60 degrees, horizontal refraction effects should be small and the estimates of the frontal position along the transmission path have about the same resolution and precision as those based on satellite observations.

Submitted to: *Journal of the Acoustical Society of America.*

Supported by: ONR Contract No. N00014-86-C-0358.

WHOI Contribution No. 7006.

CHARACTERIZATION OF DEEP SEA STORMS

Albert J. Williams III

In order to describe and quantify the physical forcing of sediment transport events at the HEBBLE site velocity, stress and sediment concentration data were obtained during a year long deployment. Through the year a variety of intense sediment transporting "events" were recorded. Careful analysis of these "events" reveals that only a small proportion of the peaks in suspended sediment concentration correspond to "local" erosion. Most sediment "events" are clouds of fine suspended material advected into the region. Analysis of progressive vector diagrams reveal that these advected clouds are bounded by regions with concentration gradients as high as 200 μgm/l/km. The high gradients suggest streams of sediment bearing water which have developed sharp fronts of sediment concentration along their sidewalls, are veering across the region. The largest concentrations of suspended sediment are observed during local suspension events. The growth and decay of the sediment clouds during the "local" events lags the changes in depth of the turbulent mixed layer. The peak in concentration occurs a short time after the peak velocity, because the source of sediment to be eroded is not depleted, but is winnowed, leaving behind sediment not so easily eroded. Thus deposition begins almost immediately after the peak velocities are past. The depositional period may last for several weeks, whereas the erosion occurred in only a few days. Photographs of the bottom reveal depositional features, crag and tail dunes, which are aligned with the post storm flow, not the erosional flow direction.

Submitted to: *Deep Sea Research, HEBBLE Edition.*

Supported by: ONR Contract No. N00014-85-C-0001.

WHOI Contribution No. 7007.

OBSERVATIONS OF SHEAR AND VERTICAL STABILITY FROM A NEUTRALLY-BUOYANT FLOAT

Eric Kunze, Albert J. Williams III, and Melbourne G. Briscoe

Measurements of shear and temperature-gradient over 0.5-5 m from a neutrally-buoyant float are used to examine the statistics and sources of shear instability in a 9-day record. "Unstable" conditions (defined as $|V_2|/N>2$) are due to higher-than-average shear rather than lower-than-average buoyancy frequency; there are no instances of unstable buoyancy frequency or overturns on the >0.5-m spacing of the thermistors. Shear is dominated by upward propagating near-inertial motions. In particular, "unstable" events occurred most frequently when a near-inertial motions. In particular, "unstable" events occurred most frequently when a near-inertial wave packet occupied the water parcel tracked by the float. Groups of events occur roughly every 5-7 h at scales <2.5 m, much more rarely at larger scales, and typically last 10 min (one buoyancy period) or longer. Turbulent and mixing quantities are estimated from these finescale measurements, giving a dissipation rate of $\varepsilon \sim 10^{9}$ W/kg and an eddy diffusivity of $K_T \sim 10^{-6} m^2$ /s.

Submitted to: *Journal of Geophysical Research.*

Supported by: ONR Contract No. N00014-85-C-0001.

WHOI Contribution No. 7008.

A DEEP-SEA SEDIMENT TRANSPORT STORM

Thomas F. Gross, Albert J. Williams III, and Arthur R.M. Nowell

Photographs taken of the sea bottom since the 1960s suggest that sediments at great depth may

be actively resuspended and redistributed. Further, it has been suspected that active resuspension/transport may be required to maintain elevated concentrations of particles in deep-sea nepheloid layers. But currents with sufficient energy to erode the bottom, and to maintain the particles in suspension, have not been observed concurrently with large concentrations of particles in the deep nepheliod layer. The high-energy benthic boundary-layer experiment (HEBBLE) was designed to test the hypothesis that bed modifications can result from local erosion and deposition as modelled by simple one-dimensional local forcing mechanics. We observed several "storms" of high kinetic energy and near-bed flow associated with large concentrations of suspended sediment during the year-long deployments of moored instruments at the HEBBLE study site. These observations, at 4,880 m off the Nova Scotian Rise in the north-west Atlantic, indicate that large episodic events may suspend bottom sediments in areas well removed from coastal and shelf sources.

Published in: *Nature*, Vol. 331, No. 6156, pp. 518-521, 11 February 1988.

Supported by: ONR Contract No. N00014-85-C-0001.

WHOI Contribution No. 7009.

ANALYSIS OF HIGH FREQUENCY MULTITONE TRANSMISSIONS PROPAGATED IN THE MARGINAL ICE ZONE

Josko A. Catipovic and Arthur B. Baggeroer

This work presents estimates of frequency and time coherence functions of acoustic transmissions centered at 50 kHz over a 1 km horizontal under-ice path in the Marginal Ice Zone (MIZ). The data were collected during the MIZEX '84 experiment as part of a feasibility study for an underwater acoustic telemetry ling. It is shown that the acoustic fluctuations are dominated by a 10 Hz process conjectured due to the turbulent under-ice boundary layer. Significant fluctuation energy in the 0.1 Hz band was also observed. The two processes differ in frequency coherence characteristics. An underwater telemetry system designed for this channel will be dominated by the high frequency fluctuations, but the slower process is capable of causing disastrous data losses unless its effects are anticipated.

Submitted to: *Journal of the Acoustical Society of America.*

Supported by: ONR Contract No. N00014-86-K-0325 and the Charles Stark Draper Lab.

WHOI Contribution No. 7022.

PERFORMANCE OF SEQUENTIAL DECODING OF CONVOLUTIONAL CODES OVER FULLY FADING OCEAN ACOUSTIC CHANNELS

Josko A. Catipovic and Arthur B. Baggeroer

Sequential decoding of long constraint convolutional codes is shown to be a feasible technique for digital data telemetry over realistic marine acoustic channels. A computational bound for sequential decoding over a fading dispersive channel is derived for hard limiting and quantizing decoders. The results indicate that a minimum of 8 dB of bit SNR is required for sequential decoder operation. Simulations indicate that 14 dB bit SNR results in simple and feasible implementations. Diversity methods for coded transmissions over Rayleigh fading channels are examined. The optimal diversity level for both minimum error probability of uncoded systems and the diversity level for minimizing the sequential decoder computational load are derived and shown to be different, with the latter requiring a higher order of diversity. Performance differences between fixed-diversity and optimal diversity systems are presented.

Submitted to: *IEEE Journal of Oceanic Engineering.*

Supported by: ONR Contract No. N00014-86-K-0751 and the Charles Stark Draper Lab.

WHOI Contribution No. 7023.

A MODEL-BASED APPROACH TO 3-D IMAGING AND MAPPING UNDERWATER

W. Kenneth Stewart

An approach to multidimensional representation of underwater environments is presented with results of applications in 3-dimensional sonar mapping. A non-deterministic model incorporates information from multiple knowledge sources and creates a framework for real-time processing. Probabilistic methods account for non-ideal sensors while spatial decomposition and numerical techniques treat amorphous underwater features and allow an incremental approach to modeling the surroundings. An emphasis on representational and modeling issues is maintained with examples drawn from computer simulations and field data from profiling and imaging sonars.

Published in: *Seventh International Conference on Offshore Mechanics and Arctic Engineering*, Vol. 5, 61-71, 1988.

Supported by: Sea Grant Contract No. NA86AA-D-FG089 and ONR Contract Nos. N00014-87-J-1111 and N00014-86-C-0038.

WHOI Contribution No. 7024.

ACOUSTIC IMAGING, PROCESSING, AND AI MODELING

W. Kenneth Stewart

Recent developments in advanced remote systems promise to extend our human perception to the deeper ocean regions, but our ability to conduct successful and efficient research, exploration, survey, work, or inspection demands an acute capability to sense and model the undersea environment. This paper describes an approach to the construction of multisensor stochastic models for intelligent systems exploring an underwater environment. The important characteristics shared by such applications are: real-time constraints; unstructured, three-dimensional terrain; high-bandwidth sensors providing redundant, overlapping coverage; lack of prior knowledge about the environment; and inaccuracy or ambiguity in sensing and interpretation.

Published in: *Proceedings of the International Ocean Technology Congress*, February 1989, Hawaii.

Supported by: Sea Grant Contract No. NA86AA-D-FG089, and ONR Contract Nos. N00014-87-J-1111 and N00014-86-C-0038.

WHOI Contribution No. 7025.

SIMPLE APPROXIMATE FORMULAS FOR BACKSCATTERING OF SOUND BY SPHERICAL AND ELONGATED OBJECTS

Timothy K. Stanton

The scattering of sound by objects is a complex process and is dealt with both analytically and numerically. Regardless of method, calculation of the exact scattered field is quite laborious and may require much computer time as well as human time to program the computer. In order to simplify calculations of the backscattering by a fluid sphere, Johnson combined low- and high-frequency limits in a heuristic manner to obtain a simple closed-form solution (named the "high-pass" solution) (J. Acoust. Soc. Am. 61, 375-377 (1977)). In this present article, his approach is refined and generalized so that the scattering by bodies of other shapes can be described. The general model is evaluated for the sphere, prolate spheroid, straight finite cylinder, and bent finite cylinder. The scattering geometries for these specific examples are limited to normal and near-normal incidence for the elongated objects, although the general model can accommodate other geometries provided the exact solutions exist. Comparisons are made of the scattering of these objects using both modal series solutions and the "high-pass" solutions for fluid, elastic, rigid and fixed, and gaseous materials over a wide range of frequencies. The high- pass solutions are formulated in a general way so as to describe scattering by idealized objects where their shape is simple (i.e. sphere, spheroid, etc.) and their material is lossless and by non-ideal more realistic objects where their shape may be irregular and their material lossy. Calculations of both "ideal" models and "non-ideal" models are compared with the modal solutions by using converged modal series for the ideal cases and truncated (keeping just the first two terms) as approximations for (irregular only) non-ideal cases. In addition to the numerical simulations, some of the high-pass solutions and corresponding modal series solutions are compared with data involving "ideal" objects (machined Dural) and "non-ideal" objects (marine organisms: shrimp, euphausiids, and fish). The numerical and experimental results show promise for use of the high-pass models for quick estimates of backscattered sound of many types of objects.

In Press: *Journal of the Acoustical Society of America.*

Supported by: ONR Contract No. N00014-79-C-0703.

WHOI Contribution No. 7026.

SOUND SCATTERING BY CYLINDERS OF FINITE LENGTH. III. DEFORMED CYLINDERS

Timothy K. Stanton

A general solution is derived for the scattering of sound by circular cylinders of finite length for a deformed axis and composition profile and (cross-sectional) radius that vary along the axis. The orientation of the axis, plane-wave source direction, and point receiver position can also vary so long as the directions of incident and scattered fields are nearly perpendicular to the tangent of the axis (this restriction can be relaxed under some conditions). This solution is a generalization of previous work [T.K. Stanton, J. Acoust. Soc. Am. 83, 55-63 (1988) and T.K. Stanton, J. Acoust. Soc. Am. 83, 64-67 (1988)] where the scattering by straight finite cylinders of uniform fluid and elastic material, respectively, were described. In those articles, the volume flow per unit length of the scattered field of the cylinders was held constant

along the length of the axis which restricted the axis to be straight and composition profile and (cross-sectional) radius to remain constant along the length of the axis. In this article, the volume flow per unit length is allowed to vary, thus allowing the above-mentioned quantities also to vary. As a result, an integral equation is derived that, in general, needs to be evaluated numerically. Examples are given in this article of the scattering of sound at all frequencies from a prolate spheroid with a high aspect ratio (i.e., high ratio of major axis to minor axis) and a uniformly bent finite cylinder of constant cross-sectional radius. There is excellent agreement between the (deformed cylinder) calculations involving the prolate spheroid and the exact spheroidal wave function solution. Furthermore, numerical integration of the deformed cylinder formula required far less computer time than calculating the exact solution. Calculations involving the bent cylinder are compared to backscatter data from preserved euphausiids and suggest that the radius of curvature of the animals plays a major role in the acoustic scatter characteristics of the marine organisms. For example, at 200 kHz the backscattering cross section of a 23-mm-long euphausiid will decrease by 6 dB if the animal bends by as little as 1.4 mm at the ends.

In Press: *Journal of the Acoustical Society of America.*

Supported by: ONR Contract No. N00014-79-C-0703.

WHOI Contribution No. 7027.

FINE SCALE PATCHINESS AT THE GULF STREAM FRONT: AN EXPLORATION USING SONAR

R.W. Nero, J.J. Magnuson, S.B. Brandt, T.K. Stanton, and J.M. Jech

The spatial distribution of animals within the Gulf Stream front is inferred from an analysis of patches that were observed in sonar echograms. Data are analyzed from a downward looking 70 kHz sonar that was towed in multiple transects that were run perpendicular to the front. Patches were defined using an arbitrarily set patch defining algorithm, selected to search for fine scale patches from within 200 X 1,200 pixel (approx. 200 m depth X 20 km width) integrated echo data. Among 17 characteristics measured for each patch, a principal component analysis identified the third component (containing the coefficient of variance among pixels in a patch, and coefficients of grain components of the integrated echo) as a good descriptor of differences between patches within layers and water masses. This component is independent of echo strength and patch size which contribute primarily to the first two components. We interpret high coefficients of variability to indicate a more contagious (clumped) distribution of animals within a patch.

A classification of patches on the third component shows that many patches are acoustically different from distant neighbors but are similar to neighbors within the same layer or region. Many of the fine scale layers are made up of small patches containing schools of either: 1) similar animals or 2), different animals exhibiting a similar spatial arrangement. In addition, a greater number of single solitary scatterers occur within the Slope Waters than within the Gulf Stream. At night, vertical migrators cause reduced acoustic grain and result in a more uniform distribution of targets.

Submitted to: *Deep Sea Research.*

Supported by: ONR Contract No. N00014-79-C-0703.

WHOI Contribution No. 7028.

THE MODULATION TRANSFER FUNCTION: CONCEPT AND APPLICATIONS

William J. Plant

This paper outlines the concept of the modulation transfer function used to relate fluctuations in power received by an active microwave system viewing the ocean to the dominant surface waves on the ocean which cause the fluctuations. Expressions are given for the purely geometric modulations related to surface tilting and changes in range. The manner in which the modulation transfer function enters into the interpretation of real and synthetic aperture radar images, wave spectrometer outputs, scatterometer wind retrievals, and altimeter measurements is reviewed. Finally, limitations of the concept are discussed.

In Press: *Workshop proceedings, "Radar Scattering from Modulated Wind Waves"*, by Komen and Oost, April 1989.

Supported by: NRL Project No. 83-1319-88.

WHOI Contribution No. 7030.

EVIDENCE OF BRAGG SCATTERING IN MICROWAVE DOPPLER SPECTRA OF SEA RETURN

William J. Plant and William C. Keller

Microwave signals backscattered from the ocean (and one lake) have been collected at many

different windspeeds and fetches. Doppler spectra of some signals obtained at low microwave frequencies exhibit double peaks clearly indicating Bragg scattering. At higher microwave frequencies, high wind speeds, long fetches, or in the presence of substantial swell, these splittings disappear. A model of microwave Doppler spectra based on Bragg- scattering, composite-surface theory is developed and used to show that the results obtained in these field studies are compatible with the hypothesis that Bragg scattering dominates microwave backscatter from rough water surfaces under many wind speed and incidence angle conditions. In particular, the model shows double peaks of the proper separation which disappear under the same conditions as those of the actual spectra. Furthermore, Doppler bandwidths given by the model agree with those of the field data under a variety of conditions. A rough angular dependence of the amplitudes of Bragg waves travelling in different directions with respect to the wind is deduced from the measurements. Finally, the implications of these findings for SAR imagery of the ocean are briefly discussed.

In Press: *Journal of Geophysical Research.*

Supported by: NRL Project No. 83-2570-88.

WHOI Contribution No. 7031.

THE NAVAL RESEARCH LABORATORY'S AIR-SEA INTERACTION BLIMP EXPERIMENT

Theodore V. Blanc, William J. Plant, and William C. Keller

The rational is given for a unique experiment in which microwave scatterometer and surface-flux measurements are to be made from a blimp to develop an improved scatterometer-model-function. A principal goal of the effort is to obtain a more accurate understanding of the relationship between the surface fluxes and the microwave power backscattered from the surface of the ocean. The limitations of previous overwater surface flux and scatterometer measurements are reviewed. The accuracy of various flux measurement techniques are compared. Evidence shows that if direct surface flux measurements are to be accurate to better than 20%, the measurements should be made at an altitude of about 5 to 10 m from a platform which is free of flow distortion. The improved surface flux measurements are required to test proposed scatterometer theories and to determine whether the radar backscatter is principally a function of surface stress or wind speed. It is concluded that scatterometer measurements accompanied by eddy- correlation technique flux measurements must be made from a platform that is highly mobile and which enables the measurements to be made over a variety of ocean conditions. To meet these requirements, the Naval Research Laboratory is undertaking a series of air-sea-interaction experiments in which a sonic anemometer and other flux-measurement instrumentation are suspended 60 m beneath a blimp flying at an altitude of 70 m while multiple K_u-band scatterometer measurements are made from the blimp's gondola. Experiments are planned for a wide range of oceanic environments beginning off the central east coast of the United States in 1989.

In Press: *Bulletin of the American Meteorological Society.*

Supported by: NRL Project No. 83-2925-88.

WHOI Contribution No. 7032.

DEPARTMENT OF PHYSICAL OCEANOGRAPHY

Robert C. Beardsley, Chairman

COASTAL CIRCULATION AND DYNAMICS

ENERGY CONSERVATION IN COASTAL-TRAPPED WAVE CALCULATIONS

K. H. Brink

A consideration of energy conservation for coastal-trapped waves shows that, for a slowly varying medium, the normalization of the wave modes is not arbitrary. Errors related to incorrect normalization are demonstrated for a simple analytic example and for a realistic case. If alongshore changes in latitude, topography or stratification are substantial, then predicted time series are shown by an example to have amplitude errors of as much as 50% if an incorrect normalization is applied.

Published in: *Journal of Physical Oceanography.*

Supported by: ONR Contract N00014-84-C-0134, NR 083-400.

WHOI Contribution No. 6895.

TIDE-INDUCED RESIDUAL CIRCULATION SIMULATED ON A PARALLEL COMPUTER

A. Capotondi, R. P. Signell, R. C. Beardsley and V. Sonnad

Tide-induced residual circulation is often the dominant dispersion mechanism in coastal regions of strong to moderate tidal currents, and the accurate prediction of waterborne tracer transport depends critically upon adequate resolution of the scale of the residual features. Since these features often have spatial scales on the order of the tidal excursion or topographic and coastline variation, the number of grid cells needed to adequately resolve the residual flow even in modest domains (of order 50 km x 100 km) can be quite large (10^4-10^5), demanding increased computer power. Parallel processing is one means to provide this increased power. To illustrate the utility of parallel processing, the tide-induced residual circulation in Buzzards Bay and Vineyard Sound, Massachusetts, has been simulated with a two-dimensional numerical model, which was solved with an explicit finite-difference scheme on a parallel processing system configured in the ICAP (loosely Coupled Array of Processors) architecture at IBM Kingston. The resulting tide-induced residual flow is generally consistent with the mean current observed at several locations. The criteria adopted for the parallelization and the performance of the parallel code are described.

Published in: *Journal of Atmospheric and Oceanic Technology.*

Supported by: NOAA Grant NA86-AA-D-SG-090, NA84-AA-O-00033, and WHOI Sea Grants R/P-21 and R/m-12.

WHOI Contribution No. 6828.

ENHANCED SUBINERTIAL DIURNAL TIDES OVER ISOLATED TOPOGRAPHIC FEATURES

David C. Chapman

Amplification of diurnal tidal currents has previously been reported over two isolated topographic features. The explanation suggested was that tidal forcing excites subinertial free waves which are trapped at the topography and propagate around it. However, only free waves were discussed and the actual forcing of the waves by the diurnal tide was not explored. To examine this forcing mechanism, a simple model of an oscillating, rectilinear, barotropic current flowing over a radially symmetric topographic feature is presented. Results support the idea of the resonant excitation of free waves and show that the amplification at the diurnal frequency is substantial for a wide range of topographic sizes. Therefore, a free-wave frequency need not occur precisely at the diurnal frequency in order for the wave to be excited.

In Press: *Deep-Sea Research.*

Supported by: NSF Grant OCE85-21837.

WHOI Contribution No. 6846.

ON THE ORIGIN OF SHELF WATER IN THE MIDDLE ATLANTIC BIGHT

David C. Chapman and Robert C. Beardsley

Based on a limited set of available oxygen isotope measurements, it is hypothesized that the mean flow in the Middle Atlantic Bight is part of a 5000 km-long buoyancy-driven, coastal current which originates along the southern coast of Greenland. This idea is consistent with most features of the known circulation of the region.

In Press: *Journal of Physical Oceanography.*

Supported by: NSF Grants OCE85-21837 and OCE84-17769.

WHOI Contribution No. 6787.

A MODEL FOR THE GENERATION OF COASTAL SEICHES BY DEEP-SEA INTERNAL WAVES

David C. Chapman and Graham S. Giese

A dynamical mechanism for the generation of coastal seiches by deep-sea internal waves is investigated using a linear, two-layer coastal model in which internal waves from the deep ocean impinge upon a step-shelf bottom topography. For periodic incident waves, a pronounced peak in the shelf response occurs at each coastal seiche frequency. The maximum amplitude over the shelf is almost directly proportional to the degree of stratification, which is consistent with the observed increase in seiche activity during periods of strong vertical stratification. The response to one or more internal-wave pulses is modelled by appropriately summing the contributions of the Fourier components based on the periodic results.

The model results are at least qualitatively consistent with observations. For geometry and stratification which are representative of the Caribbean coast of Puerto Rico, reasonably realistic incident pulses preferentially excite the basic seiche frequency, and a rather small amplitude pulse (10 m) can easily generate currents at the shelf break of 8-10 cm s^{-1}. Further, as is typical of the observed seiches, the time history of the modelled motions over the shelf can be rather irregular, depending on the pulse shape and the time delay between pulses.

Published in: *Journal of Physical Oceanography.*

Supported by: NSF Grant OCE85-21837.

WHOI Contribution No. 6927.

THE EFFECT OF COMMERCIAL TRAWLING ON SEDIMENT RESUSPENSION AND TRANSPORT OVER THE MIDDLE ATLANTIC BIGHT CONTINENTAL SHELF

James H. Churchill

Numerous field observations have revealed that turbulence created in the wake of trawl doors can generate large and highly turbid clouds of suspended sediment. Time-averaged concentrations of sediment resuspended by trawls from various areas of the Middle Atlantic Bight continental shelf have been estimated using a simple mathematical model and National Marine Fisheries Service records of commercial trawling activity. Mean concentrations of sediment put into suspension by currents have also been computed using a modified form of the Glenn and Grant model. The results indicate that sediment resuspension by trawling can be a primary source of suspended sediment over the outer shelf, where storm-related bottom stresses are generally weak. In addition, the dramatic decline in trawling activity going seaward over the outer shelf coupled with cross-shore motions in this area may result in a significant net offshore transport of sediment across shelf edge. The concentration estimates further indicate that sediment resuspended by trawls makes a sizeable contribution to the total suspended sediment load over the heavily trawled central shelf area of Nantucket Shoals during all times except winter and early spring.

Published in: *Journal of Geophysical Research.*

Supported by: DoE Contract DE-AC279EV10005.

WHOI Contribution No. 6941.

CAUSATION OF LARGE-AMPLITUDE COASTAL SEICHES ON THE CARIBBEAN COAST OF PUERTO RICO

Graham S. Giese and David C. Chapman

Coastal oscillations with amplitudes of the order of the mean tidal range have been reported from the Caribbean coast of Puerto Rico. Analysis of a 10-year time series of digital tide data from Magueyes Island, Puerto Rico, demonstrates that sea-level variance at the fundamental normal mode frequency of the shelf has a pronounced fortnightly distribution with a maximum occurring 6-7 days after new and full moon. The seasonal variation of the variance has a bimodal distribution with an inverse relationship to zonal wind stress. These results, in combination with the results of two field experiments carried out at times when large-amplitude oscillations were expected, have led to the conclusion that the waves are coastal seiches, most likely excited by deep-sea tide-generated internal solitary waves. The baroclinic-barotropic coupling appears to be strongly affected by the vertical stratification and by the relationship between mixed-layer thickness and shelf depth. In particular, it appears that thin, highly stable buoyant plumes of low-salinity water can play an important role in baroclinic-barotropic energy exchange. The phenomenon observed at Puerto Rico may be global in extent and its further study may lead to the successful prediction of destructive large-amplitude seiches throughout the world.

Published in: *Journal of Physical Oceanography.*

Supported by: NSF Grants OCE82-08621 and OCE85-21837 and University of Puerto Rico Sea Grant program under grant 04-F-158-44030.

WHOI Contribution No. 6928.

SEASONAL DIFFERENCES IN THE CURRENT AND TEMPERATURE VARIABILITY OVER THE NORTHERN CALIFORNIA SHELF DURING CODE

Steven J. Lentz and David C. Chapman

A long-term moored array was maintained over the northern California continental shelf from April 1981 to April 1983 as part of the Coastal Ocean Dynamics Experiment (CODE) to determine the seasonal differences in the current and water temperature characteristics in this region. This long-term moored array consisted of two mid-shelf moorings (C3 and R3) and one upper slope mooring (C5) deployed from April 1981 through July 1982 and one mid-shelf mooring (C3) deployed from August 1982 to April 1983. The summer and winter exhibited quite different *mean* characteristics. During the two summers, a mean southeastward wind stress (upwelling favorable) resulted in cold water over the shelf with isotherms sloping upward toward the coast and a strongly sheared equatorward mean shelf current. The intervening fall and winter of 1981-82 were characterized by a weak mean wind stress, warm shelf water, level isotherms and a poleward mean shelf current which was uniform with depth. In contrast to the means, the summer and winter current and temperature *variability* exhibited many of the same characteristics. The largest current empirical orthogonal functions (EOFs) for each of the shelf moorings during each season describe more than 75% of the subtidal variance and have a vertical structure which does not vary with season. The current is vertically sheared, oriented typically 15° - 20° clockwise relative to local isobaths near the surface and along isobaths near the bottom. Currents at the two shelf moorings (alongshore separation 29-37 km) are correlated with each other and with the local wind stress and these relationships do not exhibit a seasonal variation. Comparison of the alongshore currents at the two shelf moorings suggests that volume transport over the shelf is conserved between these two moorings during all four periods. The summer observations, which include a much denser array of wind and current observations, indicate that there can be strong, persistent variations in the wind field over relatively small scales (10's of kms) and that similar, corresponding variations are present in the current field over the shelf. Furthermore, the structure of this variability in the wind field and the associated current response varies dramatically from the summer of 1981 to the summer of 1982. Over the slope the largest EOFs for each season account for 56%-72% of the current variance.

The vertical structure is relatively uniform with depth during the summer, fall and winter of 1981, then changes abruptly during the summer of 1982, becoming strongly sheared in the upper 100 m of the water column. Current observations over the slope are not correlated with either the shelf currents or the local wind stress during any season. In contrast to the subtidal shelf current variability, the subtidal shelf temperature variability, as described by EOFs, exhibits a seasonal variation in vertical structure, with most of the variability concentrated in the upper 20-30 m in summer and the variability decreasing more uniformly with depth in winter. The shelf temperature variability is also correlated with the near-surface temperature variability over the slope accounting for about half the temperature variance at 9 m depth. The shelf temperature variability is apparently due in large part to the cross-shelf heat flux associated with wind-driven cross-shelf Ekman transport. Observations from the mid-shelf mooring maintained through the fall and winter of 1982-83 showed evidence of the 1982-83 El Niño with water temperatures remaining above 12°C during most of the fall and winter and with persistent onshore and poleward currents.

Published in: *Journal of Geophysical Research.*

Supported by: NSF Grant OCE84-17769.

WHOI Contribution No. 6832.

INSTRUMENTATION AND EXPERIMENTAL METHODOLOGY

MEASURING RELATIVE MOTION USING CLUSTERS OF SURFACE DRIFTERS

Pierre Flament

Estimates of the surface velocity gradient tensor at a scale of $\sim$ 10 km using clusters of 9 drifting buoys are presented. In a region with small velocity gradients, a cluster tracked 5 times over two semi-diurnal tidal periods resolved velocity gradients as small as $\sim 2{\cdot}10^{-6}s^{-1}$ or $f/40$. The variance of the residual displacements was consistent with aliased tidal, near-inertial oscillations. Two clusters were then deployed in an upwelling jet. Horizontal shears from $-0.5f$ to more than f were found. In regions with large gradients, the accuracy is limited by the deformation of the cluster, which prevents sampling a full tidal cycle.

Published in: *Journal of Geophysical Research.*

Supported by: ONR Contracts N00014-80-C-0440 and N00014-87-K-007.

WHOI Contribution No. 6875.

TEMPERATURE AND VELOCITY CORRECTIONS FOR VERTICAL MOTION OF A MOORING AT 35°N, 152°E IN THE KUROSHIO EXTENSION

Melinda M. Hall

Two-year time series of temperature and velocity from a mooring at 35°N, 152°E in the Kuroshio Extension have been corrected for vertical mooring motions at the top two instruments (nominal depths of 250 and 500 m). Temperature data from two CTD surveys along 152°E were used for the temperature corrections, and recorded values of velocity and pressure at the two levels were used for velocity corrections. Corrected temperatures are estimated to be accurate to within 0.18°C at both levels, while corrected velocities are estimated to be accurate to within 10% (5%) at the upper (lower) level. The time series of corrected temperature at the upper standard pressure 350 dbar is a good indicator of cross-stream distance from the center of the Kuroshio front. Magnitudes of record-length means, variances and covariances are generally larger for the corrected than for the measured series, except for $\overline{T'^2}$. A simple example is used to show that much of the apparent time variability is associated with lateral excursions of the Kuroshio Extension.

Published in: *Deep-Sea Research.*

Supported by: NSF Grants OCE85-04125, OCE85-19551 and OCE87-10929.

WHOI Contribution No. 6820.

ON IN-SITU "CALIBRATION" OF SHIPBOARD ADCP'S

Terrence M. Joyce

Methods for *in-situ* calibration of acoustic-Doppler instruments are considered for measurement of absolute current profiles from a moving ship. Errors are of two types: sensitivity and alignment. Least square error estimates are given for both, for use in the "water track" or "bottom tracking" mode. Errors in the estimation of either factor may lead to large errors in derived water velocities although the major contributions of each arise from different sources and are approximately orthogonal to one another.

In Press: *Journal of Atmospheric and Oceanic Technology.*

Supported by: NSF Grant OCE85-01176 and NASA NAGW-1026.

WHOI Contribution No. 6769.

AN INVERSE MODEL FOR CROSS-ISOTHERM VELOCITY

Kathryn A. Kelly

An inverse model was developed to infer the cross-isotherm component of velocity from a series of temperature maps from infrared satellite images. The results of this model can be used to locate regions of divergence in the near-surface velocity field, to estimate the contribution of horizontal advection in the mixed layer and to predict the location of temperature features during periods of cloud cover. The inversion is based on a simplified two-dimensional temperature conservation equation with a simple representation of surface heat fluxes. The along-isotherm component of the velocity is in the null space of this problem. Unique solutions for the underdetermined problem are obtained by minimizing the energy, divergence and roughness of the velocity solution and by examining the tradeoff curve between misfit to the equation, divergence and energy. The inversion is sensitive to the reduction in temperature gradients by the atmosphere; an empirical path length correction is first applied to each image. In tests on a series of six images from the California Current pairs of images at 12- or 24-hour separations produced reasonably consistent solutions; the estimated error for each individual solution was about 27% of the energy or about 2.7 km d^{-1}. The decorrelation time for the solutions was about one day. Horizontal advection due to the average velocity solutions was about one day. Horizontal advection due to the average velocity solutions accounted for about 20-50% of the squared temperature changes. There was little statistical skill in predicting temperature changes with the velocity fields inferred from previous images because of the short decorrelation time; however the average solutions provided a qualitative picture of movement of features seen in the series of images. The strongest region of divergence, the leading edge of a cold eddy near the coast, was consistent with average divergence calculations from acoustic Doppler surveys for the same region. The velocity solution from this series supported the theory that the cold "filaments" in the California Current are actually meanders of the current.

Published in: *Journal of Physical Oceanography.*

Supported by: ONR Contract N00014-86-K-0751.

WHOI Contribution No. 6768.

THE POLAR FLOATS PROGRAM

T. O. Manley, J.-C. Gascard and W. B. Owens

The Polar Floats Program, an adaptation of mid-latitude SOFAR float technology into the polar regions, will be used in the monitoring of subsurface circulation patterns over large spatial and temporal scales as well as tracking of mesoscale features in near real-time. This program is comprised of three major components that are now under development and will be used during the Coordinate Eastern Arctic Research Experiment (CEAREX). These components are the 80 Hz float transducer, American and French sea-ice deployable listening stations using ARGOS data telemetry (ARS and SOFARGOS, respectively), and the software needed for real-time tracking. The prototype 80 Hz transducer, developed at Webb Research Corporation in 1984 and combined with a standard SOFAR 260 Hz transducer, was deployed north of Fram Strait during the July-87 ARKTIS IV/3 Polarstern cruise. Initial results indicate that over a nominal distance of 90 km, the 80 Hz signals received and transmitted through SOFARGOS were lower than the 260 Hz signal and were heard for only a portion of the monitoring period. The consistent drop off of the 80 HZ signal through time, as well as its intermittent behavior, indicated an electro/mechanical problem which reduced its output well below expectations. Recent performance testing at the Naval Testing Platform at Lake Seneca in March of 1988 has shown that the newer 80 HZ Helmholtz resonator design (80/2) possessed an additional 7 dB of acoustic output power over the original prototype. This increase in output power is expected to meet the requisite 500-1000 km ranges needed for monitoring the central Arctic Ocean. Subsequent performance testing under continual operation will be completed at WHOI during April 1988. Experimentation with the 80 Hz and 260 Hz floats within the Arctic Ocean will commence in August of 1988 and continue for 14 months. In concert with the French ARCTEMIZ and NORDA internal wave programs, a total of eleven 80 Hz and eighteen 260 Hz floats will be deployed in Fram Strait as well as the Eurasian Basin of the Arctic Ocean. Four 260 Hz floats will be deployed within several mesoscale eddies. Near real-time float positions will then be used to adapt sampling patterns of other measurements, such as helicopter-borne CTDs, in order to follow these features and monitor their evolution in the open ocean, marginal ice zone and beneath the more interior pack ice.

Published in: *Journal of Ocean Engineering.*

Supported by: ONR Contracts N00014-86-C-0050, N00014-87-K-0204 and NSF Grant DPP-8518747 and french agencies: CNRS and IFREMER.

WHOI Contribution No. 6790.

WORLDWIDE SHIP DISTRIBUTIONS IDENTIFY MISSING DATA

P. L. Richardson

The geographical and temporal distributions of worldwide ship drift velocities were plotted in order to see where and when the observations were made and to identify what appear to be major gaps in the data. Curiously, large areas of the North Atlantic, North Pacific, and South Pacific were found to be devoid of observations in some months during the years 1920–1934 when the number of yearly observations is large. An estimated 700,000 observations are missing. These would significantly enhance the usefulness of the data set if they could be found and added to it, especially in the Pacific where the data density is low.

Published in: *Journal of Geophysical Research.*

Supported by: NSF Grant OCE87-16509.

WHOI Contribution No. 6916.

OCEAN CIRCULATION AND LOW FREQUENCY VARIABILITY

STATION "S" OFF BERMUDA PHYSICAL MEASUREMENTS 1954–1984

This book is the final data report for the first 31 years of Station "S" off Bermuda. It contains a brief account of the history of the station, a complete printed listing of pressure, temperature, salinity and oxygen measurements through station 554. A disk containing all the data plus some utility programs, in a form compatible with IBM personal computers, is included as an insert.

Published in: *Woods Hole Oceanographic Institution and Bermuda Biological Station for Research,* 189 + v pg., 1988.

Supported by: NSF Grant OCE87-13810.

WHOI Contribution No. 6894.

EVIDENCE FOR WIND-DRIVEN CURRENT FLUCTUATIONS IN THE WESTERN NORTH ATLANTIC

K. H. Brink

Two subsurface current meter moorings were deployed for 20 months along 70°W in a

low-energy portion of the western North Atlantic. The resulting data were compared with estimates of the wind stress curl to seek a relationship between currents below the mixed layer and meteorological forcing at subinertial frequencies. Currents and temperature tend to be significantly coherent with the curl, and are most coherent with the curl at remote locations, usually more than 500 km away from the mooring and generally to the east. Coherences generally decrease with increasing frequency. The current response is surface-intensified. A linear stratified model for stochastically wind-forced Rossby waves in a flat-bottom ocean is presented as an attempt to rationalize the results. The effort was not entirely successful, so that it appears that a more realistic model, perhaps including bottom topography and mean currents, will be needed to rationalize these observations fully.

In Press: *Journal of Geophysical Research.*

Supported by: ONR Contract N00014-84-C-0134, NR 083-400.

WHOI Contribution No. 6752.

OBSERVATIONS OF THE RESPONSE OF THERMOCLINE CURRENTS TO A HURRICANE

K. H. Brink

In September, 1985, the eye of Hurricane Gloria passed within about 75 km of a current meter mooring in the western North Atlantic. Data from this mooring provide a clear view of the vertical structure of the near-inertial wake in the main thermocline. The response was strong (> 25 cm s^{-1} amplitude at 159 m) and lasted about 18 days. At greater depths the response was weaker and more irregular. The phase of the near-inertial currents increased with depth, consistent with the downward spreading of energy. The total phase change across the thermocline reached about a half cycle seven days after the hurricane's passage, indicating a large vertical scale of the response. The observations are briefly compared with other time series measurements (on the continental margin) and with models.

Published in: *Journal of Physical Oceanography.*

Supported by: ONR Contract N00014-84-C-0134, NR 083-400.

WHOI Contribution No. 6899.

VELOCITY AND HYDROGRAPHIC STRUCTURE OF TWO GULF OF MEXICO WARM-CORE RINGS

Cortis Cooper, George Z. Forristall and Terrence M. Joyce

Results from an extensive survey of two Gulf of Mexico warm-core rings are presented. The data were taken during a one-week period in December 1983 using a shipboard acoustic Doppler current profiler (ADCP), expendable current probes (XCP), expendable bathythermographs (XBT), and a CTD. Two rings were observed - an older one in the western Gulf adjacent to the west Texas Shelf, and one just separated from the Loop Current. The western ring was of order 200 km in diameter with peak currents of 1 m s^{-1} at the 100 m level. Water properties were uniform and characteristic of the high-salinity Caribbean subtropical underwater. The eastern ring was of order 300 km in diameter with peak currents of near 2 m s^{-1} at the 100 m level. Water below 200 m is of Caribbean origin, while the surface waters show more variability suggesting some inflow of Gulf of Mexico common water. The evolution of the rings is also described based on the cruise measurements, satellite AVHRR, and other observations of opportunity.

Published in: *Journal of Geophysical Research.*

Supported by: CONOCO Contract # 3366.

WHOI Contribution No. 6845.

LOW FREQUENCY MEANDERING OF THE ATLANTIC NORTH EQUATORIAL COUNTERCURRENT

Silvia Garzoli and Philip Richardson

Four 19-month time series of indirect measurements of dynamic height were obtained in the tropical Atlantic along 28°W, at 0°3 °6°, and 9°N with three inverted echo sounders and one current meter mooring. The series were analyzed to study the time-latitude variability of the North Equatorial Countercurrent (NECC). The eastward flow associated with the NECC was present at 28°W from 3°to 9°N during most of the observed period except in March/April 1983 and April/May 1984, periods that coincided with the onset of the wind at the Equator. The amplitude of the NECC's annual cycle was maximum at 6°N and was larger in 1983 than 1984. The analysis of the time-latitude variability of differences in dynamic height shows a long period meridional shift of the NECC. The core of the current attains its northernmost location during the month of

August/September in both years, and its southernmost location during March/April 1983 and March 1984. The location of the core is directly related to the position of the Intertropical Convergence Zone. From the time series of dynamic height obtained from the indirect measurements, geostrophic velocities and transports were estimated and compared with direct observations of currents, and values obtained from hydrographic casts.

In Press: *Journal of Geophysical Research.*

Supported by: NSF Grants OCE85-15632 and OCE85-21082.

WHOI Contribution No. 6915.

GULF STREAM SURFACE TRANSPORT AND STATISTICS FROM GEOSAT DATA

Sarah T. Gille and Kathryn A. Kelly

Geosat altimeter height measurements for the Gulf Stream for three subtracks from the Exact Repeat Mission were processed to remove the geoid and mean Gulf Stream height. A Gaussian model for the Gulf Stream velocity profile was used to predict the form of the residual height profiles seen by GEOSAT and the mean height profile, using estimates of the width and position derived from the height residuals. Estimates of the maximum surface velocity and the surface transport were obtained by a least-squares fit of the synthetics to the data. Location statistics from GEOSAT data were in good agreement with values obtained from infrared images of the Gulf Stream. Surface velocities were consistent with historical measurements for the region. The time series showed an anomalously large increase in surface transport in the winter of 1987-88, which appeared to be correlated with an anomalous northward excursion and a 50% increase in the width of the Gulf Stream.

Published in: *Journal of Geophysical Research.*

Supported by: ONR Contract N00014-86-K-0751.

WHOI Contribution No. 6900.

VELOCITY AND TRANSPORT STRUCTURE OF THE KUROSHIO EXTENSION AT 35°N, 152°E

Melinda M. Hall

A current meter mooring maintained for two years at 35° N, 152° E as part of the "Wespac" array (Schmitz et. al., 1987) sampled the Kuroshio Extension during the last 390 days of deployment. Based on a method developed by Hall and Bryden (1985) for the Gulf Stream at 68° W, velocity and temperature time series at five depths from 350 to 6000 m have been used to construct the representative horizontal velocity structure of the current. Cross-stream position is quantified in terms of temperature at 350 dbar, and an alongstream flow direction is defined on the basis of the current shear. Integrated transport of the Kuroshio is 87 ± 21 Sv, compared to 94 ± 26 Sv for the Gulf Stream at 68° W based on analogous data sets and analysis techniques. The two currents are compared in terms of horizontal and vertical distributions of transport as well as relative strength of barotropic and baroclinic components. The Kuroshio has a larger relative barotropic component than the Gulf Stream, while the latter has a stronger, deeper thermocline expression. The effects of rotating velocity measurements to a continuously changing alongstream direction are examined for both currents; the major impact is to cut the apparent velocity variance in half, demonstrating that much of the original variance is due to the meandering of a quasi-fixed velocity profile rather than the passage of eddies. Results from these somewhat unconventional analysis methods are placed in broader geographical context and compare favorably with more traditional methods of determining these currents' transports.

Published in: *Journal of Geophysical Research.*

Supported by: NSF Grants OCE85-19551 and OCE87-10929.

WHOI Contribution No. 6909.

OBSERVATIONS OF WIND FORCED DEEP OCEAN CURRENTS IN THE NORTH PACIFIC

C. J. Koblinsky, P. P. Niiler and W. J. Schmitz, Jr.

This study examines the atmospheric response of the deep ocean using 200 instrument years of moored current measurements from across the breadth of the mid-latitude North Pacific. We have found evidence of a seasonal modulation in the ocean eddy kinetic energy beneath the thermocline at several locations north of 35°N. This modulation is often in phase with the local atmospheric forcing function. At frequencies between 0.1 and 0.01 cpd correlations between the local wind stress curl and the deep currents have been found. For a few locations the local forced response is parallel to the potential vorticity gradient $\left(\nabla \frac{f}{H}\right)$ and consistent in amplitude with a local topographic Sverdrup balance. Non-local forcing in the form of flow along isolines of potential vorticity has been

estimated and it is comparable to the observed flow at some locations, but the modeled flow is not correlated with the observations. Throughout the mid-latitude North Pacific the bottom slope tends to enhance the β-effect. This suggests that topography narrows the available bandwidth for forced barotropic Rossby waves, facilitating a quasi-steady topographic Sverdrup response over most of the basin. However, the enhanced β-effect reduces the magnitude of the ocean's response to wind forcing. Non-locally forced Sverdrup currents in the form of flow along isolines of $\frac{f}{H}$ are the dominate component, but are only order 1 $cm \cdot s^{-1}$. Locally forced Sverdrup currents, flow across isolines of $\frac{f}{H}$, are typically order 0.1 $cm \cdot s^{-1}$ *rms* and are not commonly observed. Hence, these wind forced variations are a background level signal in the mid-latitude eddy kinetic energy. In a few isolated areas the bottom slope reduces the β-effect. In these regions the local Sverdrup response is amplified and has been observed.

In Press: *Journal of Geophysical Research.*

Supported by: ONR Contracts N00014-76-C-0197, NR 083-400 and N00014-84-C-0134, NR 083-400.

WHOI Contribution No. 6780.

OBSERVATIONS AND EOF ANALYSIS OF LOW FREQUENCY VARIABILITY IN THE WESTERN PART OF THE GULF STREAM RECIRCULATION

Angelika Lippert and Melbourne G. Briscoe

This study of low frequency oceanic variability is based on data collected during the Long Term Upper Ocean Study (LOTUS), which was a two year program of (mainly) moored meteorological and oceanographic measurements. The mooring arrays were centered at 34°N and 70°W over the Hatteras Abyssal Plain. With a distance of about 300 km to the mean Gulf Stream axis and the continental slope, LOTUS was at the most northern and western long-term mooring site in the Gulf Stream recirculation region to date. The observed low-frequency variability is dominated by zonally elongated motions of the secular time scale (periods > 100 days) even at great depths (4000 m). In contrast to observations in other parts of the recirculation region, the spectral shapes are strongly depth dependent. The vertical structure of the variability was examined by EOF analysis. Different kinds of EOFs were tested; the best representation of the observed variability was obtained by an EOF representing a unidirectional non-rotating (with depth) flow. The first and second EOF together explain 96% of the observed energy. The first EOF (66%) is almost barotropic with a slight increase at the surface and the bottom of the ocean; the second mode closely resembles the first baroclinic dynamical mode. The barotropicity decreases with increasing frequency. Motions with periods less than 30 days are almost surface trapped, and a strong bottom intensification additionally exists for periods between 10 and 30 days.

Published in: *Journal of Physical Oceanography.*

Supported by: ONR Contract N00014-84-C-0134, NR 083-400.

WHOI Contribution No. 6872.

INERTIAL OSCILLATIONS IN THE UPPER OCEAN DURING THE MIXED LAYER DYNAMICS EXPERIMENT (MILDEX)

Jeffrey D. Paduan, Roland A. De Szoeke and Robert A. Weller

Surface currents in the near-inertial frequency band were analyzed from 18-day long measurements taken in October/November, 1983 as part of the Mixed Layer Dynamics Experiment (MILDEX). The currents below two drifting platforms separated by 55 km were found to have differed in their inertial response to a frontal passage on 1 November by 10 cm s^{-1}.

Wind records from the two platforms were used to compute the predicted inertial currents with a simple slab model of the wind-driven flow. The model currents reproduced most of the features of the observed inertial currents, including the disparity between the two locations following the 1 November frontal passage. The disparity was due to differences in the weak winds preceding the frontal passage which account for inertial currents of ~5 cm sec^{-1} in opposing directions at the two platforms at the time of the front. These differences in small-scale (~50 km) structure in the wind field were responsible for the disparity rather than the slight difference in the arrival time (~2 hour) of the front at the two locations. (Inertial currents, wind forcing, vertical dispersion.)

Published in: *Journal of Geophysical Research*, Vol. 94, No. C4, 4835-4842, April 15, 1989.

Supported by: ONR Contract N00014-84-C-0134, NR 083-400.

WHOI Contribution No. 6731.

ANALYSIS AND INTERPRETATION OF DEEP EQUATORIAL CURRENTS IN THE CENTRAL PACIFIC

Rui M. Ponte and James Luyten

Analysis of vertical profiles of absolute

horizontal velocity collected in January 1981, February and April 1982 in the equatorial central Pacific revealed two significant narrow band spectral peaks in zonal velocity, centered approximately at vertical wavelengths of 560 and 350 stretched meters (sm). Energy in the 560 sm band roughly doubled between the first and last cruises. Time-lagged coherence results suggested upward phase propagation at periods of about 4 years. East-west phase lines computed from coherence over zonal separations tilted downward towards the west, implying westward phase propagation and zonal wavelengths on the order of 10000 km. The peak centered at 350 sm occurred at the vertical scales of the conspicuous alternating flows in the records, generically called the equatorial deep jets in the past (the same terminology is used here). It showed a more steady character in amplitude and a higher signal-to-noise ratio in comparison with the 560 sm peak. The deep jets were best defined as a finite narrow band process in vertical wavenumber (311–400 sm), accounting for 20% of the total variance present in the broad band energetic background. At the jets' wavenumber band, latitudinal energy scaling compared reasonably well with Kelvin wave theoretical values and a general tilt of phase lines downward towards the east yielded estimates of 10000–16000 km for the zonal wavelengths. Time-lagged coherence calculations revealed evidence for vertical shifting of the jets on interannual time scales. Interpretation of both signals in terms of equatorial waves was ambiguous, because of their relatively long spatial and temporal scales compared to the records. The simplest hypothesis of linear waves in a resting basic state ocean could not be rejected, but more complicated physics can not be ruled out.

At all wavenumber bands in general, power levels decayed away from the equator over scales broader than the Kelvin wave scale. Within 1/2° of the equator, zonal current led (lagged) vertical displacement by $\pi/2$ with depth for the 933 sm (140–400 sm) band. Result at the 140–400 sm band agrees with the findings of Eriksen (*J. Phys. Oceanogr.*, 11, 48–70, 1981) in the western Pacific, and thus seems to be a general feature of the deep equatorial Pacific fields.

In Press: *Journal of Physical Oceanography.*

Supported by: NSF Grants OCE79-21786 and OCE86-00052.

WHOI Contribution No. 6819.

TRACKING THREE MEDDIES WITH SOFAR FLOATS

P. L. Richardson, D. Walsh, L. Armi and J. F. Price

Three Meddies were tracked for up to two years in the Canary Basin using neutrally buoyant SOFAR floats. These Meddies have cores of warm, salty Mediterranean water and are approximately 100 km in diameter, 800 m thick, and are centered at a depth of 1100 m. Meddy 1 was tracked for two years (1984–1986) with five floats as it drifted 1090 km southward with a mean velocity of 1.8 cm/sec. Four shipboard surveys made during these two years revealed the nearly total decay of Meddy 1 by gradual mixing processes. Meddy 2 drifted 530 km southwestward over 8.5 months with a mean velocity of 2.3 cm/sec until it collided with Hyères seamount near 31N 29W. The floats trapped in this Meddy then stopped looping abruptly, implying a major disruption of this Meddy. Meddy 3 drifted 500 km southwestward for a year and a half with a mean translation velocity of 1.1 cm/sec. A comparison of the velocity of Meddies to the velocity of nearby floats at 1100 m depth outside of the Meddies shows clearly that all three Meddies moved southwestward through the surrounding water at a speed of about 1.3 cm/sec. The floats inside the Meddies looped anticyclonically in a nearly solid-body rotation with a period of 6 days for Meddy 1, 4 days for Meddy 2, and 5 days for Meddy 3. The rotation period of Meddy 1 appeared to remain constant over nearly two years despite a large decrease in the Meddy's thickness and diameter due to mixing. Rotation velocities in the Meddies were as great as 34 cm/sec (Meddy 2), much faster than speeds of nearby floats outside of the Meddies.

In Press: *Journal of Physical Oceanography.*

Supported by: NSF Grants OCE82-14066, OCE86-00055, and OCE85-17375.

WHOI Contribution No. 6836.

STOCHASTICALLY FORCED CURRENT FLUCTUATIONS IN ZONAL SHEAR AND OVER TOPOGRAPHY

R. M. Samelson

The effects of constant zonal shear, uniform meridional bottom slope, and a deep meridional wall (representing the mid-Atlantic Ridge) on the response of a linear two-layer quasigeostrophic ocean to stochastic wind stress curl forcing are investigated. The model is motivated by discrepancies in energy levels and distributions between recent observations and a similar model

without shear or topography that predicted remote coherences relatively well. The results indicate that the presence of mean shear can significantly enhance the wind-generation of surface-intensified oceanic kinetic energy at frequencies above the zero-shear cut-off for free baroclinic waves. The primary effect of the sloping topography is enhanced barotropic response near the barotropic topographic Sverdrup resonance, where slope and planetary potential vorticity gradients cancel. The wall inhibits the barotropic response and increases coherences on the mooring side of the wall. Remote coherences for 49-day period fluctuations are due to long barotropic waves as in the previous model, so the present model only partially reconciles the previous discrepancies.

In Press: *Journal of Geophysical Research.*

Supported by: ONR Contract N00014-84-C-0134, NR 083-400.

WHOI Contribution No. 6926.

EVAPORATION MINUS PRECIPITATION AND DENSITY FLUXES FOR THE NORTH ATLANTIC

Raymond W. Schmitt, Phillip W. Bogden and Clive E. Dorman

Estimates of evaporation (E) over the North Atlantic Ocean by Bunker (1976) have been combined with estimates of precipitation (P) by Dorman and Bourke (1981) to produce new annual and seasonal maps of E-P and surface density flux. Although uncertainties about precipitation algorithms and exchange coefficients still persist, it is felt that the high spatial resolution of these data sets permits an estimate of E-P that is a significant improvement over previous work. The maps of E-P show considerably more detail than earlier maps, including a previously uncharted minimum with a northeast to southwest trend across the subtropical gyre. The two regions of *maximal* E-P display a close connection with continental air flows off Africa and North America, suggesting that the relative narrowness of the North Atlantic contributes to its status as a net evaporation basin. The zonally integrated E-P values are combined with river runoff estimates to obtain the meridional flux of freshwater, which can be compared with fluxes calculated from oceanographic sections. Maps of the surface density flux are also presented for the annual and seasonal averages. Areas of net density gain by the ocean correspond to formation regions of sub-polar mode water at high latitudes, 18°C water south of the Gulf Stream, and salinity maximum water at low latitudes in mid-gyre. The contributions of heat and salt to the density flux are separately computed. This reveals that the thermal density flux dominates at high and low latitudes whereas the haline density flux is most important in the subtropics, particularly on the eastern side of the basin. These data should facilitate the development of models of the thermohaline circulation, and aid the identification of regional differences in the dominant air-sea interaction processes.

Published in: *Journal of Physical Oceanography.*

Supported by: NSF Grant OCE84-09323, and ONR Contract N00014-87-K-0007, NR 083-004.

WHOI Contribution No. 6781.

THE MODE SITE REVISITED

William J. Schmitz, Jr.

In the 1970's, an intense physical oceanographic effort was focused on the MODE Area (centered at 28°N, 70°W) to study mesoscale eddies and their effect on the larger-scale longer-term (or general) interior ocean circulation. At that time there was considerable discussion as to the typicality of these results. It has become clear that the time-dependent field is horizontally inhomogeneous; eddies have a geography related to the general circulation. In some areas, significant temporal inhomogeneity (non-stationarity) has been observed, but this issue has not yet been clarified for the MODE Area.

Recently, a collective experiment to study the effect of fronts on mixed layer dynamics was carried out near the subtropical front in the North Atlantic. This note summarizes the (subsidiary) mean flow and eddy-based results from two subsurface moorings set as support for the main experiment, focusing on MODE Center (28°N, 70°W) where instruments at several levels from 150 to 4000 m were deployed for 20 months. Abyssal mean flow increased by an order of magnitude. The previously most stable eddy-field observable, abyssal eddy kinetic energy, changed by more than 50% from the measurement period in the 1970's to that in the 1980's. Eddy kinetic energy and mean flow in the thermocline, expected to be the least reproducible observables, hardly changed. The directionality of the thermocline eddy field is notably different, essentially reversed from the 1970's, with the meridional twice as large as the zonal variance in the 1980's. The spectral distribution in the thermocline is less "red", with the opposite tendency at abyssal depths. In summary, the MODE Area is neither particularly representative of the rest of the ocean nor are the MODE results of the 1970's quantitatively representative of measurements there ten to fifteen years later. It does seem possible, however, that many of the differences observed could be

rationalized in terms of comparatively small-scale horizontal excursions of larger-scale flow regimes, notably the subtropical frontal zone.

Published in: *Journal of Marine Research*, 45, 131-151., 1989.

Supported by: ONR Contracts N00014-76-C-0197, NR 083-400 and N00014-84-C-0134, NR 083-400.

WHOI Contribution No. 6755.

SEVEN-YEAR CURRENT METER RECORD IN THE EASTERN NORTH ATLANTIC

Walter Zenk and Thomas J. Müller

Continuous current measurements at the 1000 m level were obtained in the Central Canary Basin of the North East Atlantic near 33°N, 22°W for 2398 days. Even with this very long time series no statistically significant mean current can be estimated at that level, because the energetic fluctuations are large compared to the weak mean. In the eddy scale range, i.e. at current fluctuations with scales between 47 and 455 days, a pronounced anisotropy between zonal and meridional components is apparent. For the first time in the subtropical North Atlantic gyre our data allow a confirmation of the expected spectral decrease beyond the eddy scale peak in an Eastern Basin. With respect to future global experiments we wonder if our results from an eastern basin location are representative for the general circulation at mid-ocean sites?

Published in: *Deep-Sea Research.*

Supported by: NSF Grant OCE86-00055.

WHOI Contribution No. 6758.

THEORETICAL AND LABORATORY MODELS

THE EFFECT OF STRATIFICATION ON SEAMOUNT-TRAPPED WAVES

K. H. Brink

Circular, isolated seamounts can support the propagation of an infinite set of trapped waves. These waves exist at discrete subinertial frequencies and azimuthal wavenumbers. The wave frequencies increase as the height of the seamount or the stratification increases. Idealized examples demonstrate these trends, as well as the tendency for bottom-trapping of the velocity field to increase as stratification increases. Bottom frictional effects are weak enough that at least the simpler (graver) wave modes should last several periods before significant damping occurs. The waves should be most observable as current variations, although associated temperature fluctuations may also be measurable.

In Press: *Deep-Sea Research.*

Supported by: ONR Contract N00014-84-C-0134, NR 083-400.

WHOI Contribution No. 6855.

FINITE AMPLITUDE EFFECTS ON DEEP PLANETARY CIRCULATION OVER TOPOGRAPHY

Nelson G. Hogg

Rhines's (1983, 1988) studies of planetary geostrophic, quasi-geostrophic flow over large scale bathymetric changes are extended to finite amplitude in a two layer model. The dependence of layer depth on bottom elevation is found to be multivalued stimulating an analogy with classical hydraulic control theory. When the upstream flow is sub- or supercritical, as measured by the ratio of the incident flow speed to the long Rossby wave phase speed, and the topography is below the critical height, the interface falls or rises, respectively, over the topography as it does in the standard nonrotating situation. However, these planetary geostrophic flows are inherently two dimensional and the implied control does not occur at a Froude number of unity based on the Rossby wave phase speed. For the simple case of flow of a single layer over a uniform meridional ridge in a square basin it is found that the multivalued nature of the solution results not from hydraulic control but from the intersection of characteristics carrying information from the eastern boundary. For upstream flows which are subcritical the flow remains subcritical everywhere, no matter how high the topography, and a caustic forms downstream of the ridge where information coming from the eastern and northern boundaries intersects.

Published in: *Journal of Physical Oceanography.*

Supported by: NSF Grant OCE86-08258 and ONR Contract N00014-85-C-0001, NR 083-004.

WHOI Contribution No. 6858.

SIMULATING THE MAIN THERMOCLINE IN THE NORTH ATLANTIC WITH AN IDEAL-FLUID MODEL

Rui Xin Huang

Using an ideal-fluid model, the main thermocline in the North Atlantic is reconstructed.

The new feature in the model is the use of a nonlinear background stratification calculated from the hydrographic measurements collected on the *Discovery* cruise along 46–49°N. The basic stratification is assumed to be set up by an external thermohaline circulation and modified by a wind-driven circulation superimposed upon it. The numerical results of the model distinctly show the three-dimensional structure of the mean thermocline in the ocean. In addition, the wind-driven gyre reaches a great depth ($\approx$ 4.5 km), thus topographic effects on the gyre-scale circulation must be considered in further models. The model confirms the classical notion that the basic structure of the main thermocline and the three-dimensional density and velocity fields in the upper ocean can be simulated very well without explicitly including friction in the model.

In Press: *Journal of Physical Oceanography.*

Supported by: NSF Grant OCE86-14771.

WHOI Contribution No. 6871.

ON THE SIZE OF THE ANTARCTIC CIRCUMPOLAR CURRENT

Gregory C. Johnson and Harry L. Bryden

A model predicted transport of the Antarctic Circumpolar Current (ACC) through Drake Passage compares favorably with measured transport through the passage. The model incorporates the width of the ACC, the strong eddy presence in the region, and the deep penetration of an unstable baroclinic velocity field, all of which are characteristic features of the current. The model involves a downward transfer of wind-imparted zonal momentum by eddy form drag to a depth at which it can be removed by bottom pressure drag. The eddy form drag results from a poleward transport of heat by eddies originating from the baroclinically unstable current.

In Press: *Deep-Sea Research.*

Supported by: NSF Grant OCE85-4125 and an ONR Graduate Fellowship.

WHOI Contribution No. 6739.

SIMPLE MODELS FOR LOCAL INSTABILITIES IN ZONALLY INHOMOGENEOUS FLOWS

Joseph Pedlosky

Two very simple model equations, suggested by the form of the standard baroclinic instability dispersion relation, are studied to investigate the nature of the instability of zonally inhomogeneous flows. In particular, the simplifications of the model problems allow the consideration of examples in which the interval of instability is of the same order or even smaller than the characteristic wavelength of the free plane wave modes of the zonally homogeneous problem, a limit inaccessible to standard WKB procedures. In both model problems it is shown that the zonally gravest mode always remains, no matter how small the locally unstable interval may be. Further, this gravest mode is eddy-like rather than wave-like, *i.e.*, it has no internal nodes. When the free wave solutions are allowed to propagate, the structures of the bound modes are altered. They are squeezed against the exit edges of the unstable domain but again one mode, the bound eddy mode, is always possible. This study is complementary to the more elaborate WKB analyses recently published and, in agreement with these studies, it is shown that only local maxima in supercriticality are required to yield trapped modes. The bound eddy mode is, however, a feature allowable only when WKB analysis fails. It is suggested that such bound eddies, anchored to local maxima in supercriticality may be regarded as the preliminary stage for the production of isolated, coherent structures.

Published in: *Journal of Atmospheric Sciences.*

Supported by: NSF Grant ATM84-13515.

WHOI Contribution No. 6910.

WIND FORCING AND THE ZONAL STRUCTURE OF THE EQUATORIAL UNDERCURRENT

J. Pedlosky and R. M. Samelson

A recently-developed nonlinear inviscid model of the equatorial undercurrent is coupled to a wind-driven surface layer. The Ekman transport causes divergence and entrainment in a narrow equatorial band, determining the undercurrent transport and the value of the Bernoulli function along the equator. Solutions are presented for two zonal profiles of zonal wind stress. For eastward wind stress increasing linearly westward, eastward transport increases nearly linearly westward. For eastward wind stress with a wind-basin maximum, eastward transport has a maximum just west of the basin middle, and there is recirculation along the equator. Solutions are also presented for uncoupled models with several layers and with a deep constant potential vorticity layer.

Published in: *Journal of Physical Oceanography.*

Supported by: NSF Grant ATM84-13515.

WHOI Contribution No. 6913.

DETERMINING THE STRENGTH OF THE DEEP WESTERN BOUNDARY CURRENT USING THE CHLOROFLUOROMETHANE RATIO

Robert S. Pickart, Nelson G. Hogg and William M. Smethie, Jr.

The dilution of a passive tracer during deep water formation and the subsequent advection/mixing in a deep boundary current is modeled with application to chlorofluoromethanes (CFMs) in the North Atlantic. Two different types of boundary currents are considered: a uniform flow and a simple shear flow. In each case the core of the flow mixes with surrounding water which continually accumulates CFMs. In an extreme case the coupled system predicts that the CFM ratio in the current is unaltered from the ratio of its source water (save for a time lag). More realistic cases however suggest that the ratio is not a conserved quantity, but is substantially altered in both the overflow basin and boundary current. Matching the model results to CFM data collected near the Grand Banks gives a predicted (average) core speed of 5–10 cm/sec for the Deep Western Boundary Current, and provides a constraint on the transport and diffusivity of the flow as well.

Published in: *Deep-Sea Research.*

Supported by: NSF Grant OCE82-14925 and ONR Contracts N00014-76-C-0197, N00014-84-C-0132, NR 083-400, N00014-82-C-0019 and N00014-85-C-0001, NR 083-004.

WHOI Contribution No. 6860.

A SIMPLE MODEL FOR DEEP EQUATORIAL ZONAL CURRENTS FORCED AT LATERAL BOUNDARIES

Rui M. Ponte

Deep lateral boundary processes (e.g., western boundary currents) are hypothesized as an alternative energy source exciting the equatorial wave guide at long time scales. A linear, continuously stratified model is used to study the equatorial zonal currents generated by a time dependent, short vertical scale deep zonal jet located at the meridional walls and centered at the equator. Examples of solutions with periodic, transient and spectral forcing are presented. For low frequency forcing at the western or eastern boundaries, energy travels from the source along ray paths associated with Kelvin and long Rossby waves, respectively. Linearly damped solutions look similar in both cases.

Solutions show in general a rich baroclinic structure and a complex time dependence (e.g., periodic solutions can exhibit both upward and downward phase propagation and standing mode oscillations at different depths in the water column), with the vertical structure depending, among other factors, on the vertical scale and frequency composition assumed for the boundary jet. Results suggest the potential importance of deep forcing mechanisms to the existence of long time scale, deep baroclinic currents in the equatorial ocean. Solutions are qualitatively similar to observations of the equatorial deep jets, but any detailed comparison between model results and data is premature, given the lack of observational knowledge about the time scales, strength and spatial distribution of deep energy sources.

Published in: *Journal of Physical Oceanography.*

Supported by: NSF Grant OCE86-00052.

WHOI Contribution No. 6905.

EQUATORIAL KELVIN WAVES EMBEDDED IN MEAN FLOW, WITH APPLICATION TO THE JETS

Rui M. Ponte

Stationary equatorial Kelvin wave solutions are forced below the thermocline by a vertical velocity representing large scale convergence or divergence patterns associated with the upper ocean circulation, in the presence of a mean westward flow U mimicking the equatorial Intermediate current. For constant U, solutions exhibit a dominant vertical scale as in McCreary and Lukas (*J. Geophys. Res.*, 91, 11691-11705, 1986), but in the presence of vertical mean shear considerable changes in amplitude and vertical scale of the waves with depth occur. The combined effects of shear and linear friction on both the oscillatory and decay vertical scales of the wave flows are examined, for typical shear profiles. In general, the faster the mean flow is at the top, the deeper energy is able to propagate before being dissipated. Shallow critical layers (where $U = 0$) may provide a barrier to the penetration of wave energy to great depths. The relevance of these ideas to the dynamics of the equatorial deep jets is discussed.

Published in: *Journal of Geophysical Research*, 93 (13), 914–13,946.

Supported by: NSF Grant OCE86-00052.

WHOI Contribution No. 6827.

CRITICAL CONTROL OF ZONAL JETS BY TOPOGRAPHY

Lawrence J. Pratt

The nonlinear influence of isolated topography on an equivalent barotropic, quasigeostrophic jet is considered. The flow depends on several dimensional parameters including the mass flux Q, the mean layer thickness H, the planetary potential vorticity gradient β, the inertial boundary layer thickness $(u_0/\beta)^{\frac{1}{2}}$ and a parameter a - b measuring the north-south potential vorticity difference across the jet. Eastward jets can achieve one of two steady forms, the first supercritical and the second subcritical with respect to upstream propagation of a long potential vorticity wave. An isolated topographic feature such as a ridge can cause the jet to undergo transition from subcritical to supercritical flow and thereby achieve a steady state analogous to hydraulically controlled open channel flow. In a critically-controlled state the values of Q, a-b, H, and $(u_0/\beta)^{\frac{1}{2}}$ cannot be specified independently of the topographic parameters and the topography thereby exerts an 'upstream influence' which is felt by the general circulation of the ocean as a whole. Critically-controlled states also experience topographic form drag, whereas non-controlled states experience none. The form drag is determined by the upstream potential vorticity distribution of the flow and the critical jet width, suggesting that this type of drag might be estimated in practice by a combination of hydrographic data and satellite imagery. The Antarctic Circumpolar Current is discussed as a possible example.

In Press: *Journal of Marine Research.*

Supported by: NSF Grant OCE87-00601 and ONR Contract N00014-87-K-0007.

WHOI Contribution No. 6948.

A COUPLED MODEL OF SURFACE FORCING, WATER MASS FORMATION AND SINKING, AND DEEP INTERIOR STRATIFICATION

Kevin Speer and Eli Tziperman

A coupled model is developed of water mass formation in a marginal sea, the boundary current carrying this water towards the deep ocean, and the deep interior stratification in the ocean basin connected to the marginal sea. The model demonstrates how the interior stratification and circulation are determined by remote forcing at the ocean's surface, through the formation of water masses. The three elements of the model - marginal sea, boundary current and deep interior - are coupled together by the dynamics. Only the minimal information, that is the forcing by air-sea fluxes at the surface of the marginal sea needs to be specified externally. The model then calculates the amount of water mass formed, the structure and trajectory of the boundary current carrying this water along sloped bottom to the deep ocean, and the stratification and circulation of the deep ocean interior. In particular, the vertical structure of the circulation and stratification is calculated from the surface forcing.

As the boundary current flows along the sloped bottom towards the bottom of the ocean, it first entrains the surrounding water, and its density decreases. When the density of the boundary current approaches that of the interior. Mass continuity for the interior requires the interior upwelling velocity to increase away from the bottom, and then decrease at the levels where the boundary current entrains interior water. The interior density profile looks exponential, although the interior upwelling is not constant with depth.

Published in: *Deep-Sea Research.*

Supported by: NSF Grant OCE85-15642.

WHOI Contribution No. 6917.

A REGIONAL PRIMITIVE-EQUATION MODEL OF THE GULF STREAM: DESIGN AND INITIAL EXPERIMENTS

J. Dana Thompson and William J. Schmitz, Jr.

A primitive-equation, n-layer, eddy-resolving circulation model has been applied to the Gulf Stream System from Cape Hatteras to east of the Grand Banks (78–45 W, 30–48 N). Within the limitations of the model, realistic coastlines, bottom topography, and forcing functions have been used. A two-layer version of the model was driven by observed mean climatological wind forcing and mass transport prescribed at inflow. Outflow was determined by a radiation boundary condition and an integral constraint on the mass field in each layer. Specification of a Deep Western Boundary Current (DWBC) was included in some model runs.

Six numerical experiments from a series of over fifty integrated to statistical equilibrium were selected for detailed description and intercomparison with observations. The basic case consisted of a flat bottom regime driven by wind forcing only. Realistic inflow transport in the upper layer was then prescribed and two different outflow specifications at the eastern boundary were studied in experiments 2 and 3. Three additional experiments included (4) adding bottom

topography (including the New England Seamount Chain), (5) adding a DWBC to experiment 4 with 20 Sv. total transport, and (6) increasing the DWBC to 40 Sv. A brief discussion of the influence of parameter variations includes the modifications of dissipation (lateral eddy diffusion and bottom friction) and stratification.

Results from the sequence of experiments suggest an important role for the DWBC in determining the mean path of the Gulf Stream and consequently the distribution of eddy kinetic energy, and the character of the deep mean flow. The most realistic experiment compares to within a factor of two or better with observations of the amplitude of eddy kinetic energy and rms fluctuations of the thermocline and sea surface height. Abyssal eddy kinetic energy was less than observed. The mean flow is characterized by recirculations to the north and south of the Gulf Stream and a deep cyclonic gyre just east of the northern portion of the New England Seamount Chain, as found in the data.

In Press: *Journal of Physical Oceanography.*

Supported by: ONR Contracts ONR 32-05-3F, ONR 32-05-3G and N00014-84-C-0134, NR 083-400.

WHOI Contribution No. 6817.

DYNAMICAL REGIMES OF A FULLY NONLINEAR STRATIFIED MODEL OF THE ATLANTIC EQUATORIAL UNDERCURRENT

Sophie Wacongne

The dynamical regimes governing various regions of a nonlinear stratified mean equatorial undercurrent are investigated by computing zonal momentum balances in Philander and Pacanowski's [1984] numerical simulation of the equatorial Atlantic. Only in a narrow region of the simulation next to the western boundary does a subsurface regime exist where the positive zonal pressure gradient force overcomes the negative zonal frictional forces, resulting in a net inertial acceleration to the east and in the formation of the eastward undercurrent below westward surface flow. Elsewhere, the net force is westward and the undercurrent, experiencing a net loss of eastward momentum, weakens from west to east. For the parameterizations of frictional processes adopted in the model, zonal momentum is dissipated mostly by vertical friction in the upper thermocline and above, and by lateral friction below. Because the net retarding effect of vertical friction on the upper layers of the undercurrent is larger than that of lateral friction on the lower layers, there is on average an apparent migration of the location of the undercurrent core velocity from above the thermocline in the west of the Atlantic basin to below in the east. The bulk of the mean mid-basin model undercurrent can be described as terminating in the overlying westward flow; only a small fraction (the deeper more inertial layers) terminates at the eastern coast. It is argued that the mechanisms at work in the model are plausible ones to explain the zonal evolution of the observed undercurrent, which should motivate a re-examination of existing data. Better agreement between simulated and observed eastern undercurrent speeds might obtain by reducing the eddy coefficient of lateral mixing used in the simulation.

Published in: *Journal of Geophysical Research.*

Supported by: NSF Grant OCE85-14885.

WHOI Contribution No. 6841.

WAVE TRANSPORT OF DEEP MANTLE MATERIAL

John A. Whitehead and Karl R. Helfrich

Fluid with a certain density and viscosity can rise by buoyant Poiseuille flow through a conduit within a second fluid greater density and viscosity. Such conduits exhibit a rich behaviour characteristic of nonlinear systems, an aspect of which is the formation of solitary waves. Here we present theoretical and experimental studies of these systems. Both approaches reveal that solitary waves trap material in a cell with closed streamlines and that the central streamline velocity is faster than the wave speed. Hence, parcels of deep material are transported directly upward over large distances. This is in contrast to the usual situation in which wave propagation through a medium causes only small displacement of fluid particles. Material in these parcels will be far less contaminated by diffusion from the surroundings than would be material in ordinary pipe flow. In addition, solitary waves are more efficient than buoyant spheres at conveying material upward. We suggest that such waves might exist in the Earth's mantle, conveying uncontaminated deep mantle material to the surface of the Earth.

Published in: *Nature*, 336 (6194), 59-61.

Supported by: NSF Grant EAR87-08033.

WHOI Contribution No. 6847.

TECHNICAL REPORTS

TWO YEARS IN THE LIFE OF A MEDITERRANEAN SALT LENS

Laurence Armi, Dave Hebert, Neil Oakey, James F. Price, Philip L. Richardson, H. Thomas Rossby and Barry Ruddick

A lens of Mediterranean Water (Meddy) was tracked in the eastern North Atlantic for two years with SOFAR floats. The Meddy was first found between the Canary Islands and the Azores in October, 1984. Its center moved in an irregular pattern, at speeds of a few cm s^{-1}, and translated 1100 km to the south in two years. This Meddy was surveyed four times by CTD and velocity profilers, and once with the microstructure profiler EPSONDE. For the first two surveys the Meddy had a core which was stably and smoothly stratified in both salinity and temperature, nearly uniform in the horizontal, and was saltier than the surrounding ocean by 0.65 PSU. The Meddy was eroded from its edges, top and bottom, and lost salt and heat with an e-folding time of about one year. The salinity at the centre remained at its original value during the first year, and decreased during the second year. Evidence was seen for mixing by lateral intrusions, salt fingers, and turbulence; the intrusions are thought to be the most important mode of mixing in terms of salt and heat loss. Radial profiles of azimuthal velocity revealed a core in almost solid body rotation, with a period of 5–6 days corresponding to 0.35 times the local Coriolis parameter. At the time of the October 1984 survey, the azimuthal speed reached a maximum of 0.3 m s^{-1} at a radius of 24 km. Both the radius and magnitude of the velocity maximum decreased with time. There was very little vertical shear within the core, and the vertical shear above the core was also weak, giving a Richardson number O(100). The anticyclonic circulation attained a maximum at the radius of the salinity front. As the lens was eroded from the sides, the radius of maximum velocity and the maximum velocity both decreased, but the rotation rate of the core remained fairly steady.

Published in: *Journal of Physical Oceanography.*

Supported by: NSF Grants OCE82-14066 and OCE86-00055.

WHOI Contribution No. 6812.

SURFACE-WAVE DATA ACQUISITION AND DISSEMINATION BY VHF PACKET RADIO AND COMPUTER NETWORKING

M. Briscoe, E. Denton, D. Frye, M. Hunt, E. Montgomery and R. Payne

Waverider buoy data are normally transmitted on a 27 MHz analog radio link to a shore station a few miles away, where the buoy data are plotted on a paper strip-chart recorder or logged digitally for later computer processing. Instead, we have constructed a relay station on Martha's Vineyard island that retransmits the received Waverider data over a digital, 148 MHz packet-radio link to a personal computer in our laboratory on Cape Cod, where the data are edited, processed, spectrally analyzed, and then sent over an Ethernet line to our Institution mainframe computer for archiving. Telephone modem access of a special wave-data file on the mainframe permits unattended data dissemination to the public. The report describes the entire system, including Waverider buoy mooring hardware, computer programs, and equipment. The purpose of the project was to learn what difficulties are involved in the automated acquisition and dissemination of telemetered oceanographic data, and to gain experience with packet radio techniques. Although secondary to these purposes, the long-term surface-wave monitoring off the southwest shore of Martha's Vineyard has its own scientific, engineering, and environmental benefits.

Supported by: ONR Contract N00014-86-K-0715.

WHOI Technical Report 88-15.

A VECTOR-AVERAGING WIND RECORDER (VAWR) SYSTEM FOR SURFACE METEOROLOGICAL MEASUREMENTS IN CODE (COASTAL OCEAN DYNAMICS EXPERIMENT)

Jerome P. Dean and Robert C. Beardsley

As part of the Coastal Ocean Dynamics Experiment (CODE) field program, moored buoys were instrumented to measure and record wind speed and direction, air and water temperature, insolation, barometric pressure and relative humidity. Appropriate sensors were selected, necessary modifications to the sensors and existing current meters were made, and Vector Averaging Wind Recorders (VAWRs) were assembled. R. M. Young utility rotor and vane wind sets designed by G. Gill, Paroscientific Digiquartz pressure sensors, Eppley pyranometers and Hy-Cal relative humidity

and solar sensors were used in two field experiments. Standard VACM direction and temperature sensors were maintained in the wind recorders. Devices were constructed as needed to protect against measurement errors due to wind, sun and ocean spray. Four W.H.O.I. VAWRs with Gill Wind sensor sets were deployed CODE-1 in 1981. Seven VAWRs were deployed in CODE-2 in 1982. A modified VMCM (Vector Measuring Current Meter) was used for comparison in CODE-1, and the seventh VAWR deployed in CODE-2 carried an integral sensor set for comparison. Although several VAWRs had minor problems, all but one VAWR in the two experiments returned useful scientific data.

Supported by: NSF Grants OCE80-14941 and OCE84-17769.

WHOI Technical Report 88-20.

A COMPILATION OF DIGITIZED SATELLITE IMAGERY OF THE GULF STREAM (1982, 1983, AND 1985)

Jennifer Earles, Lawrence Pratt, Peter Cornillon and Jean-François Cayula

Ninety plots of digitized temperature boundaries from infrared satellite images of the Gulf Stream along with corresponding image snapshots were compiled to determine stream width propagation speed. The satellite images are from the years 1982, 1983, and 1985 and are often of consecutive days. In this report, these images and digitized plots are presented.

Supported by: NSF Grants OCE87-00601, OCE85-10828 and ONR Contract N00014-87-K-0007.

WHOI Technical Report 88-57.

INTELLIGENT CHILLED MIRROR HUMIDITY SENSOR

David S. Hosom, Clifford L. Winget, Sumner Weisman, Donald P. Doucet and James F. Price

A new, intelligent, chilled mirror humidity instrument has been designed for use on buoys and ships. The design goal is to make high quality dew point temperature measurements for a period of up to one year from an unattended platform, while consuming as little power as possible. Nominal system accuracy is 0.3°C, and a measure of data quality is provided to indicate possible drift in calibration. Energy consumption is typically 800 Joules per measurement; standby power consumption is 0.05 watts. Control of the instrument is managed by an on-board central processing unit which is programmable in BASIC, and communication to an external data logger is provided through an RS232 compatible interface. This report describes the preliminary sensor tests that led to this new design and provides the complete technical description required for fabrication.

Supported by: ONR Contract N00014-84-C-0134, NR 083-400 and NSF Grant OCE-09614.

WHOI Technical Report 88-61.

GIBRALTAR EXPERIMENT: SUMMARY OF THE FIELD PROGRAM AND INITIAL RESULTS OF THE GIBRALTAR EXPERIMENT

Thomas H. Kinder and Harry L. Bryden

During the period October 1985 to October 1986 a large group of oceanographers collaborated in an intensive field effort called the Gibraltar Experiment. Scientists from Morocco, Spain, France, the United Kingdom, Canada and the United States joined together to obtain an extensive suite of measurements which greatly enlarged the oceanographic data base for the Strait of Gibraltar. Primary experiment goals included obtaining one realization of the annual flow cycle, understanding the dynamical balances of the strait flow, developing strategies for long-term monitoring of the Strait, and increasing knowledge of strait effects on the adjacent ocean. Preliminary results show progress toward each of these four goals.

Supported by: ONR Contracts N00014-82-C-0019, NR 083-004, N00014-85-C-0001, NR 084-004 and N00014-87-K-0007, NR 084-004.

WHOI Technical Report 88-30.

HYDROGRAPHIC DATA FROM R.V. ENDEAVOR CRUISE 129

George P. Knapp

Hydrographic and CTD data collected during R.V. ENDEAVOR cruise 129 are presented. These data include temperature, salinity and dissolved oxygen observed at standard levels by a Neil Brown Instrument Systems' CTD-O_2 profiler and salinity, dissolved oxygen, silica, phosphate and nitrate values at the observed depths of the collected water samples. Ninety-two stations were occupied on two short sections within the Caribbean and one long meridional section at (nominally)

64°West from the British Virgin Islands to the 200 m depth contour south of Newfoundland. Also presented are a series of sectional profiles of the six observed parameters as a function of depth.

Supported by: NSF Grant OCE84-14243.

WHOI Technical Report 88-41.

EXPLORING THE NORTH ATLANTIC OCEAN ON FLOPPY DISKS

James R. Luyten and Henry M. Stommel

A selection of hydrographic station data in the Atlantic between 8°S and 70°N is packed on four $5\frac{1}{4}$" floppy disks. Sample utility programs for reading and plotting the data are also on the disks. We present this computer atlas in preliminary form for use by students and professionals, in the belief that easy access to this valuable historical data will be educational and stimulating. Criticism and comment are welcome.

Supported by: ONR Contract N00014-84-C-0134, NR 083-400 and NSF Grant OCE86-13810.

WHOI Technical Report 88-59.

FRONTAL AIR-SEA INTERACTION EXPERIMENT

Nancy J. Pennington, Robert A. Weller and Kenneth H. Brink

The Frontal Air-Sea Interaction Experiment (FASINEX) examined air-sea interaction in the vicinity of sea surface temperature fronts in the Subtropical Convergence Zone (STCZ). Mooring measurements were made from five surface, four profiling Current Meter (PCM) and two longer duration subsurface moorings. The surface and PCM moorings, which made up the FASINEX central array were set in January 1986 and remained on station for six months. The two outlying subsurface moorings, set 90 miles south and 30 miles north of the central array were deployed in October 1984 and were recovered with the central array moorings in June 1986.

The surface moorings collected oceanographic and meteorological data, using a 3-meter instrumented discus buoy and eight to ten Vector Measuring Current Meters (VMCMs) and Vector Averaging Current Meters (VACMs). The surface buoy carried a Vector Measuring Wind recorder (VAWR) and a Meteorological Recorder (MR) which measured wind speed and direction, sea surface temperature (SST), air temperature, insolation, barometric pressure and relative humidity. The MR also transmitted meteorological and engineering data via ARGOS. The VMCMs and VACMs, placed from 10 to 4000 m, measured oceanic velocities and temperatures. The subsurface moorings measured oceanic velocities and temperature from 160 to 4060 m, carrying a total of seven VACMs and a WOTAN (Wind Observations Through Ambient Noise).

This report presents meteorological and oceanographic data from the seven W.H.O.I. moorings, with major emphasis on the surface mooring data. Details of the moored array and a statement of data return and quality are also included.

Supported by: ONR Contract N00014-84-C-0134.

WHOI Technical Report 88-63.

HYDROGRAPHIC DATA FROM R/V ENDEAVOR CRUISE #143

M. C. Stalcup, T. M. Joyce, J. L. Bullister, R. L. Barbour and J. A. Dunworth

Hydrographic data collected during R/V Endeavor cruise 143 is presented as a preliminary study of subduction in the northeast Atlantic south of the Azores Front. The front is clearly defined at the northern end of CTD section #1 which also shows a layer of 16-18 deg. C water subducted to the south. Section #2, 280 km to the east, is dominated by a large cyclonic ring with characteristics similar to "eastern" rings reported earlier. An anomalously salty parcel of Mediterranean water in this section is typical of highly saline lenses seen in the Canary Basin.

Supported by: NSF Grants OCE85-15642 and OCE85-18372.

WHOI Technical Report 88-7.

SOFAR FLOAT MEDITERRANEAN OUTFLOW EXPERIMENT DATA FROM THE SECOND YEAR, 1985–1986

Marguerite E. Zemanovic, Philip L. Richardson, James R. Valdes, James F. Price and Laurence Armi

In October, 1984, the Woods Hole Oceanographic Institution SOFAR float group began a three-year-long field program to observe the low frequency currents in the Canary Basin. The principal scientific goal was to learn how advection and diffusion by these currents determine the shape and amplitude of the Mediterranean salt tongue. Fourteen floats were launched at a depth of 1100 m in a cluster centered on 32°N, 24°W, and seven other floats were

launched incoherently along a north/south line from 24°N to 37°N. At the same time investigators from Scripps Institution of Oceanography and the University of Rhode Island used four other SOFAR floats to tag a Meddy, a submesoscale lens of Mediterranean water. In October, 1985, seven additional floats were launched, four in three different Meddies, one of which was tracked during year 1. This report describes the second year of the floats launched in 1984 and the first year of the ones launched in 1985. Approximately 41 years of float trajectories were produced during the first two years of the experiment. One of the striking accomplishments is the successful tracking of one Meddy over two full years plus the tracking of two other Meddies during the second year.

Supported by: NSF Grants OCE82-14066 and OCE86-00055.

WHOI Technical Report 88-43.

MARINE POLICY CENTER

James M. Broadus III, Director

GENETIC VARIABILITY IN TWO SEASONALLY ALLOPATRIC POPULATIONS OF THE LEATHERBACK SEA TURTLE, DERMOCHELYS CORIACEA

M. Tundi Agardy

Gel electrophoresis was used to analyze blood samples taken from adult leatherback sea turtles (Dermochelys coriacea) in order to elucidate the stock structure and genetic composition of two Atlantic nesting populations. The isozyme analyses were used to estimate both the overall levels of heterozygosity in the Atlantic population and the extent to which the two samples populations could be identified as being genetically distinct. Blood samples were collected from nesting female leatherback turtles in St. Croix, U.S. Virgin Islands, and Parismina, Costa Rica, two widely separated sites representing extremes of the Caribbean nesting range for D. coriacea. Isoelectric focusing was utilized in specific isozyme identification and total protein densitometry analysis to determine whether the two populations samples represented two true demes.

Both the Chi Square tests performed on the binary data, indicating presence or absence of a particular allozyme, and the multivariate discriminant analysis of the total protein densitometry data pointed to a clear genetic separation of the stocks. In addition, the genetic baseline information was used to show how stranded animals (whose stock identities could not be otherwise determined) could be matched to the most probable nesting population of origin using a maximum likelihood estimator. Electrophoretic analysis of blood proteins was thus used in two independent ways to elaborate not only stock structure and demic integrity, but also as a tool for determining the stock affinity of untagged individuals found far from their nesting grounds.

In Press: *Copeia.*

Supported by: The Pew Charitable Trusts and the Marine Policy Center.

WHOI Contribution No. 6982.

A NOTE ON AN EASY AND EFFECTIVE METHOD TO OBTAIN BLOOD SAMPLES FROM SEA TURTLES

M. Tundi Agardy

Obtaining blood samples from sea turtles is becoming an increasingly crucial activity as researchers tackle questions about the species' physiology, reproductive biology, genetics, and population dynamics. For small species, such as the ridley turtles (Lepidochelys kempi and Lepidochelys olivacea), or for juveniles and subadults of the larger species, blood may be obtained using the technique of Owens and Ruiz (1980). However, for large turtles such as the leatherback (Dermochelys coriacea) or loggerhead (Caretta caretta) blood is more easily obtained from the paracervical sinus using a 13-gauge spinal tap needle.

In Press: *Copeia.*

Supported by: The Pew Charitable Trusts and the Marine Policy Center.

WHOI Contribution No. 6981.

SPECIAL CONSIDERATIONS IN THE CONSERVATION AND MANAGEMENT OF HIGHLY MIGRATORY MARINE SPECIES

M. Tundi Agardy

The conservation and management of highly migratory marine species is a complicated endeavor. The endangered species status of many of these species has forced agencies and managers to contend with the inherent difficulties, but the management of these animals tends to be reactionary as opposed to systematic. This is a *quality common in crisis management*, and by its nature this knee-jerk approach to management is often appallingly inefficient. The conservation of highly migratory marine species requires a sufficient body of scientific knowledge about the animal's population dynamics and habitat requirements and a management approach that is comprehensive rather than piecemeal. Without the right kind of information and a holistic approach, the conservation of highly migratory marine species teeters on the brink of disaster.

In Press: *Environmental Conservation.*

Supported by: The Pew Charitable Trusts and the Marine Policy Center.

WHOI Contribution No. 6980.

WHY INFORMATION ON POPULATION DYNAMICS IS CRITICAL TO THE CONSERVATION OF ENDANGERED SPECIES: LESSONS FROM SEA TURTLE RECOVERY ATTEMPTS

M. Tundi Agardy

Managers of endangered animal populations are often faced with the unfortunate task of having to make management decisions without the luxury

of having complete knowledge about the species. The problem is especially acute in cases where the body of knowledge about an animal's ecology pertains only to a certain portion of its life cycle. Sea turtle recovery efforts are a perfect case in point: managers worldwide are struggling to prevent local and sometimes global extinctions while knowing little about the species' demographic parameters, beyond that which is known about nesting females and emergent hatchlings. Since these segments of the populations represent the only life history stages these animals spend on land, it is these that are considered to be within the bounds of human observation and thus sufficient knowledge. However, the total time that a sea turtle spends on land within the realm of convenient study is less than one percent of its life span, even by conservative estimates.

Given that resources to study sea turtle ecology are limited and that time, especially for some critically endangered species, is short, managers must be presented with the kind of information that is necessary for formulating efficient recovery attempts. In the case of highly migratory marine animals such as sea turtles, the most important pieces of information are the following: 1) what is the size and extent of the population unit to be managed?, and, 2) what is that population's intrinsic rate of increase and how is it prevented from being fully realized? Without these basic prerequisite questions, all other data collected on the biology of the animals is useless as a basis for developing sound management.

In Press: *Conservation Biology.*

Supported by: The Pew Charitable Trusts and the Marine Policy Center.

WHOI Contribution No. 6979.

COASTAL AND MARINE BIOSPHERE IN THE ACADIAN BOREAL REGION: RESULTS OF A COOPERATIVE EFFORT BETWEEN THE U.S. AND CANADA

M. Tundi Agardy and James M. Broadus

Achievements and progress made by a U.S. and Canadian Biosphere Reserve selection panel are reported. The panel has focused on three areas within the Acadian Boreal Region as potential Biosphere Reserve nominations. The first of these is a coastal/riverine area at the mouth of the Saguenay River in Canada. The remaining two are transboundary potential Reserves, one at the mouth of the Bay of Fundy and the other extending from Cape Cod, Massachusetts to northeastern Nova Scotia. Some of the aspects of designing and implementing such largely marine and therefore unique Biosphere Reserves are discussed.

In Press: *Proceedings of the Symposium on Biosphere Reserves*, World Wildnerness Conference, Denver.

Supported by: The U.S. Man and Biosphere Committee and the Marine Policy Center.

SOCIO-ECONOMIC ISSUES AND IMPACTS OF CLIMATIC CHANGES IN THE CARIBBEAN

Anders Alm, Erik Blommestein and James M. Broadus

Many of the physical effects of climatic changes in the Wider Caribbean will have socio-economic impacts. The presumption is that, for most cases, the net effect will be costly, but this will depend on the facts of each case. For several reasons, prior work has been mostly on the potential impacts of sea level change; but other climatic changes in the region may have impacts which equal or surpass those. A matrix that relates types of climate change effects to qualitative impacts on economic sectors is presented. Potential impacts on fisheries, agriculture and forestry, tourism, settlements and structures, the immediate coastal zone, public health, and waste disposal and drainage are discussed. Descriptive and prescriptive issues of public response are examined, along with attention to techniques and research issues in efforts to estimate socio-economic impacts.

In Press: *United Nations Environment Programme.*

Supported by: The J.N. Pew, Jr. Charitable Trust and the United Nations Environment Programme.

WHOI Contribution No. 6779.

RESOLVING INTERGOVERNMENTAL CONFLICTS IN MARINE RESOURCES MANAGEMENT: THE U.S. EXPERIENCE

Jack H. Archer

Intergovernmental conflict in U.S. marine resource management programs has its source in the federalist system of separate but unequal political sovereigns. The Constitution, however, establishes several principles to guide federal and state governments and the courts in resolving such conflict. Under the supremacy and commerce clauses, the federal government may "preempt" state authority to manage marine resources. But Congress, representing constitutionally-protected sovereign states, may limit the federal role in marine resource management programs, establish joint federal-state programs, or delegate such

authority to the states. This paper examines intergovernmental conflict in four marine resource management areas (coastal resources, fisheries, offshore oil and gas, and marine mammals) and argues that, within this constitutional and political context, intergovernmental conflict in the United States tends to be resolved by expanding the policy and decision-making process to include states, local governments, and organizations whose interests have been insufficiently accommodated in an existing resource management scheme.

In Press: *Journal of Ocean & Shoreline Management.*

Supported by: The Marine Policy Center.

INTERNATIONAL WORKSHOP ON THE SOVIET MARITIME ARCTIC

Lawson W. Brigham

The Arctic Ocean is a region of increasing importance for political, scientific, environmental and strategic reasons. Primarily due to its northern location, the Soviet Union is perhaps the dominant nation in the Arctic. Thus, it is important for Western scholars to examine Soviet domestic and international policies in the Arctic Ocean. To provide an opportunity for reporting on the status of such examination and to consolidate knowledge about the Soviet Union's use of its Arctic seas, the Marine Policy Center of the Woods Hole Oceanographic Institution organized an international workshop at Woods Hole, Massachusetts on 10-13 May 1987.

Published in: *Polar Record*, 24, 149, 131-132.

Supported by: John D. and Catherine T. MacArthur Foundation and the Marine Policy Center.

WHOI Contribution No. 6717.

THE SOVIET ANTARCTIC PROGRAM

Lawson W. Brigham

The Soviet Union's programs in Antarctica are highly orchestrated, long-term in nature, and of significant scientific merit. The Soviets have been an active and influential research participant in Antarctica since the International Geophysical Year (IGY) in 1957-58. Soviet IGY observations in meteorology, glaciology, and coastal oceanography were particularly important to the development of future research objectives and methodologies of many projects. Today, approximately 15 percent of the Antarctic scientific papers contributed by treaty nations come from Soviet researchers. The Soviet Union also has a significant voice in the Scientific Committee for Antarctic Research (SCAR)–an active player in the decisions on international exchanges, the pooling of data, and the coordination of various scientific programs.

Published in: *Oceanus*, 31, 2, 87-92.

Supported by: John D. and Catherine T. MacArthur Foundation.

WHOI Contribution No. 6778.

SOVIET ARCTIC MARINE TRANSPORTATION

Lawson W. Brigham

The development of marine transportation in the Soviet Arctic during the past three decades has been an extraordinary achievement. The Northern Sea Route (NSR), which stretches approximately 5000 kilometers across the Soviet maritime Arctic, has steadily become linked to the overall development of Siberian resources.

Published in: *Northern Perspectives*, 16, 4, 20-23.

Supported by: John D. and Catherine T. MacArthur Foundation and the Marine Policy Center.

EMERGING POLAR SHIP TECHNOLOGY: AN INTRODUCTION

Lawson W. Brigham

The application of modern marine technology to polar ship design and operation has been particularly impressive during the past three decades. Several nations have designed and built remarkably capable ships for Arctic and Antarctic operations. Extraordinary polar voyages, most thought to be impossible to achieve by surface ship, have included two transits by Soviet nuclear icebreakers to the Geographic North Pole, winter transits by polar icebreakers into the Chukchi and Beaufort Seas, winter oceanographic work aboard a polar research icebreaker in the Weddell Sea, and independent icebreaking cargo ship transits across the Northern Sea Route and in the Canadian Arctic. This successful application of a broad range of new technology to polar ship design and navigation has allowed access by these ships to remote polar regions that were once deemed impenetrable.

The topics in this special Marine Technology Society Journal are illustrative of the broad spectrum of polar ship technology.

Published in: *Marine Technology Society Journal*, 21, 3, 3-5.

Supported by: The Pew Charitable Trusts and the John D. & Catherine T. MacArthur Foundation.

WHOI Contribution No. 6622.

POSSIBLE IMPACTS OF AND ADJUSTMENTS TO SEA LEVEL RISE: THE CASES OF BANGLADESH AND EGYPT

James M. Broadus

The potential economic implications of relative sea-level rise scenarios developed by physical scientists are examined for Egypt and Bangladesh for the years 2050 and 2100. Several reasons are noted for caution in the interpretation of these scenarios. The method used to indicate the potential scale of economic effects is very coarse and simplistic, but its results suggest that relatively large economic values are at stake in both cases. As a first-order indication of these economic stakes, estimates are made of the current economic output generated in the areas affected by future sea-level in each scenario. A 1 m. rise, for example, would cover areas currently accounting for about 7% of habitable land and 5% of population in Bangladesh and 22% of habitable land and 14% of population in Egypt. To demonstrate how this can be extended to an estimate of potential loss, one of the Bangladesh scenarios is developed further using strong but reasonable parametric assumptions. The result suggests that, absent mitigating adjustments, a "worst-case" relative sea-level rise of 1 m. by 2050 could impose a loss in present value terms at between 1 and 2% of the nation's current gross domestic product. It is shown further, however, that human adjustments would tend to reduce this loss; so it should be seen as a bounding value. Potential adjustments discussed are: defensive measures, recombinations of productive factors, and technological adaptation. In the near term these might include such institutional adaptations as insurance, share markets, contracts and future markets, mergers, and governmental risk-sharing schemes.

In Press: *Proceedings, International Workshop on the Effects of Climate Change on Sea Level, Severe Tropical Storms and their Associated Impacts.*

Supported by: The Pew Charitable Trusts and the U.S. Environmental Protection Agency.

DETERMINING THE STRUCTURE OF THE U. S. MARINE INSTRUMENTATION INDUSTRY AND ITS POSITION IN THE WORLD INDUSTRY

James M. Broadus, Porter Hoagland and Hanke L. Kite-Powell

This report is a general, but comprehensive, description and analysis of industrial organization in the field of marine electronic instrumentation (MEI), a broadly defined "industry," which until now has received little systematic, scholarly attention. The report reviews the current literature on international trade and competitiveness, as well as trade and scientific journals relevant to the industry. The results of a series of interviews with representatives of the industry and responsible government agencies are presented and industry and government data on R&D and output have been collected and analyzed together with other indicators of industrial performance. On the basis of these sources, the structure of the industry and its markets is characterized and the importance of marine electronic instrumentation in international high technology trade is established. Over 350 firms in the U.S. industry are identified, which annually earn total estimated gross revenues of approximately $5 billion. These firms fall into three largely distinct industry groups: (1) defense systems contractors; (2) commercial marine electronics; and (3) scientific instrumentation. The first group is by far the largest in sales volume and is oligopolistic in structure, consisting of a few large rivals for infrequent and complex defense systems contracts. The other groups are more purely competitive. Four major customer groups are distinguished: (1) military; (2) commercial and recreational shipping and boating; (3) offshore oil and gas; and (4) oceanographic/environmental. Most of the firms in the industry face international competition. The importance of marine electronic instrumentation to technological advance and economic activity in the world's oceans is strongly apparent. Parameters affecting the international competitiveness of firms in this industry, including those relating to industry structure and behavior and governmental practices and institutions such as sponsored research, procurement, intellectual property rights, tax allowances, antitrust enforcement, small business encouragements, export controls, import restrictions, exchange rates, and technology transfer are summarized. A number of issues relating to international competition, economic analysis, and government policy that are fruitful areas for further research also are identified.

Supported by: Dept. of Commerce, NOAA, National Ocean Service, Office of Marine Operations through Massachusetts Centers of Excellence Corp. grant No. NA87-AA-D-M0037.

WHOI Technical Report 88-55.

MAKING CERCLA NATURAL RESOURCE DAMAGE REGULATIONS WORK: THE USE OF THE PUBLIC TRUST DOCTRINE AND OTHER STATE REMEDIES

Cynthia Carlson

CERCLA authorizes the federal government states, as guardians of the public trust, to sue polluters to recover damages for injuries to natural resources caused by releases of hazardous substances. These causes of action are governed by the Department of the Interior's natural resource damage assessment regulations, which have recently been challenged in federal court. Critics assail the regulations as strongly biased toward the undervaluation of damaged resources. The author of this article notes that the regulations may ultimately have to be revised to address this concern. In the meantime, she argues, public trustees stand a good chance of obtaining fuller recovery for injured natural resources if they make use of available pendent state claims. By supplementing their CERCLA suits with appropriate public trust and public nuisance claims, the author submits, public trustees can widen the available remedies to include injunctions, mitigation, restitution, and other forms of equitable relief.

Published in: *Environmental Law Reporter*, 18, 10299-10307.

Supported by: The Pew Charitable Trusts and the Marine Policy Center.

WHOI Contribution No. 6851.

ON ESTIMATING COMPENSATION FOR INJURY TO PUBLICLY-OWNED MARINE RESOURCES

Steven F. Edwards and Cynthia Carlson

It is well-established that the public has the right to use certain marine resources, including fish stocks, beaches, and marine waters, for certain purposes, including recreational fishing. Rights in public resources are held "in trust" by federal and state governments for the public, both now and in the future. Given public rights, we not only argue that minimum willingness-to-accept-compensation (WTA) is the theoretically correct measure of economic damages when a publicly-owned marine resource is injured, but that it is, in fact, feasible to measure WTA, and, therefore, WTA should be used to estimate compensation. Two utility-theoretic approaches for welfare analysis which use Hausman's (1981) method and the contingent valuation method are outlined.

In Press: *Journal of Marine Resource Economics*, 6, 1.

Supported by: The Pew Charitable Trusts, the Marine Policy Center and the Northeast Fisheries Center.

WHOI Contribution No. 6974.

AN OVERVIEW-MARINE MINERAL RESERVES AND RESOURCES-1988

K.O. Emery and James M. Broadus

Marine mining has been conducted on a local and generally small scale for thousands of years. Large-scale recovery from beaches and piers began only about forty years ago, and soon afterward powered ships and tools and new exploration methods revealed the presence of economic concentrations of oil and gas, sand and gravel, and some heavy minerals beyond the beach. These materials are in relatively shallow waters of the continental shelf and now are known well enough to be considered reserve ores. Rapid success for them led to immediate expectation of marine mining of many other minerals that have higher value per unit weight, but they occur in deeper waters beyond the shelf where conditions are more difficult and costs are higher. They include phosphorite, ferromanganese nodules and crusts, and (less than a decade ago) polymetallic sulfides. All are still potential resources that cannot yet be considered reserve ores.

Increased knowledge of the deep-ocean floor and its natural processes is likely to be applied first to expanding the reserves of similar deposits now on land and perhaps later to ocean-floor mining. Moreover, ocean-floor mining must compete economically with improved methods of recovery from existing low-grade resources on land and from waste piles left from earlier and less efficient methods of mineral recovery.

In Press: *Marine Mining*, 8.

Supported by: Dept. of Commerce, NOAA, National Sea Grant Program (NA86-AA-D-SG090).

WHOI Contribution No. 6738.

PERSPECTIVES ON SCIENCE AND MANAGEMENT IN SOUTHERN NEW ENGLAND ESTUARIES

Arthur G. Gaines, Jr.

The flooded glacial coast of southern New England provides the opportunity to compare estuaries of varied geometry, tidal forcing, freshwater input and anthropogenic impact.

Observation of several of these estuaries suggest the generalizations sought by managers and legislators to serve as a basis for standards, regulations and estuarine "health" indices are less straightforward than commonly believed. Examples treating dissolved oxygen, littoral drift, nutrient loading and eutrophication are discussed.

Published in: *Program for Spring NEERS Meeting,* April 1988, Woods Hole, MA.

Supported by: The Marine Policy Center.

NITROGEN DYNAMICS IN A MARINE COVE: IMPORTANCE OF GROUNDWATER

Anne E. Giblin and Arthur G. Gaines

Most of the studies on nitrogen cycling in coastal areas has been done in large estuaries. Much less is known about nitrogen dynamics in the restricted marine coves, bays and lagoons which are common features of the coast of much of the Northeastern United States. These ecosystems differ from large river dominated estuaries in morphometry and hydrology. They are frequently separated from offshore waters by restricted inlets which may exhibit strong time and velocity asymmetries between flood and ebb tide. Surface runoff into these coves are frequently small and a significant amount of the freshwater enters these areas as groundwater.

We studied the relative contributions of groundwater, tidal water and benthic recycling to the nitrogen budget of Town Cove, Orleans, MA. Porewater profiles showed that nitrate in groundwater was carried through the sediments with very little loss. Therefore we could estimate N inputs knowing groundwater flows and nitrate concentrations in wells. We calculated that about half of the total nitrogen, and most of the dissolved nitrogen, entering the Cove was derived from groundwater. Based upon EPA statistics we estimate the majority of this nitrogen comes from septic systems but lawn fertilizer is also a significant contributor. Town Cove is similar to river dominated urban estuaries in that about half of the inorganic nitrogen entering the estuary is from sewage derived sources. The relative importance of groundwater nitrogen derived from septic systems to the nitrogen budget of other marine coves and lagoons will be discussed.

Published in: *EOS*, 69, 44, 1080, 1988.

Supported by: The Marine Policy Center and the Ecosystems Center, Marine Biological Laboratory.

CONTROLLING MARINE POLLUTION IN THE MEDITERRANEAN SEA

Peter M. Haas

An important and persistent question facing the regime literature is "Do Regimes Matter?" Much attention has been paid to regime creation and regime maintenance, but, few have studied their effects on international behavior. Although recent studies of environmental regimes exist, they do not study compliance with them. This essay investigates the link between the regime for controlling Mediterranean pollution and national compliance.

In Press: *International Organization.*

Supported by: The Pew Charitable Trusts and the Marine Policy Center.

WHOI Contribution No. 6952.

ADMINISTRATIVE DISCRETION IN THE MANAGEMENT OF OCS MINERALS

Porter Hoagland III

Mineral developers face varying kinds of risks and uncertainties associated with the exploration, development, and production of minerals from a marine deposit. These risks can be geologic (e.g., ore grade), environmental (e.g., storm frequency), or legal (e.g., lease suspension). To the miner, these types of risks all have the same result; they raise the private costs of proving-out and working a deposit. Both geologic and environmental risks could be reduced through the efforts of exploration and meteorological forecasting, for example. In the case of U.S. public minerals, legal risks might be reduced through the promulgation of new regulations, the enactment of a new law, or a favorable allocation decision made by the resource manager. We are concerned here with the special case of legal risks arising out of the exercise of administrative discretion by a resource manager over the rights to work publicly-controlled ocean minerals.

We examine the opportunities found in OCSLA for the resource manager, here the Secretary of Interior (or the MMS acting on his behalf), to apply administrative discretion to modify, suspend, or otherwise alter activities relating to the development of OCS minerals. It is useful to understand the reasons for which discretion is given to the resource manager. It is important as well to understand the extent to which the application of administrative discretion may raise the costs associated with marine nonfuel mineral development.

In Press: *Ocean Policy Study Series.*

Supported by: The Pew Charitable Trusts, Marine Policy Center and Dept. of Commerce, NOAA, National Sea Grant Program (NA86-AA-D-SG090).

WHOI Contribution No. 6831.

THE CHANNEL ISLANDS NATIONAL MARINE SANCTUARY

Porter Hoagland and Timothy K. Eichenberg

The Channel Islands National Marine Sanctuary, designated in 1981, is the keystone of the nation's marine protected areas. The marine region represented by the sanctuary, the Southern California Bight, arguably has had more influence on the shaping of United States domestic marine policy than any other.

The conflicts that surrounded establishment of the marine sanctuary at the California Channel Islands have had an important influence on the evolution of the national program during the last 10 years. In fact, the continuing controversies over the use of the resources near these islands raise questions about the efficacy of the designation "marine sanctuary" in the United States and whether management concepts, such as "multiple use," can be attained in the oceans.

Published in: *Oceanus*, 31, 1, 66-74.

Supported by: The Marine Policy Center.

CHINA SEA COASTAL AND MARINE NONFUEL MINERALS: INVESTIGATION AND DEVELOPMENT

Porter Hoagland, Yang Jinsen, James M. Broadus, David K.Y. Chu

In this paper, we survey the economic potential of coastal and marine nonfuel minerals in the East and South China Seas. We present a brief description of the mineral economies for eight China Sea countries and a review of historic and current efforts in exploration, development, and production of coastal and marine nonfuel minerals. The benefits of CCOP, an international joint prospecting organization, are described. Using 1984 data based upon production of marine sand and gravel in Kyushu, Japan, marine tin production in Indonesia, and marine salt production in China, the countries surrounding the two China Seas produce about a third of a billion dollars worth of marine nonfuel minerals annually. This figure is small in comparison, for example, with offshore crude oil production, estimated at $11 billion in that year. From a global perspective, output of marine nonfuel minerals from the East and South China Seas are proportionately much more important to world marine nonfuel production than the output of offshore hydrocarbons from the same region. Taking only sand and gravel and tin production, the marine mines in these two seas produce almost one-quarter of Broadus' (1987) estimated $500 million annual revenues from all seabed nonfuel materials worldwide. Nearshore minerals have the best prospects, and the prospects for deepsea minerals, although they occur in the region, are remote and should not influence maritime boundary settlements.

In Press: *Proceedings, Third Asian-Pacific Marine Resource Development Conference.*

Supported by: Dept. of Commerce, NOAA, National Sea Grant College Program under grant No. NA86-AA-D-SG090, the J.N. Pew, Jr. Charitable Trust, and the Marine Policy Center.

THE ANTARCTIC LEGAL REGIME AND THE LAW OF THE SEA

Christopher C. Joyner

Applying international ocean law often hinges on the legal status of the adjoining land. For example, the commonly used definitions–territorial sea, Exclusive Economic Zone, and high seas–denote varying amounts of sovereignty accorded to the coastal state/country, and similarly varying freedoms accorded to the balance of the international community.

But, Antarctica is the only continent without recognized sovereign countries. Because aspects of the international law relating to the continent are therefore ambiguous, the application of ocean law to its surrounding waters also is ambiguous.

The 1980s are an interesting period for Antarctic law–as diverse national views and international legal agreements are being tested and blended, and as nations seek new levels of international cooperation on the lands and waters surrounding the South Pole.

Published in: *Oceanus*, 31, 2, 22-27.

Supported by: The Marine Policy Center.

JAPAN AND THE ANTARCTIC TREATY SYSTEM

Christopher C. Joyner

Japan in recent years has attained prominence in shaping the course of Antarctic affairs. This commentary addresses three sets of fundamental

questions in Japan's contemporary southern polar policies. First, what is the nature and degree of Japan's commitment to the Antarctic area, and how has that relationship contributed to the regime administering activities in the region? Second, what particular national interests does Japan hold in the Antarctic, and how might these interests affect Japan's resource needs, both living and non-living, on and around the Antarctic continent? Third, what diplomatic posture has Japan assumed since 1983 in the United Nations General Assembly debates over the question of Antarctica, and what position does Japan take towards establishing a common heritage of mankind regime there? By examining these queries, Japan's foreign policy, economic priorities and legal concerns in the Antarctic should become more apparent and better appreciated.

In Press: *Ecology Law Quarterly.*

Supported by: The Marine Policy Center and The George Washington University.

WHOI Contribution No. 6811.

BOOK REVIEW: MARINE POLLUTION AND THE LAW OF THE SEA

Christopher C. Joyner

Marine pollution is not a new phenomenon. So long as man has used the oceans, he has polluted them. In this century, however, pollution of the seas has starkly intensified. This trend has been generated by several simultaneous global pressures: accelerating population growth, technological development, heightened living standards, and greater consumption demands associated with economic growth . The unmistakable consequence has been more pronounced damage to the living resources and marine ecology of coastal states shores, as well as to the world ocean environment.

In Press: *The Vanderbilt Journal of Transnational Law*, Vol. 21, 4, 1988. 843-854.

Supported by: The Marine Policy Center and The George Washington University.

WHOI Contribution No. 6770.

THE 1988 ANTARCTIC MINERALS CONVENTION: A REPORT

Christopher C. Joyner

This report has three aims. First, it generally describes the character of the Convention, with a special view to examining the institutions established to regulate mineral resource activities in the Antarctic. Second, the study addresses how internal accommodation among interested parties was sought and secured during the negotiations process. Particular attention here is focused on inter-institutional arrangements, especially as they contributed to temper conflictive views among Antarctic Treaty states concerning sovereign rights on the continent. Third, discussion is presented to outline the process of decisionmaking and how Antarctic mineral resource activities will proceed under provisions set up in the Convention. At the outset, however, explanation of the coalitions of states involved and brief treatment of the Antarctic Mineral Convention's genesis seem in order to appreciate this treaty's proper historical context.

In Press: *Marine Policy Reports.*

Supported by: The Marine Policy Center and The George Washington University.

WHOI Contribution No. 6951.

MANAGING REEFS AND INTER-REEFAL ENVIRONMENTS AND RESOURCES FOR SUSTAINED EXPLOITIVE, EXTRACTIVE AND RECREATIONAL USES

Richard A. Kenchington

The conservation of coral reefs has long been a matter of particular and expert concern to scientists who have observed and documented the problems and potential problems. The Proceedings of the International Coral Reef Symposia all contain papers documenting human impacts and reef deterioration and calling for management action.

Population growth in areas where reefs are accessible, the introduction of new technologies and the development of economies have placed many pressures on coral reefs. The likelihood of being able to manage these pressures depends in part on the extent to which the well-being of coral reefs is important to the economic well-being of the impacting human society. The management of environments is thus the management of human impacts and activities (Kenchington, 1983).

In Press: *Proceedings, Coral Reef Symposium.*

Supported by: The J.N. Pew, Jr. Charitable Trust and the Marine Policy Center.

WHOI Contribution No. 6816.

PLANNING THE GREAT BARRIER REEF MARINE PARK

Richard A. Kenchington

The Great Barrier Reef Marine Park (GBRMP) is a multiple use management approach

which aims to achieve reasonable use consistent with conservation. The Great Barrier Reef Marine Park Act (1975) anticipated the World Conservation Strategy (1981) and it may be unique in providing specifically for conservation and reasonable use, or sustainable development of a large area of recognized conservational significance. A number of general accounts of the approach and extent of the GBRMP have been published starting with Kelleher and Kenchington (1982) and most recently Kelleher (1985 and 1986).

The Great Barrier Reef Region contains about 2,900 reefs and 300 reef islands within a total area of some 350,000 square kilometers. The impetus for conservation and management of the Great Barrier Reef came in the late 1960s. It was driven by concerns over the likely impacts of petroleum exploration and production, of mining for limestone and other minerals, and the need for environmental controls over any expansion of commercial fishing over the development of a major tourist industry and over impacts reaching the Reef from terrestrial activities (Wright, 1977).

The scale and scope of the GBRMP have thus necessitated the development of a planning approach with few direct precedents in a planning environment of scarce information. This paper outlines the planning procedures and some of the background that led to them.

In Press: *Proceedings, Marine, Lake and Coastal Heritage Workshop.*

Supported by: The Pew Charitable Trusts and the Marine Policy Center.

WHOI Contribution No. 6723.

DENMARK AND THE EXCLUSIVE ECONOMIC ZONE

Finn Laursen

The purpose of this paper is to analyze those aspects of Danish marine policy in recent years which relate to what has become known as the Exclusive Economic Zone (EEZ).

Published in: *Nordic Journal of International Law*, 56, 1, 69-106.

Supported by: The J.N. Pew, Jr. Charitable Trust and the Marine Policy Center.

FISHERIES RISK IN THE MODERN CONTEXT

M. Estellie Smith

The sea has long been viewed as a threatening environment and the folktales of many peoples list an impressive inventory of the real as well as imaginary dangers that are said to lie just beyond the horizon, out in the deep. Though, for much of history, fishermen were forced (and preferred) to exploit in-shore waters, such fishing still faces risks of sudden storms, capsizing in swells, or being smashed on rocks due to an error in sailing judgment. However, if there were dangers lurking in these waters, how much more fearful were the risks once out of sight of land? Not only the fishery folk but those who studied them could not help but emphasize the natural risks of fishery ventures - and, as well, the exotic defenses such as superstitions, taboos, amulets, prayers and the like, all designed to mitigate such risks.

Published in: *Maritime Anthropological Studies*, 1, 1, 29-48.

Supported by: The J.N. Pew, Jr. Charitable Trust, the Marine Policy Center and the State University of New York at Oswego.

THE RIGHT TO CHOICE: POWER AND DECISION-MAKING

M. Estellie Smith

The chapters in this volume address a number of issues ranging from the particular–e.g., the ethnography of fishing and family dynamics–to such general concerns as development in marginal areas, political economy, and feminist issues. However, the theoretical thread of interest that seems to me to bind these papers is one that runs through much of recent scholarship, drawing increasing attention from those in many disciplines and of a variety of persuasions. That thread is the multidimensional issue of power. There is, in point of fact, a growing conviction that this "theoretical issue" is of growing common concern to those in all walks of life. Thus, whether the goal be pure science or the arenas of practical concerns, we are trying to understand power: its interrelations with its concomitants, authority and decision-making; its composition, distribution, and intended functioning, as well as actual functions; and the explicit goals and unintended consequences of all these aspects.

Published in: *To Work and To Weep*, J. Nadel-Klein and D.L. Davis (editors).

Supported by: The J.N. Pew, Jr. Charitable Trust, the Marine Policy Center and the State University of New York at Oswego.

BOOTSTRAPPING SPARSELY SAMPLED SPATIAL POINT PATTERNS

Andrew R. Solow

The bootstrap is a practical, non-parametric method that can be used to estimate the sampling distribution of a broad class of parameter estimates. We propose to use the bootstrap to estimate the sampling distribution of a distance-based estimator of intensity in a sparsely sampled spatial point pattern. An illustration of the method is given.

In Press: *Ecology.*

Supported by: The J.N. Pew, Jr. Charitable Trust and the Marine Policy Center.

WHOI Contribution No. 6791.

A RANDOMIZATION TEST FOR INDEPENDENCE OF ANIMAL LOCATIONS

Andrew R. Solow

A simple randomization test of the independence of successive observations of animal location is described. The test is exact, distribution-free, and does not depend on nuisance parameters which may be difficult to estimate in small samples. A comparison is made to an approach based on Monte Carlo simulation.

In Press: *Ecology.*

Supported by: The Pew Charitable Trusts and the Marine Policy Center.

WHOI Contribution No. 6897.

SIGNIFICANCE TESTS IN PRINCIPAL COMPONENT ANALYSIS: THE N RULE

Andrew R. Solow

Principal component analysis is commonly applied to climatological data sets having the form of spatial time series. A key problem in such applications is the choice of the number of components to be retained in the analysis. One approach to this problem is informal: components are retained until "most" of the variance in the data set is captured. A more formal approach is based on significance tests: components are retained provided that they are statistically significant in some sense. In climatological applications, the N rule is commonly used as a formal procedure. In this paper, the role of significance testing in principal component analysis is reviewed, and the N rule is shown to have no formal justification.

In Press: *Journal of Climate.*

Supported by: The Pew Charitable Trusts and the Marine Policy Center.

WHOI Contribution No. 6973.

STATISTICAL MODELING OF STORM COUNTS

Andrew R. Solow

A statistical model of a recently compiled record of monthly extratropical storm counts for the mid-Atlantic coast of the United States over the period 1942-83 is presented. The counts are modeled as a Poisson process with non-stationary mean function. The mean function is decomposed into a secular component and a seasonal cycle. Because the form of the secular component is unknown, a non-parametric regression approach suitable for Poisson data is used to estimate it. The estimated secular component is generally constant through the 1950s, then declines through the 1970s. The estimate is found to be statistically significant. A Fourier series involving two harmonics is fit to the seasonal cycle. A preliminary check indicates that the seasonal cycle remains stable through time. Some diagnostics based on suitably-defined residuals are presented that generally confirm the goodness-of-fit and distributional assumptions underlying the model.

In Press: *Journal of Climate.*

Supported by: The Pew Charitable Trusts and the Marine Policy Center.

WHOI Contribution No. 6869.

LOSS FUNCTIONS IN ESTIMATING OFFSHORE OIL RESOURCES

Andrew R. Solow and James M. Broadus

The Minerals Management Service (MMS) produces estimated probability distributions for undiscovered oil resources for several offshore planning areas. For each planning area, the mean of this distribution is taken as the point estimate of the resource quantity. We formulate the problem of point estimation in decision-theoretic terms. Under this formulation, the choice of the mean as the point estimate involves the implicit adoption of a quadratic loss function. We show that, as a consequence of the form of the distributions produced by the MMS, the optimal point estimate is very sensitive to the choice of loss function.

In Press: *Resources and Energy.*

Supported by: Dept. of Commerce, NOAA, National Sea Grant Program (NA86-AA-D- SG090).

WHOI Contribution No. 6920.

AN APPLICATION OF CIRCULAR-LINEAR CORRELATION ANALYSIS TO THE RELATIONSHIP BETWEEN FREON CONCENTRATION AND WIND DIRECTION IN WOODS HOLE, MASSACHUSETTS

Andrew R. Solow, John L. Bullister and Cynthia Nevison

Two statistical tests for correlation between a circular variate and a linear variate are presented. The tests are applied to a small data set concerning Freon-12 concentration and wind direction in Woods Hole, Massachusetts during the summer of 1987. A significant correlation is found. Further analysis suggests that this directional effect is related to onshore Freon-12 release.

Published in: *Environmental Monitoring and Assessment*, 10, 219-228.

Supported by: The Pew Charitable Trusts, the Marine Policy Center and NSF Grant No. OCE-8615289.

WHOI Contribution No. 6750.

MARINE RESERVES: RELEVANT POLICY AND MANAGEMENT ISSUES WITH EXAMPLES FROM THE GREAT BARRIER REEF MARINE PARK, AUSTRALIA, AND THE UNITED STATES

Clem Tisdell and James M. Broadus

Paying particular attention to social science considerations, this paper concentrates on two aspects of marine reserves: (a) establishment decisions and (b) general management decisions once they are established. Economic reasons are given as to why governments should establish marine reserves and a formal cost-benefit framework is outlined for determining the optimal size of reserves. This enables the approach of some conservation biologists to the determination of the size and pattern of reserves to be criticized. In addition, inadequacies in legislation as a guide to marine reserve establishment are noted. Four main aspects of the management of marine reserves are discussed.

First, the aims or objectives applicable to the management of marine reserves are considered, paying particular attention to the Great Barrier Reef Marine Park and the importance of taking account of political sustainability. The degree to which Australian legislation and that of the United States provides guidance about objectives is discussed. Secondly, the comparative difficulty of managing land-based parks and marine reserves are considered and a number of natural factors identified which make it relatively more difficult to manage marine reserves. Thirdly, the multiple-use of marine reserves and the desirability of zoning are considered. These issues are shown to be extremely important both within the Australian context and that of the United States. Fourthly, it is emphasized that social science has an important role to play in the management of marine reserves and to date insufficient weight may have been put on social science in this management.

Published in: *Research Report No. 157*, University of Newcastle, N.S.W., Australia.

Supported by: The J.N. Pew, Jr. Charitable Trust.

POLICY ISSUES RELATED TO THE ESTABLISHMENT AND MANAGEMENT OF MARINE RESERVES

Clem Tisdell and James M. Broadus

This paper considers aims or objectives relevant to the management of marine reserves, paying particular attention to the Great Barrier Reef Marine Park and the importance of taking account of political sustainability which may require some compromise of conservational goals. The comparative difficulty of managing land-based parks and marine reserves are discussed and a number of factors identified which make it relatively more difficult to manage marine reserves. Economic reasons are given as to why governments should establish marine reserves and a formal cost-benefit framework (drawing on economic analysis) is outlined for determining the optimal size of reserves. The approach of some conservational biologists to the determination of the size and pattern of reserves is criticized. The multiple use of reserves and the desirability of zoning are considered. It is pointed out that both natural science and social science have a role to play in the management of reserves. To date it seems that insufficient weight has been put on social science in this management.

In Press: *Coastal Management.*

Supported by: The J.N. Pew, Jr. Charitable Trust and the Marine Policy Center.

WHOI Contribution No. 7035.

GRADUATE STUDENTS

Abstracts of papers or theses submitted in 1988 by graduate students of the Woods Hole Oceanographic Institution Doctoral Degree Program and the Woods Hole Oceanographic Institution/Massachusetts Institute of Technology Joint Program in Oceanography/Oceanographic Engineering. Other papers authored or coauthored by graduate students are included in the departmental sections. Students are indicated by an asterisk in the Author Index.

STABILITY OF A COASTAL UPWELLING FRONT OVER TOPOGRAPHY

John A. Barth

A two-layer shallow water equation model is used to investigate the linear stability of a coastal upwelling front. The model features a surface front near a coastal boundary and bottom topography which is an arbitrary function of the cross-shelf coordinate. By combining the various conservation statements for the global properties of the system, a general stability theorem is established which allows the *a priori* determination of the stability of a coastal upwelling front.

Unstable waves are found for the modelled coastal upwelling front. The unstable wave motions are frontally-trapped and dominant in the upper layer. The wave propagates phase in the direction of the basic state flow and the primary energy conversion is via baroclinic instability. The effect of varying the model parameters is presented. Moving the front closer than ~2 Rossby radii to the coastal boundary results in a decrease in the growth rate of the fastest growing wave. Increasing the overall vertical shear of the basic state flow, by either decreasing the lower layer depth or increasing the steepness of the interface, results in an increase in the growth of the fastest growing wave.

A bottom sloping in the same sense as the interface results in a decrease of the growth rates and alongfront wavenumber of the unstable waves in the system. Linearized bottom friction is included in the stability model and results in a decrease in the growth rates of the unstable waves by extracting energy from the system. Since the unstable mode is strongest in the upper layer, bottom friction will not stabilize the upwelling front.

A comparison between the predictions from the simple two- layer model and observed alongfront variability for three areas of active upwelling is presented. Reasonable agreement is found, suggesting that observed alongfront variability can be interpreted in terms of the instability of a coastal upwelling front.

Supported by: NSF Grant OCE-84-08563 and by ONR contract N00014-84-C-0134.

THE BIOGEOCHEMISTRY OF ^{210}PB AND ^{210}PO IN FRESH WATERS AND SEDIMENTS

Gaboury Benoit

The focus of this work was geochemical cycling of ^{210}Pb in lakes, including the water column, sediments, and their interactions with each other. A special goal was to elucidate processes that might influence the distribution and fluxes of the radionuclide in ways that could effect ^{210}Pb sediment dating.

A mass balance for the epilimnion showed that ^{210}Pb inputs by precipitation were matched by outputs on settling particles, indicating that direct uptake by bottom sediments was inconsequential. Below the epilimnion, vertical eddy diffusion was calculated by the heat flux gradient method including corrections for both radiant heating and heat loss to sediments. Vertical mixing was very low because of stability imparted by a steep temperature/density gradient extending right to the reduced iron, which reprecipitated at the oxycline and returned to the bottom via settling. ^{210}Pb followed the same pattern except that, at the interface, it was scavenged rather than precipitated. Below the zone of precipitation, both ^{210}Pb and iron distributions could be described by a model consisting of constant release from anoxic sediments, horizontal transport, and simple dilution in the water column. Cycling of ^{210}Po was complicated by unidentified additional factors.

A finite difference model (SEDIMIX) was used to find the combination of sedimentation and Fickian redistribution that provided the best fit to the ^{210}Pb sediment data. Sedimentation rates were found to increase linearly with overlying water depth. The magnitude of the Fickian component of ^{210}Pb transport was equal to calculated rates of pore water diffusive flux, which is probably more important than sediment mixing in this lake.

^{210}Pb, ^{210}Po, and ancillary geochemical parameters were measured on the solid fraction and pore waters of two cores taken from the deepest basin in August and September. The radionuclides were two orders of magnitude higher than in overlaying water and had steep concentration gradients that could support substantial diffusive fluxes. Fe, Mn, S(-II), and alkalinity did not have similar gradients. ^{210}Pb partition coefficients ranged from 1500 to 15000, decreasing with depth, and seemed to be controlled by sorption on iron oxides. Remobilization to the water column apparently comes from a thin layer of iron-rich floc near the sediment water interface. Deeper in the cores, diffusive transport can cause redistribution of ^{210}Pb to an extent that can affect ^{210}Pb dating.

Supported by: United State Geological Survey through MIT.

WHERE THREE OCEANS MEET: THE AGULHAS RETROFLECTION REGION

Sara L. Bennett

The highly energetic Agulhas Retroflection region south of the African continent lies at the junction of the South Indian, South Atlantic, and Circumpolar Oceans. A new survey of the Agulhas Retroflection taken in March 1985, plus historical hydrographic data, allow its dynamical and water-mass characteristics, and its role in exchanging mass, tracers, and vorticity between the three oceans, to be extensively characterized. The 1985 survey is composed of three independent, synoptic elements: a grid of closely-spaced, full-water-depth hydrographic stations (the first entirely full-water-column survey in this area), including several transects of the Agulhas and Agulhas Return Currents; a continuous survey of the path of the currents (the first such survey in the Agulhas); and a contemporaneous and relatively cloud-free sea surface temperature image derived from satellite infrared measurements.

Mass transport balances within the closed grid boxes of the 1985 hydrographic survey provide information about current transport, recirculation (transport in excess of estimated returning interior ocean transport), and the overall Retroflection transport pattern. The current transport values exceed by as much as a factor of 1.5 the maximum interior transport computed from observed wind-stress curl and linear theory. Agulhas Current transports ranged from 56 to 95 x 10^6m s^{-1} at four 1985 transects crossing the current. Agulhas Return Current transports at the two 1985 transects were 54 and 65 x 10^6 m s^{-1}. These transports are computed relative to 2400 dbar, which lies below the deep oxygen minimum emanating from the South Indian Ocean, and above the North Atlantic Deep Water salinity maximum.

The current retroflected in two distinct branches in 1985, with a cold ring and a partially isolated warm recirculation cell found between the two branches. The satellite-derived sea surface temperature (SST) image, in agreement with the *in situ* measurements, showed that the cold ring lacked a cold SST anomaly; that the subsurface current path, as represented by a survey of the 15 C isotherm and 200 dbar surface intersection, was closely followed by a sharp front in sea surface temperature; and that most of the Agulhas's surface warm core retroflected upstream of the second retroflection branch.

Anticyclonic curvature vorticity at sharp turns in the subsurface current path was found to exceed the maximum allowed by gradient wind balance, indicating that at these locations time-dependence and cross-frontal flow are important. The current's density field is found to meet necessary conditions for baroclinic and barotropic instability. These instability mechanisms may play a role in ring formation and current meandering.

Top-to-bottom cross-stream spatial and isopycnal water-mass layering in the Agulhas Current, Agulhas Return Current, and associated rings are presented in two sets of sections, one contoured with pressure and the other with potential density as vertical coordinate. Temperature, salinity, oxygen, potential density and velocity sections are shown contoured versus pressure; and pressure, salinity, oxygen, and planetary potential vorticity are shown contoured versus potential density. These sections clearly illustrate water-mass structure both in space and relative to isopycnal surfaces. Strong salt, oxygen, and potential vorticity fronts on isopycnals in the upper ~300 m across the Agulhas and Agulhas Return Current are observed, as are deep western boundary filaments of (i) salty, low oxygen water at intermediate depths traceable to Red Sea Water influences, and (ii) salty North Atlantic Deep Water close round the tip of Africa.

The 1985 cold-core ring is the first cold-core isolated feature to be observed within the Retroflection itself. Its transport was 64 x 10^6m s^{-1}, its integrated kinetic and available portential energy anomalies were 8.3 and 61 x 10^{15}J respectively, and its integrated planetary potential vorticity anomaly was 2.8 x 10^{-12} m^{-1} s^{-1}. The potential vorticity flux associated with the exchange of 25 warm ring/cold ring pairs per year between the South Indian and Southern Oceans would balance the potential vorticity input by the wind to the entire South Indian Ocean.

Interbasin flow of warm thermocline water (warmer than 8 C) from the South Indian to the South Atlantic Ocean is reconsidered in light of the 1985 hydrographic data. Thermocline water flow from the South Indian Ocean into the South Atlantic in the 1985 and historical observations is found to range from 2.8 to <9.6 x 10^6 $m^{s}-1$. These values are less than the $\leq$10 x 10^6 m s^{-1} needed to balance the Atlantic Ocean export of deep water, and implies that the deep water export is balanced in part by water colder than 8 C.

Supported by: ONR N00014-84-C-0134, N00014-85-C-0001, and N00014-87-K-0001.

EVALUATION OF GEOSAT DATA AND APPLICATION TO VARIABILITY OF THE NORTHEAST PACIFIC OCEAN

Jeffrey W. Campbell

A portion of the northeast Pacific ocean was chosen within which to evaluate and use altimetric

data from the U.S. Navy Geodetic Satellite GEOSAT. The zero-order accuracy of the major GEOSAT geophysical data record (GDR) channels was verified, and occasional gaps in the altimeter coverage were noted. GEOSAT'S 17-day repeat orbit allowed use of collinear-track processing to create profiles of the difference between the sea surface height along a given satellite repeat, and the mean sea surface height along that repeat's groundtrack. Detrending of sea surface bias and tilt on each repeat reduced orbit and other long wavelength errors in the difference profiles.

The corrections provided on the GEOSAT GDR were examined for their effects on the difference profiles of three test arcs. It was found that only the ocean tide, electromagnetic bias, and inverted barometer corrections varied enough over the arc lengths (~4400 km) to have any noticeable effect on the difference profiles. Only the ocean tide correction was accurate enough to warrant using it to adjust the sea surface heights. The recommended processing of GEOSAT data for the area included making the ocean tide correction, three-point block averaging successive sea surface heights, and forming the mean height profiles from 18 repeat cycles (to reduce aliasing of the M2 tidal component). A set of difference profiles for one GEOSAT arc indicated that a reasonable estimate of GEOSAT's system precision was ~4.5 cm (RMS). The mid wavelength range (100-500 km) of these profiles was found to be the only range in which oceanic mesoscale features could be separated from altimeter errors.

Mean alongtrack wavenumber spectra of oceanic variability for two GEOSAT arcs were compared with a SEASAT-derived regional spectrum of FU (1983). Agreement was good, with GEOSAT showing less system noise at short wavelengths, and greater oceanic variability at long wavelengths. The GEOSAT spectra were fit well by a $k^{-1.5}$ slope at wavelengths from 100 to 1000 km.

Sea surface temporal variability as a function of location was compared with the SEASAT results of Cheney et al.(1983). Qualitative agreement was excellent and quantitative differences were largely accounted for. GEOSAT picked up the variability of the major current systems of the northeast Pacific, including the Alaskan, Californian, and North Equatorial currents. Error bounds on GEOSAT-derived oceanic variability showed that the effects of uncorrected electromagnetic bias, inverted barometer, and wet troposphere were significant. Further work in the areas of error modelling, orbit determination, and geoid calculation were called for.

Supported by: United States Navy.

A MODEL/WKB INVERSION METHOD FOR DETERMINING SOUND SPEED PROFILES IN THE OCEAN AND OCEAN BOTTOM

Kevin D. Casey

Two approaches to determining the ocean sound speed profile using measured acoustic modal eigenvalues are examined. Both methods use measured eigenvalues and mode dependent assumed values of the WKB phase integral as input data and use the WKB phase integral as a starting point for relating the index of refraction to depth. Inversion method one is restricted to monotonic or symmetric sound speed profiles and requires a measurement of the sound speed at one depth to convert the index of refraction profile to a sound speed profile. Inversion method two assumes that the sound speed at the surface and the minimum sound speed in the profile are known and is applicable to monotonic profiles and to general single duct sound speed profiles. For asymmetric profiles, inversion method two gives the depth difference between two points of equal sound speed in the portion in the profile having two turning points, and in the remainder of the profile it gives sound speed versus depth directly. A numerical implementation of the methods is demonstrated using idealized ocean sound speed profiles numerical experiments used to test the performance of the inversions using noisy data. The two methods are used to determine the sediment sound speed profiles in two shallow water waveguide models, and inversion method one is used to find the sediment sound speed profile using data from an experiment performed in the Gulf of Mexico.

Supported by: MIT by the ONR Fellowship Program.

THE EFFECTS OF ALGAL DENSITY ON GROWTH OF HETEROTROPHIC MICROFLAGELLATES

Joon Won Choi

The major role of heterotrophic nanoflagellates in the ocean is generally thought to be as grazers of bacteria, but they may also play an important role as grazers of photoautotrophs. The goal of the present study was to understand the basic growth kinetics of nanoflagellates feeding herbivorously. This was done using batch cultures in quasi steady-state growth.

Growth (increase in biomass) can involve changes in both cell numbers and cell size. Because fixed samples were examined, it was necessary to quantify the effects of fixation on the cell volume

of heterotrophic protozoa before proceeding with the growth studies. Fixation resulted in cell shrinkage, the degree of shrinkage varied with heterotrophic protozoan species and with algal prey species. It was hypothesized that egestion of food particles upon fixation was a major cause of shrinkage.

The growth rates of two heterotrophic nanoflagelates were determined to be hyperbolic functions of algal prey densities over a range of prey sizes. However, the specific response of the two species varied. Paraphysomonas imperforata appeared to respond primarily to prey cell numbers, and Strain HM-2 (unidentified species) responded most to available prey biomass (expressed as carbon or nitrogen). Minimum prey biomass for growth of both species feeding herbivorously was within the ranges reported for similar species feeding bactivorously. The growth kinetics suggest that heterotrophic nanoflagellates are adapted to heterogeneous distribution of prey within their environment.

The result of this study strongly suggests that previous studies of heterotrophic nanoflagellates based on the examination of fixed samples may have severely underestimated the role of these taxa as herbivores. Herbivory by heterotrophic nanoflagellates may be much more important than previously thought.

Supported by: NSF Grant OCE-86-00675 and OCE-86-00684.

THE SENSORY MEDIATION OF SYMBIOSIS BETWEEN HYPERIID AMPHIPODS AND SALPS

Carol E. Diebel

Hyperiid amphipods are open ocean crustaceans which use gelatinous planktonic animals for food, shelter, and brooding space for their offspring. These associations involve varying degrees of host specificity; and there are few obvious correlations between gross morphology of the amphipods and the types of host they choose. The mechanisms which allow hyperiids to find and select specific hosts in the water column were investigated through the sensory and behavioral basis of these symbioses in three genera of hyperiids, Vibilia, Lycaea, and Phronima, which differ in the nature of their association with a common host - salps. The investigation included the description of the distribution and morphology of sensilla on the dorsal surface of the exoskeleton and antennules of the three genera of hyperiids with speculation on their functions. The ultrastructure of the aesthetasc sensilla of Vibilia sp. was determined for comparison with other crustacean aesthetasc sensilla, making a chemosensory function plausible. Behavioral experiments were conducted at sea which demonstrated a chemosensory basis for the host-specific associations between species of Vibilia and Lycaea and salps. Observations on the internal anatomy and behavior of Phronima are described which underscore the importance of salps to their general ecology. Although focussed for practical and logistic reasons, on three genera of hyperiids and their salp hosts, this coordinated study of ecology, sensory structure and function, and behavior provides considerable insight into the mechanisms maintaining the symbioses which allowed hyperiid amphipods to invade and radiate within the planktonic environment.

Supported by: Lerner-Gray Fund for Marine Research of the American Museum of Natural History.

DEVELOPMENT OF AN ACTIVELY COMPLIANT UNDERWATER MANIPULATOR

David M. DiPietro

This thesis describes the design, construction, and evaluation of an actively compliant underwater manipulator for installation on the underwater remotely operated vehicle (ROV) JASON. The goal of this work has been to produce a high fidelity force-controllable manipulator exhibiting no backlash, low stiction/friction, high backdriveability, wide dynamic range, and possessing a large work envelope. By reducing the inherent dynamic nonlinearities, a wide range of joint compliances can realistically be achieved. This feature is important when implementing various force control schemes, particularly impedance control. In addition, a mechanically "clean" transmission reduces the need for sensors and allows the user to rely on integral motor sensors to provide torque, position, and velocity information.

A three axis manipulator rated to full ocean depth was built. Each of the revolute joints is driven by a DC brushless sensorimotor working through a multi-stage cable/pulley transmission. The manipulator mechanism and wiring is fully enclosed by cast aluminum housings filled with mineral oil. Mineral oil functions to pressure compensate and lubricate the system. Exterior surfaces of the manipulator are smooth and continuous, and were designed to act as work surfaces. Joints one and two have a 240°range of motion, while joint three can rotate 380°. The manipulator transmissions are modeled and predictions of manipulator stiffness, dynamic range, payload capacity, and hysteresis are compared with the results of tests conducted on

the actual system. Operation of the cable/pulley transmission are evaluated and suggestions for improvements are given.

Supported by: ONR N00014-86-C-0038, N00014-85-J-1242, and N00014-87-J-1111.

THERMAL AND MECHANICAL DEVELOPMENT OF THE EAST AFRICAN RIFT SYSTEM

Cynthia J. Ebinger

The deep basins, uplifted flanks, and volcanoes of the Western and Kenya rift systems have developed along the western and eastern margins of the 1300 km-wide East African plateau. Structural patterns deduced from field, Landsat, and geophysical studies in the Western rift reveal a series of asymmetric basins bounded by approximately 100 km-long segments of the border fault system. These basins are linked by oblique-slip and strike-slip faults cross-cutting the rift valley. Faults bounding the Kenya and Western rift valleys delineate two north-south-trending, 40-75 km wide zones of crustal extension, and little or no crustal thinning has occured beneath the uplifted flanks or the central plateau. In the Western rift, volcanism in Late Miocene time began prior to or concurrent with basinal subsidence, followed by rift flank uplift. Individual extensional basins developed diachronously, and basinal propagation may give rise to the along-axis segmentation of the rift valley. The coherence between gravity and topography data indicated that the mechanical lithosphere beneath the two rift valleys has been weakened relative to the central plateau and adjacent cratonic regions. Gravity and topography data at wavelengths corresponding to the overcompensated East African plateau can be explained by density variations within the upper mantle that are dynamically maintained.

Supported by: NSF Grant EAR-84-18120 and by Sea Grant NA84-AA-D-00033.

A COMPARISON OF CROSS-STREAM VELOCITIES AND GULF STREAM TRANSLATIONS UTILIZING IN-SITU AND REMOTELY-SENSED DATA

Clark B. Freise

In previous Gulf Stream work (Hall and Bryden, 1985, Hall 1985, 1986A, 1986B), a decomposition of multiple depth current records was developed which produced along-and cross-stream components. The cross-stream component was found to occasionally match lateral displacements of the Stream, as determined by temperature changes measured at the current meters.

This study determined where within the meander pattern of the Gulf Stream the cross-stream velocity calculated from current meters at depth correctly predicted translations of the Gulf Stream as measured by satellite data. Additionally, the effects of recently quantified cross-stream velocities associated with the curvature of Gulf Stream meanders were analyzed.

Supported by: ONR N00014-86-K-0751, N00014-87-K-0007 and by the United States Navy.

SEXUAL PATTERNS OF MONOOXYGENASE FUNCTION IN THE LIVER OF MARINE TELEOSTS AND THE REGULATION OF ACTIVITY BY ESTRADIOL

Elisabeth Snowberger Gray

Sex differences in hepatic microsomal cytochrome P-450 and monooxygenase activities were investigated in the marine teleosts scup (Stenotomus chrysops) and winter flounder (Pseudopleuronectes americanus). Microsomal cytochrome P-450 content per unit protein was 3-6 times lower in gonadally mature females than males. Ethoxyresorufin O-deethylase (EROD) activity in microsomes from females of both species was less than or equal to activity in males, reflecting sexually differentiated levels of the responsible isozyme, P-450E. Estradiol (E_2) 2-hydroxylation, demonstrated here for the first time in teleost microsomes, was measured via ^3H_2O release from [2-^{3}H]E_2. Microsomal E_2 2-hydroxylase activity in scup was P-450-mediated, although not by P-450E, and was 2-fold lower per unit protein in females than in males. Testosterone 6β-hydroxylase and aminopyrine N-demethylase (APDM) activities in scup were not sexually differentiated. In winter flounder microsomes, E_2 2-hydroxylase, testosterone 6β-hydroxylase, and APDM activities were all sexually differentiated. These three activities were decreased 2-3 fold per unit protein and increased 2-4 fold per unit P-450 in gonadally mature female winter flounder.

Levels of microsomal P-450E and P-450E were quantified by immunoblot. Specific P-450E content was lower in females than in males of both species, but P-450E per nmol P-450 was sexually differentiated only in winter flounder, where it was decreased in females. P-450A per unit protein was not sexually differentiated in either species, and in scup was not differentiated per nmol P- 450. However, in winter flounder P-450A per nmol P-450 was five times greater in females than in

males. Previously, reconstituted scup P-450A catalyzed both testosterone 6β- hydroxylase and E_2 2-hydroxylase activites (Klotz et al., Arch. Biochem. Biophys., 249 (1986): (326). P-450A levels were positively correlated to some extent with these two activities and APDM, suggesting co-regulation with or catalysis by P-450A.

E_2 injections suppressed microsomal monooxygenase activities and P-450E levels per unit protein in gonadally regressed winter flounder. Qualitatively, this change was like the decreased activities in female winter flounder. Other characteristics of the female-type pattern in monooxygenases were not reproduced by E_2 treatment. This suggests that E_2 could regulate monooxygenase activities in gonadally mature female winter flounder, but indicates that additional factors are also involved. It is speculated that testosterone or 17α,20β-dihydroxyprogesterone, which are elevated in plasma of spawning female teleosts, may also be regulatory. In rats and mice, sex differences in cytochrome P-450 are imparted by pituitary growth hormone and by the male sex steroid testosterone. In teleosts, sex differences in hepatic monooxygenases could be effected by means other than those known to function in mammals.

Supported by: Environmental Protection Agency CX-813567-01 and CR81315S-01 by National Institute of Health 1-R01-ES04220 and NSF Grant OCE-82-10505.

THE KINETICS AND THERMODYNAMICS OF COPPER COMPLEXATION IN AQUATIC SYSTEMS

Janet G. Hering

Copper complexation is ubiquitous in natural waters. Yet, many questions remain on the chemistry and biogeochemistry of naturally-occurring complexing agents. This thesis examines the sources and extent of biological cycling of such complexing agents and also the physical-chemical nature of their interactions with copper.

Investigations of copper complexation in coastal ponds and coordinated laboratory studies suggest that both labile, biogenic and refractory ligands contribute to the observed copper complexation. Culture and incubation experiments demonstrate ligand production associated with phytoplankton photosynthetic activity and suggest microbial degradation of complexing agents. However, in the coastal ponds studied, the biological cycling of natural complexing agents is obscured possibly due to contributions or refractory ligands to the observed copper complexation, mixing of pond waters with coastal seawater, or to the natural balance between biological production and degradation.

The physical-chemical nature of interactions of humic acids with copper was studied by examining both the thermodynamics and kinetics of these interactions. Extensive studies of the kinetics of metal-and ligand-exchange reactions with well-defined ligands under natural water conditions (i.e. - low concentrations of reacting species and the presence of competing metals and ligands) provide a mechanistic framework for examining the kinetics of metal-humate complexation reactions.

Study of the kinetics of copper-for-calcium metal-exchange reactions and metal titration experiments (individual metal titrations with calcium or copper and copper titrations in the presence of calcium as a competing metal) show that alkaline earth and transition metals do not compete for the same humate metal-binding sites.

Ligand exchange reactions between humate-bound copper and a fluorescent complexing agent proceed both through dissociation of the initial copper-humate species and by direct attack of the incoming ligand on the initial copper complex. The relative importance of these mechanisms is dependent on the copper-to-humate loading. Both of these mechanisms should contribute to overall ligand exchange reactions at the copper-to-humate loadings typical of estuarine and coastal waters.

The observed kinetics of ligand exchange and reactions with copper-humate species is consistent with the reactions of copper bound at discrete humate metal-binding sites. Apparent saturation of the strong copper-binding site (i.e. - slow-reacting copper-humate species) at high copper-to-humate loadings allows estimation of the strong copper-binding site density ($\approx 10^{-7}$ mol/mg humic acid) and of the conditional stability constant for copper binding at that site ($\approx 10^{10.1}$).

Investigations of ligand-exchange reactions of humate-bound copper in the presence of seawater concentrations of calcium demonstrate that the kinetics of metal coordination reactions under natural water conditions cannot be neglected. Even at high copper-to-humate loadings, the formation of CuEDTA on addition of coppper to a mixture of humic acid and EDTA (0.01 M Ca, pH - 7.3) proceeded over the course of several hours as compared with immediate formation of CuEDTA in the absence of calcium. Based on these results, equilibrium for this reaction in seawater at environmental copper-to-humate-loadings and lower EDTA concentrations is predicted to occur on a time scale of months to years.

The kinetics of coordination reaction with humic acids may be interpreted to provide information on the nature of metal-humate interactions. This information complements

equilibrium studies of such interactions. In the field, the study of the interactions of metals with naturally-occuring complexing agents is complicated by the presence of mixtures of labile, biogenic and refractory ligands. Finally, this work indicated that the assumption of fast equilibration of metals and ligands (i.e. - pseudoequilibrium) in seawater is not valid.

Supported by: MIT by NOAA; NSF; and by ONR.

COMPARISON STUDY OF SEASAT SCATTEROMETER AND CONVENTIONAL WIND FIELDS

Kristine Holderied

A demonstrated need exists for better wind field information over the open ocean, especially as a forcing function for ocean circulation models. Microwave scatterometry, as a means of remotely sensing surface wind information, developed in response to this requirement for a surface wind field with global coverage and improved spatial and temporal resolution. This development led to the 1978 deployment of the SEASAT Satellite Scattermeter (SASS). Evaluations of the three months of SEASAT data have established the consistency of SASS winds with high quality surface wind data from field experiments over limited areas and time periods. The directional ambiguity of the original SASS vectors has been removed by Atlas et al. (1987) for the entire data set, and the resulting SASS winds provide a unique set of scattermeter wind information for a global comparison with winds from conventional sources.

A one-month (12 August to 9 September 1978) subset of these dealiased winds, in the western North Atlantic, is compared here with a conventional, pressure-derived wind field from the 6- hourly surface wind analyses of the Fleet Numerical Oceanographic Center (FNOC), Monterey, CA. Through an objective mapping procedure, the irregularly spaced SASS winds are regridded to a latitude-longitude grid, facilitating statistical comparisons with the regularly spaced FNOC wind vectors and wind stress curl calculations. The study includes qualitative comparisons to synoptic weather maps, calculations of field statistics and boxed mean differences; scatter plots of wind speed, direction, and standard deviation; statistical descriptions of the SASS-FNOC difference field, and wind stress curl calculations.

The SASS and FNOC fields are consistent with each other in a broad statistical sense, with wide scatter of individual values about a pattern of general agreement. The FNOC wind variances are slightly smaller than the SASS values, reflecting smoothing on larger spatial scales than the SASS winds, and the SASS mean values tend to be slightly higher than the FNOC means, though the increase is frequently lost in the large scatter. Exceptions to the pattern of relatively small consistent variations between the two fields are the pronounced differences associated with extremely strong winds, especially during Hurricane Ella, which traveled up the East Coast of the United States during the latter part of the study period. These large differences are attributed mainly to differences in the inferred positions of the pressure centers and in the response at the highest wind speeds (> 20m/s). The large statistical differences between the SASS and FNOC fields, present under high wind conditions, may yield significantly different ocean forcing, especially when the strong winds persist over longer periods of time. Under less intense wind conditions, usually prevailing over the ocean, the two fields correspond well statistically and the ocean responses forced by each should be similar.

Supported by: United States Navy through MIT.

AN ORGANIC GEOCHEMICAL APPROACH TO PROBLEMS OF GLACIAL-INTERGLACIAL CLIMATE VARIABILITY

John P. Jasper

The concentration and carbon isotopic composition ($\delta^{13}C$) of sedimentary organic carbon (C_{org}), N/C ratios, and terrigenous and marine $\delta^{13}C$-C_{org} end-members form a basis from which to address problems of Late Quaternary glacial-interglacial climatic variability in a 208.7 m hydraulic piston core (DSDP 619) from the Pigmy Basin in the northern Gulf of Mexico. Paired analyses of $\delta^{13}C$-C_{org} and N/C are consistent with the hypothesis that the sedimentary organic carbon in the Pigmy Basin is a climatically-determined mixture of C_3 photosynthetic terrigenous and marine organic matter, confirming the model of Sackett (1964). A high resolution (~ 1.4-2.7 ky/sample) $\delta^{13}C$-C_{org} record shows that sedimentary ogranic carbon in interglacial oxygen isotope (sub)stages 1 and 5a-b are enriched in $^{1}3C$ (average $\pm$ 1σ values are -24.2 $\pm$ 1.2°/$_{oo}$ and -23.0 $\pm$ 0.8°/$_{oo}$ relative to PDB, respectively) while glacial isotope stage values 2 are relatively depleted (-25.6 $\pm$ 0.5°/$_{oo}$). Concentrations of terrigenous and marine sedimentary organic carbon are calculated using $\delta^{13}C$-C_{org} and C_{org} measurements, and terrigenous and marine $\delta^{13}C$-C_{org} end-members. The net accumulation rate of terrigenous organic carbon is 3.7 $\pm$ 3.1 times higher in isotope stages 2-4 than in (sub)stages 1 and 5a-b, recording higher erosion

rates of terrigenous organic material in glacial periods than interglacial periods. The concentration and net accumulation rates of marine and terrigenous C_{org} suggest that the nutrient-bearing plume of the Mississippi River may have advanced and retreated across the Pigmy Basin as sea level fell and rose in response to glacial-interglacial sea level change.

A study of selected organic biomarker compounds which could serve as tracers or terrigenous and marine sedimentary organic matter sources was performed by comparison with contemporaneous sedimentary organic carbon isotopic composition (δ^{13}C-C_{org}). Organic carbon-normalized concentrations of total long chain (C_{37}-C_{39}) unsaturated alkenones and individual C_{27}-C_{29} desmethyl sterols were determined to be useful proportional indicators of preserved marine and terrigenous organic carbon, respectively. The alkenones, whose source is marine phytoplankton of the class Prymnesiophyceae, generally occurred in higher concentrations in interglacial isotope stages 1 and 5a-b than in the intervening stages, including glacial stages 2 and 4. Sterols (C_{27}-C_{29}) of a dominantly terrigenous origin and lower concentrations during interglacial stages than in glacial stages. The sedimentary records of both terrigenous and marine organic carbon-normalized biomarker compound concentrations appear to be systematically altered by the remineralization of sedimentary organic carbon, is indicated by a simple, first-order organic carbon decay model. The sedimentary deposition of some terrigenous 4-desmethylsterols may be affected by differential hydraulic particle sorting as they are transported from river deltas across the continental shelf and slope to the hemipelagic Pigmy Basin. The marine phytoplanktonic alkenones which originate in the surface ocean and sink through the water column would not be subject to comparable particle sorting. The lack of any 4-desmethyl-or 4-α -methylsterol which was linearly related to the proportion of marine sedimentary organic matter (as scaled by δ^{13}C-C_{org}) indicated that either (1) sedimentary diagenesis had obscured the biomaker/C_{org} versus δ^{13}C-C_{org} record, or (2) the selected compounds were not proportional indicators of preserved marine organic carbon input.

The diagenetic alteration of the sedimentary sterol concentration records in which marine sterols were apparently more susceptible to degraduation than terrigenous sterols was consistent with present-day sediment trap and recent (10^{-1}-10^{2}y) sediment core observations. Preferential preservation of terrigenous sterols may result in a biased sedimentary record of sterol input which could be misinterpreted as indicating solely terrigenous sterol sources. The value and limitations of a simple model which characterizes the effects of sedimentary disgenesis and source input changes on the relationship between organic carbon-normalized biomarker compounds and sedimentary organic matter carbon isotopic composition are discussed.

The potentail occurence of sterol double bond hydrogenations (Δ^5, Δ^{22}) in the three classes of $C_{27\text{-}29}$-4-desmethylsterols was evaluated by examining the time series of expected product/precursor relationships with sterol data from the ~2- 100kybp DSDP 619 record. Only the Δ^5-hydrogenations of the C_{29} sterols (24-ethylcholest-5-en-3β-ol, 24-ethylcholest-5, 22-dien- 3β-ol) showed significant temporally-increasing trends. The 24-ethylcholestan-3β-ol/24-ethyl-cholest-5-en-3β-ol ($C_{29}\Delta^{o}$ /$C_{29}\Delta^{5}$) ratio also positively correlated with paired sedimentary organic carbon isotropic composition (δ^{13}C-C_{org}) values. This may be due to increased susceptibility to diagenetic transformation reactions by the organic matter accompanying finer grain-sized terrigenous sediment particles. A long-term source change of 24- ethylcholestan-3β-ol relative to 24-ethylcholest-5-en-3β-ol to explain the correlation with δ^{13}C-C_{org} seems less likely since both compounds are predominantly of a terrigenous origin in the Pigmy Basin. A comparison of histograms of stanol/stenol (Δ^{o}/Δ^{5}) ratios for the $C_{27\text{-}29}$-4-desmethylsterols indicates the following sequence in the relative degree of transformation: $C_{27} > C_{28} > C_{29}$. The $C_{27\text{-}}$ and $C_{28\text{-}}$ sterols appear to have attained their respective degrees of tranformation before ~2kybp, perhaps prior to deposition in the Pigmy Basin. However, differential rates of competing reactions of both the precursor and products may have obscured these simple transformation ratio records.

The sedimentary record of a ratio (U^{K}_{37}) of long chain (C_{37}) unsaturated alkenones is a useful indicator of glacial- interglacial climatic change inthe Late Quaternary northern Gulf of Mexico where a planktonic foraminiferal δ^{18}O-CaCO record is complicated by meltwater and/or fluvial events (Williams and Kohl, 1986). Using laboratory temperature calibration data of the U^{K}_{37} ratio (Prahl and Wakeham, 1987), it is suggested that the minimum glacial surface mixed layer (SML) temperature was 8±1°C colder than the Holocene high SML temperature of 25.6±0.5°C in a Pigmy Basin hydraulic piston core (DSDP 619). However, this glacial-interglacial $U^{K}_{37\text{-}}$-temperature difference was significantly larger than the differences predicted by either the foraminiferal δ^{1}8O or foraminiferal assemblage temperature methods (0.8-2.0°C). A possible cause for this large difference is that the Prymnesiophyte assemblages in this area may vary in response to climatically-induced hydrographic changes.

Interglacial periods may be dominated by pelagic Prymnesiophyte assemblages, while glacial periods may be dominated by neritic assemblages. Correlation of the U^{K}_{37} ratio with the sedimentary organic carbon composition ($\delta^{13}C$-C_{org}) is consistent with the predominance of preserved input of erosive terrigenous over marine organic carbon during glacial stages in the northern Gulf of Mexico when sea level was as much as 150m lower than in the present interglacial stage. Marine organic carbon burial dominated in warmer interglacial stages 1 and 5a-b.

Supported by: NSF Grant OCE-84-15720 and by the Andrew A. Mellon Foundation.

HEAT FLOW AND TECTONICS OF THE LIGURIAN SEA BASIN AND MARGINS

John P. Jemsek

Heat flow, tectonic subsidence and crustal thickness distributions in the Ligurian Basin are best explained by asymmetric lithospheric thinning mechanisms. Over 150 heat flow measurements are made on several transects between Nice, France and Calvi, Corsica on continental slope and rise settings. Thermal gradient determinations are improved using an optimization technique. Piston core data and surface sediment 3.5 kHz reflectivity patterns help constrain thermal conductivity obtained from over 100 in situ stations. Plio-Quaternary stratigraphy is revised using new seismic reflection profiles: a boundary fault system associated with postrift margin uplift, a Pleistocene-age Var Fan constuction, and recent diapirism of Messinian salt are indicated. After assessing local thermal disturbances (mass-wasting, microtopography, and salt refraction), positive heat flow corrections are made for multi-lithologic sedimentation histories and glacial paleotemperatures. Using boundary-layer cooling models, equilibrium heat flow estimates support geologic evidence for Oligocene and early Miocene rifting. Heat flow maxima correlate well with two "oceanic" sub-basins, suggesting that the southeastern trough near Corsica is ~5 Myr younger, consistent with the southeastern progression of volcanism and back arc rifting in the Western Mediterranean. Tectonic subsidence-crustal thickness trends indicate lithospheric stretching, with heat flow supporting asymmetric sub-crustal lithospheric thinning during the conjugate margin formation.

We report 176 new heat flow measurements which are distributed on several transects across the Ligurian Basin and margins between Nice, France and Calvi, Corsica. Improved heat flow instrumentation provides in situ thermal conductivity data at points where equilibrium temperatures are known for over 100 gradients determinations. Analytical studies of the in situ continuous-heating method indicate uncertainties of 5%, comparable to those of needle-probe measurements on piston cores. Gamma ray attenuation logs of sediment cores predict vertical variations in conductivity and indicate possible instrumental bias for discretely-spaced thermistor arrangements. Piston core data and 3.5 kHz reflection records demarcate regions of predominantly hemipelagic sediment on the slopes and turbiditic sediment on the Var fan. Mean conductivity values correlate well with surficial sediment patterns and morphology, so that conductivity may be reliably estimated for thermal gradient stations without in situ conductivity. To automate as well as improve equilibrium temperature estimates, the Golden Section Search method is used to optimize effective origin times for heating incurred on probe impact. Numerical modeling of probe thermal structure indicates that an initial temperature perturbation in sediments surrounding the probe may account for observed nonlinearities in standard temperature versus reciprocal-time plots. This technique has the largest effect on equilibrium values where high velocities are necessary for successful probe entry.

Heat flow measurements for the entire basin have a weighted mean of 70 ± 28 mW m^{-2}. Systematic regional variations are characterized by an overall asymmetic trend in heat flow, with heat flow averaging about 20% to 50% higher on the Corsican side. Significant scatter in regional heat flow values is mainly attributed to variability in the thermal gradients, Sites with very low scatter ($\pm$5-10%) are located on the continental rise and on the lower Var fan level. High variability on the continental slope is attributed to environments and processes of canyon formation: microtopography and mass-wasting. To a lesser extent, central basin values are perturbed by narrow salt structures and shallow faults. A reliability assessment suggests that heat flow averages are altered for sites where diapirism produces isolated high values. Contrary to the situation for most young oceanic crust, the sediment cover is extensive so that variability due to hydrothermal circulation is neglibible.

New high-resolution (100-300Hz) seismic records enable a revised Plio-Quaternary stratigraphy for the basin and a reassessment of the causes of margin uplift. We infer a Pleistocence age for the Var fan development, which is about 1 Myr younger than previous estimates. Recent margin subsidence has been affected by a "boundary fault" system at the base-of-slope, with up to 1 km uplift near the Cote d'Azur region of southern France. The uplift is consistent with Messinian and Glacial paleostrand line positions and suggests that an erosional-rebound phase occuring within the Alpine folded-and-thrusted

complex is responsible for the vertical movement. The boundary fault system is the main seaward dislocation for the uplift is associated with reactivated basement faults residing near the transition to highly-attenuated crust (<10 km). We associate the timing and geometry of the Var fan development with this uplift.

In order to determine equilibrium lithospheric heat flow, we account for the effects of deposition of up to 5km of sediments in the central basin. Sedimentation rates are reconstructed from the shallow and deep seismic data and physical properties are inferred from piston core and borehole data located within the northwestern Mediterranean. We develop a multi-layer compaction and sedimentation history, including the effects of salt deposition and marginal erosion during the Messinian. Sensitivity analyses of the sedimentation model reveal that composite media effects between the sediment layer and basement are similar in magnitude to the effects of compaction. Basement burial rate is the overall determining factor of the heat flow alteration, rather than surface sedimentation rate. Overpressuring in pre-Messinian sediments may decrease the heat flow by an additional 10%. Sedimentation corrections range from 30% for the Var levee to zero for the Corsican upper margin. Paleoclimatic corrections of 8-10 mW m^{-2} are also deemed necessary for the Mediterranean Sea Basins, assuming about a 4 °C change in bottom water temperature since the late Pleistocene. Uncertainties in corrected heat flow averages due to environmental corrections are generally <10%, which is smaller than data variability in most cases. Differences in sedimentation rates cannot account for local variations between stations (~2 km spacing), but somewhat reduces regional deviations between sites. The final corrected basin heat flow retains an asymmetric pattern, consistent with the asymmetric continental heat flow values observed on the conjugate borderlands.

Corrected values of 102 to 120 mW m^{-2} for northwestern and southeastern central basin sites, respectively, are consistent with boundary-layer cooling estimates for basin opening between 18-25 Myr ago. These results, integrated with calculations of basement subsidence and recent crustal thickness measurements, require a nonuniform spatiotemporal development for the Ligurian Basin. Heat flow correlates well with two basement troughs oriented parallel to the basin axis. Two modes of asymmetric lithospheric thinning account for the basin development: an intrabasinal rift jump (pure shear) and low-angle detachment faulting (simple shear). Some progression in rifting ages across the basin is suggested by younger volcanics on the Corsican-Sardinian block and the general southeastern arc-trench migration for the Western Mediterranean. The NW and SE margin heat flow and crustal data are consistent with asymmetic nonuniform lithospheric extension similar to that predicted by detachment faulting models. Thus, the asymmetic development of the Ligurian is envisioned to be quite similar to the drilling and seismic stratigraphic evidence for the multiple-rifting history of the Tyrrhenian Basin (Mascle and Rehault, 1988).

With our detailed environmental analysis, we may place more confidence in tectonic models derived from heat flow than low- amplitude magnetic anomaly patterns which favor a symmetric basin opening. Lateral heat flow appears to be suppressed for marginal basins, despite their generally narrow widths. Back arc extention in the Liguro-Provencal Basin is deemed important to the subsidence history of the basin. Negative residual basement depths of almost 1 km are explained by an anomalously cool upper mantle maintained by the limited influence of deep asthenospheric upwelling behind subduction zones. We speculate that "normal" high heat flow observed in marginal basins is an artifact of higher mantle thermal conductivity for highly-depleted mantle, created by plate recycling and hydrous melting in the back arc setting.

Supported by: NSF Grant OCE-80-25181 and OCE-84-09170.

CENOZOIC DEEP-WATER AGGLUTINATED FORAMINIFERA IN THE NORTH ATLANTIC

Michael A. Kaminski

Cenozoic (predominantly Paleogene) "flysch-type" agglutinated foraminiferal assemblages and their modern analogs in the North Atlantic and adjacent areas have been studied to provide an overview of their spatial and temporal distribution and utility for paleoenvironmental analysis. Over 200 species of agglutinated foraminifera have been recognized in Paleogene sediments from North Atlantic and Tethyan basins. This unified taxonomic data base enables the first general synthesis of biostratigraphic, paleobiogeographic and paleobathymetric pattern in flysch-type agglutinated assemblages from upper Cretaceous to Neogene sediments in the North Atlantic. The majority of taxa are cosmopolitan, but latitudinal, temporal and depth-related trends in diversity and species composition are observed among flysch-type assemblages.

Modern deep-sea agglutinated foraminiferal faunas provide an analog to fossil flysch-type assemblages and serve as models for paleoecologic studies. Core-top samples from the Panama Basin, Gulf of Mexico and Nova Scotian continental rise

were examined in order to determine the habitats of modern species of agglutinated foraminifera. The ecology of modern taxa provides constraints on the paleoenvironmental significance of fossil agglutinated assemblages in the North Atlantic, and their utility for paleoceanography.

Towards this end, spade core samples from a 3912 m deep station in the Panama Basin were studied to determine abundance and microhabitat partitioning among living agglutinated foraminiferal populations and the preservation of dead assemblages. The genera Dendrophrya, Cribrostomoides and Ammodiscuc have epifaunal habitats and the genus Reophax is predominantly infaunal. Species of Reophax are probably responsible for fine reticulate burrows observed in x-radiographs. An experiment using recolonization trays in the Panama Basin was designed to identify opportunistic species of benthic foraminifera, and to assess the rate at which a population can colonize an abiotic substrate. The most successful colonizer at this site is Reophax, while Dendrophrya displays the lowest capability for dispersal. After nine months the abundance of living individuals in sediment trays was one-tenth to one-third that of background abundance, but the faunal diversity did not differ greatly from control samples. Recolonization by bethnic foraminifera is more rapid than among macrofaunal invertebrates.

Modern agglutinated assemblages from the Louisiana continental slope were examined to determine changes in species composition associated with hydrocarbon seeps. Organic-rich substrates are characterized by a decrease in astrorhizids and an increase in trochamminids and textulariids. Highly organic-enriched substrates with chemosynthetic macrofauna are dominated by Trochammina glabra and Glomospira charoides.

The biostratigraphy of fossil agglutinated foraminifera in the North Atlantic is based on detailed analysis of 670 samples from 14 wells and one outcrop section, and examination of additional picked faunal slides from industry wells. Local biostratigraphic schemes are established for Trinidad, Northern Spain, the Labrador Sea, Baffin Bay, and the Norwegian-Greenland Sea. These schemes are compared with existing biostratigraphic frameworks from the Labrador Margin, the North Sea, and the Polish Carpathians. A number of species show utility for biostratigraphy in the North Atlantic. Lineages which contain stratigraphically useful species include the Haplophragmoides cf. glabra - Reticulophragmium group, Hormosina, and Karreriella.

Significant faunal turnovers are observed at the Paleocene/Eocene, Ypresian/Lutetian and Eocene/Oligocene boundaries. A reduction in diversity occurs at the Paleocene/Eocene boundary in all bathyal sections studied, and agglutinated forminifera disappear entirely from abyssal low-latitude DSDP sites. In the Gibraltar Arch, the Labrador Sea and the Norwegian-Greenland Sea, the Ypresian/Lutetian boundary is characterized by a Glomospira-facies. This is attributed to a rise in the lysocline associated with increased paleoproductivity and the NP14 sealevel lowstand. The Eocene/Oligocene boundary is delimited by another major turnover and the last occurence of a number of important taxa. At Site 647, where recovery across the Eocene/Oligocene boundary was continuous, the change from an Eocene agglutinated assemblage to a predominantly calcareous assemblage in the early Oligocene took place gradually, over a period of about 4 m.y. The rate of change of the faunal turnover accelerated near the boundary. This faunal turnover is attributed to changes in the preservation of agglutinated foraminifera, since delicate species disappeared first. Increasingly poorer preservation of agglutinated foraminifera in the late Eocene to earliest Oligocene reflected the first appearance of cool, nutrient-poor deep water in the southern Labrador Sea. The approximately coeval disappearance of agglutinated assemblages along the Labrador Margin was caused by a regional trend from slope to shelf environments, accentuated by the "mid"-Oligocene sealevel lowstand.

Paleobiogeographic patterns in flysch-type foraminifera were examined in the Paleogene of the North Atlantic. In the early Paleogene, general decrease in diversity is observed from low to high latitudes and from the continental slope to the deep ocean basins. The diversity of these microfossils declines in most studied sections throughout the Paleogene. The last common occurrence (LCO) of flysch-type foraminifera in the North Atlantic exhibits a pattern of diachrony with latitude and depth. Extinctions occurred first at abyssal depths and at low latitudes. Agglutinated assemblages disappeared from the northern Atlantic region in the early Oligocene. However, the deep Norwegian-Greenland Sea served as a refuge for many species, and agglutinated assemblages persisted there until the early Pliocene. The LCO of flysch-type foraminifera may have been related to the transition from a warm, sluggish deep sea environment to a cooler, more oxygenated, thermohaline-driven deep circulation pattern caused by bipolar cooling.

The paleobathymetry of Paleogene agglutinated assemblages in the North Atlantic differs from Cretaceous patterns. Shallow-water assemblages of Paleogene are contain robust astrorhizids, loftusiids and coarse lituolids, whereas deep assemblages possess delicate tubular forms, ammodiscids, and smooth lituolids. At low latitudes, upper bathyal assemblages contain

abundant calcareous ataxophragmiids. Paleocene paleobathymetric patterns in the North Atlantic compare well with patterns observed in the Carpathian troughs.

The utility of agglutinated foraminifera in paleoceanography in illustrated by a study of the paleocommunity structure of fossil assemblages in ODP Hole 646B on the Eirik Ridge (Labrador Sea). They synecology of benthic foraminifera in the Hole 646B places constraints on the history of Denmark Straits Overflow water over that site. Below seismic horizon "R3", a Miocene assemblage contains smooth agglutinated species with abundant Nuttalides umbonifera, indicating corrosive bottom water and tranquil conditions. A coarse agglutinated assemblage with "NADW-type" calcareous benthics is observed above the seismic horizon. This faunal turnover at horizon "R3" reflects the onset (or renewal) of significant Denmark Straits overflow at ~7.5 Ma. Agglutinated species disappear between reflector "R2", and the base of the sediment drift, indicating a change in deep-water properties associated with the re-opening of the Mediterranean. The onset of drift sedimentation at the Eirik Ridge is dated at ~4.5 Ma. Drift formation ceased at ~2.5 Ma, concomitant with the appearance of ice-rafted sediments.

Supported by: NSF Grant OCE-82-17586 and by Texas A&M Research Foundation/U.S. Scientific Program.

MEASUREMENTS OF A BAROTROPIC PLANETARY VORTICITY MODE IN AN EDDY-RESOLVING QUASI-GEOSTROPHIC MODEL USING ACOUSTIC TOMOGRAPHY

Wendy B. Lawrence

A tomographic array is placed in a 2-layer, flat bottom, steady-wind driven quasi-geostrophic circulation model to investigate whether the analysis of acoustic travel time changes can detect large-scale barotropic oscillations. Time series of sea surface elevation and upper and lower layer meridional currents are generated for comparison against a series of acoustic travel times. The spectra of these time series exhibit a broad mesoscale peak near a period of 40 days. The spectrum of the acoustic travel time contains a significant peak due to a resonant barotropic oscillation with a period of 28.6 days which is not present in the spectra of the point measurements. In this numerical model, basin-scale tomographic measurements are a better method of sensing the large-scale resonant barotropic oscillations than are conventional point measurements because the tomographic system attenuates the "noise" from the mesoscale.

Supported by: United States Navy.

FLUID FLOW AND SOUND GENERATION AT HYDROTHERMAL VENT FIELDS

Sarah A. Little

Several experiments are presented in this thesis which examine methods to measure and monitor fluid flow from hydrothermal vent field.

Simultaneous velocity, temperature, and conductivity data were collected in the convective flow emanating from a hydrothermal vent fluid located at 10°56'N, 103°41'W on the East Pacific rise. The horizontal profiles obtained indicate that the flow field approaches an ideal plume in the temperature and velocity distribution. Such parameters as total heat flow and maximum plume height can be estimated using either the velocity or the temperature information. Such parameters as total heat flow and maximum plume height can be estimated using either the velocity or the temperature information. The results of these independent calculations are in close agreement, yielding a total heat flow from this vent site of 3.7 ± 0.8 MW and a maximum height of 150±10 m. The nonlinear effects of large temperature variations on heat capacity and volume changes slightly alter the calculations applied to obtain these values.

In Guaymas Basin, a twelve day time series of temperature data was collected from a point three centimeters above a diffuse hydrothermal flow area. Using concurrent tidal gauge data from the town of Guaymas it is shown that the effects of tidal currents can be strong enough to dominate the time variability of a temperature signal at a fixed point in hydrothermal flow and are a plausible explanation for the variations seen in the Guaymas Basin temperature data.

Theoretical examination of hot, turbulent, bouyant jets exiting from hydrothermal chimneys revealed acoustic source mechanisms capable of producing sound at levels higher than ambient ocean noise. Pressure levels and frequency generated by hydrothermal jets are dependent on chimney dimensions, fluid velocity and temperature and therefore can be used to monitor changes in these parameters over time.

A laboratory study of low Mach number jet noise and amplification by flow inhomogeneities confirmed theoretical predictions for homogeneous jet noise power and frequency. The increase in power due to convected flow inhomogeneities, however, was lower in the near field than expected.

Indirect evidence of hydrothermal sound fields (Reidesel et al., 1982; Bibee and Jacobson, 1986) showing anomalous high power and low frequency noise associated with vents is due to processes other than jet noise.

On Axial Seamount, Juan de Fuca Ridge, high quality acoustic noise measurements were obtained by two hydrophones located 3 m and 40 m from an active hydrothermal vent, in an effort to determine the feasibility of monitoring hydrothermal vent activity through flow noise generation. Most of the noise field could be attributed to ambient ocean noise sources of microseisms, distant shipping and weather, punctuated by local ships and biological sources. Water/rock interface waves of local origin, were detected which showed high pressure amplitudes near the seafloor and, decaying with vertical distance, produced low pressures at 40 m above the bottom.

Detection of vent signals was hampered by unexpected spatial nonstationarity due to shadowing effects of the caldera wall. No continuous vent signals were deemed significant based on a criterion of 90% probability of detection and 5% probability of false alarm. However, a small signall near 40 Hz, with a power level of $1X10^{-4}$ Pa^2/Hz was noticed on two records taken near the Inferno black smoker. The frequency of this signal is consistent with predictions and the power level suggests the occurrence of jet noise amplification due to convected density inhomogeneities.

Ambient noise from the TAG (Trans-Atlantic Geotraverse) hydrothermal area on the Mid-Atlantic Ridge near 26°N, in the frequency band 1-30 Hz at a range of 0.75-14 km from the site of an extremely active high temperature hydrothermal vent field (Rona, 1986) was examined. The ambient noise field exhibits great temporal and spatial variations attributed in part to typical ocean noise sources such as distant shipping and microseisms. Power spectral levels as measured at each of six ocean bottom hydrophones (OBH) were used to estimate the location of point sources of sound in the area, if any.

The hydrothermal vent did not produce enough sound to be located as a point source using data from the OBH array. The only consistently identifiable point source found with the data set was generating sound in a 0.8-3.5 Hz bandwidth the located outside the median valley. It appears to be harmonic tremor associated with the tip of a ridge on the western side of the spreading axis and may be volvanic in origin.

Supported by: ONR N00014-87-K-0007, NSF Grant OCE-83-10175 and NOAA Grant NA86AA-D-SG090.

REGISTRATION AND VARIABILITY OF SIDE SCAN SONAR IMAGERY

John W. Nicholson

This thesis presents the results of several experiments performed on side scan sonar equipment and imagery with the aim of characterizing the acoustic variability of side scan sonar imagery and applying this information to image rectification and registration. A static test tank experiment is presented which analyzes the waveform, power spectral density, and temporal variability of the transmitted waveform. The results of a second static experiment conducted from the Woods Hole Oceanographic Institution Pier in Woods Hole, Massachusetts permit determination of the distribution and moments of intensity fluctuations of echoes from objects imaged in side scan sonograms. This experiment also characterizes temporal and spatial coherence of intensity fluctuations. A third experiment is presented in which a side scan sonar towfish images the bottom adjacent to the pier while running along an underwater track which reduces towfish instability. Imagery from this experiment is used to develop a rectification and registration algorithm for side scan sonar images. Preliminary image processing is described and examples presented, followed by favorable results for automated image rectification and registration.

Supported by: Marine Imaging System; Mass. Commonwealth Center; and United States Navy.

GEOSTROPHIC VORTEX DYNAMICS

Lorenzo M. Polvani

By generalizing the method of contour dynamics to the quasigeostrophic two layer model, we have proposed and solved a number of fundamental problems in the dynamics of rotating and stratified vorticity fields. A variety of rotating and translating potential vorticity equilibria (V-states) in one and two layers have been obtained, shedding new light on potential vorticity dynamics in the geostrophic context. In particular, the equivalent barotropic model is shown to be a singular limit of the two-layer model for scales large compared to the radius of deformation.

The question of coalescence of two vortices in the same layer (merger) and in different layers (alignment) is studied in detail. Critical initial separation distances for coalescence are numerically established as functions of the radius of deformation and the relative thickness of the layers at rest. The connection between coalescence and the existence of stable rotating

doubly-connected V-states is shown to be an illuminating generalization of the Euler results.

The question of filamentation of two-dimensional vorticity interfaces is addressed from a new geometrical perspective. The analysis of the topology of the streamfunction in a frame of reference rotating with the instantaneous angular velocity of the vorticity distribution (the corotating frame) is shown to yield new powerful insights on the nonlinear evolution of the vorticity field. In particular, the presence of hyperbolic (critical) points of the corotating streamfunction that come in contact with the vorticity interface is found to be directly responsible for the generation of filaments.

The importance of the position of the critical points of the comoving streamfunction is found to generalize to the two-layer quasigeostrophic context. They are shown to play the crucial role in determining the limits, in parameter space, on the existence of a number of two-layer rotating and translating potential vorticity equilibria.

Supported by: ONR through MIT.

OBSERVATIONS AND MODELLING OF DEEP EQUATORIAL CURRENTS IN THE CENTRAL PACIFIC

Rui Vasques De Melo Ponte

Analysis of vertical profiles of absolute horizontal velocity collected in January 1981, February 1982 and April 1982 in the central equatorial Pacific as part of the Pacific Equatorial Ocean Dynamics (PEQUOD) program, revealed two significant narrow band spectral peaks in the zonal velocity records, centered at vertical wavelengths of 560 and 350 stretched meters (*sm*). Both signals were present in all three cruises, but the 350 *sm* peak showed a more steady character in amplitude and a higher signal-to-noise ratio. In addition, its vertical scales corresponded to the scales of the conspicuous alternating flows generically called the equatorial deep jets in the past (the same terminology will be used here). Meridional velocity and vertical displacement spectra did not show any such energetic features.

Energy in the 560 sm band roughly doubled between January 1981 and April 1982. Time lagged coherence results suggested upward phase propagation at time scales of about 4 years. East-west phase lines computed from zonally lagged coherences, tilted downward towards the west, implying westward phase propagation. Estimates of zonal wavelength (on the order of 10000 *km*) and period based on these coherence calculations, and the observed energy meridional structure at this vertical wavenumber band, seem consistent, within experimental errors, with the presence of a first meridional mode long Rossby wave packet, weakly modulated in the zonal direction.

The equatorial deep jets, identified with the peak centered at 350 *sm*, are best defined as a finite narrow band process in vertical wavenumber (311-400 *sm*), accounting for only 20% of the total variance present in the broad band energetic background. At the jets wavenumber band, latitudinal energy scaling compared well with Kelvin wave theoretical values and a general tilt of phase lines downward towards the east yielded estimates of 10000- 16000 *km* for the zonal wavelengths. Time-lagged coherence calculations revealed evidence for vertical shifting of the jets on interannual time scales. Interpretation of results in terms of single frequency linear wave processes led to inconsistencies, but finite bandwidth (in frequency and wavenumber) Kelvin wave processes of periods on the order of three to five years could account for the observations. Thus, the records do not preclude equatorial waves as a reasonable kinematic description of the jets.

At all wavenumber bands in general, power levels decayed away from the equator over scales broader than the Kelvin wave scale, suggesting the presence of Rossby wave energy. Cross-spectral analysis showed Rossby and Kelvin wave motions to be dominant at the equator over the 933 *sm* and the 140-400 *sm* vertical wavelength bands, respectively. The latter agrees with the findings of Eriksen (1981) in the western Pacific, and thus seems to be a climatological feature of the deep equatorial Pacific fields.

In an attempt to model the observed zonal velocity signals, alternative forcing mechanisms for the deep ocean (other than direct surface winds) were tried. The probable presence of deep energy sources at the ocean side walls (e.g., Kawase, 1987) was explored by considering the linear response of an equatorial ocean to a time varying zonal jet placed at the lateral boundaries. In another simple model, we examined the character of stationary Kelvin wave solutions obtained in the presence of vertically sheared mean westward flows. In this case, the waves are forced below the thermocline by a vertical velocity representing large scale convergence or divergence patterns associated with the upper ocean circulation. Results suggest that both ideas remain potentially important to the existence of deep baroclinic currents in the equatorial ocean.

Supported by: NSF Grant OCE-8600052.

MASS, HEAT AND NUTRIENT FLUXES IN THE ATLANTIC OCEAN DETERMINED BY INVERSE METHODS

Stephen R. Rintoul

Inverse methods are applied to historical hydrographic data to address two aspects of the general circulation of the Atlantic Ocean. The method allows conservation statements for mass and other properties, along with a variety of other constraints, to be combined in a dynamically consistent way to estimate the absolute velocity field and associated property transports.

The method is first used to examine the exchange of mass and heat between the South Atlantic and the neighboring ocean basins. The Atlantic Circumpolar Current (ACC) carries a surplus of intermediate water into the South Atlantic through Drake Passage which is compensated by a surplus of deep and bottom water leaving the basin south of Africa. As a result, the ACC loses $.25\pm.18x10^{15}$W of heat in crossing the Atlantic. At 32°S the meridional flux of heat is $.25\pm.19x10^{15}$ W equatorward, consistent in sign but smaller in magnitude than other recent estimates. This heat flux is carried primarily by a meridional overturning cell in which the export of 17 Sv of North Atlantic Deep Water (NADW) is balanced by an equatorward return flow equally split between the surface layers, and the intermediate and bottom water. No "leak" of warm Indian Ocean thermocline water is necessary to account for the equatorward heat flux across 32°S; in fact, a large transfer of warm water from the Indian Ocean to the Atlantic is found to be inconsistent with the present data set. Together these results demonstrate that the Atlantic as a whole acts to convert intermediate water to deep and bottom water, and thus that the global thermohaline cell associated with the formation and export of NADW is closed primarily by a "cold water path," in which deep water leaving the Atlantic ultimately returns as intermediate water entering the basin through Drake Passage.

The second problem addressed concerns the circulation and property fluxes across 24°and 36°N in the subtropical North Atlantic. Conservation statements are considered for the nutrients as well as mass, and the nutrients are found to contribute significant information independent of temperature and salinity. Silicate is particularly effective in reducing the indeterminacy of circulation estimated based on mass conservation alone. In turn, the results demonstrate that accurate estimates of the chemical fluxes depend on relatively detailed knowledge of the circulation.

The zonal-integral of the circulation consists of an overturning cell at both latitudes, with a net export of 19 Sv of NADW. This cell results in a poleward heat flux of $1.3\pm.2x10^{15}$W and an equatorward oxygen flux of 2900 ± 180 $kmols^{-1}$ across each latitude. The net flux of silicate is also equatorward: 138 ± 38 $kmols^{-1}$ and 152 ± 56 $kmols^{-1}$ across 36°and 24°N, respectively. However, in contrast to heat and oxygen, the overturning cell is not the only important mechanism responsible for the net silicate transport. A horizontal recirculation consisting of northward flow of silica-rich deep water in the eastern basin balanced by southward flow of low silica water in the western basin results in a significant silicate flux to the north. The net equatorward flux is thus smaller than indicated by the overturning cell alone.

The net flux of nitrate across 36°N is 119 ± 35 $kmols^{-1}$ to the north and is indistinguishable from zero at 24°N (-8 ± 39 $kmols^{-1}$), leading to a net divergence of nitrate between these two latitudes. Forcing the system to converse nitrate leads to an unreasonable circulation. The dominant contribution to the nitrate flux at 36°N results from the correlation of strong northward flow and relatively high nitrate concentrations in the sub-surface waters of the Gulf Stream. The observed nitrate divergence between 24°and 36°N, and convergence north of 36°N, can be accounted for by a shallow cell in which the northward flow of inorganic nitrogen (nitrate) in the Gulf Stream is balanced by a southward flux of dissolved organic nitrogen in the recirculation gyre. Oxidation of the dissolved organic matter during its transit of the subtropical gyre supplies the required source of regenerated nitrate to the Gulf Stream and consumes oxygen, consistent with recent observations of oxygen utilization in the Sargasso Sea.

Supported by: NASA through MIT and NSF by MIT.

IMPROVEMENT OF THREE DIMENSIONAL ACOUSTIC FIELD ESTIMATION USING TOMOGRAPHIC RECONSTRUCTIONS OF THE OCEAN

Elizabeth A. Rowe

In order to determine the efficacy of tomographic reconstructions of the ocean sound speed structure in improving acoustic field predictions for source localization, a 150 km by 350 km volume of ocean 3000 meters deep was synthetically modeled to be similar to the Gulf Stream system, including an eddy and a front. The features were Gaussian, with the eddy's maximum sound speed perturbation being $10ms^{-1}$ and the front's maximum perturbation $15ms^{-1}$. Two vertical slices through this system were inverted in

a synthetic tomography experiment using linear optimal estimation theory. Inversions were also performed using XSV and satellite sea surface temperature data. Gaussian fits to the reconstructed features were constructed for use with a three dimensional raytrace program (HARPO). Three dimensional rays were propagated both through the reconstructions and the original model. Travel time versus intensity (transmission loss) for the eigenrays was used as a basis for intercomparison. Tomographic results showed good reconstruction for a first iteration of the inversion, but inadequate vertical resolution. Iterations and the use of more refractive eigenrays are needed for improvement of the reconstruction, especially for the front. Reconstructed results for the acoustic field should improve conventional beamforming, but are probably inadequate for matched field processing.

Supported by: United States Navy.

THE INFLUENCE OF GEOTHERMAL SOURCES ON DEEP OCEAN TEMPERATURE, SALINITY, AND FLOW FIELDS

Kevin G. Speer

This thesis is a study of the effect of geothermal sources on the deep circulation, temperature and salinity fields. In Chapter 1 background material is given on the strength and distribution of geothermal heating. In Chapter 2 evidence for the influence of a hydrothermal system in the rift valley of the Mid-Atlantic Ridge on nearby property fields and a model of the flow around such a heat source are presented, with an analysis of a larger-scale effect. Results of an analytical model for a heat source on a β-plane in Chapter 3 show how the response far from the source can have a structure different from the forcing because of its dependence on two parameters: a Peclet number (the ratio of horizontal advection and vertical diffusion), and a Froude-number-like parameter (the ratio of long wave phase speed to background flow speed) which control the relative amount of damping and advection of different vertical scales. The solutions emphasize the different behavior of a dynamical field like temperature compared to tracers introduced at the source. These ideas are useful for interpreting more complicated solutions from a numerical model presented in the final chapter.

Supported by: NSF Grant OCE-82-13967, OCE-85-15642 and by the WHOI/MIT JP OVF Fund.

HYBRID STATE ESTIMATORS FOR THE CONTROL OF REMOTELY OPERATED UNDERWATER VEHICLES

Gregory M. Vaughn

This paper explores the use of "hybrid" state estimators to increase the accuracy and flexibility of acoustic position measurement systems used in the control of underwater vehicles. Two different approaches to extend the range of acoustic position measurement systems are explored. The first approach is the use of an inexpensive Strapdown Inertial Measurement System (SIMS) to augment the acoustic with inertial position information. The approach is based on the experience gained using an attitude and inertial measurement package fielded on the JASON JUNIOR Remotely Operated Vehicle (ROV). The second approach is the use of a mobile, platform-mounted, acoustic net in conjunction with a platform tracking system. This second investigation used the JASON ROV as the basis for the simulation work. As motivation, some of the theoretical and practical difficulties encountered when range is extended using an unaugmented system are explored. Simulation results are used to demonstrate the effects of these difficulties on position estimation accuracy and on the performance in closed loop control of the vehicle. Using measured sensor noise characteristics, a hybrid Kalman filter is developed for each approach to take the greatest advantage of the available information. Formulation of the Kalman filter is different for each case. In the second case, the geographic position of the ROV is the sum of the acoustic net's geographic position, measured at a different interval by RF positioning system, and the position of the ROV relative to the net, as measured acoustically. Closed loop vehicle performance evaluations are made for representative noise levels and update rates with and without the augmentation discussed in the first approach. Finally, conclusions are drawn about the benefits and applications of the hybrid Kalman filter to the control of Remotely Operated Vehicles.

Supported by: United States Navy.

SIMILARITY RELATIONS OF WIND WAVES IN FINITE DEPTH

Padmaraj Vengayil

Three formulations for the rear face of a growing wind-sea spectrum in finite depth based on Phillips (1958), Toba (1972) and Donelan et al. (1985) are tested using spectral measurements from Lake St. Clair. Assuming spectral similarity in wave number space relations between the

energy, equilibrium parameters and peak wave number are derived. Using a regression analysis, relations are obtained from the data and compared to the theoretical relations. Results indicate that the formulation based on a high-frequency $\mathcal{F}^{-4}$ tail (Toba, 1972 and Donelan et al., 1985) is better than the Philliphs $\mathcal{F}^{-5}$ high-frequency tail. Based on the effective fetch formulation, wave propagation directions are calculated. Relations between the spectral parameters, growth-stage variables and fetch are also determined from the data. The relations indicate a weak dependence of the spectral parameters on depth. Various source terms in the energy balance equation for wave growth in finite depth water are estimated for two cases of wave evolution. The relative importance of wind input, bottom dissipation, white-capping dissipation and nonlinear transfer in the evolution of the spectra is analyzed.

Supported by: NOAA Grant NA86-AA-D-SG090.

THE INFLUENCE OF A STEADY BAROCLINIC DEEP OCEAN ON THE SHELF

M. Ross Vennell

The degree to which a baroclinic deep ocean could be responsible for the mean flow on the shallow continental shelf is examined using steady, boundary forced models which incorporate bottom friction. One set of models, for a vertically well mixed shelf, includes the horizontal advection of density. The second set of models comprises a three-layer model without and a two-layer model with interfacial friction.

It is found that near bottom flow has a short cross isobath scale due to the steep continental slope and consequently that the deep oceans lower water column could not be responsible for the observed mean flow. The cross isobath scale of flow in the upper deep ocean is predominantly determined by the oceans velocity profile. In a barotropic or near barotropic flow the upper water column follows the near bottom flow and therefore has little influence on the shelf. A surface intensified deep ocean flow is able to cross isobaths until it encounters the bottom. If deep ocean flow is confined to a surface layer thinner than the depth at the shelf break it could be responsible for the observed flow. The depth scale for velocity and density over the slope in the Mid-Atlantic Bight is generally larger than the shelf break depth and consequently it is concluded that the steep continental slope "insulates" this particular shelf from baroclinic deep ocean influence and therefore that the observed shelf flow is not of oceanic origin.

Using oxygen isotope data, Chapman et al (1986) found that the Scotian shelf is the major source of Mid-Atlantic Bight shelf water. Their barotropic modeling results are extended to show that a baroclinic deep ocean also acts to hold shelf water on the shelf.

Supported by: NSF through MIT.

DYNAMICS OF THE EQUATORIAL UNDERCURRENT AND ITS TERMINATION

Sophie Wacongne

This study focuses on the zonal weakening, eastern termination and seasonal variations of the Atlantic equatorial undercurrent (EUC). The main and most original contribution of the dissertation is a detailed analysis of the Atlantic EUC simulated by Philander and Pacanowski's (1986) general circulation model (GCM), which provides a novel description of the dynamical regimes governing various regions of a nonlinear stratified undercurrent.

Only in a narrow deep western region of the simulation does one find an approximately inertial regime corresponding to zonal acceleration. Elsewhere frictional processes cannot be ignored. The bulk of the mid-basin model EUC terminates in the overlying westward surface flow while only a small fraction (the deeper more inertial layers) terminates at the eastern coast. In agreement with observations, a robust feature of the GCM not present in simpler models is the apparent migration of the EUC core from above the thermocline in the west to below it in the east. In the GCM, this happens because the eastward flow is eroded more efficiently by vertical friction above the base of the thermocline than by lateral friction at greater depths. This mechanism is a plausible one for observed EUC. A scale analysis using a depth scale which decreases with distance eastwards predicts the model zonal transition between western inertial and eastern inertio-frictional regimes.

Historical and recent observations and simple models of the equatorial and coastal eastern undercurrents are reviewed, and a new analysis of current measurements in the eastern equatorial Atlantic is presented. Although the measurements are inadequate for definitive conclusions, they suggest that Lukas' (1981) claim of spring surge of the Pacific EUC to the eastern coast and a seasonal branching of the EUC into a coastal southeastward undercurrent may also hold for the Atlantic Ocean. To improve the agreement between observed and modelled strength of the eastern undercurrent, it is suggested that the eddy coefficient of horizontal mixing should be reduced in future GCM simulations.

Supported by: NSF Grant OCE-82-08744 and OCE-85-14885.

THE ROLE OF SEDIMENT TRANSPORT IN THE EXCHANGE OF CHEMICALS ACROSS THE BED-WATER INTERFACE

John L. Wilkin

A sediment transport formulation is developed for the prediction of the fate of sediment borne chemical contaminants in river and marine environments.

The model is based on the physical principle that the bottom shear stress in excess of the critical value for initiation of motion is supported: (i) at low transport rates by fluid drag on sediment grains sliding along the bottom, and (ii) at high transport rates by transfer of fluid momentum to sediment grains ejected from the bed. For physically reasonable choices of model parameters the predicted transport rates compare favorably with published experimental data.

The model requires as input the grain size and critical shear strength τ_c of the sediment and the bottom stress due to the flow. An experimental facility for measuring τ_c is developed and tested as part of the study.

The particular advantage of this sediment transport formulation is its prediction of the sediment exchange rate between the immobile bed and the overlying moving fluid. Using this exchange rate a simple two-layer model for tracer dispersal is derived. The model solution resembles the solution of the diffusion equation. An expression for the equivalent diffusion coefficient as a function of sediment and flow parameters is derived for both steady uni-directional and oscillatory transport systems. The tracer dispersal model is applied to: (i) the steady problem of exchange of contaminants between bottom sediments and the water column, and (ii) the unsteady bottom sediments tracer dispersal in the surf zone.

Supported by: NSF Grant OCE-84-17769 and OCE-85-21837.

CHARACTERIZATION OF SWIMMING MOTILITY IN A MARINE CYANOBACTERIUM

Joanne M. Willey

The structural mechanism, behavior, energetics and functional significance of the unique swimming motility displayed by some oceanic isolates of the cyanobacterium Synechococcus was investigated. A variety of analytical techniques confirmed that these strains swam through liquids without flagella or flagellar-like appendages. No extracellular structures were observed in a broad range of cell preparations examined by transmission electron microscopy (TEM), or by high-intensity dark field microscopy. The possibility that a structure might be present that eluded visualization was eliminated by the lack of motility-dependent amplitude spectra, the absence of discrete circulation of microspheres around the cell body and the inability of shearing forces to arrest motility. TEM and gel electrophoretic analysis of spheroplasts, cell wall-enriched fractions from motile and nonmotile strains, and cell material collected following the application of a flagellar hook-basal body complex isolation technique to a motile Synechococcus strain provided no further evidence of a structure or protein unique to motile strains.

The motile Synechococcus strains represent the only cyanobacterium reported to date capable of swimming rather than gliding motility. Swimming behavior was characterized by several features: between 50 - 80% of cells were actively motile during logarithmic phase of growth, with speeds that ranged from 5 - 40 um s^{-1}; the average speed was 13 um s^{-1}. Swimming patterns were entirely random, consistent with the absence of bacterial flagella. Synechococcus motility resembled flagellar-mediated motility in that thrust (forward motion) was accompanied by torque (cell rotation) as demonstrated by i) dividing cells which swam with the daughter cells at an angle, ii) individual cells that were sometimes seen to rotate end over end at a rate or 3 to 5 rev s^{-1}, iii) polystyrene beads attached to the cell body served as a point of reference as the cell rotated concomitant with translocation and iv) cells attached to the coverslip or slide spun about one pole at an average rate of 1 rev s^{-1}. When observed in the same plane of focus, 50% of the cells spun clockwise and 50% spun counterclockwise, but unlike flagellated cells, Synechococcus was never seen to change direction of rotation, as would be predicted if the cell body were rotating as a single unit and the motility apparatus were incapable of reversing direction of rotation. This motility apparatus appeared to operate at a constant torque, as indicated by the relationship between swimming speeds and the fluidity of the surrounding medium.

Investigation of the energetics of motility in Synechococcus WH8113 demonstrated that swimming was sodium coupled. There was a specific sodium requirement such that cells were immotile at external sodium concentrations below 10 mM, with speeds increasing with increasing sodium to a maximum speed at 150 to 250 mM sodium, pH 8.0 to 8.5. The sodium motive force increased similarly, but other energetic parameters including proton motive force, electrical potential, and the proton and sodium diffusion gradients lacked correlation to levels of motility. When components of the sodium motive force were

diminished by monensin or carbonyl cyanide m-chlorophenyl-hydrazone, motility was arrested. Motility was independent of the magnitude of internal ATP pools, which were depleted to 2% of control values without affecting cell motitlity. These results suggest that the direct source of energy for Synechococcus motility is a sodium motive force, and that the device driving motility is located in the cytoplasmic membrane, as is the case for flagellated bacteria.

The ecological role of Synechococcus motility was explored and several lines of evidence indicated that cells lacked behavioral photoresponses but were able to detect and respond to very low concentrations of simple nitrogenous compounds. When 23 compounds were tested in spatial gradients established in blind well chemotaxis chambers, cells displayed positive chemoresponses only when placed in gradients of NH_4Cl, $NaNO_3$, urea, glycine and alanine. Cells also failed to respond in chambers which lacked gradients due to the presence of only seawater or an equal distribution of chemoeffector, demonstrating that a gradient was required to elicit a response. The apparent threshold levels of 10^{-10} M - 10^{-9} M for Synechococcus chemoresponses are 4 to 5 orders of magnitude lower than those for most other bacteria and place them in the range of ecological significance. The presence of chemotaxis in this oceanic cyanobacterium may help support the notion that nutrient enriched microaggregates may play an important role in picoplankton nutrient dynamics.

Supported by: NSF Grant PCM-86-8698.

Index